Optimising CAR T cell immunotherapy with a tumour microenvironment targeted immunocytokine

Runbeck, Erin

Awarding institution:
King's College London

Optimising CAR T Cell Immunotherapy with a Tumour Microenvironment Targeted Immunocytokine

Erin Runbeck (1558169)

Submitted to King's College London for the award of

Doctor of Philosophy

ImmunoEngineering Group, School of Cancer and Pharmaceutical Studies, King's College London

August 2019

Abstract

Prostate cancer (PCa) is the most common malignancy in men in the UK. However, the 5-year survival rate of stage IV PCa is 30% and the median survival for the castrate resistant phenotype is less than 2 years. This illustrates a clinical need for improved therapies for metastatic castrate resistant prostate cancer. Chimeric antigen receptor (CAR) T cell therapy has shown unprecedented success in blood cancers. The application of this platform in solid cancers, including PCa, has been less efficacious. A 2nd generation CAR, P28z, has previously been developed to retarget T cells to PSMA. When co-expressed with the IL-4 responsive 4αβ chimeric cytokine receptor, the resultant P4 transduced T cells proliferate and enrich in the presence of IL-4. The aim of my project was to develop an IL-4 immunocytokine targeted to the tumour microenvironment to provide P4 CAR T cells with a proliferative signal and thereby increase anti-tumour efficacy. Fibroblast activation protein (FAP) was chosen as the target for the immunocytokine because of its overexpression in the stroma of epithelial cancers. An immunocytokine designed from a published anti-FAP single chain variable fragment (scFv) sequence, eFAP-4, showed FAP specificity and signalling capabilities through the 4αβ receptor. For drug development, PCa cell lines were characterised and developed to express PSMA and reporter genes. Additionally, FAP^{+} stromal cell lines were characterised and engineered with a reporter gene. When P4 CAR T cells were cultured on PSMA^{+}FAP^{+} PCa/stroma monolayers in the presence of eFAP-4, increased T cell proliferation, cytokine secretion and persistence were observed. However, when PCa xenografts were established *in vivo*, stromal engraftment was insufficient. To model this interaction, PCa cells were transduced with FAP. In a pilot study using this PSMA^{+}FAP^{+} PCa xenograft model, increased survival and tumour control was seen in the group treated with P4 + eFAP-4. This study has indicated the potential for the improvement of CAR T cell immunotherapy of PCa using tumour microenvironment targeted immunocytokines.

Table of Contents

List of Figures

List of Tables

Abbreviations

4-1BB	Tumour necrosis factor receptor superfamily member 9
4-1BBL	Tumour necrosis factor receptor superfamily member 9 ligand
ADCC	Antibody-dependent cellular cytotoxicity
Ag	Antigen
aHSCT	Allogeneic haematopoietic stem cell transplantation
AIDS	Acquired immunodeficiency syndrome
ALCL	Anaplastic large cell lymphoma
ALT	Alanine aminotransferase
AML	Acute myeloid leukaemia
APC	Allophycocyanin
AR	Androgen receptor
ASCO	American Society of Clinical Oncology
AST	Aspartate aminotransferase
B-ALL	B-cell acute lymphoblastic leukaemia
BCA	Bicinchoninic acid
BCG	Bacillus Calmette-Guerin
Bcl-2	B-cell chronic lymphocytic leukaemia/lymphoma 2
Bcl-xL	B-cell lymphoma-extra large
BLI	Bioluminescent imaging
BM-MSC	Bone marrow mesenchymal stromal cell
bp	Base pair
BTK	Bruton tyrosine kinase
CAF	Cancer-associated fibroblast
CAIX	Carbonic anhydrase 9
CAR	Chimeric antigen receptor

CCL19	C-C chemokine ligand 19
CCL2	C-C chemokine ligand 2
CCL22	C-C chemokine ligand 22
CCR	Co-stimulation chimeric receptor
CCR2b	C-C chemokine receptor 2b
CCR4	C-C chemokine receptor 4
CD	Cluster of differentiation
CD40L	CD40 ligand
CDC	Complement-dependent cytotoxicity
CDR	Complementarity-determining region
CEA	Carcinoembryonic antigen
cFLIP	Cellular FLICE-inhibitory protein
$CH_{1/2}$	Constant heavy chain ½
CLEC14a	C-type lectin domain family member 14a
CLL	Chronic lymphocytic leukaemia
CM	Conditioned media
CPI	Checkpoint inhibitors
CRC	Colorectal carcinoma
CRPC	Castrate resistant prostate cancer
CRS	Cytokine release syndrome
CRUK	Cancer Research UK
CSCC	Cutaneous squamous cell carcinoma
CTLA-4	Cytotoxic T-lymphocyte associated protein 4
CXCL11	C-X-C chemokine ligand 11
DAPI	4′,6-diamidino-2-phenylindole
DLBCL	Diffuse large B-cell lymphoma

DLI	Donor lymphocyte infusion
DMEM	Dulbecco's Modified Eagle Medium
dMMR	deficient DNA mismatch repair
DMSO	Dimethyl sulfoxide
DNA	Deoxyribonucleic acid
dNTP	Deoxynucleotide triphosphate
DPPIV	Dipeptidyl peptidase IV
DRE	Digital rectal exam
ECL	Enhanced chemiluminescence
ECM	Extracellular matrix
ED-B	Extra-domain B
EDTA	Ethylenediaminetetraacetic acid
EGFR	Epidermal growth factor receptor
ELISA	Enzyme-Linked Immunosorbent Assay
EpCAM	Epithelial cell adhesion molecule
EphA2	Ephrin type-A receptor 2
Fab	Fragment antigen binding
FAO	Fatty acid oxidation
FAP	Fibroblast activation protein
FBP	Folate binding protein
FBS	Foetal bovine serum
Fc	Fragment crystallisable region
FDA	Federal Drug Administration
FGFR	Fibroblast growth factor receptor
FITC	Fluorescein isothiocyanate
FKBP	FK506 binding protein

FL	Follicular lymphoma
FR	Folate receptor
GAM-PE	Goat anti mouse-PE
GD2	Disialoganglioside
GEJ	gastro-esophageal junction
GM-CSF	Granulocyte-macrophage colony-stimulating factor
gp100	Glycoprotein 100
GvHD	Graft-versus-host disease
H&E	Haematoxylin and eosin
HBS	Hepes buffered saline
HCC	Hepatocellular carcinoma
HCL	Hairy cell leukaemia
Her2/ErbB2	Human epidermal growth factor 2
HL	Hodgkin's Lymphoma
HLA	Human leukocyte antigen
HNSCC	Head and neck squamous cell carcinoma
HRP	Horseradish peroxidase
HSV-1	Herpes simplex virus 1
HSV-tk	Herpes simplex virus thymidine kinase
hTERT/hT	Human telomerase reverse transcriptase
HVEM	Herpes virus entry mediator
IC	Immunocytokine
ICAM-1	Intercellular adhesion molecule 1
iCas9	Inducible Caspase 9
ICOS	Inducible T-cell co-stimulator
IDO	Indoleamine-pyrrole 2,3-dioxygenase

IFN-γ	Interferon γ
IFNα	Interferon α
IgG	Immunoglobulin G
IHC	Immunohistochemistry
IL-12	Interleukin 12
IL-15	Interleukin 15
IL-15R	IL-15 receptor
IL-18	Interleukin 18
IL-1R	Interleukin 1 receptor
IL-2	Interleukin 2
IL-21	Interleukin 21
IL-2R	IL-2 receptor
IL-4	Interleukin 4
IL-4Rα	IL-4 receptor α
IL-7	Interleukin 7
IL-7Rα	IL-7 receptor α
IP	Intraperitoneally
ITAM	Immunoreceptor tyrosine-based activation motif
IU	International units
IV	Intravenously
IVIG	Intravenous immunoglobulins
K_D	Equilibrium dissociation constant
kDa	Kilodalton
L	Leader sequence
LAG-3	Lymphocyte-activation gene 3
LAK	Lymphokine activated killer

LB	Luria-broth
LMP-2	Low molecular mass protein 2
LMP-7	Low molecular mass protein 7
LT	ffLuciferase-tdTomato
mAb	Monoclonal antibody
MAGE-A3	Melanoma antigen gene family member A3
MAGE-A4	Melanoma antigen gene family member A4
MAGE-C1	Melanoma antigen gene family member C1
MART-1	Melanoma antigen recognised by T cells
MCC	Merkel cell carcinoma
mCRPC	Metastatic castrate resistant prostate cancer
MDSC	Myeloid-derived suppressor cell
MEK	Mitogen-activated protein kinase kinase
MFI	Median fluorescent intensity
MHC I	Major histocompatibility complex I
MMP-2	Metalloproteinase 2
MMP-9	Metalloproteinase 9
MOPS	3-(N-morpholino)propanesulfonic acid
MRI	Magnetic resonance imaging
mRNA	Messenger ribonucleic acid
MSI-H	High microsatellite instability
MTT	3-(4,5-dimethylthiazol-2-yl)-2,5-diphenyltetrazolium bromide
MUC-1	Mucin-1
MW	Molecular weight
n.d.	No data
n.s.	Not significant

NAAG	N-acetylaspartylglutamate
NaCl	Sodium chloride
NFAT	Nuclear factor of activated T cells
NHL	Non-Hodgkin's Lymphoma
NK	Natural killer
NSCLC	Non-small cell lung carcinoma
NY-ESO-1	New York esophageal squamous cell carcinoma-1
OX40	Tumour necrosis factor receptor superfamily member 4
P4	P28z + 4αβ
P4Tr	Truncated P4
PAP	Prostatic acid phosphatase
PBMC	Peripheral blood mononuclear cell
PBS	Phosphate buffered saline
PCa	Prostate cancer
PCR	Polymerase chain reaction
PD-1	Programmed cell death protein 1
PD-L1	Programmed death ligand 1
PD-L2	Programmed death ligand 2
PDGFRα	Platelet-derived growth factor receptor α
PDX	Patient-derived xenograft
PE	Phycoerythrin
PED	Phosphoprotein enriched in diabetes
PEI	Polyethylenimine
PFS	Progression free survival
PHA	Phytohemagluttinin-L
PI3K	Phosphoinositide 3-kinase

PIPE	Polymerase incomplete primer extension
PKR	Protein kinase R
PMBCL	Primary mediastinal B-cell lymphoma
PSA	Prostate specific antigen
PSCA	Prostate stem cell antigen
PSMA	Prostate specific membrane antigen
RANKL	Receptor activator of nuclear factor kappa-B ligand
RCC	Renal cell carcinoma
rhIL-4	Recombinant human IL-4
rIL-4	Recombinant IL-4
RPM	Revolutions per minute
RPMI	Roswell Park Memorial Institute
SC	Subcutaneously
scFv	Single chain variable fragment
SCLC	Small cell lung carcinoma
SDS-PAGE	Sodium dodecyl sulfate polyacrylamide gel electrophoresis
SEM	Standard error of the mean
SLAMF7	Signaling lymphocytic activation molecule family member 7
SOC	Super optimal broth with catabolite repression
SOCS1	Suppressor of cytokine signaling 1
SPECT	Single photon emission computer tomography
SRC	Spare respiratory capacity
STAT6	Signal transducer and activator of transcription 6
T-VEC	Talimogene laherparepvec
TAG72	Tumour associated glycoprotein 72
TAM	Tumour-associated macrophage

TAP-1	Transporter associated with antigen processing 1
TAP-2	Transporter associated with antigen processing 2
TBE	Tris-borate-EDTA
TBST	TBS-Tween 20
TCR	T-cell receptor
tEGFR	Truncated epidermal growth factor receptor
TGF-β	Transforming growth factor β
TGF-βR	Transforming growth factor β receptor
TIL	Tumour infiltrating lymphocyte
TIM3	T-cell immunoglobulin and mucin-domain containing-3
TNBC	Triple negative breast carcinoma
TNFα	Tumour necrosis factor α
TNM	Tumour, lymph node and metastasis
Treg	Regulatory T cell
TRUCK	T-cell redirected universal cytokine killing
UCOE	Ubiquitous chromatin opening element
VEGF	Vascular endothelial growth factor
VEGFR2	Vascular endothelial growth factor receptor 2
V_H	Antibody heavy chain variable region
V_L	Antibody light chain variable region
VSVG	Vesicular stomatitis virus G
WT-1	Wilms' Tumour 1
αSMA	α Smooth muscle actin

Acknowledgements

The last 4 years of my life have really been a time of growth, discovery and amazement. I never thought I would one day be living in London, England pursuing my PhD in translational cancer research. It has been a truly breath taking experience to be involved in an area of work so close to my heart. This journey has been trying to say the least, but I am so grateful for the impact it has had on my life and my self-improvement. There have definitely been a couple of mental (and necessary) slaps to the face… what doesn't kill you!

My undying gratitude goes to my primary supervisor and mentor Sophie Papa. She has guided me through lessons of cell culture, subcutaneous injections, presenting my work to a range of audiences and above all, how to be a leader that people want to follow. She was nurturing, but also knew when I needed a little kick of encouragement. I will forever appreciate our work meetings that turned into mentoring sessions and always left me feeling a bit better about everything going on in my life. Thank you.

My second supervisor, John Maher is just a wealth of knowledge about literally all things CAR T cell! It has been humbling to attend weekly lab meetings with him and catching glimpses of the wheels turning in his head. I am appreciative of the guidance he has been able to offer me on my project and potential career choices.

All the members of ImmunoEngineering (especially my team with Rob and Olivier), CAR Mechanics and Leucid have been beyond helpful throughout this degree. I realise how fortunate I am to work in such a friendly and caring environment and everyone really goes out of their way to help a follow lab mate in need. Special thanks to Marc Davies who was silly enough to give me his personal number and has been receiving random thesis/lab questions ever since. Marc is an inspiring researcher and friend. Nia Emami-Shahri will always have a special place in my heart as my first post-doc mentor.

Antonella, Caroline, Leena, Ana and Lynsey have always been able to magically make the hard times seem a little brighter. Thank you, ladies.

My family is my rock in turbulent times. It has been difficult being so far away from them for so long, but they have helped me recognise this as growing pains. My mother, my father and my sister are so supportive of my endeavours and I feel so lucky to be such great friends with them as well. How many people can say they actively enjoy grabbing a pint with the parents and the sis?

Lastly, I am ever so grateful for my partner Sonny Dormer. He has been on the front lines of my PhD meltdowns and thesis panics and has managed to remain patient, understanding, attentive and loving through it all. Life would have been a lot more stressful these last 3 years without him and for that I will forever be indebted.

Chapter 1: General Introduction

1.1 Immunotherapy for cancer

1.1.1 History

The potential beneficial association between infection and tumour control has been recorded as far back as ancient Egypt (Ebbell, 1937). Studies evaluating the use of infectious agents to treat tumours were documented in 1891 when William Coley recorded the effect of injecting cancer patients with *Streptococcus* strains to induce erysipelas. He first described the trials of Dr. Friedrich Fehleisen, credited for the isolation of the microbe responsible for the erysipelas infection, and his seven patients with different sarcoma and carcinoma malignancies. These patients were injected with bacteria to cause erysipelas; six developed infection and three had visible reduction in both swollen glands and tumour size. Independent of this, Coley reported seven more cases of complete tumour regression or decrease in tumour size following accidental or intentional induction of erysipelas (Coley, 1891). Based on these observations, Coley went on to treat ten patients with intratumoural injections of *Streptococci* and seven manifested some degree of tumour regression/growth control. In most cases, an incapacitating erysipelas infection preceded anti-tumour events including high fever, chills, vomiting, malaise and fatigue (Coley, 1893). Known as "the father of immunotherapy", Coley treated nearly 1,000 patients in his lifetime with Coley's Toxins (a mixture of heat-inactivated *Streptococci* and *Serratia marcescens*). However due to poorly controlled experiments and the severity of infections, Coley's Toxins were no longer regarded as a viable treatment for cancer by the mid-20th century (McCarthy, 2006). The role of immunology in cancer progression or treatment had not been described by that time and consequently it wasn't completely understood why Coley's Toxins appeared to induce tumour regression. Building on this concept, the first widely established cancer immunotherapy was the Bacillus Calmette-Guerin (BCG) vaccine,

which was originally administered to prevent tuberculosis. The BCG vaccine was first used to treat superficial bladder cancer in 1976 and this live attenuated vaccine is still in use for non-invasive bladder cancer (Chang et al., 2016, Morales, 2017, Morales et al., 1976).

It is now understood that the immune system is involved in the control of malignancy through 'immunosurveillance' and, paradoxically, contributes to cancer progression through 'immunoediting'. This impact of the immune system on tumour evolution is characterised by 3 states: elimination, equilibrium and escape of the malignant cells (Dunn et al., 2002). Immunologic control of tumour formation/growth was debated for most of the 20th century, but expansion of the field of immunology and further development of tissue-specific transgenic mouse models has allowed for a more thorough investigation into the immunosurveillance theory. An initial study using fibrosarcoma cells expressing a dominant negative IFN-γ receptor rendering the cells IFN-γ insensitive in immunocompetent mice resulted in a loss of tumour control in the model (Dighe et al., 1994). Additional investigations using transgenic mice lacking the crucial cell-mediated cytotoxicity molecules or receptors for IFN-γ and perforin led to a higher rate of chemically induced tumour development, increased tumour growth of syngenic xenografts and an elevated proportion of metastases (Street et al., 2002, Street et al., 2001, van den Broek et al., 1996). This loss of IFN-γ/perforin dependent tumour elimination was amplified by additionally knocking out the tumour suppressor gene *p53* (Kaplan et al., 1998, Smyth et al., 2000b). Observational studies of immunosuppressed organ transplant recipients and patients with Acquired Immunodeficiency Syndrome (AIDS) show an increased incidence of both viral and non-viral associated malignancies compared to the general population, further supporting the concept of cancerous cell elimination through immunosurveillance (Biggar et al., 1987, Birkeland et al., 1995,

Frisch et al., 2001, Penn, 1999). One report showed a remission rate of 32% and 60% for sarcoma patients with superficial and visceral lesions, respectively, in whom post-transplantation immunosuppressive drugs were discontinued without any additional therapeutic intervention (Penn, 1995). Additionally, multiple studies have shown a beneficial association between overall survival and tumour-infiltrating lymphocyte count (Clark et al., 1989, Clemente et al., 1996, Epstein and Fatti, 1976, Lipponen et al., 1992).

Elimination is considered the first phase of immunoediting. This phase corresponds to the immunosurveillance theory previously described involving immune-mediated control of mutated cells. The second phase in the immunoediting process is equilibrium, which hypothesises that immune cells can positively select for cancerous cells that are more resistant to killing and thus shape the microenvironment to promote tumour cell survival. This ultimately leads to the third phase, the escape/outgrowth of these evolved cancerous cells into a clinical disease capable of producing an immunosuppressive factor milieu. The immune-driven selection of robust variants was described in an early study evaluating the effect of IFN-γ and lymphocytes in the process of tumour formation. In this report, chemically induced tumours were harvested from either wildtype or $RAG2^{-/-}$ immunosuppressed mice and subsequently injected into either wildtype or $RAG2^{-/-}$ mice. Tumour progression was seen for all mice in each condition apart from the wildtype mice receiving $RAG2^{-/-}$ tumours in which 40% of tumours were rejected. This is consistent with the evolution of more immunogenic tumour variants in the absence of a functioning immune system (Shankaran et al., 2001). Since then, murine studies have shown that pressure from the innate and adaptive immune system can result in tumour cell dormancy/cell cycle arrest and lead to later tumour progression (Koebel et al., 2007, Muller-Hermelink et al., 2008, O'Sullivan et al., 2012, Teng et al., 2012). The maintenance of this state of equilibrium is reliant on a balance between pro-tumour and

anti-tumour cytokines and leukocytes within the microenvironment that is distinct from the escape phase (Wu et al., 2013). Tumours that escape control and progress have been shown to express a number of factors to dampen down immune regulation and promote tumour cell survival, growth and motility. Such factors include vascular endothelial growth factor (VEGF), galectin-1, transforming growth factor β (TGF-β), indoleamine-pyrrole 2,3-dioxygenase (IDO), programmed death ligand 1 (PD-L1), prostaglandin E2, arginase and metalloproteinase 2 and 9 (MMP-2/9) (Dublin et al., 1993, Gobin et al., 2019, Kremer et al., 1992, Mittal et al., 2014, Reed et al., 1991, Rubinstein et al., 2004, Senger et al., 1986). There is also an increase of immunosuppressive cell types in the tumour microenvironment such as regulatory T cells (Tregs), M2 macrophages, cancer-associated fibroblasts (CAFs) and myeloid-derived suppressor cells (MDSCs) (Bhome et al., 2016). Cancerous cells can also show downregulation or aberrant expression of major histocompatibility complex I (MHC I) enabling avoidance of recognition by T cells (Garrido et al., 1997).

The emergence of lower immunogenicity variants has also been seen in different malignancies undergoing immunotherapeutic intervention. In patients with New York oesophageal squamous cell carcinoma-1 (NY-ESO-1)-expressing melanoma or breast cancer who were vaccinated against this antigen, disease relapse was characterised by downregulation of NY-ESO-1 in 11/17 cases (Nicholaou et al., 2011). One relapsed melanoma patient displayed continuous expression of two cancer associated antigens, melanoma antigen gene family member C1 (MAGE-C1) and Melan-A, throughout the duration of disease; however, loss of expression of NY-ESO-1 was noted in metastases. This loss of expression of the vaccine target antigen was associated temporally with an observed immune response to NY-ESO-1 (von Boehmer et al., 2013). This has also been documented in B-cell acute lymphoblastic leukaemia (B-ALL) patients treated with

CD19-specific chimeric antigen receptor (CAR) T cell therapy resulting in a number of relapses with $CD19^-$ disease (Grupp et al., 2013, Lee et al., 2015, Maude et al., 2016). Evidence of immunological influence on malignancy development has impacted immunotherapy/trial design and emergence of antigen negative disease has highlighted a need for multi-targeted therapies.

1.1.2 Monoclonal antibodies and immune checkpoint blockade

Monoclonal antibodies are the immunotherapeutic class with the greatest number of Food and Drug Administration (FDA) approvals to date [Table 1.1]. Antibodies have been used in a clinical setting since the late 19th century. Emil von Behring first described 'anti-toxin'; the phenomenon whereby serum from an immunised animal conferred protection against infection in an un-immunised animal (Behring, 1890). This polyclonal therapy heralded the use of intravenous immunoglobulin (IVIG) in humans, both to treat immunodeficiency and for the management of some auto-immune conditions (Hooper, 2015). With the introduction of hybridoma technology (Kohler and Milstein, 2005), it became possible to create large libraries of monoclonal antibody-producing clones in order to specifically target antigens of interest. This method was translated into the clinic by monoclonal antibody generation targeted against B-cell lymphoma patient-derived tumour cells in two separate case studies (Miller et al., 1982, Nadler et al., 1980). With the discovery of a B-cell specific antigen, CD20, that was also present on all assessed B-cell cancers (Stashenko et al., 1980), the anti-CD20 monoclonal antibody Rituximab was developed by IDEC pharmaceuticals and became the first FDA approved cancer therapeutic monoclonal antibody (Maloney et al., 1997). This was followed by a cascade of FDA approvals for therapeutic antibody treatment in multiple blood cancers and solid tumours.

While initial antibody development was targeted against tumour-associated molecules, there was a paradigm shift towards development of antibodies that instead disrupted natural immune checkpoints which would otherwise suppress immune responses. The application of checkpoint inhibitors (CPIs) has led to the largest class of approved antibodies to date with the most indications in advanced solid tumours [Table 1.1]. This class of monoclonal antibodies target and block inhibitory immune checkpoints that naturally dampen down immune responses. So far, monoclonal antibody therapies targeting the immune checkpoints CTLA-4, PD-1 and PD-L1 have become commercially available. Cytotoxic T-lymphocyte associated protein 4 (CTLA-4) was first described as a T-cell specific immunoglobulin superfamily marker that is highly expressed in activated T cells (Brunet et al., 1987). Later, it was established that CTLA-4 is structurally related to the co-stimulation receptor CD28 and, like CD28, it binds to CD80/86 (Harper et al., 1991, Linsley et al., 1991). Further investigation revealed that administration of soluble CTLA-4 could halt transplant rejection in mice, suppress T cell expansion/activation and protect against the development of multiple sclerosis in *in vivo* models (Cross et al., 1995, Lin et al., 1993, Linsley et al., 1992). Owing to its higher affinity, CTLA-4 outcompetes CD28, displacing it from co-stimulatory ligands, leading to inhibition of T cell responses. A key early observation was the demonstration that antagonistic anti-CTLA-4 antibodies inhibit its interaction with its ligands permitting tumour rejection and development of anti-tumour memory. This study which involved a colon cancer model marked the beginning of the development of CPIs for cancer therapy (Krummel and Allison, 1995, Leach et al., 1996). In 2011, the anti-CTLA-4 antibody ipilimumab was approved for the treatment of advanced unresectable melanoma after a phase III trial illustrated an increase in overall survival of 4 months for patients receiving the drug. This was also accompanied by high grade adverse events in 10-15% of patients in the ipilimumab treatment groups, resulting in 14 drug-related deaths (Hodi et al., 2010). A 2015 report encompassing the

data from multiple trials for melanoma showed a median overall survival of 11.4 months, but a 3-year overall survival of 22% accompanied by a plateau of the survival curve extending to 10 years. This suggests that ipilimumab conveys long term survival benefits surpassing 3 years for almost a quarter of patients treated (Schadendorf et al., 2015).

The programmed cell death protein 1 (PD-1) receptor was first described as a new immunoglobulin superfamily member that was restricted to the murine thymus and upregulated in programmed death induced cells (Ishida et al., 1992). Later studies demonstrated PD-1 upregulation on activated leukocytes, not solely on dying cells. Programmed cell death protein 1 knockout mice develop autoimmune-type features with an increase in circulating leukocytes, highlighting a role for PD-1 in immune tolerance (Nishimura et al., 1998, Nishimura et al., 1999, Vibhakar et al., 1997). The ligands for PD-1 are known as PD-L1 and PD-L2 and are naturally expressed on antigen presenting cells, in addition to certain epithelial tissues such as lung and heart. Activation of PD-1 by its ligands results in the inhibition of co-stimulation signalling, reduced T cell proliferation and control of inflammation in healthy tissues (Freeman et al., 2000, Latchman et al., 2001). It is also apparent that PD-L1/2 are expressed on a wide variety of solid tumours and blood cancers. The presence of PD-L1/2 in a tumour microenvironment enabled the induction of apoptosis of T cells *in vitro* (Dong et al., 2002). In mouse models of leukaemia in which PD-L1 was either naturally expressed or induced, *in vivo* progression of the tumour and abrogation of T cell responses were associated with its expression. This was reversed by targeting antibodies to PD-L1 and the enhanced tumour progression was lost in a PD-1 knockout model (Iwai et al., 2002). These observations led to the clinical development of antibodies targeting PD-1/PD-L1. An initial phase I trial of the anti-PD-1 antibody nivolumab in patients with advanced solid tumours indicated a tolerable safety profile with no grade 4 toxicities and 5/39

clinical responses (Brahmer et al., 2010). A phase I trial of pembrolizumab (which also targets PD-1) in advanced solid tumours also showed acceptable toxicity with no grade 3/4 adverse events, although one patient died of infection after prolonged corticosteroid administration due to drug-related gastric inflammation. There were 2 complete responses, 3 partial responses and 15 cases of stable disease out of 30 treated patients (Patnaik et al., 2015). Pembrolizumab was the first anti-PD-1 drug approved for clinical use and was followed soon thereafter by nivolumab [Table 1.1]. Both drugs are humanised IgG4 antibodies that block the interaction of PD-1 with its ligands. Initially approved for the treatment of advanced melanoma, they both have since gained approvals for the treatment of a variety of malignancies. Anti-PD-1 CPIs have a better safety profile than ipilimumab and have shown efficacy in PD-L1^{-} tumours. Monoclonal antibodies against PD-L1 such as atezolizumab, avelumab and durvalumab have also been approved (Alsaab et al., 2017).

Not all patients treated with CPIs respond to treatment. In fact, across all indications, most patients do not respond or relapse. Because CTLA-4 and PD-1 inhibit T cell cytotoxicity via different cellular signalling pathways involving pre- and post-engagement of the TCR (Carter and Carreno, 2003, Parry et al., 2005), combinations of CTLA-4 and PD-1 checkpoint blockade antibodies have been investigated in order to augment anti-tumour efficacy. A combination of ipilimumab and nivolumab has been approved to treat advanced melanoma after a phase III trial reported an almost doubling of overall survival in the combination group compared to ipilimumab alone (Wolchok et al., 2017). This combination has also been approved for the treatment of metastatic colorectal carcinoma with high microsatellite instability or mismatch repair deficiency and for renal cell carcinoma after observations of increased efficacy in response rates and survival (Motzer et al., 2018, Overman et al., 2018). However, this increased anti-tumour

activity is accompanied by a higher toxicity profile and the occurrence of immune related adverse events (Zhou et al., 2019). Additional combinations are being investigated for CPIs including new checkpoint blockade antibodies targeted against lymphocyte-activation gene 3 (LAG-3) and agonistic tumour necrosis factor receptor superfamily member 4 (OX40), vascular targeting drugs and small molecule inhibitors (Ascierto et al., 2017, Infante et al., 2016, Mitchell et al., 2018, Siu et al., 2017, Wallin et al., 2016).

Antibody Name	Target	Disease	Year of approval
Rituximab	CD20	NHL FL DLBCL CLL	1997
Trastuzumab	Her2/ErbB2	Breast carcinoma Metastatic gastric carcinoma GEJ adenocarcinoma	1998
Gemtuzumab ozogamicin (ADC)	CD33	Adult/pediatric AML	2017
Alemtuzumab	CD52	B-cell CLL	2001
Ibritiumomab Tiuxetan (ADC)	CD20	B-cell NHL	2002
Cetuximab	EGFR/Her1/ErbB1	mCRC Advanced/metastatic HNSCC	2004
Bevacizumab	VEGF	mCRC Advanced/metastatic non-squamous NSCLC Metastatic breast carcinoma Glioblastoma mRCC Metastatic cervical carcinoma Ovarian/peritoneal carcinoma	2004
Panitumumab	EGFR/Her1/ErbB1	mCRC	2006
Ofatumumab	CD20	CLL	2009
Ipilimumab	CTLA-4	Melanoma Advanced RCC mCRC	2011
Brentuximab vedotin (ADC)	CD30	HL ALCL $CD30^+$ T-cell lymphoma	2011
Pertuzumab	Her2/ErbB2	Breast carcinoma	2012
Ado-Trastuzumab emtansine (ADC)	Her2/ErbB2	Metastatic breast carcinoma	2013
Denosumab	RANKL	Giant cell tumour of bone	2013
Obinutuzumab	CD20	CLL FL	2013
Ramucirumab	VEGFR2	Advanced gastric carcinoma GEJ adenocarcinoma mNSCLC mCRC	2014

Antibody Name	Target	Disease	Year of approval
Pembrolizumab	PD-1	Advanced melanoma mNSCLC Non-squamous mNSCLC mHNSCC Adult/pediatric HL Advanced/metastatic urothelial carcinoma Advanced/metastatic gastric carcinoma GEJ adenocarcinoma Solid tumours with MSI-H or dMMR Recurrent/metastatic cervical cancer Adult/pediatric PMBCL HCC Adult/pediatric advanced/mMCC	2014
Blinatumomab (BiTE)	CD3 CD19	Adult/pediatric B-cell ALL	2014
Nivolumab	PD-1	Advanced/metastatic melanoma mNSCLC Advanced RCC HL mHNSCC Advanced/metastatic urothelial carcinoma mCRC HCC mSCLC	2014
Dinutuximab	GD2	Pediatric neuroblastoma	2015
Daratumumab	CD38	Multiple myeloma	2015
Necitumumab	EGFR/Her1/ErbB1	mNSCLC	2015
Elotuzumab	SLAMF7	Multiple myeloma	2015
Atezolizumab	PD-L1	Advanced/metastatic urothelial carcinoma mNSCLC Non-squamous mNSCLC Advanced/mTNBC Advanced SCLC	2016
Olaratumab	PDGFRα	Soft tissue sarcoma	2016
Avelumab	PD-L1	Adult/pediatric metastatic MCC Advanced/metastatic urothelial carcinoma	2017
Durvalumab	PD-L1	Advanced/metastatic urothelial carcinoma Unresectable NSCLC	2017
Inotuzumab ozogamicin (ADC)	CD22	B-cell ALL	2017
Moxetumomab pasudotox (ADC)	CD22	HCL	2018
Cemiplimab	PD-1	Advanced/metastatic CSCC	2018

Table 1.1 United States Federal Drug Administration (FDA) approved cancer therapeutic antibodies.
Targets, indicated diseases and year of approval for antibodies. Abbreviations for targets include EGFR: epidermal growth factor receptor, VEGF: vascular endothelial growth factor, CTLA-4: cytotoxic T-lymphocyte associated protein 4, RANKL: receptor activator of nuclear factor kappa-B ligand, VEGFR2: vascular endothelial growth factor receptor 2, PD-1: programmed cell death protein 1, GD2: disialoganglioside, SLAMF7: signalling lymphocytic activation molecule family member 7, PD-L1: programmed cell death ligand 1, and PDGFRα: platelet derived growth factor receptor alpha. Abbreviations for diseases include NHL: non-Hodgkin's lymphoma, FL: follicular lymphoma, DLBCL: diffused large B-cell lymphoma, CLL: chronic lymphocytic leukaemia, GEJ: gastro-esophageal junction, AML: acute myeloid leukaemia, mCRC: metastatic colorectal carcinoma, HNSCC: head and neck squamous cell carcinoma, NSCLC: non-small cell lung carcinoma, mRCC: metastatic renal cell carcinoma, HL: Hodgkin's lymphoma, ALCL: anaplastic large cell lymphoma, MSI-H: high microsatellite instability, dMMR: deficient DNA mismatch repair, PMBCL: primary mediastinal B-cell lymphoma, HCC: hepatocellular carcinoma, mMCC: metastatic Merkel cell carcinoma, ALL: acute lymphoblastic leukaemia, mSCLC: metastatic small cell lung carcinoma, mTNBC: metastatic triple negative breast carcinoma, HCL: hairy cell leukaemia, and CSCC: cutaneous squamous cell carcinoma. Cross-referenced at https://www.accessdata.fda.gov/scripts/cder/daf/, https://www.fda.gov/Drugs/DevelopmentApprovalProcess/DrugInnovation/default.htm; accessed on 3rd May, 2019.

1.1.3 Cancer vaccines and oncolytic viruses

Another area of cancer immunotherapy aims to elicit a systemic anti-tumour response through the principles of vaccination. Theoretically, injection of cancer-specific antigens would recruit the immune system to respond similarly as it would to pathogens, and thus target and destroy the malignant cells. Attempts to achieve this have included vaccination with whole tumour cells, proteins/peptides derived from viruses and cancer neo-antigens, carbohydrates, DNA, mRNA and antigen-loaded dendritic cells. Cytokines, adjuvants and antigen expression on bacterial/viral vectors are often utilised in order to increase the body's response to the antigen. Pre-clinical studies have achieved tumour eradication, but clinical trials have been less successful (Goldman and DeFrancesco, 2009). Cancers caused by viral infection are theoretically more accessible to this platform as they often express foreign antigens that are immunogenic. However, difficulty arises from the need to overcome the mechanisms of central tolerance to self-antigens, a process that deletes or inactivates most self-reactive T cell and B cell clones (Kang et al., 2013, Kumai et al.,

2017). A further important challenge in the cancer vaccine field is presented by the immunosuppressive tumour environment. Approaches to enhance vaccine efficacy by co-targeting the microenvironment have been investigated (Ohshio et al., 2015, Rice et al., 2015). The first major success story in this field is the FDA approval of the prostate cancer vaccine, Provenge. This dendritic cell-based vaccine involves loading autologous dendritic cells with a fusion protein derived from the pro-inflammatory cytokine granulocyte-macrophage colony-stimulating factor (GM-CSF) and the prostate cancer associated protein, Prostatic Acid Phosphatase (PAP). In a phase III clinical trial in metastatic castrate resistant prostate cancer, a modest 4-month increase in median survival was seen for the vaccine compared to the placebo. There was an observed increase in T cell proliferation and antibody titre in the vaccine arm. The toxicity profile was tolerable with high grade adverse reactions occurring in only 6.8% of patients receiving Provenge, most of which resolved within 48 hours after vaccine administration (Kantoff et al., 2010). This pivotal study led to its approval for clinical use in 2010, although its application clinically remains low due to high treatment cost and a moderate therapeutic benefit. Investigations into optimising cancer vaccines as a viable treatment modality are ongoing.

A more recent development in vaccination strategy is the use of oncolytic viruses. This therapy uses viruses that have been attenuated for growth in healthy cells, but preferentially infect and replicate in tumour cells. Studies into underlying therapeutic mechanisms have indicated that anti-tumour activity derives from the inherent cytolytic component of viral replication as well as the recruitment of the immune system targeted towards tumour-derived antigens that become available after cell death (Kaufman et al., 2015). Different viruses that have been investigated for their anti-tumour capabilities include adenoviruses, vaccinia viruses, herpes viruses, Newcastle disease virus, measles

virus, polio virus, coxsackievirus and reovirus (Andtbacka et al., 2015, Au et al., 2011, Breitbach et al., 2013, Dispenzieri et al., 2017, Freeman et al., 2006, Garcia-Carbonero et al., 2017, Kicielinski et al., 2014, Toyoda et al., 2011). Wildtype viruses achieve tumour specific replication as the process of malignant transformation often includes dysregulation in the cell's intrinsic anti-viral pathways. Cellular distress signalling through the protein kinase R (PKR) pathway normally alerts the cell to viral infection and disrupts protein synthesis/viral replication. The aberrant regulation of signalling via this pathway, due to mutated oncogenes encoding Ras and mitogen-activated protein kinase kinase (MEK), is one mechanism by which viruses evade detection and continue to replicate preferentially in cancer cells (Farassati et al., 2001, Smith et al., 2006, Strong et al., 1998). Related to the PKR pathway, type I interferon signalling (a key regulator of viral survival and replication) is often down-regulated in cancer cells allowing for unchecked growth. Oncolytic viruses can also take advantage of this mutated pathway for tumour-specific replication (Pansky et al., 2000, Zhang et al., 2010). Some oncolytic viral strains also enter the cell via receptors that are consistently overexpressed in cancer, including herpes virus entry mediator (HVEM), intercellular adhesion molecule 1 (ICAM-1), CD46, integrin α2β1 or CD155 (Anderson et al., 2004, Montgomery et al., 1996, Shafren et al., 2004, Shafren et al., 2005, Tsang et al., 2017, Zhand et al., 2018). Other viruses have been genetically engineered to preferentially infect cancer cells through modifications in tropism targeting tumour-associated antigens such as human epidermal growth factor 2 (Her2), EGFR and fibroblast growth factor receptor (FGFR) (Petrovic et al., 2018, Uusi-Kerttula et al., 2015). Additionally, viruses can be attenuated in healthy cells and directed to tumour cell-specific replication via mutations in virulence proteins such as E1B and ICP34.5 (Braidwood et al., 2014, Heise et al., 1997). Although oncolytic viruses can directly destroy cancer cells, it is the recruitment of the immune response following cell death that is crucial for sustained anti-tumour efficacy. Greater

efficacy is seen with oncolytic viruses that express cytokines/chemokines to induce and attract a systemic immune response (Bernt et al., 2005, Li et al., 2011). Talimogene laherparepvec (T-VEC), a GM-CSF expressing herpes simplex virus 1 (HSV-1) oncolytic virus with deleted virulence genes ICP34.5 and ICP47, was approved in 2015 for the treatment of metastatic melanoma. Approval was based on a phase III trial in patients with unresectable advanced melanoma. Complete responses were seen in 47% of injected lesions in 277 patients. Evidence of systemic anti-tumour immunity was seen with 22% of un-injected non-visceral and 9% of un-injected visceral lesions disappearing completely. The safety profile was acceptable, with high grade toxicity occurring in only 2.1% of those receiving T-VEC (Andtbacka et al., 2015, Andtbacka et al., 2016). Further investigations into increasing the efficacy of T-VEC are being evaluated and include combination therapy with ipilimumab in advanced melanoma patients. In a phase I study, no dose-limiting toxicities were seen although 26.3% of treated patients experience grade 3-4 adverse events. Fifty percent of patients demonstrated a progression free survival (PFS) of greater than 1.5 years (Puzanov et al., 2016). Additionally, T-VEC in combination with pembrolizumab yielded a 62% overall response rate in melanoma patients. This was accompanied by a greater than 60% PFS extending to 19 months and no dose limiting toxicities in a phase Ib clinical study (Ribas et al., 2017). This combination therapy is being evaluated in comparison to pembrolizumab alone in a phase III/IV clinical trial for melanoma (Ribas et al., 2015).

1.1.4 Adoptive cellular therapy; advances in CAR T cells

The natural ability of T cells to control and target cancer has led to their development as therapeutic agents. Allogeneic haematopoietic stem cell transplantation (aHSCT) for haematopoietic malignancies was the first adoptive cell therapy to be developed. This procedure is undertaken to reconstitute the haematopoietic and immune system of patients

undergoing lympho/myeloablative therapy. A second early example of the use of adoptive T cell immunotherapy entails the use of donor lymphocyte infusion (DLI). This may be performed in the event of relapse following aHSCT and serves to induce a graft-versus-leukaemia effect through donor T cell recognition of allogeneic malignant cells (Bonini and Mondino, 2015, Caldemeyer et al., 2017, Mitani et al., 2019). The discovery of interleukin 2 (IL-2), and its role in T cell expansion, enabled *ex vivo* culture and expansion of T cells for therapeutic use (Mochizuki et al., 1980, Morgan et al., 1976). Early studies compared systemic IL-2 with autologous 'lymphokine activated killer' (LAK) cells in the context of solid tumours. Cells isolated from peripheral blood were expanded *ex vivo* in IL-2 and infused back with co-administered IL-2. While there were objective responses in both treatment arms, there wasn't a significant increase in survival or responses in patients given both LAK cells and IL-2 compared to IL-2 alone. Additionally, IL-2 infusion was associated with high levels of severe toxicity highlighted by a 3.3% treatment related mortality rate (Rosenberg et al., 1993). The observation that tumour infiltrating lymphocytes (TILs) were seen to be at least 50-times more effective in killing cancer cells than LAK cells *in vivo* lead to the development of protocols isolating and *ex vivo* expanding TILs for cancer therapy. When applied to a murine sarcoma and colon cancer model, in conjunction with IL-2 and conditioning chemotherapy, TILs were able to ablate all micrometastases in contrast to LAK cells (Rosenberg et al., 1986). A small single centre trial of TILs, IL-2 and chemotherapy for patients with metastatic melanoma, renal cell, breast and colon carcinoma demonstrated tolerable toxicity. Partial responses were observed in 3/12 patients treated (Topalian et al., 1988). Soon after, a larger study in 20 metastatic melanoma patients reported a 55% objective response rate (Rosenberg et al., 1988). While no TIL therapies have been approved by the FDA for clinical application, the expansion of the endogenous tumour-specific T cell population that can be isolated from patients' tumours has undergone

extensive investigation. Efforts to improve clinical responses have included the use of various conditioning chemotherapy regimens, depletion of Tregs, co-administration of IL-7/15, development of minimal *ex vivo* culture methods and $CD8^+$ T cell enrichment. Lymphodepletion has become standard conditioning therapy prior to adoptive cell therapy after it was shown to increase efficacy of the treatment in melanoma patients (Dudley et al., 2002). Observations have indicated that this is partially due to a depletion of endogenous Tregs and creating a physical niche for the adoptive cells to populate without competition for resources (Antony et al., 2005, Gattinoni et al., 2005). One study in metastatic melanoma patients reported prolonged disease remission which, in some responders, continued beyond 10 years (Feldman et al., 2015, Rosenberg et al., 2011). However, major limitations of this therapy include insufficient/failed TIL expansion and the need for cumbersome manufacturing protocols.

Genetic re-programming of whole T cell populations using T-cell receptors (TCRs) engineered towards tumour-associated antigens has also been explored. Tumour specific TCR clones have been identified through the expansion of TILs and genetically transferred to polyclonal populations, resulting in larger numbers of cancer targeting T cells. Early trials in melanoma led to the identification of TIL TCR clones specific for glycoprotein 100 (gp100) and melanoma antigen recognised by T cells 1 (MART-1) (Kawakami et al., 1994a, Kawakami et al., 1994b). These two proteins were described as cancer-associated antigens that are overexpressed in melanoma, but which are also present in healthy tissue. Because of this, it has been difficult to safely and effectively direct T cells to target only malignant cells (Bonini and Mondino, 2015). Early pre-clinical studies in which a MART-1 targeting TCR was delivered using a retroviral vector into the Jurkat human T-cell leukaemia cell line established the functionality of this approach (Cole et al., 1995). When transduced into human peripheral blood mononuclear

cells (PBMCs), these MART-1 specific clones demonstrated cytolytic activity and increased IFN-γ/GM-CSF secretion upon culture with a melanoma cell line, when compared with non-transduced MART-1 specific T cells (Clay et al., 1999, Hughes et al., 2005). In a murine melanoma model, utilising the B16 cell line that endogenously expresses gp100, adoptive transfer of gp100 directed TCR-engineered T cells demonstrated marked tumour regression (Abad et al., 2008). However, a pilot trial in 15 melanoma patients with MART-1 TCR engineered peripheral blood T cells resulted in low clinical efficacy with only two partial responses. No significant toxicity was reported (Morgan et al., 2006). A different trial utilising a TCR with higher affinity for MART-1 yielded greater clinical efficacy with a 30% partial response rate. This was accompanied by an 18.7% objective response rate with gp100 transgenic TCR T cells. There was also an increase in skin, ear and eye toxicity as these antigens are also expressed in these healthy tissues (Johnson et al., 2009). Continued investigation into TCRs engineered to target MART-1 showed 11/14 objective responses in patients with metastatic melanoma. None of these responses continued beyond 6 months and severe respiratory toxicities occurred in two patients treated at the higher T cell dosages (Chodon et al., 2014). Engineered TCRs have also been clinically investigated that target other antigens such as Wilms' Tumour 1 (WT-1), MAGE-A3, MAGE-A4, NY-ESO-1 and carcinoembryonic antigen (CEA) in patients with an array of carcinomas, sarcomas and haematological cancers (Kageyama et al., 2015, Linette et al., 2013, Lu et al., 2017, Morgan et al., 2013, Parkhurst et al., 2011, Robbins et al., 2011, Tawara et al., 2017). However, severe toxicities have been associated with targeting MAGE-A3. Illustrating this, one group treated melanoma patients with MAGE-A3 specific TCR engineered T cells and observed neurological toxicity in 3/9 patients. Two of these patients subsequently died. It was later discovered that the engineered TCR could cross-react with MAGE-A9/A12. Expression of these family members was discovered in brain tissue by quantitative RT-PCR (Morgan

et al., 2013). A second group found severe toxicity in cardiac tissue resulting in the death of a melanoma and a myeloma patient. It was determined that this was due to off-target recognition of titin, a protein expressed in cardiomyocytes, by the affinity matured engineered MAGE-A3-specific TCR (Linette et al., 2013). Mismatched pairing of endogenous and transgenic αβ TCR chains leading to the potential for novel specificity is also a theoretical concern with TCR gene modification of T cells. In practice this has not, as yet, been shown to cause clinical toxicity. Attempts to mitigate this risk include knocking out the endogenous α and β chains using zinc finger nucleases, interfering RNA and more recently CRISPR/Cas9 technology (Bunse et al., 2014, Knipping et al., 2017, Legut et al., 2018, Provasi et al., 2012).

In an attempt to improve tumour specificity and reduce 'on target, off tumour' toxicity, tumour specific neo-antigens are being studied as potential targets. Effective methods for discovery of personalised neo-antigens expressed solely on cancerous tissue and not in health are being extensively explored (Chheda et al., 2018, Lu et al., 2018, Tubb et al., 2018). Whole exome sequencing of tumours in gastrointestinal carcinoma patients found unique neo-epitopes that were recognized by the patient's TILs. One patient experienced partial tumour regression following two injections of the neo-antigen specific expanded TILs (Tran et al., 2015, Tran et al., 2014). Recently, a breast cancer patient treated with *ex vivo* expanded TILs that were specific for 4 different tumour neo-antigens resulted in a complete response reaching 22 months (Zacharakis et al., 2018).

Major limitations of engineered TCR adoptive cell therapy are the requirement for HLA restriction and the downregulation of co-stimulation in malignancy. In order for transgenic TCR recognition of cognate antigen, processing and presentation of peptide antigens via the human leukocyte antigen (HLA) pathway is required by the cancer cells

along with co-stimulation. However, antigen processing is consistently downregulated in malignant tissue, and dysregulation of trafficking of processed peptides to MHC I for cell surface presentation has been partially attributed to decreased expression of genes encoding for HLA, transporter associated with antigen processing 1 and 2 (TAP-1/2) and low molecular mass protein 2 and 7 (LMP-2/7) (Garrido et al., 1997, Restifo et al., 1993).

Chimeric antigen receptor (CAR) T cells offer a solution to the challenge imposed by HLA restriction, as seen with TCR engineering. Chimeric antigen receptors are artificial fusion receptors that combine the targeting of native cell surface antigens in an antibody-like manner with T cell activation. Engineering of CARs has led to many different formats but, critically, CARs include an antigen recognition portion (most commonly a single chain variable fragment, or scFv, derived from a monoclonal antibody) fused to a transmembrane and intracellular signalling domain. In the simplest 'first generation' form, the signalling domain generally takes the form of the CD3ζ signalling portion of the TCR/ CD3 complex [Figure 1.1]. T cells transduced with a CAR-encoding vector can theoretically target and induce cytolysis against extracellular antigens independent of HLA processing and presentation. Initial studies involved the design of chimeric TCRs in which the variable heavy and light chain domains of phosphorylcholine, digoxin or TNP-specific antibodies were individually fused to the α and β chains of TCRs. These chimeric receptors were successfully expressed in T cells and induced TCR signalling and cytotoxicity against target cells. Mismatched pairing of endogenous and transgenic chains also occurred (Becker et al., 1989, Goverman et al., 1990, Gross et al., 1989, Kuwana et al., 1987). The TNP targeting chimeric receptor was subsequently applied in the context of cancer treatment and reactivity to a TNP-transduced murine lymphoma cell line was observed (Eshhar and Gross, 1990). Non-functional mispairing of CD3 complex chains was avoided by adopting the format of an scFv linked directly to the signalling

CD3ζ or the FcR chain and continued to show MHC-independent targeting of antigen expressing cells (Eshhar et al., 1993, Gross and Eshhar, 1992). Comparison of the CD3ζ and FcεRI-γ signalling domains of a CEA-specific CAR demonstrated the superiority of CD3ζ for T cell activation (Haynes et al., 2001). Application of CAR expressing T cells directed towards tumour associated antigens including different members of the ErbB family, folate binding protein (FBP), CEA and tumour associated glycoprotein 72 (TAG72) indicated antigen specific targeting and lysis *in vitro* and *in vivo* (Altenschmidt et al., 1996, Darcy et al., 1998, Hombach et al., 1997, Hwu et al., 1993, Hwu et al., 1995, Moritz et al., 1994, Stancovski et al., 1993). One study suggested a ligand for the ErbB receptors could be used as the binding portion of a CAR instead of an scFv (Altenschmidt et al., 1996). Early studies also reported the importance of a hinge region between the scFv and the CD3ζ, allowing for antigen accessibility. Commonly, the Fc portion of antibodies or the CD8α hinge/ spacer region is used for this purpose (Abken et al., 1997).

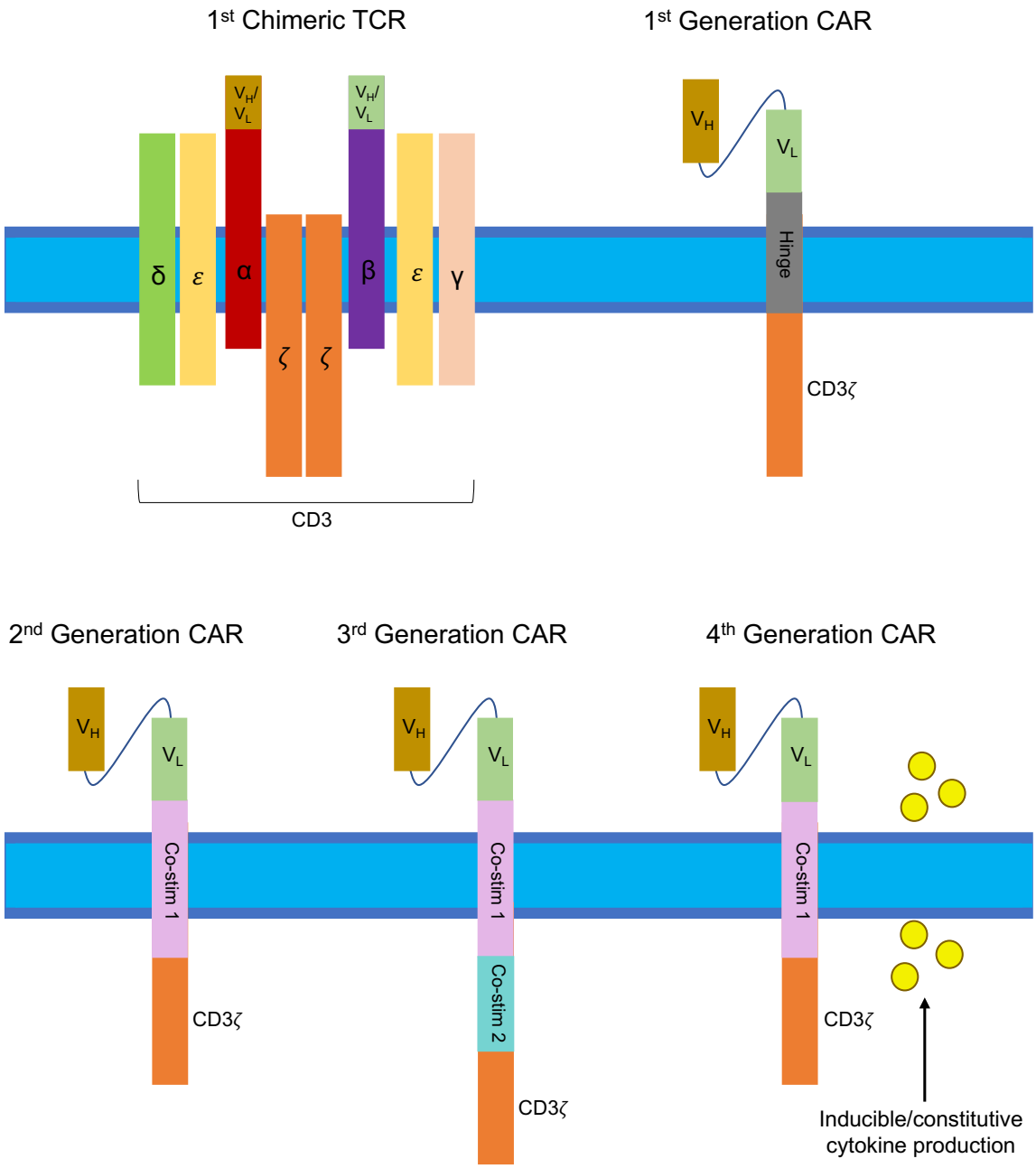

Figure 1.1 Evolution of chimeric antigen receptors (CARs).
Chimeric antigen receptors have been defined by generational distinctions that are illustrated here. TCR: T-cell receptor; V_H: antibody heavy chain variable region; V_L: antibody light chain variable region; Co-stim 1: co-stimulatory region 1; Co-stim 2: co-stimulatory region 2.

Signalling through the scFv-CD3ζ alone was not enough to stimulate the activation of naive primary murine T cells (Brocker and Karjalainen, 1995). The additional delivery of co-stimulation signals to the T cell via the introduction of a second chimeric receptor could increase T cell activation and cytokine secretion after antigen specific CAR engagement (Alvarez-Vallina and Hawkins, 1996). This led to the development of '2nd

generation' CARs that included the intracellular signalling domain of the CD28 co-stimulation molecule in the same construct as the CAR; downstream of the hinge and upstream of CD3ζ. Functionality of this platform was first demonstrated in Jurkat cells using a CD33-targeting CAR and exhibited a marked increase in IL-2 production for the 2nd generation CAR compared to the original CAR (Finney et al., 1998). Validation of 2nd generation CAR technology in primary human T cells was first shown using the prostate-specific membrane antigen (PSMA) CAR that is the subject of this PhD project. In that setting, it was observed that inclusion of the CD28 co-stimulatory domain enabled PSMA-activated human T cells to proliferate and to release IL-2, properties that were not seen with 1st generation CAR T cells. Tumour cell killing was seen at equivalent levels with both 1st and 2nd generation CAR T cells (Maher et al., 2002). This CD28-containing 2nd generation CAR platform is now marketed as axicabtagene ciloleucel (Yescarta), which is one of the two FDA-approved CAR T cell products for the treatment of B cell malignancy.

Investigations have explored the use of different co-stimulatory molecules such as tumour necrosis factor receptor superfamily member 9 (4-1BB), inducible T-cell co-stimulator (ICOS), CD27 and OX40 for increased CAR T cell therapeutic potential (Finney et al., 2004, Imai et al., 2004, Pule et al., 2005, Song et al., 2012). Debate between the superiority of CD28 or 4-1BB as co-stimulatory regions has been ongoing. CD28 appears to produce a more immediate effector response and 4-1BB provides a more persistent population of CAR T cells; both aspects being important for efficacious durable clinical responses (van der Stegen et al., 2015). Studies comparing CAR constructs with different co-stimulatory domains have indicated that CD28 containing CARs show increased proliferation, greater cytotoxic effect *in vitro* and secrete enhanced levels of cytokine, while CARs incorporating 4-1BB have a slower initial response, but persist longer *in vivo*

and express less exhaustion markers as a result of tonic CAR signalling (Finney et al., 2004, Guedan et al., 2014, Long et al., 2015, Milone et al., 2009). This increased persistence leads to improved tumour control in murine models. Clinical trials for CD19 directed CARs have indicated that incorporation of 4-1BB into the construct increases the longevity of the T cells in patients (Lee et al., 2015, Maude et al., 2014, Maude et al., 2016). Investigations into the mechanisms behind the differences in CAR co-stimulation have illuminated diverging metabolic pathways associated with CD28 and 4-1BB. One study illustrated the increased proliferative capacity, survival and central memory phenotype of 4-1BB CARs compared to CD28 CARs targeting CD19 and mesothelin. Chimeric antigen receptor T cells with CD28 co-stimulatory domains produced a more effector memory phenotype. Metabolically, 4-1BB CARs yielded higher fatty acid oxidation (FAO), spare respiratory capacity (SRC) and mitochondrial mass which is characteristic of long-term memory cells. Comparatively, CD28 CARs exhibit an increased rate of glycolysis, which has been associated with effector T cells (Kawalekar et al., 2016). Another study showed an increase in memory-associated gene expression in 4-1BB CARs and a more effector cell gene signature in CD28 CARs. Chimeric antigen receptors incorporating CD28 also had a higher signalling intensity in terms of the number of phosphorylated proteins and it was determined that this was due to tonic signalling through Lck association (Salter et al., 2018).

There is some evidence for a benefit of 3rd generation CARs combining CD28 and 4-1BB. Enhanced anti-tumour cytotoxicity through 4-1BB and CD28 combination in CAR constructs has been reported for T cells redirected towards prostate cancer and lymphoma in pre-clinical models. These studies show an increased persistence, greater tumour control and increased expression of the anti-apoptotic marker Bcl-X_L for 3rd generation CARs compared to 2nd generation CARs (Tammana et al., 2010, Zhong et al., 2010).

However, a mesothelioma mouse model showed similar anti-tumour capabilities between 2nd and 3rd generation CAR constructs utilising 4-1BB and CD28 co-stimulatory domains (Carpenito et al., 2009). A CD19-specific CAR in a NALM6 leukaemia model compared CD28 and 4-1BB containing 3rd generation CARs with a CD28 2nd generation CAR that constitutively expresses 4-1BBL and addition of 4-1BBL expression in the CD19-specific CD28ζ generation CAR resulted in increased tumour regression, CAR T cell persistence and survival compared to the 3rd generation CAR (Zhao et al., 2015). This indicates insufficient signalling of the 4-1BB domain in the 3rd generation constructs. Inclusion of both CD28 and 4-1BB co-stimulation in a CD19 CAR showed a 23-fold greater expansion and longevity in lymphoma patients than the 2nd generation CAR with CD28 alone (Gomes da Silva et al., 2016). Further safety analysis of the 3rd generation CARs in lymphoma indicate tolerability and 6/15 complete responses (Enblad et al., 2018). Application of this approach in pre-clinical solid tumour models has been inconclusive.

Co-stimulation regions including CD28, 4-1BB, OX40 and ICOS have been arranged variably into 3rd generation CARs targeting antigens such as prostate stem cell antigen (PSCA), mesothelin, prostate specific membrane antigen (PSMA) and GD2. Reports have suggested enhanced persistence of CAR T cells *in vivo* with or without an accompaniment of greater tumour control compared to 2nd generation CARs (Carpenito et al., 2009, Guedan et al., 2018, Hillerdal et al., 2014, Quintarelli et al., 2018, Zhong et al., 2010). A 3rd generation CAR-specific for GD2 is currently being investigated in neuroblastoma patients. Data published to date demonstrates no dose limiting toxicity, but the best response has only been stabilisation of disease. The addition of anti-PD-1 blockade did not enhance efficacy (Heczey et al., 2017). In contrast, one group found that a 3rd generation CEA-targeting CAR, incorporating CD28 and OX40 co-stimulation domains, led to increased activation-induced cell death and worse function *in vivo* than the CD28

2nd generation CAR (Hombach et al., 2013). This illustrates the variable outcomes of different CAR construct designs and the need for optimisation.

There has been significant clinical success with CAR modified T cells for haematological malignancies. Two different CD19-targeting 2nd generation CAR T cell products, Tisagenlecleucel-T and Axicabtagene ciloleucel, have been approved for B-ALL and diffuse large B-cell lymphoma (DLBCL) (Maude et al., 2018, Neelapu et al., 2017). These are the first ever genetically modified cells licensed for cancer therapy. Tisagenlecleucel-T was first reported as a case study in two patients with paediatric ALL. One patient showed elevated liver enzymes aspartate aminotransferase (AST) and alanine aminotransferase (ALT) indicating toxicity and the other patient experienced cytokine release syndrome (CRS), a toxicity associated with activation of immune cells and subsequent secretion of inflammatory cytokines manifesting by fever, headache, fatigue, malaise, myalgia, nausea, hypotension, hypoxia, tachycardia and organ toxicity. The patient entered into complete remission one month after treatment. One of the patients relapsed within two months. The relapsing leukaemia was found to have lost expression of the CAR target CD19 (Grupp et al., 2013). The trial was continued and 30 patients received CAR therapy. Ninety percent achieved complete response initially with 19 remaining in remission at 6 months. High grade CRS was seen in all patients. A correlation was observed between CRS and disease burden. This was effectively treated with tocilizumab, an anti-IL-6R monoclonal antibody (Maude et al., 2014). Cytokine release syndrome is a common adverse event in CAR T cell therapy. A grading and management guide was recently published to address CRS scoring/treatment in the clinic and trials (Lee et al., 2019). High grade CRS is treated with vasopressors, oxygen and anti-cytokine interventions including tocilizumab, etanercept (TNFα recombinant receptor), infliximab (anti-TNFα) and anakinra (IL-1R antagonist) (Lee et al., 2014). In

some cases, corticosteroids may be used although there are concerns that this may compromise therapeutic benefit. A larger study reported a 93% complete remission rate and a 55% relapse-free survival at 12 months, reaffirming the CD19-CAR T cell efficacy in B-ALL (Maude et al., 2016). However, in a cohort of 27 adult patients, 3 patients died due to refractory CRS. No additional fatal toxicities were seen when the CAR T cell dose was separated across different injection time points (Frey et al., 2016). A trial in DLBCL demonstrated an overall response rate of 59%. Chimeric antigen receptor T cells were detected in responders almost 1 year after treatment (Schuster et al., 2017). These trials led to regulatory approvals in paediatric and young adult B-ALL and DLBCL. This CAR has also been evaluated in chronic lymphocytic leukaemia (CLL) patients with a 57% response rate, but has not yet achieved clinical approval (Porter et al., 2015).

While Tisagenlecleucel-T incorporates a 4-1BB co-stimulation domain, the Axicabtagene ciloleucel CAR construct utilises CD28. Similar to Tisagenlecleucel-T, this CAR was first reported in a case study involving treatment of a single patient with relapsed follicular lymphoma (FL). The patient demonstrated a partial response durable for 32 weeks (Kochenderfer et al., 2010). When the trial was expanded to 8 patients with FL or CLL, 6 experienced objective responses (Kochenderfer et al., 2012). A large trial in DLBCL demonstrated efficacy with an 82% response rate and an 80% survival rate at 6 months. There were 3 deaths from adverse events in this study (Locke et al., 2017). The amounting evidence of clinical efficacy for the CAR in B-cell lymphomas led to its FDA approval for treatment of DLBCL. Although it is not yet approved for this disease, studies have explored its anti-leukemic capabilities in a dose escalation for ALL patients achieving a 66.7% complete response rate and 6/21 patients experiencing high grade reversible CRS (Lee et al., 2015). A caveat of the CD19-targeting CARs appears to be a high rate of toxicity. However, there is also a high relapse rate partially due to insufficient

CAR T cell persistence. Methods to improve the therapeutic window of these CARs in the clinic have explored dual targeting to avoid antigen escape, decreasing T cell exhaustion and improving persistence through co-treatment with a Bruton tyrosine kinase (BTK) inhibitor, which has shown to decrease T cell PD-1 expression and increase *ex vivo* CAR T cell expansion (Fraietta et al., 2016, Ruella et al., 2016). Patient stratification is also being investigated to predict serious adverse reactions (Teachey et al., 2016).

Solid tumour CAR T cell therapy has demonstrated less success to date. Similar to engineered TCRs, selection of an appropriate target antigen has proven difficult. Tumour-associated antigens are often expressed on healthy tissue as well and cases of normal tissue destruction by CAR T cells have highlighted this obstacle. One patient died after treatment with Her2-targeting CAR T cells due to low antigen expression in lung tissue (Morgan et al., 2010). Treatment was halted in another trial using carbonic anhydrase 9 (CAIX)-specific CAR T cells because of high grade liver toxicity seen in half of the patients caused by unexpected on-target-off-tumour destruction of bile duct tissue (Lamers et al., 2013). The CD19-specific CARs also target normal pre-B cells leading to B cell aplasia. This toxicity however is manageable with regular antibody replacement with IVIG (Doan and Pulsipher, 2018). Demonstrated challenges to successful solid tumour CAR T cell therapy include poor tumour trafficking and penetration, as well as an inability for CAR T cells to proliferate and function in immunosuppressive tumour microenvironments. Methods to improve these deficiencies have explored CAR T cell expression of chemokines/chemokine receptors, pro-inflammatory cytokines and targeting the vascular network (Adachi et al., 2018, Bocca et al., 2017, Craddock et al., 2010, Yeku et al., 2017b). Alternatively, intratumoural delivery may be employed in some selected indications (Tchou et al., 2017). Improving efficacy is covered in more detail later [section 1.3]. Insufficient persistence of CAR T cells has also been reported

in some of the CD19 CAR trials (Knochelmann et al., 2018). Many CAR T cell therapies have undergone or are currently in clinical trial for solid cancers. Therapies targeting solid tumours have not progressed past phase I clinical trials and many of the preliminary reports have indicated low efficacy and persistence (Yeku et al., 2017a). A GD2-targeting CARs expressed in EBV-specific T cells were administered to 19 neuroblastoma patients and 3/11 with active disease had complete responses. No dose limiting toxicities occurred (Louis et al., 2011). Recently an abstract at American Society of Clinical Oncology (ASCO) annual meeting reported a phase I trial for the intrapleural treatment of 20 patients with mesothelin-specific CAR T cells. No CAR T cell related toxicities above grade 1 were observed and 14 received subsequent anti-PD-1 monoclonal antibodies. Among the anti-PD-1 co-treated patients, this resulted in 2 patients with durable complete responses extending to 62 and 39 weeks (ongoing), 5 with partial responses and 4 patients with stable disease (Adusumilli et al., 2019). Continued investigations into CAR T cell immunotherapy for solid tumours seeks to overcome these limitations in efficacy and illustrate the viability of this treatment modality in non-haematological malignancies.

1.2 Prostate Cancer

1.2.1 Prevalence

Prostate cancer is the most common malignancy in men in the UK and Europe and is second only to lung carcinoma worldwide. While the incidence rate is high, with over 47,000 new cases in the UK each year, the prognosis of this disease is generally good compared to other cancers with an 84% 10-year survival in men diagnosed with any stage prostate cancer (www.cancerresearchuk.org/health-professional/cancer-statistics/statistics-by-cancer-type/prostate-cancer, viewed 3 May 2019). Further dissection of this statistic shows that the survival for late stage metastatic prostate cancer differs drastically from early stage disease. The 5-year survival rate of stage I-III prostate

cancer patients is over 90% in the UK and United States. The 5-year survival rate drops to 29-34% for men of any age diagnosed with stage IV metastatic prostate cancer (Howlader et al., 2019) (www.cancerresearchuk.org/health-professional/cancer-statistics/statistics-by-cancer-type/prostate-cancer, viewed 3 May 2019). This illustrates an unmet need for improved treatments in advanced stage prostate cancer.

1.2.2 Prostate cancer development

Prostate adenocarcinoma is the most common form of prostate cancer and arises from the glandular epithelium of this male organ. This pathology is associated with an older population as the median age at diagnosis is 67. The incidence of prostate cancer increases with age. Factors that have been identified as contributors to the development of disease are family history (a close family member's diagnosis at least doubles an individual's risk), a high-fat diet and aberrant hormone levels (Grozescu and Popa, 2017).

Prostate cancer progression is defined in stages using the tumour, lymph node and metastasis (TNM) I-IV staging system. Progression occurs by spreading to surrounding tissue, draining lymph nodes and ultimately metastasise to distant sites in late stage disease, most commonly bone tissue. The Gleason scoring system is a prostate cancer specific diagnostic that indicates how aggressive the cancer from a histopathological perspective. The technique was developed in 1966 and involves haematoxylin and eosin (H&E) staining and morphological analysis of prostate needle biopsies. The calculated grade is based on cell differentiation and can predict how quickly the cancer will progress. This score is presented on a scale of 1-5 and encompasses a score of the two largest areas, meaning that the highest possible score is 10. The Gleason index is still universally used for prognostic assignment and treatment decisions in prostate cancer (Epstein et al., 2016, Gleason, 1966).

The prostate is made up of glandular tissue and is involved in the production and secretion of seminal fluid. This process is driven by androgen hormones like testosterone. Mutational disruption of the androgen pathway is often involved in malignancy and has become the target of therapies. This pathway is critical for healthy prostate development, but overexpression/activation of the androgen receptor in disease correlates with progression, drug resistance and increased cell growth (Schrecengost and Knudsen, 2013). The androgen receptor is a transcription factor responsible for the translation of genes associated with proliferation and resistance to apoptosis. The crucial role of the androgen receptor in the pathogenesis of prostate cancer has made androgen signalling a key focus of therapeutic intervention. As early as the 1940's, physicians observed a regression in prostate cancer when androgen deprivation was initiated through surgical castration (Huggins, 1967, Huggins and Hodges, 1941). However, while this treatment is often effective at the start, cancer will progress to a castrate-resistant phenotype. Exploration into the mechanisms underlying this drug resistance have identified additional mutations in the androgen signalling pathway, allowing evasion of therapy. It is believed that signalling through the androgen receptor (AR) is achieved via higher expression of the receptor, mutations allowing for non-specific ligand binding, and/or cell survival/proliferation signalling independent of AR-ligand interactions altogether (Arora et al., 2013, Culig et al., 1994, Koivisto et al., 1997, Veldscholte et al., 1990). Progression to castrate-resistant prostate cancer (CRPC) is associated with poor prognosis and a median overall survival of between 14 and 26 months (Halabi et al., 2014, James et al., 2016a).

1.2.3 Current treatment options

There are a number of treatments available for prostate cancer patients depending on disease stage and prognosis. Population data shows that 65-80% of men diagnosed with

prostate cancer in the UK or United States present with localised disease (Li et al., 2018, National Collaborating Centre for Cancer (UK)). These early stage diagnoses are often indolent and slow-growing. Therefore, a common management option for low risk patients is active surveillance. This avoids unnecessary complications of active treatment such as incontinence and impotence. Studies have shown that there is no significant increase in prostate cancer associated mortality for patients between 5-10 years with localised malignancy that undergo active surveillance compared to definitive therapy. However, 27-53% converted to require active therapy within the evaluation period (Hamdy et al., 2016, Klotz et al., 2015). Active surveillance generally includes frequent digital rectal exams (DREs), prostate specific antigen (PSA) testing, magnetic resonance imaging (MRI) scans and biopsies. Higher-risk early stage patients, or those that have experienced tumour progression during active surveillance, are candidates for external beam radiation/brachytherapy, or prostatectomy. External beam radiotherapy is generally a well-tolerated outpatient procedure. There are long term complications such as rectal toxicity, incontinence and impotence associated with treatment (Pickles et al., 2010). The implantation of radiation-emitting seeds into the prostate (brachytherapy) requires short term hospitalisation, which is often a deterrent. The brachytherapy approach has the benefit of limiting radiation exposure to surrounding healthy tissue with resultant reduction in complications of therapy (Cesaretti et al., 2007, Keyes et al., 2009). Prostatectomy is a more invasive procedure. Surgery is associated with a greater risk than radiotherapy of long term side effects including incontinence and erectile dysfunction (Alemozaffar et al., 2011, Mettlin et al., 1997).

Locally advanced prostate cancer refers to tumours that begin to invade the surrounding tissue and have a high risk of progressing. Treatment options available include the definitive treatments described above in addition to hormone therapy. Current best

practice for this stage of disease is still undetermined, but usually involves a combination approach. Radical prostatectomy is generally less utilised due to its invasive nature, high rate of side effects and the difficulty of obtaining negative resection margins. However, there is evidence that surgical removal of the prostate increases the overall survival outcomes of patients (Engel et al., 2010, Heidenreich et al., 2011). The standard treatment for locally advanced prostate cancer is radiotherapy plus hormone therapy. Clinical studies have shown a significant increase in progression-free survival and overall survival in patients receiving combination therapy versus monotherapy (Fahmy et al., 2017, Fossa et al., 2016).

As previously stated, metastatic prostate cancer is associated with poor long-term survival. First line treatment for advanced disease is life-long hormone therapy, which is usually effective for a few years before escape of a hormone resistant phenotype. This therapy includes surgical (removal of the testes) or chemical (luteinizing hormone releasing hormone agonists and antagonists) androgen deprivation, thereby removing the proliferative signals delivered by androgen hormones when they interact with the AR on prostate cancer cells (Nevedomskaya et al., 2018). Androgen deprivation therapy is now generally administered in conjunction with the chemotherapeutic agent docetaxel. This approach has been substantiated by a large clinical trial which showed improved survival for patients who received this combination therapy (James et al., 2016b). When progression to a metastatic CRPC (mCRPC) disease state occurs, alternative drugs are available such as Sipuleucel-T (not widely utilised), the chemotherapy agent cabazitaxel, radium-223 for bone metastases (common in this disease), and the androgen synthesis inhibitor, abiraterone acetate or androgen receptor blocker, enzalutamide. Because AR mutations cause a refractory cancer type, stronger blockade of this pathway is required. Mutations that increase the expression of AR and therefore the sensitivity to androgen

hormones could benefit from abiraterone acetate that blocks androgen production in the testes, tumour and adrenal glands (Barrie et al., 1997, Potter et al., 1995). Additionally, targeting the AR pathway directly with enzalutamide can circumvent mutations that enable ligand independent signalling (Tran et al., 2009). Both of these second line anti-androgen therapeutics have demonstrated improved overall survival compared to standard of care in advanced disease (Dreicer et al., 2014, Scher et al., 2012). Treatment of mCRPC improves duration of overall survival, but ultimately the median survival of these patients is approximately 2 years (Francini et al., 2019).

1.2.4 CAR T cell immunotherapy for prostate cancer

Immunotherapy for mCRPC has not achieved clinical success to date. Because of the heterogeneity of the disease there is motivation for improved clinical trial design to optimally target patients that might have a higher response to immunotherapy. The dendritic vaccine Sipuleucel-T is still the only approved immunotherapeutic for use in mCRPC, but production is expensive and survival benefit modest. Overall survival improvement was 31.7% for patients at 3-years compared to 23% for the placebo group (Kantoff et al., 2010). Prostate cancer has been identified as a good candidate for targeted immunotherapy due to tumour-associated markers commonly expressed in the tissue. However, the microenvironment has been described as immunosuppressive and needs to be addressed for effective immunotherapeutic intervention (Pasero et al., 2016, Sfanos et al., 2008, Zhang et al., 2011b). Investigation of ipilimumab therapy in mCRPC showed no improved overall survival and 9 treatment related deaths out of 399 ipilimumab treated patients. An increase in progression free survival was reported (Beer et al., 2017). These shortcomings illustrate a need for novel immunotherapeutic approaches to mCRPC.

Chimeric antigen receptors have been developed to target prostate cancer through recognition of PSMA, prostate stem cell antigen (PSCA), mucin-1 (MUC-1), Her2 and epithelial cell adhesion molecule (EpCAM) (Deng et al., 2015, Ma et al., 2014, Maher et al., 2002, Morgenroth et al., 2007, Pinthus et al., 2003, Sanchez et al., 2013). The primary targets for CARs directed against prostate cancer are PSMA and PSCA, which are commonly overexpressed in prostate neoplasms. Prostate specific membrane antigen expression correlates with disease stage and is found on the vasculature of most solid tumours, making it a versatile target (Bostwick et al., 1998, Chang et al., 1999a). Every completed clinical trial for CAR T cell treatment of mCRPC to date has utilised PSMA-targeting constructs. Results from one trial indicated tolerable toxicity of the CAR T cells with significant adverse reactions being attributed to the conditioning chemotherapy rather than the CAR activation and cytokine release syndrome (CRS). While not the primary objective of the study, two partial responses in PSA levels were seen in the five patients treated (Junghans et al., 2016). Another phase I trial, using the same CAR construct presented in the current project, indicated that patients could be safely treated with up to 30 million CAR^+ T cells/kg with reports of manageable pyrexia and increased levels of circulating cytokines. Out of seven patients treated, two displayed stable disease for over 6 months and CAR T cells persisted in patients for 2 weeks (Slovin et al., 2013). A phase I trial has been designed to evaluate a PSMA-targeting CAR co-expressing a dominant-negative TGF-β receptor providing resistance to TGF-β signalling (Narayan et al., 2019). Three phase I trials are planned to assess the safety of PSCA- and EpCAM-targeting CAR T cells in metastatic prostate cancer (clinicaltrials.gov NCT03873805, NCT02744287 and NCT03013712, viewed on 3 May 2019). So far, CAR T cell trial results suggest acceptable safety without clinically meaningful efficacy in prostate patients. This highlights the need to improve efficacy for PSMA targeting of solid tumours with CAR T cells.

1.3 Methods from improving CAR T cell therapy in solid tumours

1.3.1 Improving specificity and safety

Because antigens targeted by immunotherapy are often not entirely restricted to tumour tissue, efforts have been made to increase the specificity and safety of adoptive T cell therapy. One approach involves the inclusion of 'suicide genes' in the CAR expression constructs. These genes are expressed alongside the CAR in the construct and permit inducible cell death in case of severe toxicities. One such suicide gene is inducible Caspase 9 (iCas9), a fusion protein of the human caspase 9 and FK506 binding protein (FKBP). The FKBP region binds to the dimerising drug AP1903 and causes a signalling cascade within the transduced cell that results in rapid apoptosis of 99% of the engineered population (Straathof et al., 2005). This system is well described for control of adoptive cellular therapy. In a clinical trial, patients' graft-versus-host disease (GvHD) was reversed within 24-hours of AP1903 administration and >90% of the transgenic cells were ablated (Di Stasi et al., 2011, Iuliucci et al., 2001). The iCas9 suicide system has been applied to CAR T cell therapy as a means to treat uncontrollable toxicity due to T cell activation. Inducible elimination of transduced cells *in vivo* has been demonstrated (Hoyos et al., 2010). Additional suicide genes that have been included with CAR constructs for adoptive cell therapy are the herpes simplex virus thymidine kinase (HSV-tk) and an inert/truncated version of EGFR (tEGFR). Elimination of transduced cells expressing HSV-tk is achieved by administration of the anti-viral agent, ganciclovir, and this has been shown to be effective in patients who developed GvHD following donor leukocyte infusion (Bonini et al., 1997). The tEGFR suicide system is activated through complement-dependent cytotoxicity (CDC)/antibody-dependent cellular cytotoxicity (ADCC) which may be induced using anti-EGFR antibodies like cetuximab. Pre-clinical studies demonstrate that this system can be used to effectively target and kill CD19 CAR T cells expressing this gene (Kao et al., 2019). These approaches afford some degree of

therapeutic control for clinicians at the onset of severe T cell mediated toxicity. It is hypothesised that the use of suicide systems may also avoid the development of fatal toxicities as seen in earlier trials (Lamers et al., 2013, Morgan et al., 2010). Suicide genes are currently in use in a number of CAR T cell clinical trials (Adusumilli et al., 2019, Brown et al., 2015). Limitations of suicide systems include the loss of all therapeutic adoptive cells upon activation of the suicide gene and immunogenicity, particularly with viral proteins such as HSV-tk.

Inducible activation of CARs has also been developed to improve the safety of this therapy. The strategy employs 'switches' in order to activate and de-active the CAR, allowing for control of possible acute toxicities without eliminating the CAR T cells and curtailing potential future therapeutic effects. The concept of a universal CAR (UniCAR) renders activation a two-step process in which a CAR that recognises non-tumour associated structures is inactive until the administration of a CAR-specific targeting molecule. This targeting molecule is either an antibody specific for a tumour-associated antigen or a fusion of a CAR-recognising protein and an antibody fragment specific for the tumour. This type of CAR has been developed to bind molecules such as biotin, antibodies/fragments, fluorescein, peptide neoepitopes or the human nuclear protein La/SS-B. The targeting molecules then recognise tumour markers including CD19, CD20, CD33, CD123, mesothelin, EpCAM, folate receptor (FR), EGFR, Her2, PSCA and PSMA (Cartellieri et al., 2016, Feldmann et al., 2017, Koristka et al., 2014, Raj et al., 2019, Rodgers et al., 2016, Tamada et al., 2012, Urbanska et al., 2012). This platform has shown efficacy in a number of xenograft models. Efficacy can be titrated such that the level of anti-tumour response can be controlled by the quantity of target molecule injected (Feldmann et al., 2017). This can also combat disease recurrence after antigen loss by adjusting the specificity of the targeting molecule, avoiding laborious and expensive

additional production of a different CAR vector or T cell population. Using a murine $CD19^+$ B-cell lymphoma model, one study demonstrated that the ability to give the CAR T cell intermittent breaks from activation using a CD19-specific targeting molecule resulted in increased expansion of CAR T cells, adoption of a higher effector memory phenotype and longer persistence of central memory CAR T cells (Viaud et al., 2018). Controllable activation has also been achieved using a CD19-specific CAR design to express the intracellular co-stimulation and CD3ζ signalling regions separately. These regions are induced to dimerise on exposure to a mutant rapamycin (rapalog), activating the signalling cascade upon drug administration (Wu et al., 2015).

Other attempts to improve tumour specificity and reduce on-target-off-tumour effects have involved dual targeting CAR constructs. Transduced T cells express two chimeric receptors, one encompassing CD3ζ (CAR) and one encompassing the co-stimulation signal (CCR), that each target unique tumour-associated antigens with engagement of both necessary to fully activate anti-tumour cytotoxicity (Kloss et al., 2013). This increases the tumour specificity of the CAR T cells by requiring the tumour cells to express multiple markers and reduces the chance of toxicity to healthy tissues. In a model targeting mesothelin (CAR) and FR (CCR), dual targeting T cells showed similar cytotoxicity *in vitro* and *in vivo* as a 2nd generation CAR when the malignancy expressed both antigens and diminished effects similar to a 1st generation CAR when the cell only expressed one of the antigens. More importantly, healthy tissue that only expressed mesothelin was spared (Lanitis et al., 2013). Illustrating the variability between CAR constructs, another group targeting ErbB2 (CAR) and MUC-1 (CCR) in the same manner found that the dual targeting CAR produced less cytokine *in vitro* compared to the 2nd generation equivalent CAR. Elimination of cells expressing ErbB2 alone was similar to dual expressing cells, indicating no increase in tumour specificity. Proliferation, however,

was increased when the dual targeting CAR T cells were co-cultured with dual expressing cell lines specifically (Wilkie et al., 2012). Combination of a CAR with suboptimal tumour killing and a CCR incorporating both a CD28 and 4-1BB co-stimulation sites resulted in enhanced tumour specificity. Targeting PSCA with the CAR and PSMA with the CCR led to tumour regression *in vivo* of cells expressing both antigens only. This study also warns that the antigen with less tumour restriction should only be targeted using the CCR to lower the risk of off-tumour toxicity (Kloss et al., 2013). With the use of dual targeting, fully functional 2nd generation CARs, antigen escape can be tempered through destruction of the cancer cells based on two tumour-associated antigens (Lee et al., 2018).

Apart from controllable activation, inducible CAR expression has also been described in the context of dual targeting. A synthetic Notch receptor developed to target a specific antigen cleaves an intracellular transcription factor that explicitly promotes expression of a CAR gene with specificity for a different antigen. SynNotch receptors illustrate another method of increasing tumour specific lysis and reducing cell death in healthy tissue (Roybal et al., 2016).

The use of dual targeting receptors has also incorporated an inhibitory function to increase CAR T cell safety. By targeting less restrictive tumour antigens with a CAR and a healthy tissue marker with an inhibitory CAR (iCAR), CAR signalling/T cell activation can be interrupted upon dual receptor binding on healthy tissue and remain active on tumour tissue. This was demonstrated using CD19-specific CAR T cells co-expressing a PSMA-specific iCAR utilising either the PD-1 or CTLA-4 signalling domains. This dual targeting approach achieved complete CD19^{+} tumour cell destruction and abrogation of cytotoxic activity on cells that expressed both CD19 and PSMA. Control of T cell

activation by the iCAR was superior with a PD-1 signalling domain compared to CTLA-4 (Fedorov et al., 2013). Ultimately, clinical trials will define the role of these safety approaches.

1.3.2 Improving efficacy

While safer CAR T cell application has been discussed, one of the more confining obstacles for CAR therapy is a lack of efficacy against solid tumours. Attempts to improve efficacy have focused on persistence, cytotoxicity, trafficking and overcoming suppressive factors. Fourth generation 'Armoured' CARs or T-cell redirected universal cytokine killing ('TRUCKs') utilise co-expression of cytokines/chemokines/receptors alongside the CAR. Previously described TRUCKs deliver a payload to the tumour site and not only further stimulate CAR T cell anti-tumour performance, but potentially recruit and encourage surrounding TILs to also attack the malignant tissue (Yeku et al., 2017b). This could be helpful in avoiding recurrence of disease due to antigen escape by inducing a polyclonal anti-tumour response. Interleukin-12 is a relevant cytokine of choice for its potent ability to promote expansion and cytotoxicity of NK cells and T cells and IFN-γ production (Smyth et al., 2000a, Zhao et al., 2012). Initial reports of inducible IL-12 under the control of a nuclear factor of activated T cells (NFAT) promoter in TCR and CAR engineered T cells demonstrated enhanced tumour growth control and an influx of activated macrophages (Chmielewski et al., 2011, Zhang et al., 2011a). In the CAR study, macrophages activated by the inducible IL-12 were able to kill an antigen negative cell line demonstrating potential epitope spreading and the scope to control a solid tumour consisting of diverse cell populations (Chmielewski et al., 2011). However, administration of the IL-12 inducible engineered TCR T cells to metastatic melanoma patients resulted in increased circulating IL-12 levels, accompanied by limited responses and severe liver and haematopoietic toxicity (Zhang et al., 2015). Construct designs for

solid tumour treatment have extended to include constitutive or inducible production of cytokines, including IL-15 and IL-18, to enhance the efficacy and persistence of the CAR T cells. Interleukin-15 supports differentiation of $CD8^+$ memory T cells and recruits leukocytes, while IL-18 activates T cells/NK cells and enhances IFN- γ production (Lodolce et al., 1998, Mortier et al., 2009, Okamura et al., 1995). In CEA^+ pancreatic and lung tumours *in vivo*, CARs co-expressing IL-18, but not the CARs alone, ablated xenografts and skewed the tumour microenvironment towards a pro-inflammatory state (Chmielewski and Abken, 2017). Interleukin-15 promoted increased CAR mediated anti-tumour activity against glioma murine models compared to the CAR alone. However, tumours escaped with antigen negative/low disease (Krenciute et al., 2017). Co-stimulatory ligands such as CD40L or 4-1BBL co-expressed in CAR transduced T cells further stimulate activation and cytotoxicity (Curran et al., 2015, Zhao et al., 2015). Cytokines in addition to IL-2 have also been co-administered with CAR T cells (Dwyer et al., 2019).

Co-expression of receptors to further enable CAR T cell persistence and trafficking have been developed. Investigations indicate that traditionally immunosuppressive signals can be translated into T cell stimulatory signals. One such study evaluated a dominant negative transforming growth factor-β receptor (TGF-βR) that is preferentially expressed in a CAR T cell system targeting $PSMA^+$ prostate cancer. By sequestering TGF-β from signalling through its endogenous receptor, CAR T cells exhibited greater persistence in a generally immunosuppressive tumour microenvironment (Kloss et al., 2018). This conversion of signals has also been shown using IL-4 chimeric receptors that induce an IL-2/15 or IL-7 intracellular signal upon ligand binding (Mohammed et al., 2017, Wilkie et al., 2010). These IL-4 chimeric receptors are further described in chapter 3. Chemokines and their receptors co-expressed with CARs can enhance CAR T cell

trafficking to the tumour. Investigations show that CAR T cell co-expression of chemokine receptors CCR2b and CCR4 enable the cells to home to tumours that naturally express their respective ligands CCL2 and CCL22 (Craddock et al., 2010, Rapp et al., 2016). Expression of chemokines themselves in CAR T cells such as CCL19 and the IL-7 cytokine resulted in higher leukocyte and antigen-presenting cell infiltration and increased tumour clearance (Adachi et al., 2018). One study modified the tumour to express the chemokine CXCL11 using an oncolytic virus and preferentially increased CAR T cell presence in the tumour in comparison to the CAR T cells co-expressing CXCL11 (Moon et al., 2018).

A limitation of CAR T cell therapy is the inability to recognise intracellular peptides, which make up the majority of tumour-associated antigens. T-cell receptor-like CARs have been developed using the same structure as 2nd generation CARs, but incorporating an scFv that recognises MHC-bound peptide. Potent killing was demonstrated when directed towards intracellular targets including gp100 and MART-1 in melanoma models (Walseng et al., 2017, Zhang et al., 2014).

Signalling through CAR engagement with antigen differs from physiological TCR/CD3 complex signalling on engagement of antigen-MHC. Endogenous TCRs are more sensitive than CARs with the same specificity and affinity and produce more cytokines in response to lower levels of antigen stimulation (Harris et al., 2018). It is believed that this is due to inherent differences in the structure between CARs and TCRs. The endogenous TCR signalling machinery includes more domains with a total of 10 immunoreceptor tyrosine-based activation motifs (ITAMs), whereas CARs usually only contain the CD3ζ domain with 3 ITAMs in each CAR monomer. Increasing the number of ITAMs in the signalling complex of CARs could enhance the activation to mimic an

endogenous TCR (James, 2018). Chimeric antigen receptors have also exhibited constant activation in the absence of antigen, or tonic signalling, correlated to the intensity of CAR surface expression, resulting in antigen-independent proliferation and eventual exhaustion (Frigault et al., 2015). Tonic signalling in CARs has also been partially explained by aggregation of the scFv domains in CD28 containing constructs (Long et al., 2015).

Manufacturing cell products is complex and costly. It is also open to intervention to enhance the functional efficacy of the resultant cell product. Various amendments to production protocols have been made to increase the anti-tumour capacity of the therapy. Expansion of CAR T cells in IL-4, IL-7, IL-21 and/or IL-15 can result in a more memory or stem-cell like phenotype enabling greater proliferative capacity (Gargett and Brown, 2015, Ptackova et al., 2018). Decreasing *ex vivo* production time has shown to increase efficacy. Chimeric antigen receptor T cells against CD19 demonstrated a more naïve phenotype and had greater anti-leukaemia efficacy when cultured for only 3 days compared to 9 days (Ghassemi et al., 2018). Concentrating effort on the manufacturing conditions might help augment the therapeutic efficacy of CAR T cells.

1.3.3 Targeting the tumour microenvironment

The tumour microenvironment has been widely accepted to play a key role in suppressing the immune system's endogenous anti-cancer mechanisms. It also plays a key role in limiting the efficacy of cancer immunotherapy. These effects are largely mediated through the non-malignant cells (stroma) that reside within the tumour and which secrete factors that dampen down inflammatory conditions necessary for adequate cancer elimination [Figure 1.2]. The stroma can be classified into various cellular categories including mesenchymal, vascular and immune and these elements can adversely affect

CAR T cell immunotherapy in numerous ways. The density of tissue and erratic vessel formation facilitate hypoxic conditions and impede penetration of tumour-infiltrating cells and drugs. Tumour-associated macrophages (TAMs), regulatory T cells (Tregs) and cancer-associated fibroblasts (CAFs) express anti-inflammatory molecules which decrease immune recognition and activation. Cancer cells and stroma express inhibitory ligands such as PD-L1/2 to attenuate T cell cytotoxicity (Bhome et al., 2016). The more that tumours exhibit these characteristics, the more resistant they are to immunotherapy (Gasser et al., 2017). Many combination therapies have investigated the potential to permit CAR T cells to overcome these obstacles. Targeting the inhibitory checkpoint interaction between PD-1 and PD-L1 through co-administration of CPIs or oncolytic viruses expressing antibody fragments to PD-L1 have been investigated. Combination approaches enhance efficacy of PSMA and Her2 CAR T cells in solid tumours for which CAR T cells alone had limited anti-tumour effects (Serganova et al., 2017, Tanoue et al., 2017). Increased penetration and migration was seen for CAR T cells rendered insensitive to the inhibitory protein kinase A or co-injected with bevacizumab to reorganise the vasculature (Bocca et al., 2017, Newick et al., 2016). Regulatory immune cells can also be targeted to yield greater combination therapy results. Sarcoma patient-derived xenograft (PDX) models were treated with all-trans retinoic acid which ablated the substantial numbers of myeloid-derived suppressor cells (MDSCs) in the tumour, allowing for control of tumour growth with CAR T cells (Long et al., 2016). Chimeric antigen receptors are also being developed against the aberrant vascular networks within the tumour microenvironment. Prostate specific membrane antigen is overexpressed in the neo-vasculature of many tumours and a 3rd generation CAR directed against PSMA exhibited vessel specificity and tumour control *in vivo* (Santoro et al., 2015). Another vasculature target that has recently emerged is C-type lectin domain family member 14a (CLEC14a). Targeting CLEC14a with a CAR T cell platform demonstrated efficacy in

murine lung cancer models with no observed toxicity in healthy tissues (Zhuang et al., 2014).

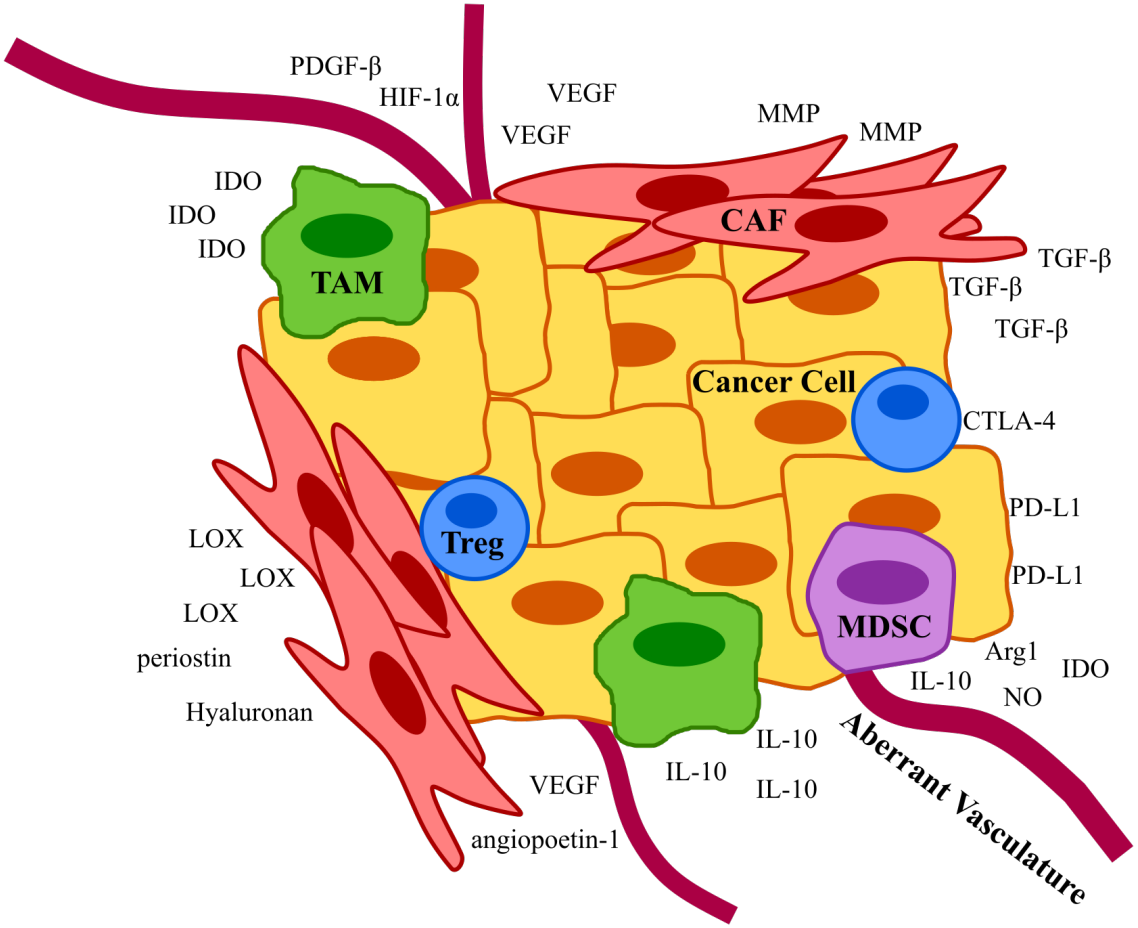

Figure 1.2 Suppressive stroma and factors within the tumour microenvironment. Cancer cells are surrounded by stroma of different cell origins in the tumour. Along with the cancer cells, they each express proteins/molecules to dampen down the anti-tumour immune response and aid in cancer progression and metastasis. CAF: cancer-associated fibroblast; TAM: tumour-associated macrophage; Treg: regulatory T cell; MDSC: myeloid-derived suppressor cell; PDGF-β: platelet-derived growth factor β; HIF-1α: hypoxia inducible factor 1 α; VEGF: vascular endothelial growth factor; MMP: matrix metalloproteinase; IDO: indoleamine-pyrrole 2,3-dioxygenase; TGF-β: transforming growth factor β; CTLA-4: cytotoxic T-lymphocyte-associated protein 4; PD-L1: programmed death ligand 1; LOX: lysyl oxidase; IL-10: interleukin 10; Arg1: arginase 1; NO: nitric oxide.

Cancer-associated fibroblasts (CAFs) are considered any fibroblast within the tumour stroma. These cells have been described as having an activated phenotype, similar to myofibroblasts found in acute injury, in that they are metabolically active, proliferate, express α smooth muscle actin (αSMA) and produce extracellular matrix (ECM)

proteins. However, studies have shown that CAFs phenotypically differ from normal myofibroblasts and remain chronically activated partially due to epigenetic regulation of gene expression (Bechtel et al., 2010, Bozoky et al., 2013, Sadlonova et al., 2009). Generally, CAFs promote tumour proliferation, survival and metastasis through cell-cell contact, ECM manipulation and cytokine/chemokine/growth factor secretion (Erdogan et al., 2017, Gaggioli et al., 2007, Hodkinson et al., 2006, Orimo et al., 2005, Otomo et al., 2014). Exosomes released by chemoresistant CAFs in pancreatic ductal adenocarcinoma were able to deliver transcription factor Snail and miRNA-146a to cancer cells, increasing their chemoresistance and proliferation (Richards et al., 2017). Additionally, CAFs aid in tumour immunity evasion by creating a protumour, immunosuppressive environment. This is partly accomplished through CAF secreted chemokines/cytokines including CCL2, CXCL16, Chitinase 3-like-1 (Chi3L1) and IL-6 that recruit and drive immunosuppressive phenotypes such as MDSCs and M2 polarised macrophages (Allaoui et al., 2016, Chomarat et al., 2000, Cohen et al., 2017, Yang et al., 2016). Cancer-associated fibroblast secreted factors such as tryptophan 2,3 dioxygenase (TDO), VEGF, arginase II (Arg2) and MMPs affect dendritic cell maturation, T cell metabolism and NKG2D ligand expression on tumour cells leading to a loss of functional immune response (Gabrilovich et al., 1998, Hsu et al., 2016, Ino et al., 2013, Ziani et al., 2017). Supernatant from CAFs of head and neck squamous cell carcinoma significantly increased the proportion of Tregs in PBMC cultures compared to matching normal fibroblasts from patients (Takahashi et al., 2015). Another study showed that CAFs in colorectal carcinoma samples expressed high levels of the immunoregulatory marker CD70 and this correlated with increased Treg accumulation in the tumour. Fibroblasts expressing high levels of this protein were also superior to low expressers for supporting Treg expansion in culture (Jacobs et al., 2018). Transforming growth factor-β (TGF-β) has been widely implicated in immunosuppression. This factor has been shown to activate

CAFs to a myofibroblastic phenotype and sustain activation via autocrine signalling (Kojima et al., 2010, Tang et al., 2019). In addition to self-sustainment, TGF-β decreases cytokine secretion and cytotoxicity of $CD8^+$ T cells and reduces their penetration into the tumour (Ahmadzadeh and Rosenberg, 2005, Mariathasan et al., 2018, Thomas and Massague, 2005). Further to this immunosuppressive milieu, CAFs create a physical barrier against infiltrating immune cells and therapies through increased ECM deposition and tissue tension, leading to poor vascularisation and hypoxic conditions (Chauhan et al., 2013, Salmon et al., 2012).

The fibroblast compartment is widely heterogenous and not well understood to date. Heterogeneity of CAFs may be intrinsic of the cell origin. Resident tissue fibroblast phenotypes differ between organs and fibroblasts can be induced from precursor cells including bone marrow MSCs (BM-MSCs), adipocytes, endothelial cells, epithelial cells and pericytes (Chang et al., 2002, Marangoni et al., 2015, Quante et al., 2011, Sun et al., 2016). Single-cell RNA data showed that wound-derived fibroblasts clustered into 12 distinct genetic expression profiles (Guerrero-Juarez et al., 2019). In a cancer context, the MMTV-PyMT transgenic murine model of breast cancer showed 4 subtypes of CAFs with varying genetic expression, protein markers, function, origin and location within the tumour (Bartoschek et al., 2018). In patients with breast cancer, CAFs with a downregulated caveolin-1 phenotype were correlated with a worse disease-free survival rate. Caveolin-1 silencing in fibroblast cell lines increased the invasive potential of the breast cancer cell lines MDA-MB-468 and T47D (Simpkins et al., 2012). A new subset of CAFs in breast and lung tumours has been identified by the expression markers CD10 and GPR77. These CAFs promote chemoresistance and enrichment of cancer stem cells (Su et al., 2018). In contrast to the described active myofibroblast, studies have exposed a subset of CAFs that acquire senescence, in which they remain metabolically active but

no longer divide. These senescent CAFs are able to promote tumorigenesis and cell proliferation through various factor secretion (Bavik et al., 2006, Pazolli et al., 2009). A study utilising oesophageal squamous cell carcinoma cultures demonstrated that a genetically unstable disease variant correlated with an increased senescent CAF population. Senescence was induced through reactive oxygen species secreted by the cancer cells and an increase in TGF-β expression in the fibroblasts. The senescent CAF phenotype was able to increase invasive capabilities of tumour cells *in vitro* and was partially explained by an increase of CAF-derived MMP-2 (Hassona et al., 2013, 2014).

Emerging evidence indicates that targeting the CAF compartment with therapeutic intervention can increase treatment efficacy. A strategy currently being investigated involves reversing the cancer-promoting phenotype of CAFs to a less active, more quiescent state. Knocking down NADPH oxidase 4 (NOX4) using either a selective NOX inhibitor or shRNA reverted myofibroblast differentiation in human foetal foreskin fibroblasts *in vitro* and reduced myofibroblast presence and tumour growth in a xenograft model of head and neck cancer (Hanley et al., 2018). All-trans retinoic acid (ATRA) induced a quiescent phenotype in the pancreatic stellate cell line PS1, as assessed by gene expression. Treatment with ATRA also induced PS1-dependent cancer cell apoptosis, diminished invasion potential and slowed proliferation in pancreatic cancer cells in 3D cultures via Wnt-β-catenin signalling disruption (Froeling et al., 2011). Similar effects have been observed with pancreatic stellate cells treated with a vitamin D receptor ligand, increasing the efficacy of the chemotherapy drug gemcitabine in a pancreatic cancer transgenic mouse model (Sherman et al., 2014). Cytotoxic drug targeting to CAFs has also been investigated. Exploitation of the off-target uptake of therapeutic nanoparticles in tumour fibroblasts was designed to deliver plasmids encoding secreted TNF-related apoptosis-inducing ligand (sTRAIL) to CAFs, triggering apoptosis in the neighbouring

cancer cells. A xenograft model of bladder cancer co-injected with NIH3T3 fibroblasts showed accumulation of the nanoparticles in the fibroblasts, reduction in tumour growth and decreased fibroblast activation (Miao et al., 2017). A phase I trial exhibited increased anti-tumour efficacy in 3/12 patients with a combination therapy of the Hedgehog signalling inhibitor Sonidegib and docetaxel. Investigation into the mechanism determined that Hedgehog signalling in CAFs results in upregulation of ECM remodelling and supports a cancer stem cell phenotype (Cazet et al., 2018). Further development of therapies targeting CAFs may illustrate greater clinical efficacy for combination cancer treatments.

1.3.4 Fibroblast Activation Protein (FAP) as a therapeutic target

The 170kDa homodimer Fibroblast Activation Protein (FAP) is a serine protease in the Dipeptidyl Peptidase IV (DPPIV) family. While dipeptidyl peptidase activity is a feature of all DPPIV members, FAP is also uniquely capable of endopeptidase cleavage (Aertgeerts et al., 2005). The physiological expression pattern of this protease is well characterised in embryonic mesenchyme, scar formations/wound healing and bone marrow-derived mesenchymal stromal cells (Bae et al., 2008, Rettig et al., 1988). Although abundant in embryonic tissue, its role seems to be non-essential in the development of the foetus as FAP knockout mice exhibit a healthy phenotype (Niedermeyer et al., 2000). The role of FAP in cell biology and the discovery of its substrates are still under investigation. Neuropeptide Y, B-type natriuretic peptide, peptide YY and substance P are among the natural substrates identified for FAP dipeptidyl peptidase activity (Keane et al., 2011). The ECM proteins $\alpha 2$-antiplasmin, type I collagen and gelatin are known substrates of soluble and membrane-bound FAP endopeptidase activity (Lee et al., 2006, Park et al., 1999). This enzymatic ECM remodelling activity is central to FAPs role in scar resolution and cancer progression.

In contrast to the highly restricted presence of FAP in health, the enzyme is widely expressed in diseased tissues. In 1986, FAP was first identified through the relative restriction of binding of a monoclonal antibody to astrocytomas, sarcomas and fibroblasts (Rettig et al., 1986). It was further characterised while analysing biopsies from 18 different tumour types. Overexpression of FAP was detected in the stroma of epithelial cancers including colorectal, breast, ovarian, bladder, lung, mesothelioma, skin, gastric, pancreatic, endometrial and melanoma, but not in the surrounding healthy tissue (Garin-Chesa et al., 1990). Overexpression of FAP in the tumour microenvironment is associated with increased invasiveness of the cancer, which could be due to its collagenolytic activity. Forced expression of FAP in the HT1080 sarcoma cell line results in increased migration of the cells in chambers containing different types of ECM, as well as an upregulation of integrin-related intracellular signalling proteins. These changes are abrogated upon treatment with an antibody that causes FAP internalisation (Baird et al., 2015). Knocking down endogenously expressed FAP in cancer-associated fibroblasts decreases the migratory capacity of the cancer cells (Teichgraber et al., 2015). A meta-analysis of 15 different studies of FAP expression in multiple solid tumour types identified a statistically significant correlation between FAP overexpression and lymph node metastases, distant metastases and poorer overall survival. Notably, worsened overall survival was only significant in cases where tumour cells, as opposed to stroma, expressed FAP (Liu et al., 2015). Numerous carcinomas show significantly increased levels of TGF-β (Friess et al., 1993, Travers et al., 1988, Truong et al., 1993) which is a primary upregulator of FAP (Chen et al., 2009). Illustrating this, TGF-β containing conditioned media from colorectal cancer cells upregulated FAP expression in fibroblasts (Henriksson et al., 2011). The expression of FAP in the tumour microenvironment highlights its potential as a target for cancer therapy.

Cancer-associated fibroblasts (CAFs) are genetically stable cells within the tumour microenvironment (Qiu et al., 2008, Walter et al., 2008). Many immunotherapies have been developed to take advantage of this stability by targeting CAF antigens including FAP. In an early phase I study, the F19 antibody used to discover FAP was radiolabelled with iodine-131 in order to image liver metastases originating from colorectal cancer. In 15/17 patients who received the tracer, metastases were successfully imaged by single-photon emission computed tomography (SPECT) in the absence of dose-limiting toxicity. Moreover, imaging findings correlated to the extent of disease as identified at the time of subsequent resection (Welt et al., 1994). The antibody was subsequently humanised and underwent evaluation of safety and therapeutic efficacy in a phase I trial in FAP^+ tumours and a phase II trial in metastatic colorectal carcinoma patients. In both studies the immunotherapy was well-tolerated, but exhibited little clinical efficacy (Hofheinz et al., 2003, Scott et al., 2003). Dendritic cell and DNA vaccines directed against FAP have been tested in animal models of colon and breast carcinoma, melanoma and lymphoma. Significant slowing of tumour growth, reduction in metastases and $CD8^+$ T cell mediated anti-FAP responses were seen (Lee et al., 2005, Loeffler et al., 2006, Wen et al., 2010). One study noted there was a slight delay in wound healing ability in vaccinated mice, although this difference was short lived (Lee et al., 2005). However, none of these studies demonstrated that tumour regression could be induced after vaccination alone. Chimeric Antigen Receptor (CAR) engineered T cells directed against FAP have also been investigated in mouse models of lung cancer and mesothelioma. Slowing of tumour growth was observed in these studies which was further enhanced by combination with other therapies (Kakarla et al., 2013, Wang et al., 2014). Treatment of lung tumour bearing mice with co-injections of two separate CAR^+ T cell populations, targeting FAP and lung carcinoma associated antigen ephrin type-A receptor 2 (EphA2), resulted in an improved anti-tumour efficacy beyond that seen with either CAR construct alone. By

contrast, FAP-specific CAR T cells elicited weak or negligible anti-tumour activity in models of melanoma, colon cancer, fibrosarcoma, breast and kidney cancer. In these studies, animals exhibited bone necrosis and cachexia which was attributed to the targeting of FAP expressed on bone-marrow mesenchymal stromal cells (Tran et al., 2013). Similar toxicity was not seen with FAP directed CARs in other studies (Kakarla et al., 2013, Wang et al., 2014). Despite these disappointing results, a F19 derived FAP-specific CAR T cell immunotherapy is currently under study in a phase I trial in patients with malignant mesothelioma (Petrausch et al., 2012).

Although FAP tends to localise in epithelial cancer stroma, the aforementioned studies suggest that the targeting of FAP expression alone may not be sufficient to result in tumour clearance. These studies indicate that combination therapies that include a FAP-directed therapeutic agent could lead to enhanced anti-tumour activity.

1.3.5 Utilising immunocytokines

As a method of targeted cytokine delivery, antibody-cytokine fusion molecules termed 'immunocytokines' [Figure 1.3] have been widely developed and assessed in clinical trials involving a variety of cancers [Table 1.2]. Pre-clinical studies have demonstrated the efficient targeting capabilities of immunocytokines to the tumour site. Given the toxicity profiles of many systemically delivered cytokines, use of an immunocytokine approach can often broaden the therapeutic window of the cytokine under study (Borsi et al., 2003, Carnemolla et al., 2002). Immunocytokines incorporating IL-4 have been investigated *in vivo*, but they have primarily been assessed in the treatment of auto-inflammatory conditions including arthritis, endometriosis and psoriasis (Hemmerle et al., 2014a, Hemmerle et al., 2014b, Kawalkowska et al., 2016, Quattrone et al., 2015). However, one study described an IL-4 immunocytokine targeted to an alternatively

spliced extra-domain A of fibronectin that is aberrantly expressed in a range of cancers. This agent demonstrated anti-tumour activity in mouse models of teratocarcinoma, lymphoma and colon cancer (Hemmerle and Neri, 2014). The use of FAP as a target for immunocytokine delivery has also been validated using a number of cancer models. Illustrating this, FAP-specific immunocytokines carrying the inflammatory cytokine tumour necrosis factor-α (TNF) or a *trans*-signalling variant of IL-15 demonstrated good localisation to the tumour microenvironment, leading in turn to the induction of potent anti-tumour immune responses (Bauer et al., 2004, Kermer et al., 2012). A bi-specific molecule coupling a FAP-specific scFv to the co-stimulatory ligand 41BB-L also elicited enhanced co-stimulation in co-cultures of T cells with FAP-expressing tumour cells (Muller et al., 2008).

Immunocytokines have been investigated previously in combination with CAR T cells in a $CD19^+$ $CD20^+$ plasma cell leukaemia model. Increased persistence *in vivo* was described for CD19-specific CAR T cells co-administered with a CD20-targeting IL-2 immunocytokine compared to CAR alone, CAR with untargeted IL-2 or an irrelevant GD-2-specific IL-2 immunocytokine. Tumour eradication achieved in the CAR T cell plus CD20 IL-2 immunocytokine group continued for 83 days (Singh et al., 2007). This study has highlighted the potential to support and improve CAR T cell therapy with tumour targeted immunocytokines.

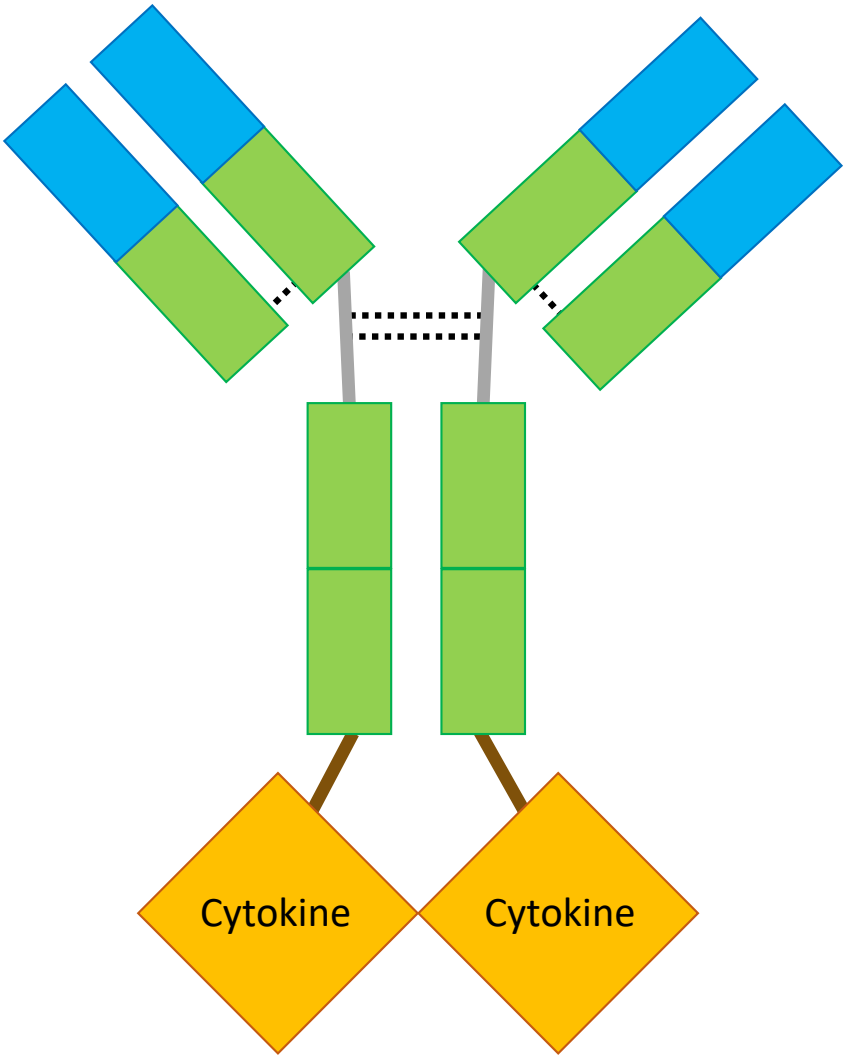

Figure 1.3 Structure of an immunocytokine.
An example of an immunocytokine format is shown. In this case, a full-length native antibody conformation has been conjugated to the cytokine payload which has been attached to the C-terminus of the heavy chain. Immunocytokines can incorporate a variety of antibody fragments including Fab and scFv domains. They can also differ in the location at which cytokine attachment is situated (blue boxes = antibody variable regions; green boxes = constant regions; grey lines = hinge domain; black dotted lines = disulphide bonds; brown lines = serine-glycine linker).

Target Antigen	Disease	Cytokine Delivered	Reference
GD2	Neuroblastoma Melanoma	IL-2	(Albertini et al., 2012, Albertini et al., 2018, King et al., 2004, Ribas et al., 2009, Shusterman et al., 2010)
A1 domain of Tenascin C	Solid tumours Breast carcinoma	IL-2	(Catania et al., 2015)
EpCAM	Solid tumours Small cell lung carcinoma Prostate carcinoma	IL-2	(Connor et al., 2013, Gladkov et al., 2015, Ko et al., 2004)
ED-B isoform of fibronectin	Melanoma Renal cell carcinoma Solid tumours	IL-2 IL-12 TNF	(Danielli et al., 2015, Eigentler et al., 2011, Johannsen et al., 2010, Papadia et al., 2013, Rudman et al., 2011, Spitaleri et al., 2013, Weide et al., 2014)
DNA fragments	Solid tumours Non-small cell lung carcinoma	IL-2	(Gillessen et al., 2013, van den Heuvel et al., 2015)

Table 1.2 Clinical trials utilising immunocytokines.
Targets, diseases, delivered cytokines and references that describe clinical trials involving immunocytokines. Antigen targets include GD2: disialoganglioside, EpCAM: epithelial cell adhesion molecule, ED-B: extra-domain B.

1.4 Project hypothesis and objectives

I hypothesised that the efficacy of PSMA-targeted CAR T cell immunotherapy for prostate cancer could be significantly improved through the delivery of a tumour stroma-specific immunocytokine. The objectives of this PhD thesis were to:

- Develop a functional FAP-specific IL-4 immunocytokine.
- Generate a prostate cancer/stroma model for *in vitro* and *in vivo* experimentation.
- Observe the effects of the immunocytokine on CAR T cell anti-tumour capabilities *in vitro* and in *in vivo* xenograft models.

Chapter 2: Materials and methods

2.1 Media and solutions

D10 Media = 500 mL Dulbecco's Modified Eagle Medium (DMEM) + 4.5 g/L glucose (Lonza)

50 mL Foetal Bovine Serum (Autogen Bioclear)

3.6 mM L-Glutamine (Lonza)

R5 Media = 500 mL Roswell Park Memorial Institute (RPMI) Medium without L-Glutamine

(Lonza)

25 mL Foetal Calf Serum

3.6 mM L-Glutamine

PS1 Media = 500 mL DMEM/Ham's F-12 50/50 mix with 2.5 mM L-glutamine (Corning)

50 mL Foetal Bovine Serum (Autogen Bioclear)

Expi293F™ Expression Media (Gibco)

EX-CELL® Hybridoma Media (Sigma)

Trypsin-Versene = 25 mL 2x Trypsin (Pierce)

25 mL 2x Versene

1X PBS = 9.55 g/L phosphate-buffered saline in deionised water (Biochrom AG)

1X HBS = 8.76 g/L NaCl and 2.38 g/L hepes in deionised water (Provided by Dr. Jim McDonnell)

Tissue Digestion Buffer = 500 mL RPMI (Lonza)

1 mg/mL collagenase (Sigma)

0.1 mg/mL Deoxyribonuclease I (Sigma)

2.2 Cell cultures

All cells were maintained in incubators at 37˚C and 5% CO_2 apart from Expi293F™ cells which were maintained at 37˚C and 8% CO_2 in 120 RPM shaking conditions. Cells were passaged once ≥ 90% confluency was reached. All cell lines were kept in D10 media during culture. Exceptions were PS1 cells cultured in PS1 media, Expi293F™ kept in Expi293F™ Expression Media and hybridomas which were cultured in serum free EX-CELL media. H29 cultures in D10 were supplemented with 2 μg/mL tetracycline to suppress expression of the cytotoxic VSVG *env* protein that is under control of a tetracycline repressed promoter. H29 cultures were also supplemented with 3 μg/mL puromycin and 6 μg/mL G418 for *gag*/*pol* suppression.

2.2.1 Cell lines

Cell Line	Derived From (Envelope Protein)	Source
H29	Human embryonic kidney (Vesicular stomatitis virus G)	Memorial Sloan Kettering Cancer Center, N.Y
293vec-RD114 (RD114)	Human embryonic kidney (RD114 endogenous feline virus)	BioVec Pharma
DU145	Human prostate	CRUK
PC3-LN3 (PL)	Human prostate	Dr. Sue Eccles (Institute of Cancer Research, Sutton)

PC3-LN3-PSMA (PLP)	Human prostate	Dr. Sophie Papa (Research Oncology, King's College London)
LT-PLPFAP	Human prostate; transduced to express LT and FAP	Developed in the lab
MRC5hT (hTERT transduced)	Human foetal lung fibroblast	Dr. Gabriele Saretzki (Institute for Ageing and Institute for Cell and Molecular Biosciences, Newcastle)
PS1 (hTERT transduced)	Pancreatic stellate cells	Dr. Hemant Kocher (Centre for Tumour Biology, Bart's Cancer Institute)
HT1080/HT1080-FAP	Human sarcoma	Ulf Petrausch (OnkoZentrum, Zürich)
Hybridomas	FAP-specific splenocytes and myeloma	GenScript
CTLL-2/4αβ	Murine T cell	Dr. Alastair Noble (King's College London)
Expi293F™	Suspension human embryonic kidney cells	Dr. Sophia Karagiannis (King's College London)

Table 2.1 Cell lines used in this study.
Includes the name, their origin and where they were sourced from.

2.2.2 Peripheral blood mononuclear cells (PBMCs)

Blood was collected into 5 mL of anticoagulant citrate-dextrose solution (Sigma) from healthy volunteer donors under approval of the Guy's Hospital Research Ethics Committee (09/H0804/92; Use of Donor Blood Samples for Pre-Clinical Development of Active and Passive Immunotherapy for Cancer). Fifteen millilitres of Ficoll-Paque (Sigma) was aliquoted into a 50 mL Falcon tube and 25 mL of blood was slowly layered on top. This was centrifuged at 800 x g for 35 minutes with the acceleration and brakes turned off. A Pasteur pipette was used to transfer the buffy coat of PBMCs into a new Falcon tube. The cells were washed with PBS and spun at 400 x g for 10 minutes twice. The pellet was resuspended in R5, counted and diluted to 3 x 10^6 cells/mL. Phytohemagglutinin-L (PHA) (Sigma) was added at 5 μg/mL and cells were plated across 6 well plates and incubated overnight. Twenty-four hours later, 100 IU/mL IL-2 was added and cultures were supplemented with IL-2 every 2-3 days.

2.3 Molecular biology techniques

2.3.1 Construct design

Gene constructs in the SFG vector were previously developed and used to transduce cell lines for this project [Figure 2.1]. Fibroblast activation protein (FAP) was cloned into SFG for experiments in this thesis and is described later [section.2.3.2]. The variable regions of the B1 and C11 hybridomas generated for this project by GenScript were initially sequenced by GenScript. The Snapgene software was used for scFv-Fc and immunocytokine design and Genedesigner (ATUM) was utilised for codon optimisation of the B1HL, B1LH and C11 scFv-Fc constructs. All leader sequences for the scFv-Fc and immunocytokine constructs were derived from the heavy chain of the C11 hybridoma or the CSPG4 antibody, kindly gifted by Dr. Sophia Karagiannis. The ESC11 V_H and V_L sequences were sourced from a patent application for the anti- human and murine FAP

antibody (application no.: 13/499,718) (https://patents.google.com/patent/US20120258119A1/en). The V_H and V_L domains were connected by a 15-amino acid serine-glycine linker in each scFv-Fc and immunocytokine construct. The immunocytokine was designed to link recombinant human IL-4 to the C-terminus of the ESC11 scFv by a 15-amino acid serine-glycine linker. Construct sequences were confirmed using Sanger sequencing by Source Bioscience.

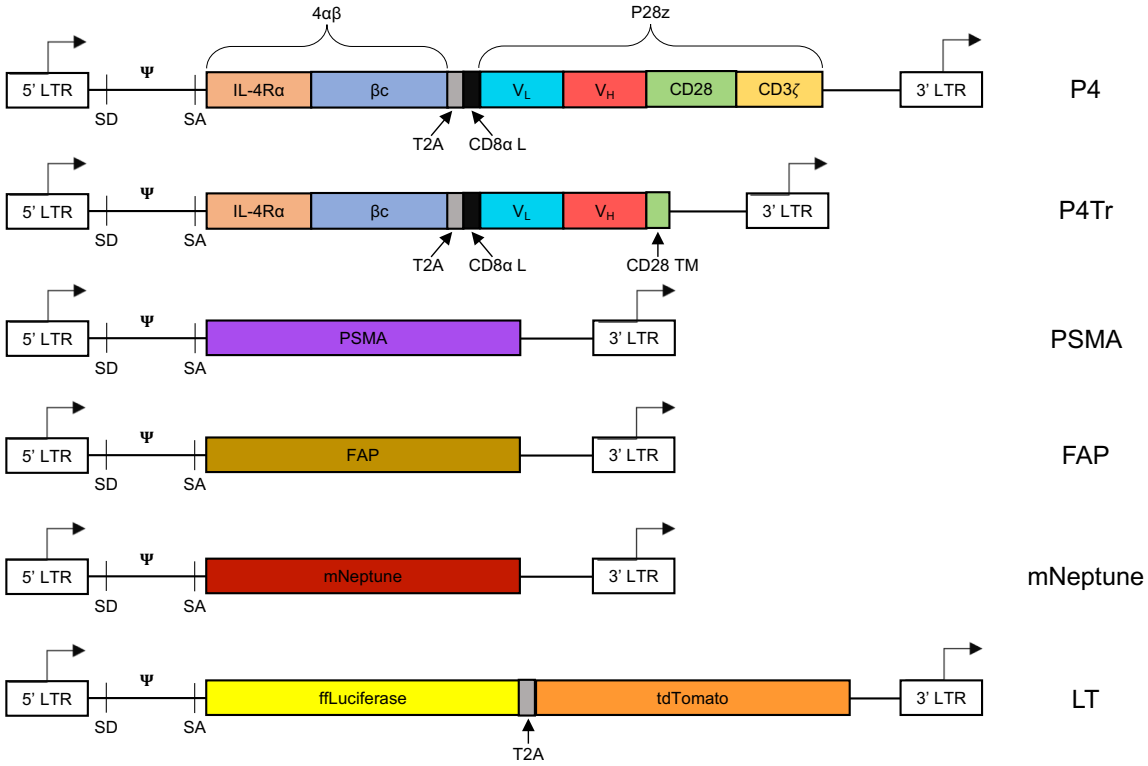

Figure 2.1 Constructs for stable transduction of cell lines.
The constructs for SFG plasmids containing P4, P4Tr, PSMA, FAP, mNeptune and ffLuciferase-tdTomato (LT) are illustrated. LTR: long terminal repeats; SD: splice donor; SA: splice acceptor; **Ψ**: packaging signal; T2A: furin cleavage site; CD8α L: CD8α leader sequence.

2.3.2 Subcloning FAP into SFG

The commercially available plasmid FAP-pcDNA3.1-(k)DYK (GenScript) was used as a source of Fibroblast Activation Protein DNA sequence which was subcloned into the SFG retroviral vector previously described (Riviere et al., 1995). Fibroblast Activation Protein

and SFG were both amplified using the polymerase chain reaction (PCR) technique with primers harbouring overlapping regions to insert FAP into the SFG cloning site. The FAP-pcDNA3.1-(k)DYK and SFG plasmids were diluted to 1 ng/µL in nuclease free water and primers [Table 2.2] were diluted to a working concentration of 10 µM. A master mix was generated with 10 µL Q5® Reaction Buffer (NEB), 10 µL GC enhancer (NEB), 1 µL dNTP (NEB) and 0.5 µL Q5® High Fidelity DNA Polymerase (NEB) into 21.5 µL water. The master mix was used at 21.5 µL/reaction with 0.5 µM forward/reverse primers and 1 ng plasmid DNA templates. The FAP and SFG reactions were carried out as follows: a 3-minute denaturation period at 98˚C followed by 35 cycles of 15 seconds denaturation at 98˚C, 15 seconds annealing at 67˚C and a 30 seconds/kilobase extension at 72˚C. A final extension was run at 72˚C for 2 minutes and reactions were held at 10˚C. Reactions were visualised on an agarose gel [section 2.3.6] for correct size and template strands were digested with 0.5 µL DpnI enzyme at 37˚C for 15 minutes. The SFG and FAP amplicons were mixed together and transformed into competent bacteria [section 2.3.3]. Colonies were chosen, expanded and a miniprep [section 2.3.4] was performed to extract plasmid DNA for sequencing.

PCR	Forward Primer	Reverse Primer	Size of Fragment
FAP Subcloning into SFG			
FAP insert	ccccgggggtggaccatcctctagactgcc atgaagacttgggtaaaaatcgtatttggag	gactaatccggatccctcgagtggctgtta gtctgacaaagagaaacactgctttagg	2,340 bp
SFG backbone	taacagccactcgagggatccg	ggcagtctagaggatggtccac	6,358 bp

Table 2.2 Primers used for the FAP-SFG PCR reactions.
The sequences of the primers used for each reaction are listed along with the expected size of the fragment. bp = base pair.

2.3.3 PIPE cloning

This technique was used to produce the eFAP-4 and scFv-Fc recombinant antibodies. A UCOE02 (Merck Millipore) plasmid containing the sequence for a human IgG1 heavy

chain was donated by Dr. Sophia Karagiannis, King's College London. The eFAP-4 immunocytokine or scFv was sourced from a pUC57 plasmid (GenScript) containing the relevant sequence. The UCOE backbone was used as the template for 3 PCRs to generate 3 different fragments and the pUC57-scFv/immunocytokine plasmids were used to generate the insert fragment. All reactions included 10 ng of template DNA, 10 µM of forward primer, 10 µM of reverse primer and a 1X concentration of Phusion™ Flash High-Fidelity PCR Master Mix (Thermo Scientific) diluted to 50 µL in nuclease free water. Generation of the scFv-Fc was carried out as follows: a 30 second denaturation at 98˚C followed by 30 cycles of 1 second denaturation at 98˚C, 5 seconds annealing at 60˚C and 15 seconds/kilobase extension at 72˚C. Amplicons were visualised on 1% agarose gels [section 2.3.6]. The template strands in each reaction were digested in 1X CutSmart® buffer with DpnI (NEB) at 37˚C for 2 hours. One microliter each of the 3 UCOE backbone products were mixed with 1 µL of the relevant insert fragment in 4 µL nuclease free water and left overnight at room temperature. Competent bacteria were transformed the following day.

2.3.4 Bacterial transformation

Competent K12 ER2925 *E. coli* (NEB) were thawed on ice for 30 minutes and 4µL DNA was added. Cells were incubated on ice for 30 minutes and heat shocked at 42°C for 1 minute. Bacteria were allowed to rest briefly, then 300µL super optimal broth with catabolite repression (SOC) media (Invitrogen) were added and cells were shaken at 200RPM, 37°C for 1 hour. Bacteria was then pelleted down at 13,000RPM for 3 minutes. Three-hundred microliters of supernatant were removed and the cells were resuspended. Cells were added to an agar plate containing 100µg/mL ampicillin and spread. The plate was incubated at 37°C overnight. Colonies were selected and added to 5mL 100µg/mL

ampicillin Luria-broth (LB). Bacteria were placed in an orbital shaker at 200RPM, 37°C overnight.

2.3.5 Miniprep

The QIAprep spin Miniprep kit (Qiagen) for bacteria colonies was used and instructions provided were followed. Colonies were grown overnight in 5mL 100µg/mL ampicillin LB and pelleted at 3,000 x g. Pellets were resuspended in 250 µL Buffer P1. Resuspended bacteria were then mixed with 250 µL Buffer P2 and gently mixed by inverting. Cell lysis was neutralised by invert mixing in 350 µL Buffer N3 and pelleted at 16,800 x g for 10 minutes. The supernatant was applied to a spin column and centrifuged for 1 minute. The spin column was washed with 500 µL Buffer PB and centrifuged for 1 minute. The column was washed with 750 µL Buffer PE and centrifuged for 1 minute. An additional 1 minute centrifugation was applied to remove any liquid. The column was then placed in a clean Eppendorf and the plasmid DNA was eluted with 50 µL Buffer EB. The membrane was allowed to stand for 1 minute and then centrifuged for 1 minute. Concentrations were analysed using a Nanodrop. The plasmids were stored at -20°C.

2.3.6 Maxiprep

Colonies grown overnight in 5mL 100µg/mL ampicillin LB were transferred to 200 mL of the same broth and expanded overnight in the orbital shaker at 200RPM and 37°C. The QIAprep spin Maxiprep kit (Qiagen) for bacteria colonies was used and instructions provided were followed. Harvested cultures were split into aliquots of 50 mL and pelleted at 3,000 x g for 15 minutes at 4˚C. Pellets were resuspended in 20 mL Buffer P1 and vortexed. Equal volume of Buffer P2 was added, mixed by inverting and incubated at room temperature for 5 minutes. Twenty millilitres cold Buffer P3 was added and mixed by inverting before incubating on ice for 20 minutes. Solutions were centrifuged at 3,000

x g for 30 minutes at 4˚C. Supernatant was applied to equilibrated QIAGEN-tips and allowed to flow through the membrane. Tips were washed twice with 30 mL Buffer QC. DNA was eluted in 15 mL Buffer QF and precipitated by adding 10.5 mL isopropanol. Precipitated DNA was centrifuged at 3,000 x g for 90 minutes and the supernatant discarded. The DNA pellet was washed with 70% ethanol, centrifuged at 3,000 x g for 60 minutes and the supernatant discarded. The pellet was dried at 37˚C for 10 minutes and the DNA was dissolved in 500 µL TE Buffer. Concentrations were analysed using a Nanodrop. The plasmid was stored at -20°C.

2.3.7 Agarose gel

Digestions with relevant restriction enzymes were incubated at 37°C for 1 hour. A 1% agarose gel was made in 1X TBE buffer and a 1:10,000 concentration of SYBR™ safe (Invitrogen). Samples were prepared with 6X gel loading dye and loaded with 10µL 1kb DNA ladder (NEB). Electrophoresis was run at 150 volts for ~1 hour and the gel was imaged using UV light.

2.4 Protein purification, quantification and characterisation

2.4.1 Purification

Hybridoma and recombinant scFv-Fc antibodies were purified using Protein G GraviTrap columns (GE Healthcare) and instructions provided were followed. Purification of the eFAP-4 immunocytokine was achieved using the AminoLink Immobilisation Kit (Thermo Scientific) and 1.5 mg of purified mouse anti-human IL-4 (Biolegend UK: 8D4-8) was immobilised on the column. Company instructions were followed for protein coupling and purification. Eluents were concentrated and buffer was exchanged to 1X PBS using Amicon Ultra centricons (Merck Millipore) with a 3,000 MW cutoff.

Concentrations were analysed using a Nanodrop. The extinction coefficient for eFAP-4 was calculated to be 72475 $M^{-1}cm^{-1}$ using the ExPaSy ProParam tool online.

2.4.2 Western blot

Pre-cast NuPAGE Gel (Invitrogen) was used and 50 ng of protein was loaded. Samples were prepared with 4X NuPAGE loading buffer (Invitrogen), containing 1 mM dithiothreitol in reduced conditions, protein sample and PBS. Reduced samples were boiled for 5 mins at 94°C. Samples were loaded alongside the PageRuler Plus Prestained Protein Ladder (Thermo Scientific) and run in 1X NuPAGE MOPS running buffer (Invitrogen) at 150 volts for 1 hour. The proteins were transferred to a nitrocellulose membrane (GE Healthcare) in 1X transfer buffer in the cold room at 100 volts for 1 hour. The membrane was washed in 1X TBST. Blocking was done in 3% milk for 1 hour. Primary antibody was diluted in 3% milk and stained for 1 hour. The membrane was washed, the HRP-conjugated secondary antibody was diluted in blocking buffer and incubated for 1 hour. The membrane was washed before incubation with developing reagents 1 and 2 from the ECL kit (GE Healthcare) for 1 minute. The membrane was wrapped and taped inside a developing case. High performance chemiluminescent hyperfilm (GE Healthcare) was used.

2.4.3 Coomassie stain

Pre-cast NuPAGE Gel (Invitrogen) was used and 3 μg of protein was loaded unless otherwise specified. After running the gel (as with the western blot), it was submerged in InstantBlue Coomassie stain (Expedeon) overnight. The gel was rinsed with distilled water and visualised.

2.4.4 Bicinchoninic acid (BCA) assay

The Pierce BCA Protein Assay Kit (Thermo Scientific) was used and bovine serum albumin (BSA) concentration standards were made. Reagents A and B were mixed at a 50:1 ratio. In a plate, 25µL of each standard and sample were used in replicates of 2. Two-hundred microliters of the reagent mixture were added quickly and incubated at 37°C for 30 minutes. The plate was read at a 562nm wavelength.

2.4.5 Biacore binding kinetics

A Biacore T100 instrument was used to assess the binding kinetics of proteins. Recombinant ESC11 scFv-Fc was immobilised on Series S Protein A sensor chip (GE Lifesciences) at a 50 nM concentration diluted in 1X HEPES Buffered Saline (HBS) running buffer. Recombinant hFAP (R&D Systems) was washed over the chip at decreasing doses starting at 50 nM and ranging to 0 nM also diluted in 1X HBS. Regeneration was carried out according to the manufacturer's guidelines. The binding data was plotted in GraphPad Prism and non-linear regression curve analysis was used to determine the dissociation constant.

2.5 Transfection and transduction of cells

2.5.1 Transfection of H29

Tetracycline, G418 and puromycin were removed two hours prior to transfection. A polyethylenimine (PEI) solution (1.5mL serum-free DMEM, 1.5µL of 1mM PEI and 20µL DNA plasmid) was incubated at room temperature for 30 minutes. The cells were washed with serum-free media and the PEI solution was added for two hours at 37°C. D10 was added and incubated at 37°C for 72 hours. The media was changed 72-hours post transfection. Supernatant (3mL) was harvested daily.

2.5.2 Transduction of RD114-pseudotyped HEK293vec (RD114)

Supernatant from transfected H29 cells was placed on pantropic RD114-pseudotyped HEK293vec cells. After 72 hours, flow cytometry was performed to assess transgene expression analysis.

2.5.3 Transduction of cancer and stroma cell lines

Cells were plated at 25-30% confluency on a 6 well plate treated with 200 μg of RetroNectin® (Takara) in D10. The relevant RD114-pseudotyped packaging cell line was plated at ~30% confluency in 2 mL D10. Twenty-four hours later, supernatant harvested from transduced RD114 cells was added to the cancer/stromal cell lines. Cells were repeatedly exposed to RD114 supernatant until transgene expression levels were >90%, as assessed by flow cytometry.

2.5.4 Transduction of PBMCs

The relevant RD114-pseudotyped packaging cell line was plated at 30-35% confluency in 2 mL D10. Twenty-four hours later, supernatant was harvested from RD114 cells and the media replaced. Harvested supernatant was added to 6 well plates treated with 200 μg RetroNectin® (Takara) and kept at 4˚C for 4 hours. Supernatant was then aspirated and replaced with 2 mL of freshly harvested RD114 supernatant and 48 hour PHA-activated PBMCs were added at 1 x 10^6 cells/well. Wells were topped up to 3 mL with fresh R5 media and given 100 IU/mL IL-2 (Novartis). Transduced PBMCs were continuously expanded in R5 media supplemented with 30 ng/mL IL-4 (Peprotech) and transgene expression was analysed using flow cytometry.

2.5.5 Transfection of Expi293F cells

Expi293F cells (Gibco) were transfected with plasmid DNA encoding recombinant scFv-Fc or immunocytokine protein. Protocol for transfection was provided by the supplier. Cells were seeded at 7.5 x 10^7 cells in 25.5 mL of Expi293™ Expression Medium. Eighty microliters ExpiFectamine™ Reagent was diluted in 1.5 mL Opti-MEM™ Medium and incubated at room temperature for 5 minutes. At the same time, 30 µg DNA was diluted in 1.5 mL Opti-MEM™ Medium at room temperature for 5 minutes. The DNA solution and the ExpiFectamine™ Reagent solution were mixed and incubated at room temperature for 20 minutes. This DNA-Reagent mixture was added to the cells and incubated for 16 hours at 37˚C and 8% CO_2 in 120 RPM shaking conditions. The following day, 150 µL ExpiFectamine™ 293 Transfection Enhancer 1 and 1.5 mL ExpiFectamine™ 293 Transfection Enhancer 2 were added to the transfected cells and incubated at 37˚C and 8% CO_2 in 120 RPM shaking conditions. On day 8 post transfection, cells were pelleted at 300 x g for 5 minutes and the supernatant was transferred to a new Falcon tube. The cells were pelleted again at 3571 x g for 50 minutes at 4˚C. Supernatant was collected and filtered through 0.2 µm syringe filters. Sterile supernatant was stored at 4˚C until purification.

2.6 Flow Cytometry

Primary antibodies [Table 2.3] were diluted in 1X PBS and incubated with cells in 100 µL volume for 45 mins on ice unless otherwise specified. Flow cytometric analysis of autofluorescent cells was performed without antibody incubation. Corresponding isotype control antibodies were used to detect non-specific antibody binding. Cells were washed with PBS, centrifuged and the supernatant decanted. Samples were incubated with appropriate secondary antibody [Table 2.3] in 100 µL 1X PBS for 25 minutes on ice. Cells were washed, resuspended in PBS and kept in the dark until analysis on a BD

LSRFortessa™ (BD Biosciences). In samples that were incubated with multiple colour stains, compensation was carried out using single colour and Fluorescence Minus One (FMO) controls.

Name	Company (Clone)	Dilution	Application
Primary			
Mouse anti-human FAP	eBioscience (F11-24)	1:100	FC
Mouse anti-human PSMA	MBL Life Science (107-1A4)	1:100	FC
Mouse anti-human CD124 PE	BD Pharmingen (hIL4R-M57)	20 µL/test	FC
Mouse IgG1 κ isotype PE	BD Pharmingen (MOPC-21)	20 µL/test	FC
Mouse anti-human CD3 APC	BioLegend (UCHT1)	5 µL/test	FC
Mouse anti-human Ki-67 PE/Cy7	BioLegend (Ki-67)	5 µL/test	FC
Mouse IgG1 κ isotype APC/ PE/Cy7	BioLegend (MOPC-21)	5 µL/test	FC
Mouse IgG isotype control	Life Technologies	1:100	FC
Human IgG isotype control	Invitrogen	1:100	FC
Mouse anti-human CD8 FITC	BioLegend (OKT8)	5 µL/test	FC

Mouse anti-human CD4 FITC/APC	BioLegend (OKT4)	5 μL/test	FC
Mouse anti-human PD-1 PE	BioLegend (EH12.2H7)	5 μL/test	FC
Rat anti-human CD44 PE/Cy7	BioLegend (IM7)	1:100	FC
Mouse IgG1 κ isotype PE	BioLegend (MOPC-21)	1:100	FC
Rat IgG2b κ isotype PE/Cy7	BioLegend (RTK4530)	1:100	FC
Mouse Unpurified Hyb S.C. anti-FAP	GenScript (22F8C6)	Neat, 1:10, 1:100	FC
Mouse Unpurified Hyb S.C. anti-FAP	GenScript (22F8H1)	Neat, 1:10, 1:100	FC
Mouse Unpurified Hyb S.C. anti-FAP	GenScript (23D7D5)	Neat, 1:10, 1:100	FC
Mouse Unpurified Hyb S.C. anti-FAP	GenScript (23D7G11)	Neat, 1:10, 1:100	FC

Mouse Unpurified Hyb S.C. anti-FAP	GenScript (26F6A3)	Neat, 1:10, 1:100	FC
Mouse Unpurified Hyb S.C. anti-FAP	GenScript (26F6A11)	Neat, 1:10, 1:100	FC
Mouse Unpurified Hyb S.C. anti-FAP	GenScript (30E9C11)	Neat, 1:10, 1:100	FC
Mouse Unpurified Hyb S.C. anti-FAP	GenScript (30E9G4)	Neat, 1:10, 1:100	FC
Mouse Unpurified Hyb S.C. anti-FAP	GenScript (30H2B1)	Neat, 1:10, 1:100	FC
Mouse Unpurified Hyb S.C. anti-FAP	GenScript (30H2C8)	Neat, 1:10, 1:100	FC
Mouse Purified Hyb S.C. anti-FAP; scFv-Fc	GenScript (22F8**C6**)	0.1 mg/mL, 0.15 mg/mL, 0.01 mg/mL, 0.015 mg/mL, 0.005 mg/mL, 0.0075 mg/mL, 50 ng	FC; WB

Mouse Purified Hyb S.C. anti-FAP; scFv-Fc	GenScript (23D7**D5**)	0.1 mg/mL, 0.15 mg/mL, 0.01 mg/mL, 0.015 mg/mL, 0.005 mg/mL, 0.0075 mg/mL, 50 ng	FC; WB
Mouse Purified Hyb S.C. anti-FAP; scFv-Fc	GenScript (30E9**C11**)	0.1 mg/mL, 0.15 mg/mL, 0.01 mg/mL, 0.015 mg/mL, 0.005 mg/mL, 0.0075 mg/mL, 50 ng	FC; WB
Mouse Purified Hyb S.C. anti-FAP; scFv-Fc	GenScript (30H2**B1**)	0.1 mg/mL, 0.15 mg/mL, 0.01 mg/mL, 0.015 mg/mL, 0.005 mg/mL, 0.0075 mg/mL, 50 ng	FC; WB
ESC11 scFv-Fc; eFAP-4 Immunocytokine	Renner Laboratory (University Hospital Zürich)	0.1 mg/mL, 0.01 mg/mL, 0.001 mg/mL, 0.0001 mg/mL	FC

Secondary			
Goat anti-mouse HRP	Dako	1:500	WB
Goat anti-mouse (GAM) PE	Dako	1:100	FC*
Goat anti-mouse FITC	Dako	1:100	FC
Goat anti-human/mouse Alexa Fluor 647	Jackson ImmunoResearch	0.25 µL/test	FC
Mouse anti-human IL-4 PE/APC	eBioscience/Biolegend UK (8D4-8)	5 µL/test	FC

Table 2.3 Common antibodies used during the project.
Primary and secondary antibodies used in various experiments are outlined by their specificity, clone name, company source, dilution and application. Hyb S.C. = Hybridoma Subclone; FC = flow cytometry; Co = Coomassie; WB = Western Blot.

*This antibody was also used as a directly conjugated detection reagent for PSMA-targeted CARs.

2.7 Growth kinetics and antigen expression studies

2.7.1 CTLL-2 and PBMCs

The functionality of eFAP-4 was assessed by measuring the growth kinetics of CTLL-2 and healthy donor PBMCs expressing the 4αβ chimeric receptor. The samples were diluted 1:4 in trypan blue and counted in a haemocytometer. Total cells/mL were calculated by [Average cells of squares counted]x(dilution factor)=cell number x 10^4/mL. CTLL-2 and PBMCs were plated in 48-well plates at 5x10^4 cells/well in 500 µL. Cultures were treated every 48-hours with either 100 IU/mL of IL-2 (Novartis), stated

concentrations of IL-4 (Peprotech) or eFAP-4, or no cytokine. After 4 days, 250 µL media was added. Cells were counted using a haemocytometer at various time points. Transduced PBMCs were analysed for proportions of $CD8^+$ and $CD4^+$ cells using flow cytometry.

2.7.2 Prostate cancer (PCa) cells

Wells of a 6-well plate were seeded with 10^5 cells in 2 mL of D10 media and cultured at 37°C for pre-determined time points. Antigen expression was analysed after 24 hours in wells seeded at 5 x 10^5 cells in 2 mL.

2.7.3 Conditioned media

The prostate cancer cell lines were plated at 9 x 10^3 cells/well in a 24-well plate in D10 media. PS1 cells were plated similarly at 3.6 x 10^4 cells/well and MRC5hT cells were plated at 8 x 10^4 cells/well. Conditioned media was generated by plating cells at 10^5 per well in a 24-well plate in 1 mL D10 media. Twenty-four hours later the media was collected, spun at 800 x g for 10 mins and added 0.6 mL to respective cell cultures to assess growth kinetics or diluted 1:2 for 50% conditioned media cultures. Cells were cultured in conditioned media for 24, 48, 72 and 96 hours. The fold change in growth of conditioned media cultures compared to fresh D10 cultures was analysed using MTT assay [section 2.8.3]. Fibroblast Activation Protein expression in PS1 and MRC5hT was assessed by flow cytometry at 24 and 72-hour time points.

2.7.4 Co-culture ratio determination

mNeptune transduced PS1 or MRC5hT and firefly Luciferase-tandem dimer (td)Tomato (LT) transduced PL, PLP, DU145 and DU145P cells were plated at various ratios in 24-well plates in D10 media. Each well contained a total of 4 x 10^4 cells and co-cultures were

plated at stroma:prostate cancer ratios of 1:1, 2:1, 4:1, 8:1 and 16:1. Cultures were grown for 24 and 96 hours and then assessed by flow cytometry. The fluorescent reporters were used to identify each population and their relative percentage of the whole culture. Final values were presented as percentages of total cells that were single positive for either tdTomato or mNeptune.

2.7.5 Prostate cancer and stroma co-culture growth kinetics

mNeptune transduced PS1 and LT transduced PCa cells were plated at a 4:1 ratio in 24-well plates in D10 media for a total of 4 x 10^4 cells/well. Cell lines were also plated as monocultures at 4 x 10^4 cells/well or at co-culture densities (PS1 = 3.2 x 10^4 cells/well; PCa = 0.8 x 10^4). mNeptune transduced MRC5hT and LT transduced PCa cells were plated similarly, but at an 8:1 ratio and with monoculture of 4 x 10^4 cells/well and corresponding co-culture densities (MRC5hT = 3.6 x 10^4; PCa = 0.4 x 10^4). Cells were cultured for 24, 48, 72 and 96 hours and cell number at each time point was assessed by flow cytometry using CountBright™ beads (Invitrogen). Cells were resuspended in 300 µL PBS and 25 µL beads were added. Cell count was determined using the equation: (# cell events expressing relevant fluorescent reporter/ # bead events) X (Lot # concentration/ volume of sample). At 24 and 72 hours, FAP expression was assessed in the stromal cell lines by gating on mNeptune$^+$ events.

2.8 Killing assays

2.8.1 Specification of cell death populations in killing assays

The prostate cancer cell lines LT-PL, LT-PLP, LT-DU145 and LT-DU145P and the stromal cell line mN-MRC5hT were plated either alone or as mixed MRC5hT:PCa co-cultures. This was performed at an 8:1 MRC5hT:PCa ratio for a total of 1 x 10^5 cells/well in a 24 well plate in 500 µL D10. Twenty-four hours later, 0.5 x 10^5 P4 or P4Tr CAR

[Figure 2.1] transduced T cells were washed with PBS, resuspended in 500 µL R5 and added to the MRC5hT/PCa monolayers for a 1:2 effector to target (E:T) ratio. Twenty-four hours later, 200 µL supernatant was collected for cytokine analysis and the monolayers were trypsinised and resuspended in 300 µL D10 with 25 µL CountBright™ beads (Invitrogen) and analysed using flow cytometry. Cell number of each population (identified by their individual fluorescent reporters) was calculated as stated before [section 2.7.5] and compared to T cell untreated monolayers to determine the percent viability.

2.8.2 Enzyme-Linked Immunosorbent Assay (ELISA)

Cytokines secreted during the killing assays were quantified by ELISA. T cell production of the pro-inflammatory cytokine interferon-γ (IFN-γ) was analysed using the DuoSet® Human IFN-γ kit (R&D Systems) and manufacturer's instructions were followed. Samples collected were diluted 1:30 with reagent diluent for the assay. Additionally, the production of the proliferative cytokine IL-2 was measured using the Human IL-2 Uncoated ELISA kit (Invitrogen) and manufacturer's instructions were followed. Samples collected were diluted 1:15 with ELISA diluent for the assay. For both ELISA procedures, capture antibody was diluted and coated on 96 well plates. Plates were washed with wash buffer and blocked at room temperature for 1 hour with the appropriate reagent. Diluted samples and standards were added to the plates and incubated overnight at 4˚C. The detection antibody was added to washed plates and incubated at room temperature for 1 hour (IL-2) or 2 hours (IFN-γ). Plates were washed and a working dilution of streptavidin-HRP was added for 20 minutes (IFN-γ) or 30 minutes (IL-2) at room temperature in the dark. Plates were washed and incubated at room temperature in the dark with the substrate solution until the plate developed according to the standard curve (20-30 minutes). The stop solution was added and plates were read immediately.

The absorbance of both ELISAs were read on a FLUOstar Omega (BMG LABTECH) plate reader at 450 nm wavelength.

2.8.3 Cell viability assay

The 3-(4,5-dimethylthiazol-2-yl)-2,5-diphenyltetrazolium bromide (MTT) assay was used to determine cell viability of monolayers by the processing of MTT in metabolically active cells to produce purple formazan crystals. Cell supernatant was aspirated and cells were washed with PBS before 500 µg/mL MTT (Sigma) in D10 was added at 500 µL/well. Cells were incubated at 37˚C for 1.5 hours. The MTT was aspirated and the resulting formazan crystals were dissolved in 300 µL dimethyl sulfoxide (DMSO) (VWR). Absorbance was read on a FLUOstar Omega (BMG LABTECH) plate reader at 570 nm and the percentage of viability was calculated as: (absorbance/absorbance of untreated) x 100.

2.8.4 Restimulation assays

Continuous killing assays were set up to determine the persistence and proliferation capacity of CAR T cells with and without cytokine/immunocytokine supplementation. Monolayers of PCa/MRC5hT were plated as before [section 2.8.1]. Twenty-four hours later, 0.001 mg/mL eFAP-4 was added to the media of respective wells and incubated at 37˚C for 1 hour. The media was aspirated and replaced with 500 µL fresh D10. P4 or P4Tr CAR T cells were washed with PBS, resuspended in 500 µL R5 media and added at 0.5 x 10^5 cells/well. Interleukin-4 (Peprotech) was added to the corresponding cultures at a 2 nM concentration. Twenty-four hours later, 100 µL supernatant was collected for cytokine analysis. At 72-96 hours after addition to monolayers, CAR T cells were collected, centrifuged at 800 x g for 5 mins, resuspended in 500 µL fresh R5 and counted using trypan blue. All of the CAR T cells were added onto fresh monolayers that had been

plated the day before and treated as above with either eFAP-4 or IL-4. T cell restimulations onto new monolayers were continued until killing was no longer observed. After the removal of CAR T cells, monolayers were subjected to MTT assays [section 2.8.3] to determine killing capacity with and without eFAP-4/IL-4 addition. After 3 antigen stimulations on monolayers and the last stimulation, CAR T cells were collected for flow cytometric analysis of markers including CD8, CD4, PD-1 and CD44. The CD8:CD4 ratio was recorded as the percentage of $CD8^+$ cells/$CD4^+$ cells and the deviation from the baseline.

2.9 *In vivo* experiments

All animal experiments were in accordance with the UK Home Office guidelines as outlined in project licence numbers 70/7794 and P23115EBF and under the authority granted by personal licence number, I31DF0FE0. The mice used were male NOD scid gamma (NSG) mice with ages ranging from 7-20 weeks old. Mice used for fluorescent imaging were kept on an alfalfa-free 5V75 diet (LabDiet®).

2.9.1 Establishment of PCa/MRC5hT xenograft models

The prostate cancer lines LT-PL, LT-PLP, LT-DU145 and LT-DU145P and the fibroblast line mN-MRC5hT were trypsinised, washed with PBS and mixed at an 8:1 ratio of MRC5hT:PCa. Complete matrigel matrix (BD BioSciences) was thawed overnight on ice in the cold room. A total of 9 x 10^5 mixed cells were resuspended in either 200 µL PBS, or resuspended in 100 µL PBS and mixed with 100 µL matrigel. Mice aged 11-20 weeks were injected with the tumour cells subcutaneously (SC) into the right flank using 23G needles (Terumo). Each group consisted of 3-4 mice. Tumour growth was monitored using bioluminescent imaging (BLI) and *in vivo* fluorescence imaging on an IVIS® Lumina Series III (Perkin Elmer) system. Bioluminescence imaging was performed after

administration of 200 µL of the substrate D-luciferin (Source BioScience) at 15 mg/mL. This was injected intraperitoneally (IP) using 29G insulin needles (Terumo). Mice were anaesthetised using vaporised isofluorane and imaged 12 minutes post injection. In order to image MRC5hT engraftment, mN-MRC5hT, PLP and DU145P were trypsinised, washed with PBS and mixed at an 8:1 ratio of MRC5hT:PCa. A total of 9 x 10^5 mixed cells or mN-MRC5hT alone were resuspended in 100 µL PBS and mixed with 100 µL matrigel and injected SC into the right flank of mice. Mice were anaesthetised and imaged using *in vivo* fluorescence imaging on an IVIS® Lumina Series III (Perkin Elmer). Weight was monitored as indications of toxicity. At the end of the *in vivo* experiment, mice were sacrificed using cervical dislocation and tumours were resected and temporarily stored in PBS. Tumour tissue was cut in half using a scalpel and either snap frozen in Tissue-Tek® OCT compound (Sakura) on dry ice and stored at -80˚C, or digested for flow cytometric analysis. Digestion involved weighing the tissue and mincing finely using a scalpel, followed by shaking incubation at 37˚C for 1 hour in Tissue Digestion Buffer at 3 mL/0.5 g of tissue. Tissue was strained through 40 µm cell strainers (Fisher Scientific), washed with PBS, and single cell suspensions were stained for flow cytometry.

2.9.2 *In vivo* efficacy study

The prostate cancer cell line LT-PLPFAP, transduced to express the FAP antigen and the reporter gene LT, was trypsinised, washed with PBS and resuspended to a total of 2.5 x 10^5 cells in 200 µL PBS. Mice aged 7-9 weeks were injected with the cells SC into the right flank using 23G needles (Terumo). Each group consisted of 3 mice. On day 12 post tumour inoculation, 250 pmols of either IL-4 (Peprotech) or eFAP-4 diluted in 200 µL PBS was injected IP into relevant treatment groups. T cells transduced with either P4 or P4Tr and expanded for 11 days in IL-4 [section 2.5.4] were washed with PBS and resuspended to 1 x 10^6 CAR^+ T cells in 200 µL. CAR T cells were injected intravenously

(IV) 20 minutes after IL-4/eFAP-4 injection into corresponding treatment groups. Control group mice received 200 μL PBS injections IP and IV. A subsequent 3 IP injections of IL-4/eFAP-4 were administered 2, 4 and 7 days after CAR T cell injection. Tumour growth was monitored using BLI and weight recorded as stated above [section 2.9.1]. Mice were sacrificed, tumours harvested, digested and frozen as previously described [section 2.9.1].

2.10 Histochemistry

2.10.1 Haematoxylin and Eosin (H&E) staining

Frozen tumours were cut into 6 μm sections using a cryostat and stained with Haematoxylin and Eosin by the Pathology Services at Bart's Cancer Institute.

2.10.2 Immunohistochemistry (IHC)

Frozen tumours were cut into 6 μm sections using a cryostat and stained for mouse αSmooth Muscle Actin (αSMA) and mouse/human FAP (Abcam) by the Pathology Services at Bart's Cancer Institute.

2.10.3 Fluorescence microscopy

Frozen tumours were cut into 6 μm sections using a cryostat by the Pathology Services at Bart's Cancer Institute. Slides were fixed in 4% formaldehyde (VWR Chemicals), washed 3-times in PBS and mounted using ProLong™ Gold Antifade Mountant with DAPI (Invitrogen). After drying in the dark for 24 hours, slides were imaged on an A1R Confocal microscope (Nikon) using a 10x or 20x objective lens. DAPI was used to visualise nuclei and was excited by the 405 nm laser and read in the 450/50 detection range. For tdTomato and mNeptune, the 561nm laser was used to excite both

fluorophores. The tdTomato reporter was detected in the 525/50 range and mNeptune was detected with the 595/50 filter.

2.11 Statistics

Investigation for statistical significance was performed using GraphPad Prism software (version 7) and p values < 0.05 were considered significant. Data was subjected to a student's unpaired t-test or a two-way ANOVA when stated. A Log-rank and Gehan-Wilcoxon statistical test was applied to survival curve data to determine significance.

Chapter 3: Development of a FAP-specific Interleukin-4 immunocytokine

3.1 Introduction

3.1.1 Role of Interleukin-4 in tumour immunology

Amounting data has depicted opposing effects of endogenous and exogenous IL-4 on tumour biology. There is considerable evidence to suggest that endogenous (e.g. tumour-associated) IL-4 can play an important role in cancer progression, contrasting with many anti-tumour activities that have been ascribed to exogenous IL-4. Pre-clinical models indicate that IL-4 promotes tumour progression and metastasis through multiple pathways (Venmar et al., 2014). Interleukin-4 polarises immunity towards a Th_2 response which is generally considered to be less favourable to anti-tumour activity (Kumar et al., 2017). Illustrating this, higher levels of IL-4 have been detected in the tumour draining lymph node in a CT26 mouse colon cancer model, associated with skewing of the response towards a Th_2 phenotype through increased expression of Th_2 associated cytokines including IL-5, IL-10, IL-13 and TGF-β. The same upregulation of IL-4 in the draining lymph node is present in mouse tumour models of TC-1 lung and 4T1 breast carcinoma. When IL-4 is knocked down in the lymph nodes, a reduction in tumour growth is seen. In the same study, macrophages within the tumour microenvironment are polarized towards a M2 immunosuppressive phenotype as a result of IL-4 (Shirota et al., 2017). Analysis of the tumour microenvironment of primary breast cancer shows an expansion of IL-4 and IL-13 secreting $CD4^+$ T cells. Dendritic cells within the breast cancer samples also express OX40L, which promotes a Th_2 response, and supernatant from these breast cancer tissues polarize healthy dendritic cells further propagating the Th_2 arm of immunity (Pedroza-Gonzalez et al., 2011). Moreover, IL-4 causes $CD8^+$ T cells to become less cytotoxic (Erard et al., 1993, Kienzle et al., 2005). Tumour associated macrophages are a primary source of the protease cathepsin B and S which enhances the progression *in vivo* of RT2 tumours of a transgenic model of pancreatic cancer. These

tumours express IL-4 which is responsible for the upregulation of these cathepsins in the macrophages (Gocheva et al., 2010). In addition to dampening the host's immune response to the cancer, IL-4 has been shown to promote cancer cell survival by inhibiting apoptotic pathways. Primary cancer cells from breast, colon, lung, prostate and bladder samples all have increased expression of the anti-apoptotic proteins phosphoprotein enriched in diabetes (PED), cellular FLICE-inhibitory protein (cFLIP), B-cell lymphoma-extra large (Bcl-xL) and B-cell chronic lymphocytic leukaemia/lymphoma 2 (Bcl-2) as well as IL-4, consistent with autocrine/paracrine survival promotion. Following the abrogation of IL-4 signalling with a blocking antibody, there was a decrease in the expression of these anti-apoptotic proteins, accompanied by tumour cell sensitisation to chemotherapy and CD95 (Fas)-induced cell death (Conticello et al., 2004, Todaro et al., 2008). Many cancer types exhibit an increased expression of IL-4Rα that correlates to tumourgenicity including colon, thyroid, pancreatic, colon cancer stem cells and fibrosarcoma cancer models (Koller et al., 2010, Li et al., 2008, Prokopchuk et al., 2005, Todaro et al., 2007, Todaro et al., 2006). Some evidence for IL-4 autocrine/paracrine signalling has been shown in various pancreatic cell lines and the lung carcinoma cell line A549 due to IL-4 expression and the effects that knocking down IL-4 has on the proliferation and stemness characteristics of the cancer cells (Prokopchuk et al., 2005, Zhao et al., 2018). However, these studies do not address the expression of IL-13Rα which is necessary for IL-4 signalling in non-hematopoietic cells (Aman et al., 1996, Palmer-Crocker et al., 1996). High serum levels of IL-4 are found in colon, gastric, oesophageal and metastatic melanoma cancer patients (Baier et al., 2005, Cardenas et al., 2018, Gao et al., 2014b, Nevala et al., 2009). Circulating IL-4 levels are correlated with more advanced disease in renal cell carcinoma, pulmonary adenocarcinoma and prostate cancer and is linked to increased chances of relapse in NSCLC patients after resection (Goldstein et al., 2011, Li et al., 2014a, Onishi et al., 2001, Takeshi et al., 2005).

In contrast to the effects of endogenous IL-4, several studies suggest that exogenous IL-4 exerts anti-tumour effects against different solid tumours. In part, this is mediated through direct interaction with the cancer cells and is further contributed indirectly via the recruitment of eosinophils and $CD8^+$ T cells to the site of disease (Golumbek et al., 1991, Obiri et al., 1993, Tepper et al., 1992, Topp et al., 1995). Studies have shown exogenous IL-4 significantly inhibits the growth of colon and breast carcinoma cell lines. Furthermore, IL-4 reverses the growth advantage effects of oestradiol in breast carcinoma similar to tamoxifen and, together, IL-4 and tamoxifen elicit an additive response (Toi et al., 1992). Interleukin-4-induced growth inhibition and an increase in apoptosis has been observed in breast cancer cells which is partially explained by phosphorylation of STAT6 (Gooch et al., 2002). There is a reduction in volume of established colon cancer tumours when mice are vaccinated with IL-4 expressing colon carcinoma cells. Granulocytes are implicated in early anti-tumour response in this model, while $CD8^+$ and $CD4^+$ T cells are responsible for long-term immunity. When tumour cell vaccines are engineered to release IL-4 together with IFNα, Th_1 polarised anti-tumour responses are induced (Eguchi et al., 2005). A further potential therapeutic action of exogenous IL-4 relates to its anti-angiogenic properties (Volpert et al., 1998). One study has shown that an IL-4 secreting plasmacytoma tumour causes stromal fibroblasts to acquire a less angiogenic phenotype in the tumour microenvironment, thereby facilitating IL-4 mediated tumour rejection (Schuler et al., 2003). These pre-clinical studies prompted early clinical trials involving administration of exogenous IL-4, which disappointingly resulted in low anti-tumour efficacy. Nonetheless, administration of IL-4 was generally well-tolerated with few adverse effects, establishing a safe dose range for this agent (Gilleece et al., 1992, Majhail et al., 2004, Margolin et al., 1994, Prendiville et al., 1993, Stadler et al., 1995, Taylor et al., 2000).

The contradictory role of IL-4 in cancer progression is still being investigated. In part, the contrasting effects reported for IL-4 could be related to the study of different cancer types, cell lines and/ or model systems (Olver et al., 2007). Additionally, as indicated above, there is considerable evidence that the divergent effects of this cytokine are due to the source of IL-4 – in other words, whether it is of endogenous (intratumoural) or exogenous (therapeutic) origin. In the former case, while levels are elevated, they generally do not reach very high concentrations. By contrast, therapeutic delivery of overexpressed quantities of the cytokine can achieve local concentrations that vastly exceed those that occur in physiological or pathological states (Li et al., 2009). Therefore, high levels of intratumoural IL-4 achieved through the targeted administration of this cytokine could provide therapeutic benefit in the treatment of malignancies.

3.1.2 Use of IL-4 to support CAR T cell expansion

In order to harness endogenous IL-4 in the microenvironment of tumours, the chimeric cytokine receptor 4αβ was developed. To construct 4αβ, the ectodomain of IL-4Rα has been coupled to the βc endodomain subunit of IL-2R/IL-15R. Upon binding of IL-4, this synthetic receptor co-localises with and signals together with the common-gamma chain via the JAK/STAT pathway (Wilkie et al., 2010). When co-expressed with a CAR, IL-4 binding to 4αβ will produce an IL-2-like proliferation signal and CAR T cell specific expansion is achieved. Therapeutically, this cytokine receptor can harness increased endogenous IL-4 within tumours in order to support CAR T cells at this location. This chimeric cytokine receptor system also offers the possibility that CAR T cells may benefit from exogenous IL-4 administration. A third potential use of 4αβ is to achieve selective enrichment of CAR transduced T cells during *ex vivo* manufacture of cell products. This application of 4αβ is currently being used to enable CAR T cell manufacture from a blood

draw rather than a leukapheresis in a phase I clinical trial in patients with relapsed refractory head and neck cancer (van Schalkwyk et al., 2013). Early studies used this type of chimera to test the signalling capacity of the IL-2Rβ subunit in various T cell subsets (Gasser et al., 2000, Izuhara et al., 1993). More recently, a related chimeric receptor has been designed to take advantage of the increased levels of IL-4 associated with malignancy. Akin to 4αβ, this receptor utilizes the ectodomain of IL-4Rα, but is genetically conjugated to the endodomain of IL-7Rα. In animal models, this chimeric cytokine receptor promotes anti-tumour activity and T cell proliferation when expressed in EBV-specific T cells (Leen et al., 2014) and PSCA-targeted CAR T cells (Mohammed et al., 2017).

To ensure the CAR T cell specific proliferation and persistence *in vivo* for which the 4αβ receptor was designed, it may be beneficial to deliver additional rIL-4 to the tumour microenvironment in a targeted fashion. Conceptually, this would be preferable to IL-2 co-administration due to the adverse clinical safety profile associated with high dose IL-2 therapy (Rosenberg, 2014). Moreover, use of the 4αβ system provides a selective stimulus to the CAR T cells, reducing the enrichment of undesired cell types such as regulatory T cells. Furthermore, directed cytokine delivery to the tumour would lower the effective concentration required and decrease systemic reactions. With this foundation, the aim of this project was to target IL-4 to the tumour microenvironment using a FAP-specific antibody, thereby potentiating the proliferation and survival of co-administered CAR T cells that express the 4αβ receptor [Figure 3.1]. In particular, I set out to evaluate this system in support of the P28z second generation CAR that is targeted against PSMA (Maher et al., 2002). Human T cells engineered to express P28z have previously shown anti-tumour activity both *in vitro* (Maher et al., 2002) and *in vivo* against $PSMA^{+}$ prostate tumours (Emami-Shahri et al., 2018, Zhong et al., 2010).

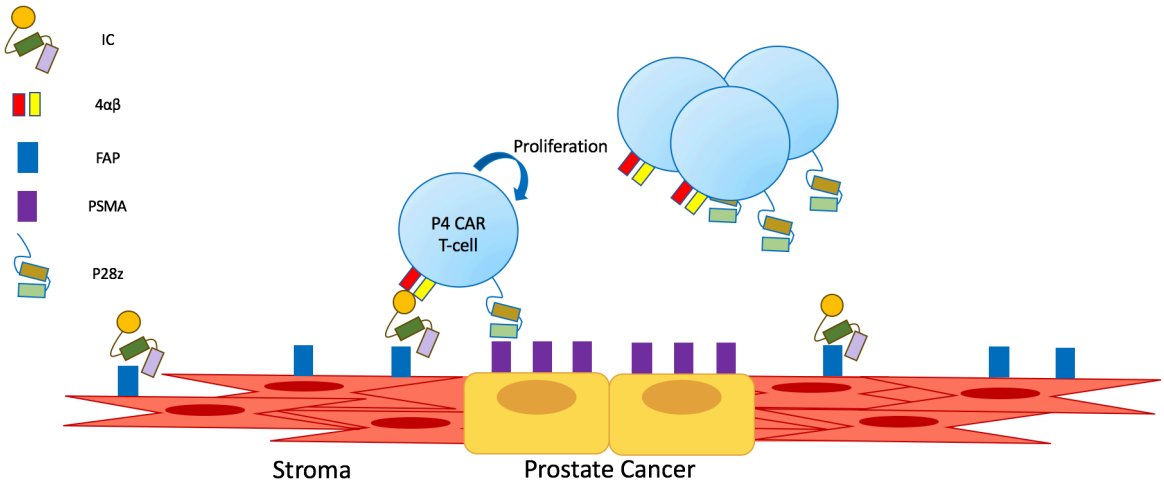

Figure 3.1 Illustration of project concept.
Localisation of the immunocytokine (IC) and the PSMA-targeting CAR (P28z) T cells co-expressing the chimeric 4αβ receptor (P4) to the tumour site via targeting the stroma and the prostate cancer cells. In this case, the immunocytokine is shown as comprising an scFv (dark green and lilac rectangles) coupled to IL-4 (orange).

3.1.3 Specific aims

1. Generate a FAP-specific scFv

2. Design and develop a FAP-targeted immunocytokine conjugated to IL-4

3. Determine the functionality of the immunocytokine

3.2 Results

3.2.1 FAP-specific hybridoma generation and screening

Mouse hybridomas specific for FAP were generated by GenScript following immunisation with the extracellular domain of the protein followed by a boost of HT1080-FAP^{+} cells. After screening of resultant hybridoma supernatants for binding to human (h) and murine FAP, 19 hybridoma clones were selected for further study. Murine FAP shares 89% homology with hFAP and cross-species binding ability was considered desirable for future toxicity assessments in mouse models (Niedermeyer et al., 1997). Antibody-containing supernatants were screened for their ability to bind to membrane-bound FAP specificity using the HT1080 sarcoma cell line that lacks FAP, making

comparison with an engineered version that highly expresses FAP [Figure 3.2A]. Using this method, 7 cell lines showed differential binding to cell-bound FAP [Figure 3.2B] and these were subsequently subcloned by GenScript (the two hybridoma lines 27C12 and 29E3 could not be subcloned).

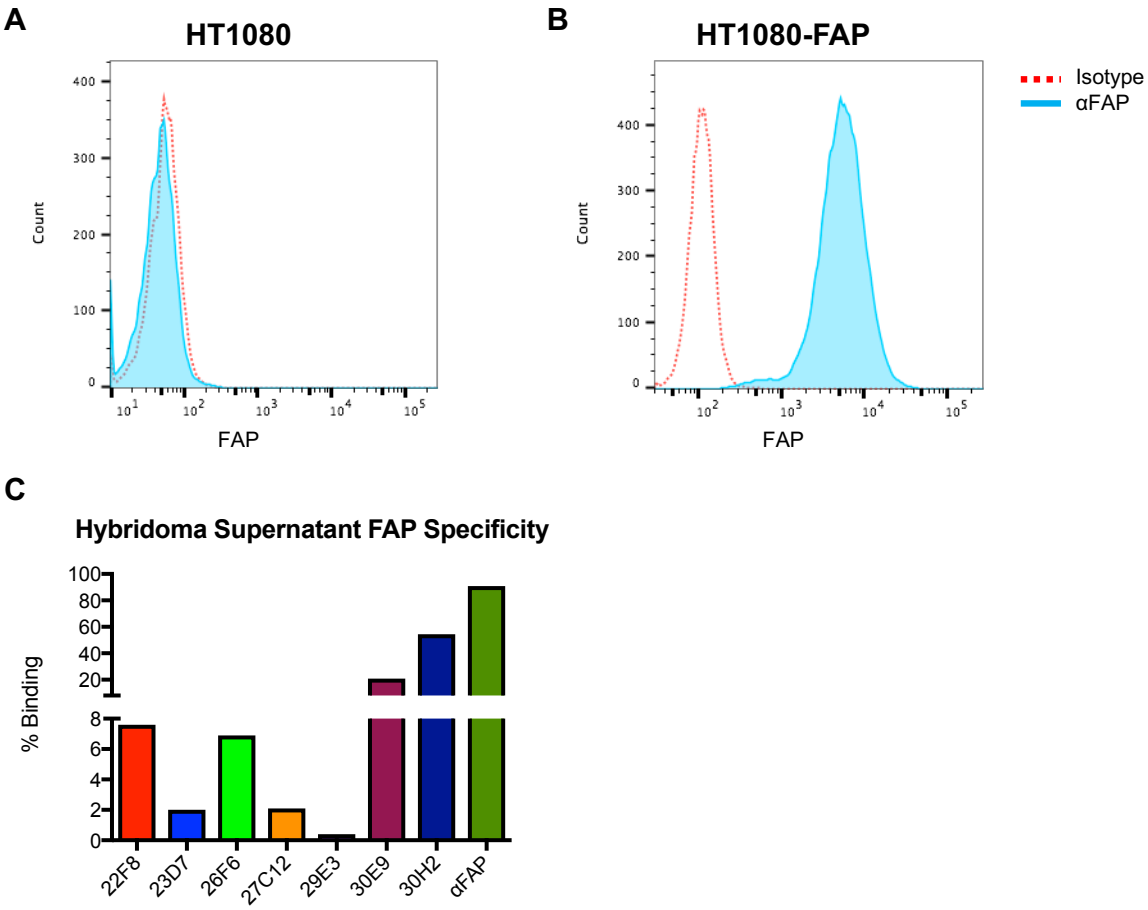

Figure 3.2 FAP-specificity screening of hybridoma supernatants.
Unpurified supernatant was collected from the indicated hybridoma cell lines and added at a 1:10 dilution to A) FAP^- sarcoma cell line HT1080 and B) HT1080 cells that had been engineered by retroviral transduction to be FAP^+. C) Seven hybridoma cell lines showed preferential binding to HT1080-FAP when compared to unmodified H1080 cells and these were sent for subcloning (n=1). αFAP is a commercially available mouse IgG FAP-specific antibody which was used as a positive binding control. This experiment was performed once prior to subcloning of hybridomas.

Two subclones were generated from each original clone and these were rescreened for production of FAP-specific antibody using the FAP^- and FAP^+ HT1080 cell lines [Figure 3.3]. The two original clones that showed the highest FAP binding, 30E9 and 30H2, maintained the highest FAP-specificity within their subclones. One subclone was chosen

from each original clone and taken forward in the project as follows 30H2B1, 22F8C6, 23D7D5 and 30E9C11 (further referred to by their subclone name which is underlined). All antibodies produced by these hybridomas were subclass IgG1, except C6 which was IgG2a. Since supernatants from 26F6A3 or 26F6A11 failed to bind membrane-bound FAP, these subclones were abandoned.

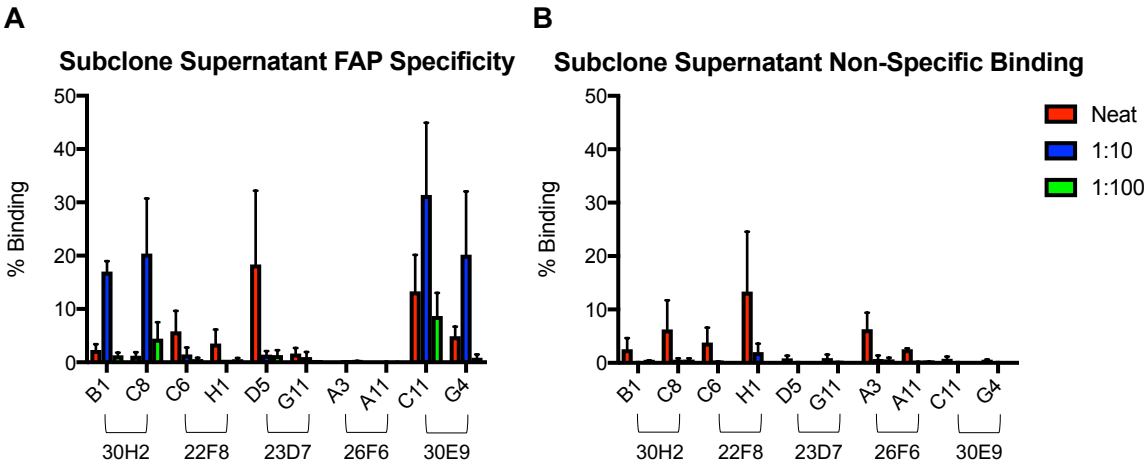

Figure 3.3 FAP-specificity of hybridoma subclones.
The subclones generated were screened again for A) FAP specific binding to HT1080FAP$^+$, or B) Non-specific binding to HT1080. Unpurified supernatant was filtered and incubated either neat (no dilution in media) or at different dilutions in D10 media (1:10 = 1 part subclone supernatant: 9 parts media; 1:100 = 1 part subclone supernatant: 99 parts media) (mean ± SEM, n=3).

Selected hybridoma supernatants were purified using Protein G GraviTrap columns (GE Healthcare). A Coomassie blue stain of an SDS-PAGE gel was performed to assess purity and to observe any aggregation. Appropriate banding patterns for IgG were visualised in reduced and non-reduced conditions. Under reduced conditions, the heavy chain can be seen at 55 kDa and the light chain is at 25 kDa while the non-reduced antibody is seen as a band at 150kDa [Figure 3.4A]. A western blot was performed using an anti-mouse IgG detection antibody and produced similar results as the protein stain for the reduced conditions [Figure 3.4B]. The two bands seen for the IgG2a C6 hybridoma in both the protein stain and western blot are most likely due to asymmetrical glycosylation (Ha et

al., 2011). A BCA assay quantification of the newly purified hybridoma antibodies showed concentrations over 1mg/mL in each case [Figure 3.4C].

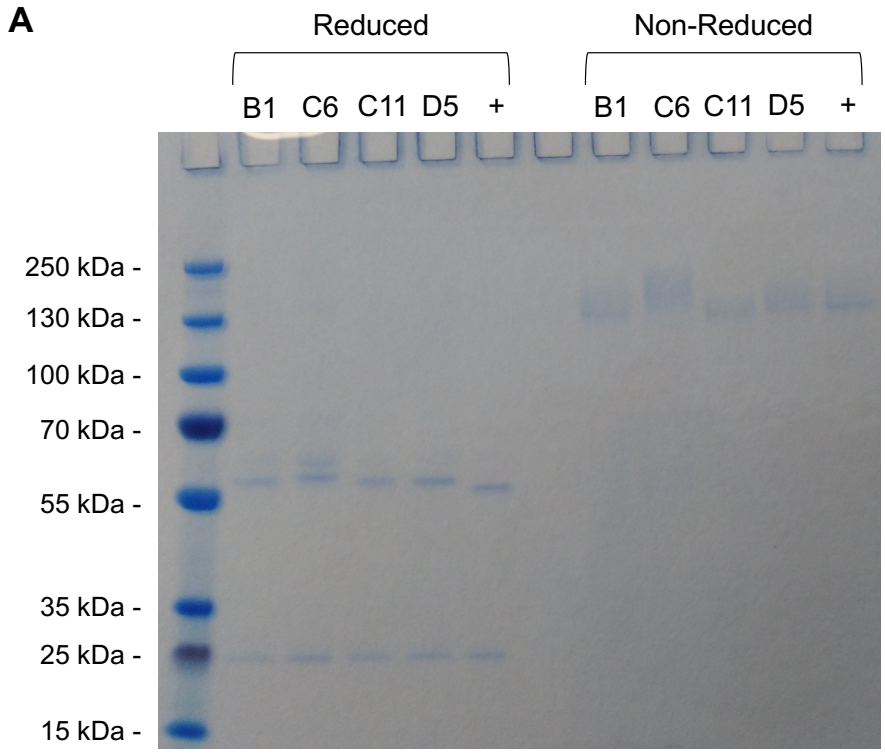

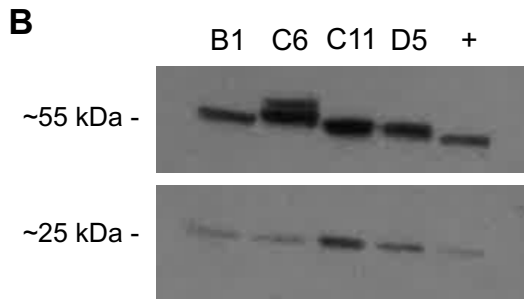

C

B1	C6
1.59 mg/mL	1.38 mg/mL

C11	D5
1.33 mg/mL	1.41 mg/mL

Figure 3.4 Purification and quantification of the hybridoma supernatant.
Purification of the hybridoma supernatants yielded no protein contamination or aggregation as seen by A) Coomassie stain or B) Western blot. C) BCA assay quantification indicated that high protein concentrations were obtained for all purified antibodies. For both A) and B) the positive control was a commercially available mouse IgG FAP-specific antibody.

Freshly purified antibody supernatants were rescreened for FAP-specificity at various concentrations. The first flow cytometric analysis showed relatively high binding capacity of the B1 and C11 antibodies and optimal binding capacity in 0.01 mg/mL at 64.5% and 29% respectively [Figure 3.5A]. However, the following screen performed 3 days later showed a marked decrease in binding capacity at every concentration [Figure

3.5B]. All subsequent screenings indicated a further reduction in binding and no non-specific binding [Figure 3.5C&D]. When protein levels were quantified again, concentrations were relatively unchanged except for C6, which had decreased by more than half [Figure 3.5E].

Although no protein aggregates were seen in the Coomassie blue stain [Figure 3.6A], it is possible that non-covalent aggregates were present but not-visible due to SDS-mediated denaturation in the gel assay. To rescue binding capabilities, antibodies were spun at 18,407 x g (14,000 RPM) for 5 mins to sediment any large aggregates. The supernatant was tested again for FAP-specific binding [Figure 3.6]. This method appeared to restore some of the antibody binding capacity in B1 and C11 at 0.01 mg/mL, suggesting potential aggregate formation after purification. There was no non-specific binding to HT1080 [data not shown].

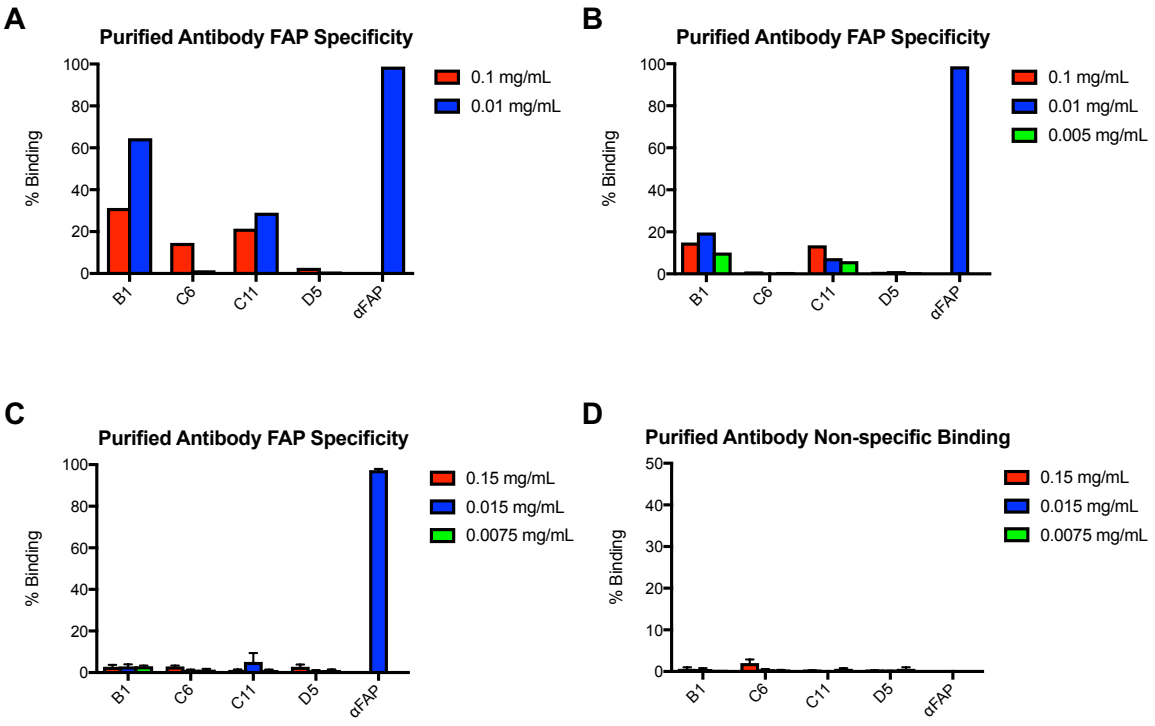

E

B1	C6	C11	D5
1.28 mg/mL	0.52 mg/mL	1.19 mg/mL	1.34 mg/mL

Figure 3.5 FAP-specificity screening of newly purified hybridoma supernatants. FAP-specific binding of antibody purified from hybridoma supernatants was investigated at various times after antibody purification using HT1080-FAP cells. A) Initial assay, performed immediately after purification, B) The second assay was performed 3 days later and C) combined analysis of the subsequent 3 assays (mean ± SEM, n=3). D) No non-specific binding to HT1080 cells was observed at any time throughout the analysis (mean ± SEM, n=3). There was no loss of FAP expression on the HT1080-FAP cell line as seen with binding of the commercial αFAP. E) A BCA assay showed that all antibody concentrations remained above 1 mg/mL, except for C6.

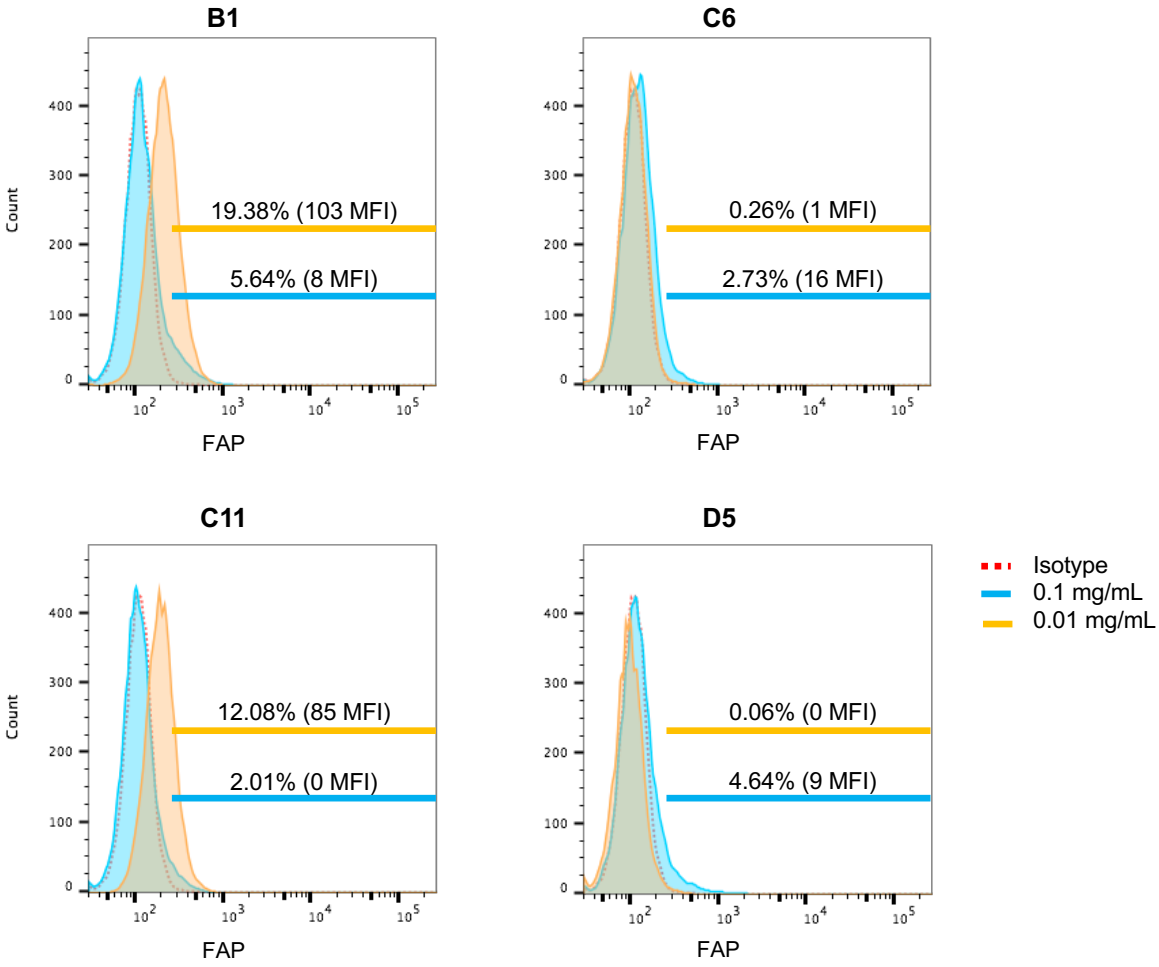

Figure 3.6 Screening of centrifuged and purified antibodies.
Purified supernatant was centrifuged to remove aggregates and screened again for the ability to bind FAP by addition to HT1080-FAP cells at the indicated concentrations. An isotype control was used to set the gate. Results shown were performed in a single experiment.

The antibodies B1 and C11 were produced, purified, quantified and screened again. This second production of the antibodies yielded lower concentrations that had been obtained previously [Figure 3.7E]. Both antibodies showed optimal FAP-binding at 0.01 mg/mL, albeit at lower levels than the 1st production round [Figure 3.7A]. As seen before, the binding capacity dropped between the first and second screening (8 days apart) and C11 had lost most of its FAP-specificity [Figure 3.7B]. In order to exclude loss of binding signal due to internalisation of the antibodies during the incubation period, primary incubations were maintained for 15 minutes, 30 minutes and 45 minutes on ice. B1 in particular show a small increase in FAP-binding with elongation of the incubation time

[Figure 3.7C]. This suggests that the loss of FAP-specificity is not due to antibody internalisation. At no point was non-specific binding to HT1080 seen [Figure 3.7D].

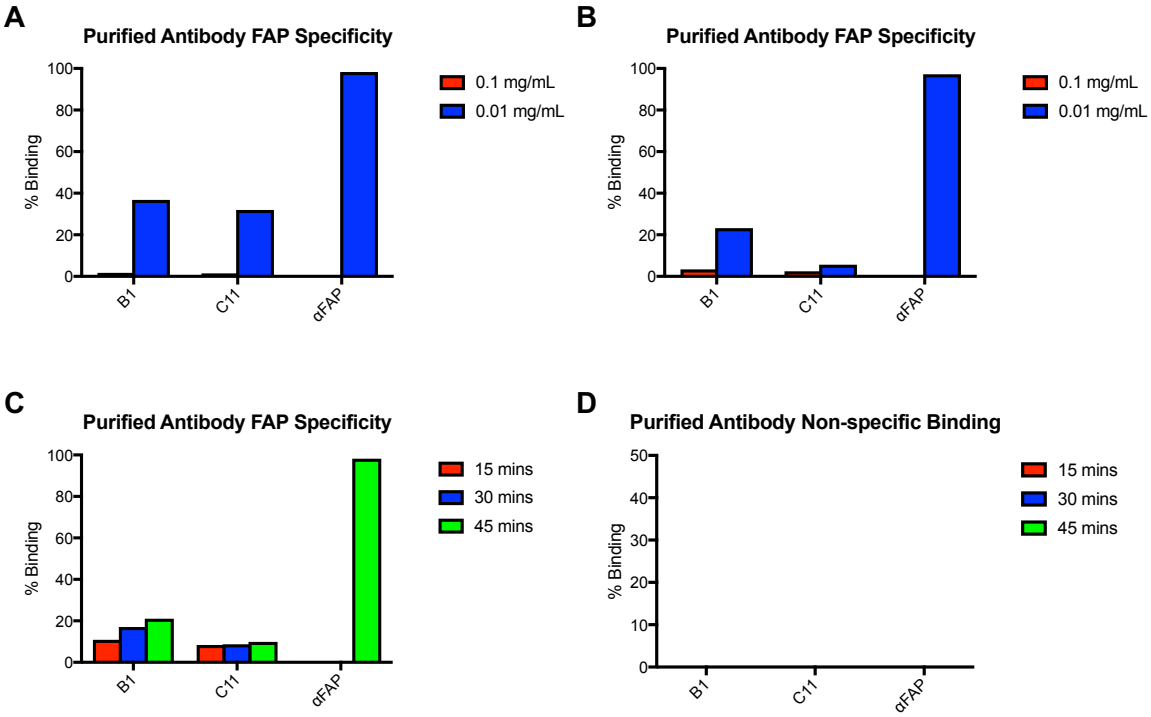

E

B1	C11
0.76 mg/mL	0.65 mg/mL

Figure 3.7 Screening of FAP-specificity of purified antibody after 2nd round of production.

Purified antibody derived from B1 and C11 were A) screened for FAP-binding after purification by addition to HT1080-FAP cells at the indicated concentration. B) They were similarly assayed once again 8 days later. C) The antibodies were tested at a concentration of 0.01 mg/mL with incubation times of 15, 30 and 45 minutes. A-C) Antibodies were screened against HT1080-FAP. D) The antibodies never bound to the FAP$^-$ HT1080 cell line (mean $\pm$ SEM, n=3). E) A BCA assay was used to quantify the purified antibodies.

3.2.2 Humanized scFv-Fc development from FAP-specific antibodies

Because B1 and C11 showed optimal FAP specificity, the variable regions were sequenced by GenScript and scFvs designed. Codon optimisation was undertaken for human cell production. Two versions of the B1-scFv were designed with reversal of the heavy and light chain variable region positioning [Figure 3.8]. A previously validated FAP-specific antibody ESC11 (Fischer et al., 2012), was incorporated as a positive

control for FAP binding. These scFv sequences were cloned into a pUC57 background vector for *E. coli* transformation and expansion.

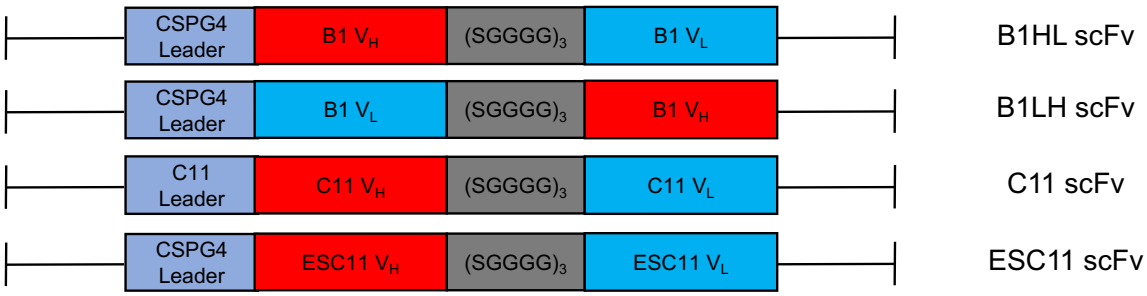

Figure 3.8 Design of scFvs for B1, C11 and ESC11.

All antibody fragments were designed to contain the CSPG4 heavy chain leader sequence except C11 for which its codon optimised endogenous heavy chain leader sequence was used, the heavy chain variable region (V_H), the light chain variable region (V_L) and a 15 amino-acid flexible serine-glycine linker. B1 included two orientations of the variable regions for testing with either the V_H in the first position, or the V_L in the first position.

The method of Polymerase Incomplete Primer Extension (PIPE) cloning was used to insert the new scFv sequences into a human heavy chain IgG1 backbone. The designated scFvs were subcloned upstream of the human IgG hinge and Fc portion to yield scFv-IgG chimeric proteins for production in mammalian cells [Figure 3.9].

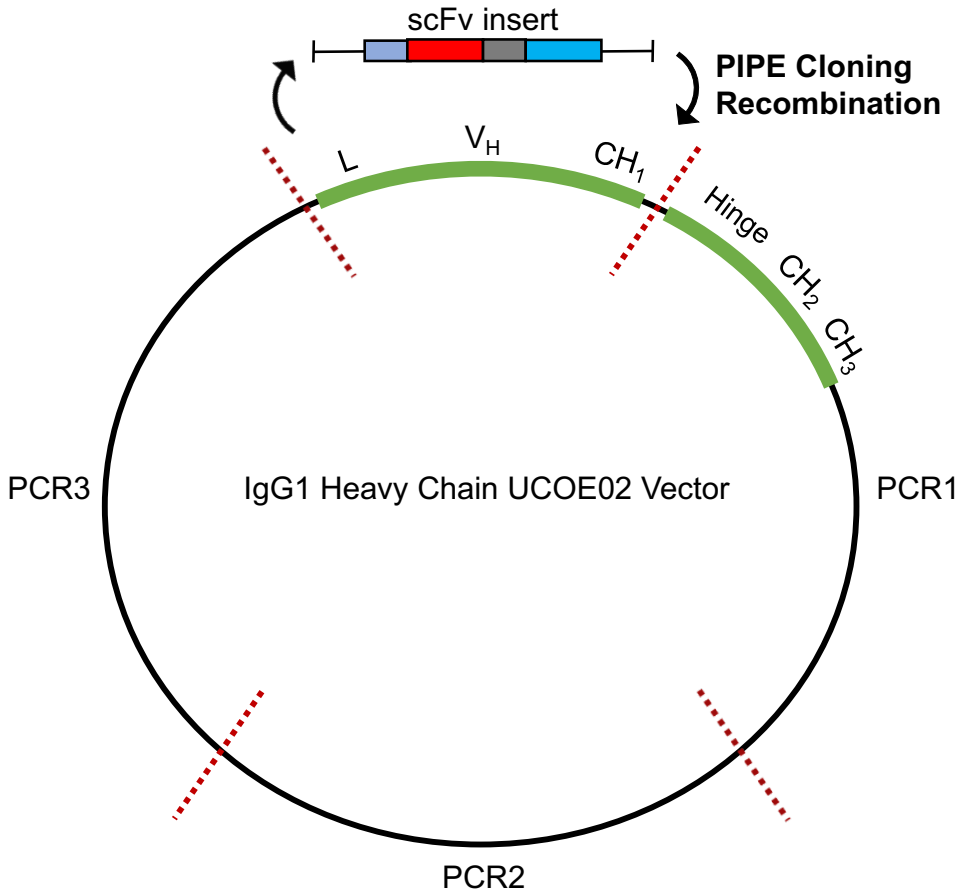

Figure 3.9 PIPE cloning method diagram
This diagram indicates where the scFv insert recombines into the vector by replacing the leader sequence (L), variable heavy chain (V_H) and the constant heavy chain 1 (CH_1). The hinge and constant heavy chain 1 (CH_1) and 2 (CH_2) remain in the vector. Dotted lines indicate the PCR fragments generated.

The PCR products were visualised on an agarose gel and were of the correct predicted size. The backbone PCR fragments produced bands as follows 1: 3726 bp, 2: 2890 bp and 3: 2422 bp. The scFv PCR bands were as follows: C11: 774 bp and B1HL/B1LH: 762 bp [Figure 3.10A]. The backbone PCR products yielded the same bands for the second round of PIPE cloning with ESC11 correctly sized at 813 bp [Figure 3.10B]. Sanger sequencing confirmed the predicted sequence of all plasmids.

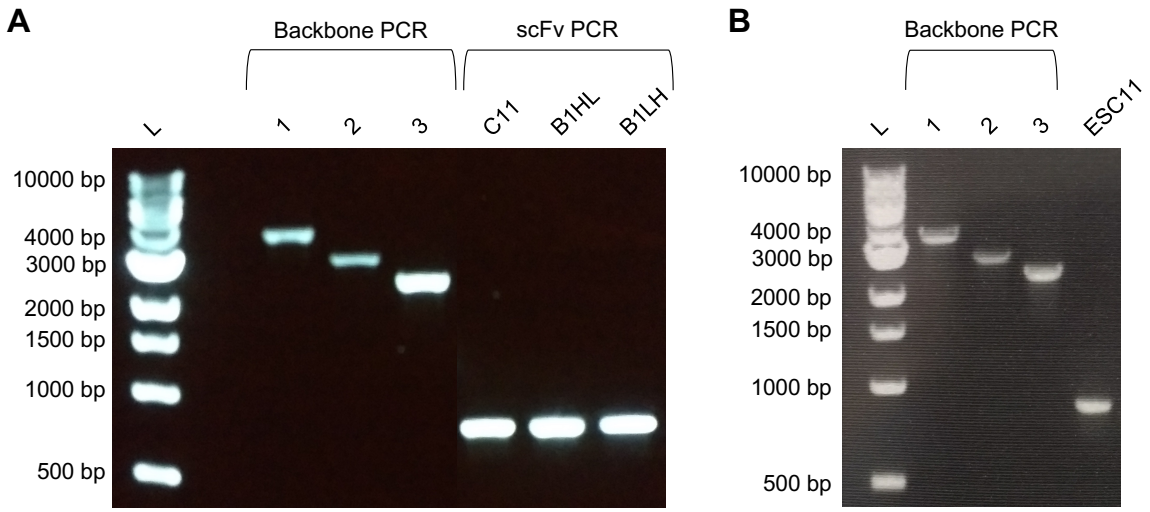

Figure 3.10 PIPE cloning PCR product analysis.
The PCR products were visualised on an agarose gel for A) scFv inserts C11, B1HL and B1LH and B) ESC11. A 1 kb ladder (L) was used.

Following expression in Expi293F™ mammalian cells and purification on a Protein G column, the scFv-Fcs were stained with Coomassie blue on an SDS-PAGE to assess their purity. This analysis revealed the presence of unidentified bands in reduced and non-reduced conditions for B1HL, B1LH and C11 [Figure 3.11A]. Aggregation was also seen in the non-reduced B1HL and B1LH scFv-Fcs, indicated by the appearance of streaks and protein stuck in the wells. The ESC11 scFv-Fc displayed bands expected for reduced (55 kDa) and non-reduced (110 kDa) conditions [Figure 3.11B]. The three distinct bands in the non-reduced condition are most likely due to alternative glycosylation. Protein yield was low for the hybridoma derived scFv-Fcs, but a high quantity of ESC11 was produced [Figure 3.11C].

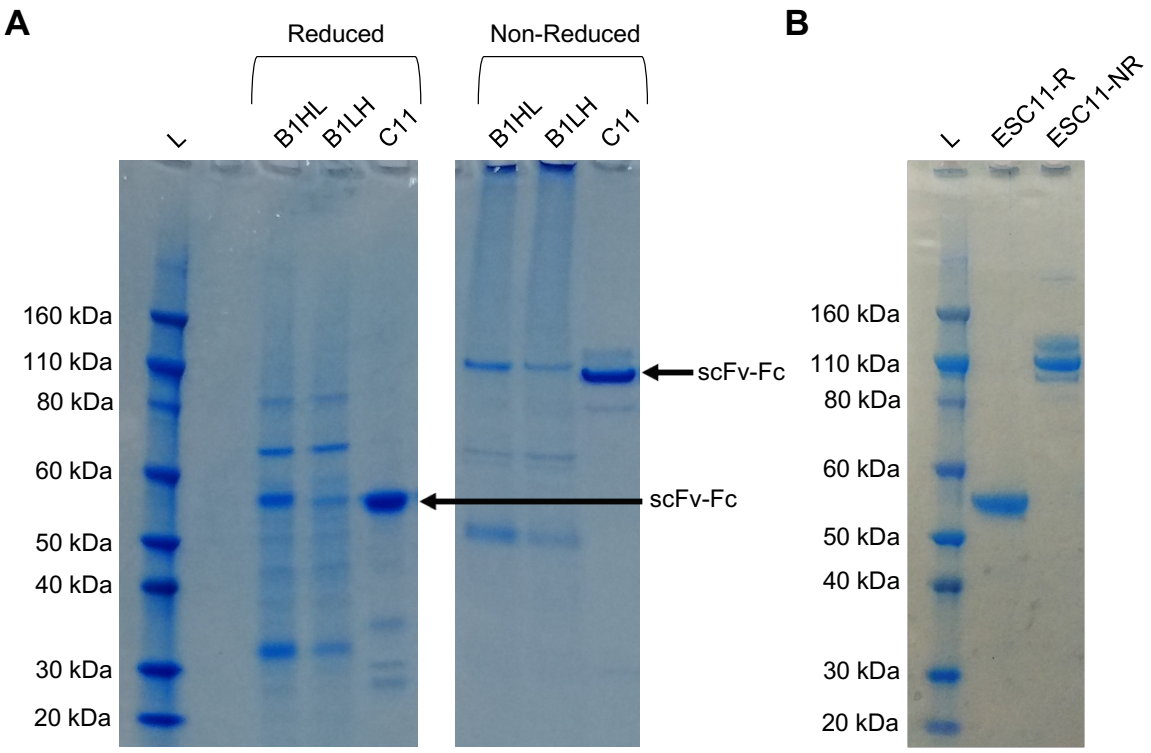

C

B1HL	B1LH	C11	ESC11
0.27 mg/mL	0.22 mg/mL	0.79 mg/mL	4.7 mg/mL

Figure 3.11 Purification and quantification of the scFv-Fc recombinant antibodies. Purified proteins were visualised on an SDS-PAGE with Coomassie blue stain for A) the hybridoma derived scFv-Fcs B1HL, B1LH and C11 (arrowed). B) The ESC11 scFv-Fc was visualised in reduced (ESC11-R) and non-reduced (ESC11-NR) conditions. For both A) and B) the Novex Sharp pre-stained protein standard was used as the ladder (L). C) The protein concentration was quantified using a Nanodrop.

Despite the apparent contaminating bands present in the new hybridoma scFv-Fc preparations, they were screened against the HT1080FAP^{+} and FAP^{-} cell lines to establish specificity of binding to FAP. Initial screening of the new scFv-Fcs indicated a high level of binding to FAP at concentrations of 0.1 mg/mL for both B1HL and B1LH, but relatively no binding for C11 [Figure 3.12A]. A small amount of non-specific binding was seen at the highest concentration of B1HL and B1LH. However similar to the native hybridoma antibodies, there was a rapid reduction in FAP binding capacity over the next 4 weeks. The hybridoma scFv-Fcs showed a higher level of binding to the FAP^{-} cell line than to the HT1080FAP in later testing [Figure 3.12B]. HT1080-FAP^{+} cells retained FAP

expression as demonstrated by maintained staining with a commercial αFAP antibody. To further exclude a spurious anomaly attributable to the HT1080 cells, two other cell lines were assessed to provide confirmatory evidence that FAP-specific binding had been lost. The pancreatic stromal cell line (PS1) naturally expresses FAP and was used to determine specific binding capacity. The prostate cancer cell line (PL) expresses little to no FAP and was used to evaluate non-specific binding. The same pattern was observed with higher scFv-Fc binding to the FAP^- PL than the FAP^+ PS1 [Figure 3.12C].

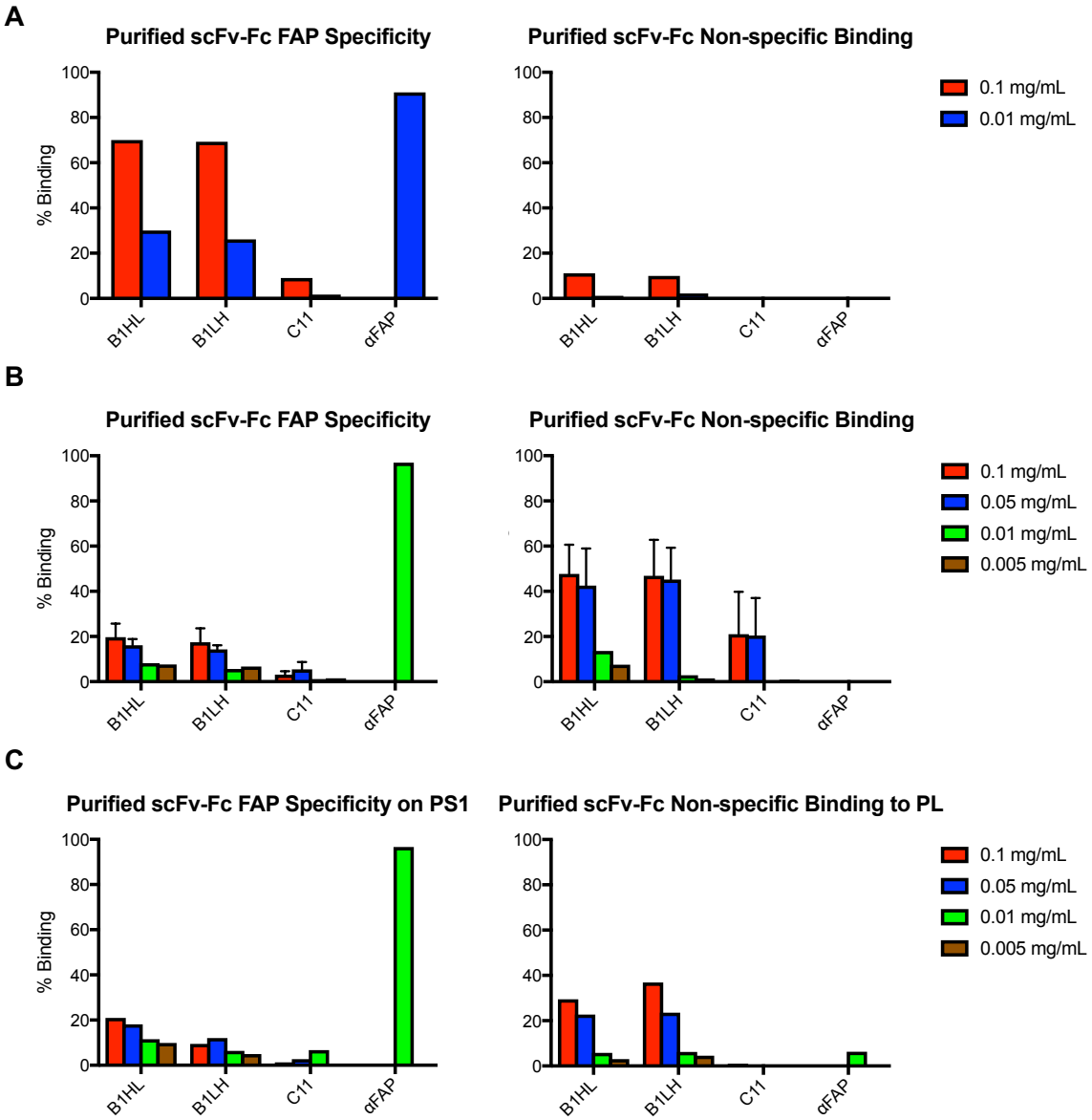

Figure 3.12 FAP-specificity evaluation of the hybridoma scFv-Fc antibodies.

The hybridoma scFv-Fc engineered antibodies were first screened for their ability to bind to the A) HT1080-FAP (left) and HT1080 cell lines (right). B) After 7 days, binding analyses to HT1080-FAP (left) and HT1080 cells (right) was repeated (mean ± SEM, n=3). C) Hybridoma scFv-Fcs were screened for their ability to bind to FAP^+ PS1 cells (left) and FAP^- PL cells (right). A commercially available αFAP antibody was used as a positive control and a relevant isotype was used to set the gate.

By contrast to the new hybridoma-derived scFv-Fc preparations, analysis of the ESC11 scFv-Fc confirmed high FAP-specificity [Figure 3.13A] with negligible non-specific binding [Figure 3.13B]. This was the case even at the lowest concentration of 0.0001 mg/mL, suggesting a strong interaction with FAP. The binding kinetics of ESC11 scFv-Fc were analysed by Biacore. High affinity of the ESC11 scFv-Fc for FAP was demonstrated [Figure 3.13C]. A two-phase decay model was fitted to the data and

indicated two kinetically different reactions. The prevailing slow K_D had a value of 120 pM and the fast K_D, which makes up 9.3% of the reactions, had a value of 40 nM [Figure 3.13C]. More than 90% of the protein-protein interaction between ESC11 scFv-Fc and rhFAP has a strong binding in the picomolar range.

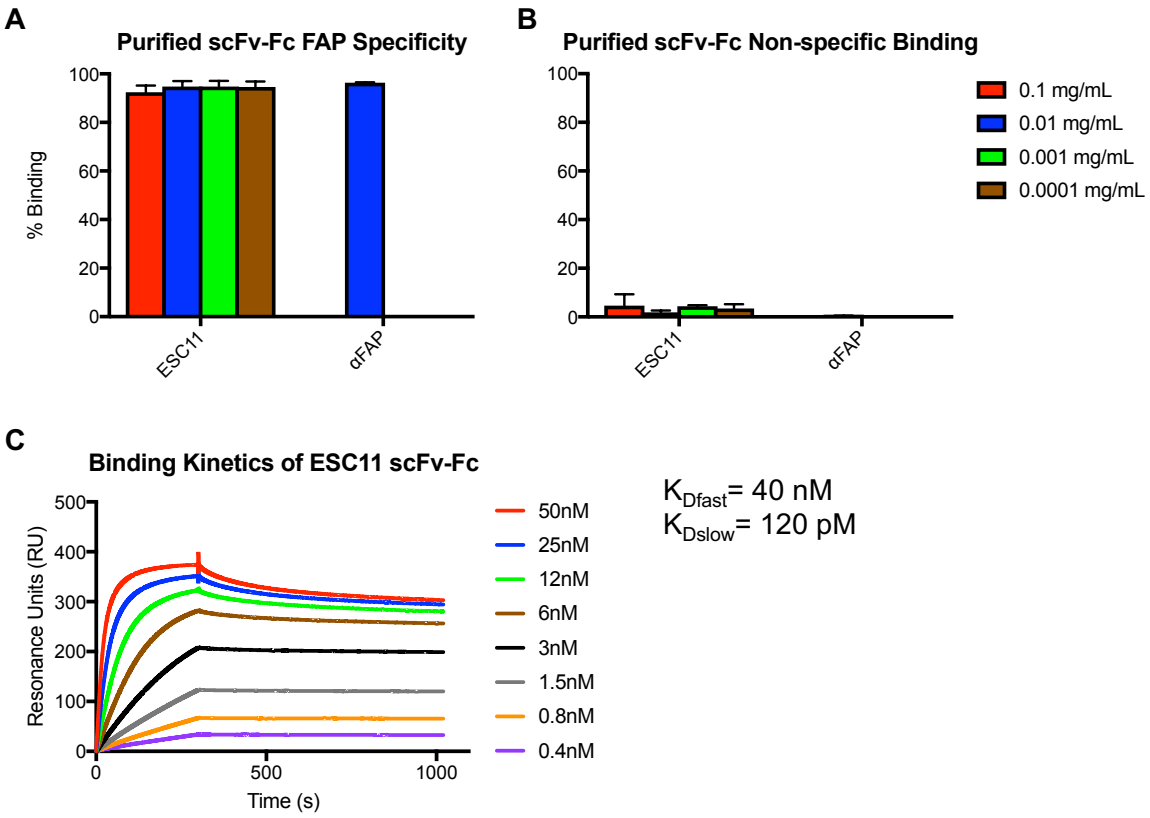

Figure 3.13 FAP-specificity and binding kinetics of ESC11 scFv-Fc.
Purified ESC11 scFv-Fc was assayed for its ability to bind to A) HT1080-FAP cells, indicating specific binding and B) HT1080 cells, for non-specific binding (mean ± SEM, n=3). B) Binding kinetics at different concentrations were plotted. The K_{Dfast} and the K_{Dslow} were calculated using a two-phase decay model fitted to the graph.

3.2.3 IL-4 immunocytokine design and function

Because ESC11 showed superior stability and FAP-specificity, this was taken forward into production of the immunocytokine designated eFAP-4. Recombinant human IL-4 was linked to the C-terminus of the ESC11 scFv via a 15-amino acid serine-glycine linker [Figure 3.14A]. eFAP-4 was cloned into a pUC57 backbone by GenScript, and then PIPE cloning was used to insert the immunocytokine into the UCOE02 lentiviral vector

(lacking the hinge-Fc portion). The PCR fragments produced bands of predicted size showing backbone PCR fragment 1 at 3042 bp, fragment 2 at 2890 bp, fragment 3 at 2422 bp and eFAP-4 at 1248 bp when analysed on an agarose gel [Figure 3.14B]. These products were validated by sequencing. The immunocytokine was produced in Expi293F™ mammalian cell cultures again and was purified using an antigen affinity column (ThermoFisher Scientific). The column covalently linked αIL-4 antibodies to activated agarose beads to immobilise eFAP-4. The success of this method of purification was seen on a Coomassie blue stained SDS-PAGE gel in non-reduced conditions [Figure 3.14C]. In the unpurified supernatant, the correct band of 49 kDa was present along with additional protein bands. After purification, only the eFAP-4 band remained, with no indication of aggregation. Purified protein yields were concentrated to around 1 mg/mL [Figure 3.14D].

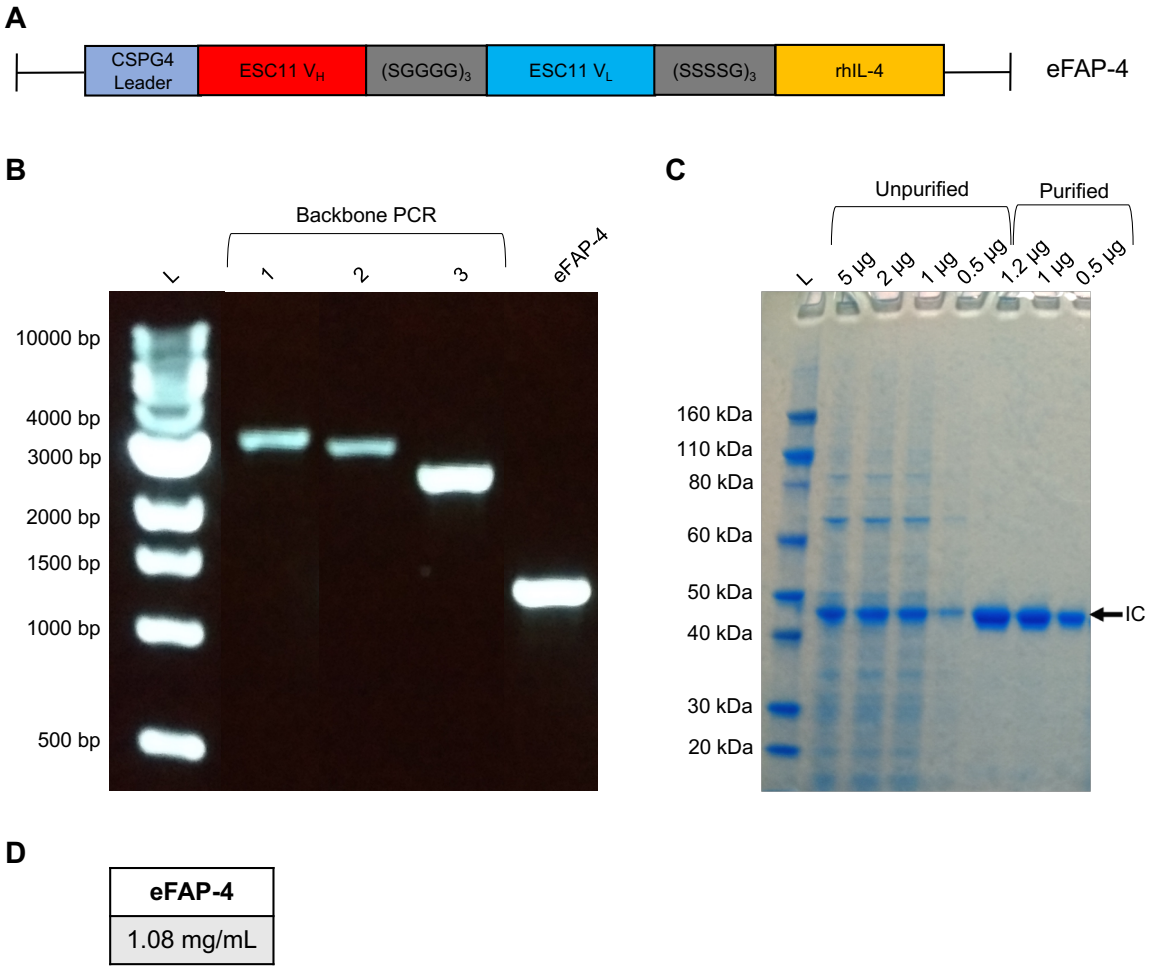

eFAP-4
1.08 mg/mL

Figure 3.14 Design, production and purification of the eFAP-4 immunocytokine.
To design the immunocytokine, A) recombinant human (rh) IL-4 was conjugated to the previously designed FAP-specific ESC11 scFv. B) PIPE cloning products were visualised on an agarose gel. C) Unpurified and column purified supernatants were analysed on a non-reduced Coomassie blue stained SDS-PAGE gel at labelled loading concentrations. Arrow indicates the bands representing the eFAP-4 immunocytokine (IC). D) Purified eFAP-4 was quantified using a Nanodrop with a calculated extinction coefficient using the ExPaSy ProtParam tool.

Purified eFAP-4 was assessed for FAP-specificity using HT1080-FAP cells, making comparison with parental HT1080 cells. The immunocytokine retained its original specificity for FAP and had no off-target binding activity [Figure 3.15]. While the percentage binding was the same across the different concentrations tested [Figure 3.15A-B], the median fluorescence intensity was the greatest at the concentration of 0.001 mg/mL and significantly decreased at a concentration of 0.0001 mg/mL [Figure 3.15C-D]. For this reason, it was decided that this is the optimal immunocytokine concentration to bind cell-bound FAP.

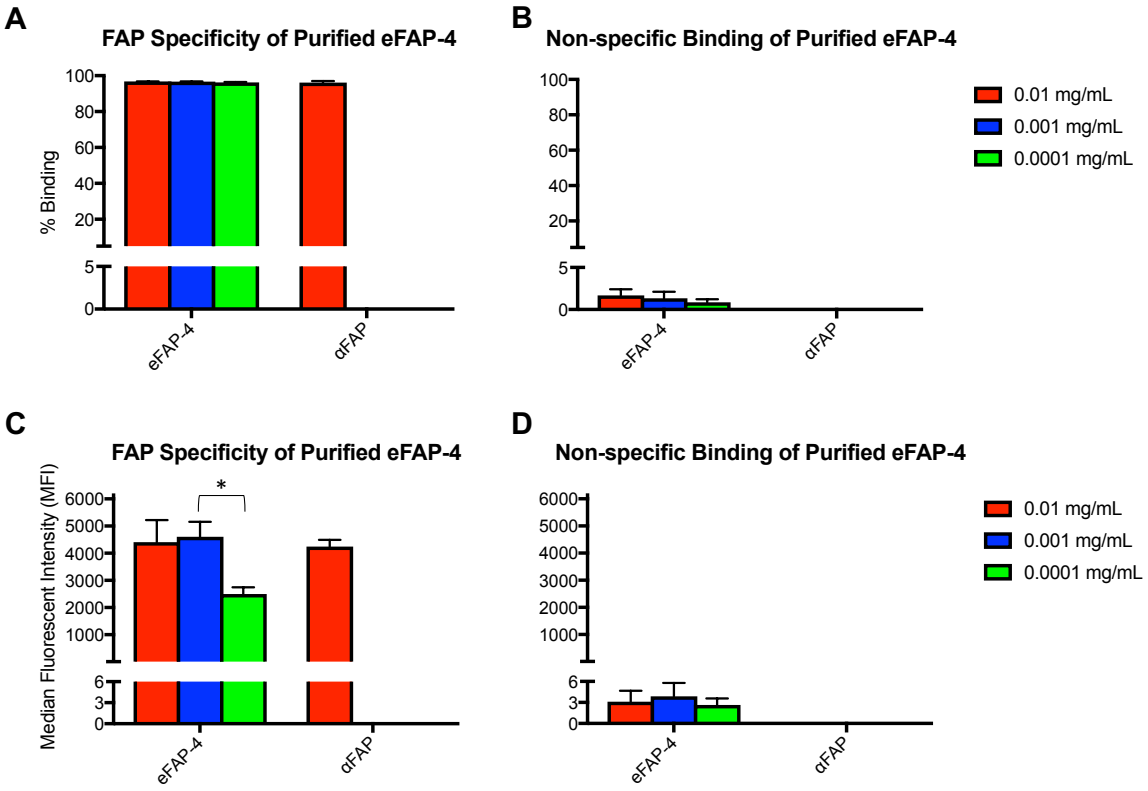

Figure 3.15 FAP-specificity of the eFAP-4 immunocytokine.

Specificity of the eFAP-4 immunocytokine for FAP was quantified by performing binding studies with A) HT1080-FAP cells (specific binding) and B) HT1080 cells (non-specific binding) (mean ± SEM, n=3). C) The median fluorescent intensity (MFI) signal was also determined for FAP-specific binding to HT1080-FAP cells and D) FAP non-specific binding to HT1080 cells (mean ± SEM, n=3). Statistical significance was determined using a student's t-test (* = $p < 0.05$).

To confirm these findings, similar binding studies were performed using two FAP$^-$ prostate cancer cell lines (PLP and DU145P) and one stromal line, (MRC5hT), which strongly expresses FAP [Figure 3.16]. As expected, the immunocytokine did not bind the FAP$^-$ prostate cancer lines. By contrast, eFAP-4 and the commercially available αFAP mAb bound with similar intensity to MRC5hT cells.

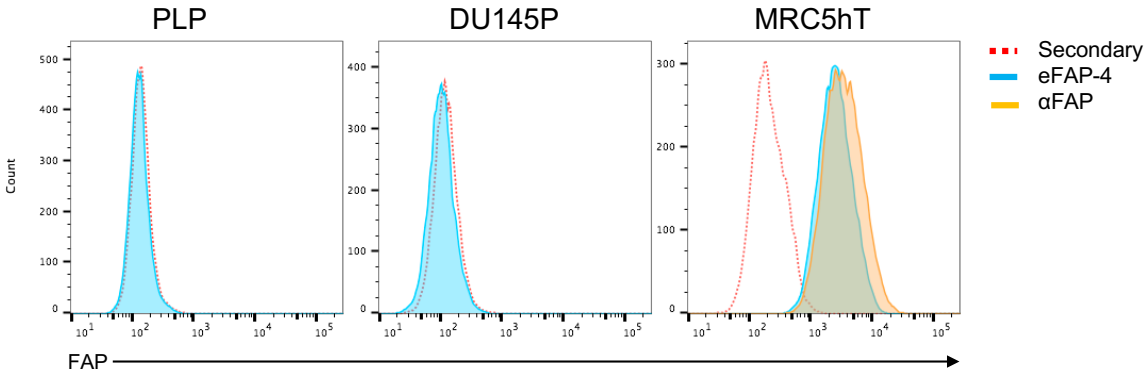

Figure 3.16 eFAP-4 binding to other cell lines.
The eFAP-4 immunocytokine was incubated with the two FAP$^-$ prostate cancer cell lines, PLP and DU145P, and the FAP$^+$ stromal cell line MRC5hT at 0.001 mg/mL. Binding of eFAP-4 was subsequently detected with an αIL-4 antibody. Expression of FAP in MRC5hT cells was confirmed with a commercial αFAP antibody. Data are representative of 3 replicates which yielded similar results.

The functionality of the cytokine signalling properties of eFAP-4 was tested using an IL-2 dependent murine leukaemic cell line, CTLL-2. While the parental line requires IL-2 to survive and proliferate, expression of 4αβ renders these cells IL-4 responsive (Wilkie et al., 2010). Following retroviral transduction, expression of 4αβ in CTLL-2 cells was determined by staining for the human IL-4Rα [Figure 3.17A]. CTLL-2 and CTLL-4αβ cells were cultured for 6 days with either IL-2, IL-4 or eFAP-4 and were counted to monitor their expansion [Figure 3.17B]. Parental CTLL-2 cells only expanded in the presence of IL-2. By contrast, CTLL-4αβ expanded in all cytokine conditions but failed to expand in the absence of cytokine support. There was no statistical difference between the various concentrations of IL-4 and eFAP-4, suggesting comparable 4αβ chimeric receptor occupancy and signalling at the range of concentrations tested.

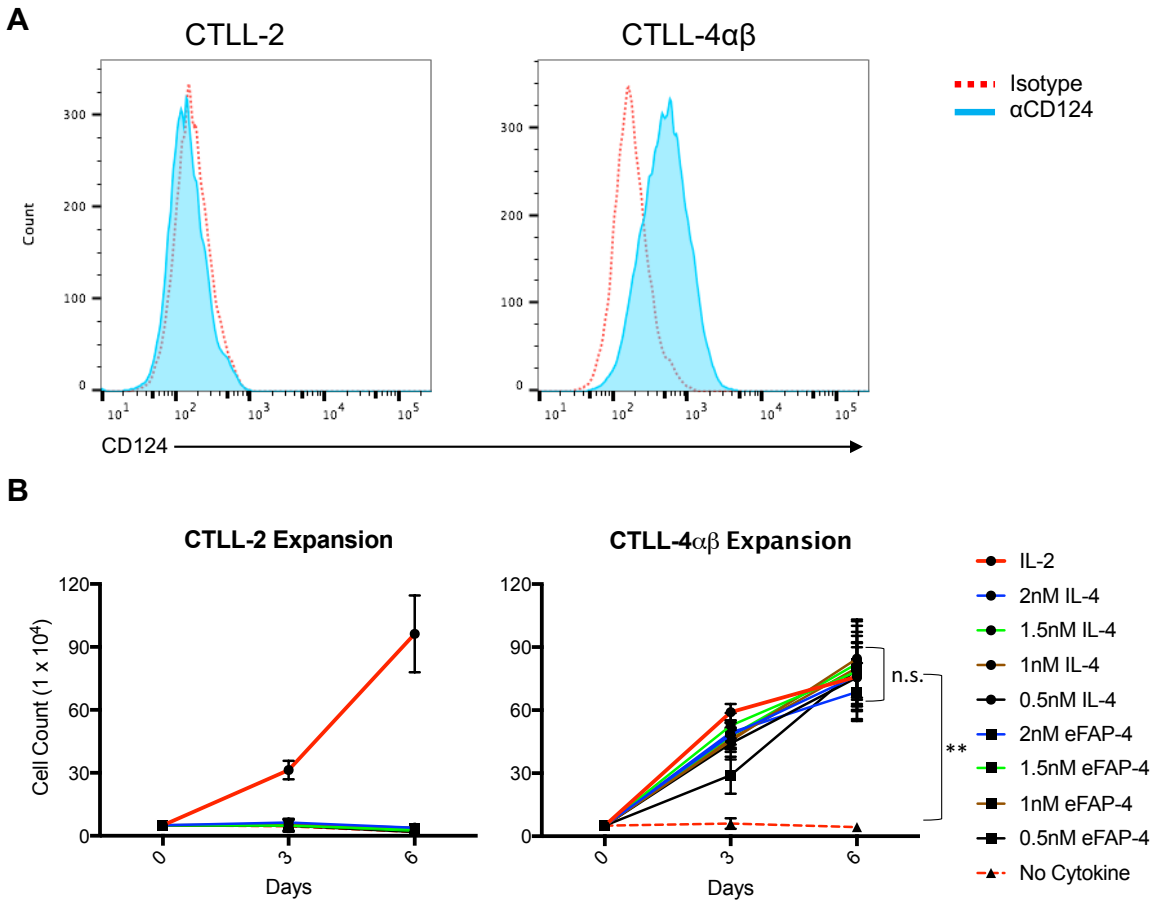

Figure 3.17 eFAP-4 signalling through the 4αβ receptor.
Functional binding of the IL-4 portion of eFAP-4 was validated using a CTLL-2 model system. A) CTLL-2 parental cells were transduced to express the 4αβ chimeric cytokine receptor. Expression was demonstrated by staining with anti-CD124-PE. B) Cell growth was determined by manual counting at days 3 and 6 post seeding of $5x10^4$ cells/well (mean ± SEM; n=3). CTLL-2 and CTLL-2-4αβ cells were cultured with the indicated concentrations of IL-2, IL-4 or eFAP4. A two-way ANOVA test was used to determine statistical significance between the cytokine conditions (n.s. – not significant) (2 nM eFAP-4 vs. no cytokine = **) (** = $p < 0.01$).

3.3 Discussion

Fibroblast activation protein (FAP) has been validated as a tumour stroma-associated target for cancer immunotherapy. Co-expression of the 4αβ receptor with a CAR results in effective expansion of CAR^+ T cells when cultured with IL-4 (Wilkie et al., 2010). This led to the hypothesis that the anti-tumour activity of CAR^+ T cells that co-express the 4αβ receptor could be potentiated through the FAP-dependent delivery of IL-4 to the tumour microenvironment at high concentration. To exploit this for therapeutic benefit, I set out to engineer a FAP-directed IL-4 immunocytokine. I envisioned that this agent

would not only exert a net anti-tumour effect in its own right, but would also potentiate the anti-tumour activity of 4αβ-expressing CAR T cells.

My initial attempt to generate an in-house FAP-specific antibody via hybridoma technology yielded promising subclones. However, further manipulation of derived monoclonal antibodies demonstrated that they had poor stability. This was indicated by rapid loss of FAP-specificity for the native antibody conformations and a loss of specificity and aggregation of the hybridoma-derived engineered scFv-Fc. This could be explained through several factors. When FAP-binding capacity of original hybridoma-derived antibodies was lost, they were centrifuged to remove aggregates. Rescreening of these antibodies showed a moderate rescue of binding. This result suggested the presence of aggregation, even though none could be visualised on a gel. Murine hybridoma aggregation can occur at many stages of production due to high temperature of the culturing environment, low pH during culture and purification, agitation and adsorption to container surfaces (Vázquez-Rey and Lang, 2011). The occurrence of these obstacles in both the native conformation and engineered version of the hybridoma antibodies, but not the ESC11 engineered antibody, suggests that there is an inherent stability issue with the hybridoma variable domains. The scFv-Fc antibody format has been validated (Powers et al., 2001) and shown to be compatible with successful expression in mammalian cells (Cao et al., 2009, Jager et al., 2013). Therefore, I think a reasonable explanation for the instability of the hybridoma-derived antibodies could be due to imperfect folding interactions of the variable domains. This could lead to an increased incidence of unfolding and subsequent aggregation of the protein (Honegger, 2008). Future manipulation of these FAP-specific hybridomas could investigate the benefits of humanisation through cloning of the CDRs into an established human IgG1 backbone.

This would remove the majority of the variable domains and could allow for greater protein expression and stability.

In order to move forward with the project, the validated FAP-specific antibody ESC11 was selected. This human Fab was originally produced via phage display and cloned into an IgG1 backbone for further testing. Preliminary assessment showed strong binding to human and mouse FAP, no cross-reactivity with the closely related CD26 protein and overnight internalisation of the antibody upon antigen recognition (Fischer et al., 2012). Internalisation was later shown to ensue when the antibody had a bivalent format, and monovalent Fabs did not share this characteristic. For this reason, I designed a monovalent immunocytokine in which the variable domain sequences of the ESC11 heavy and light chain were joined to generate an scFv. The binding kinetics seen in this study indicate a stronger affinity of ESC11 to hFAP than previously described (10 nM) (Renner et al., 2012). This is probably due to the format of the scFv tested. The original publication analysed the binding affinity of a Fab fragment while I produced and tested a dimeric scFv-Fc. Analysis of this material demonstrated that it had a slower off-rate and thus a higher K_D (MacKenzie et al., 1996). The ESC11 antibody also binds to murine FAP with a K_D of approximately 51 nM (Renner et al., 2012).

The CTLL-2 murine cell line provided a convenient model system to test the ability of eFAP-4 to signal through the 4αβ chimeric receptor. CTLL-2 cells are absolutely growth factor dependent and are generally propagated in IL-2 for this reason (Gillis and Smith, 1977). Cells engineered to express 4αβ can also be cultured in human IL-4. Binding of this cytokine is harnessed to deliver an IL-2/15 signal through the chimeric receptor, which can associate with the endogenous mouse common gamma chain that is also present in these cells (Wilkie et al., 2010). Since human IL-4 is inactive on the mouse IL-

4 receptor orthologue, CTLL-2 cells that do not express 4αβ cannot survive in human IL-4. Addition of the eFAP-4 immunocytokine to CTLL-4αβ but not parental CTLL-2 cells elicited strong proliferation that rivalled the effect of rhIL-4 alone. This immunocytokine also maintained comparable binding specificity and strength for FAP as was detected using the parental antibody. The functionality of both ends of eFAP-4 have been validated and further testing will be undertaken with human CAR^+ T cells.

3.4 Summary

- Two hybridoma cell lines, B1 and C11, showed superior FAP-specificity and were used to design scFv-Fc antibodies along with ESC11.
- Instability of the hybridoma-derived scFv-Fcs led to the advancement of the ESC11 engineered antibody only.
- ESC11 displayed high specificity and affinity for membrane-bound and soluble FAP.
- The immunocytokine eFAP-4 fully retains the binding capacity of the ESC11 antibody and delivers a comparable mitogenic signal to IL-4 through the 4αβ complex.

Chapter 4: Effects of eFAP-4 on P4 CAR T cells *in vitro*

4.1 Introduction

4.1.1 Prostate Specific Membrane Antigen (PSMA) as a target for immunotherapy

Prostate Specific Membrane Antigen was first identified as a transmembrane glycoprotein expressed by the prostate cancer cell line LNCaP (Horoszewicz et al., 1987, Israeli et al., 1993). Enzymatic activity of PSMA has been seen with the neurotransmitter neuropeptide N-acetylaspartylglutamate (NAAG) and polyglutamated folates (Carter et al., 1996, Pinto et al., 1996). More recently, the folate hydrolase activity of PSMA has been implicated in prostate tumour progression through phosphoinositide 3-kinase (PI3K) activation using vitamin B9 as a substrate (Kaittanis et al., 2018). While strong mRNA expression is seen in prostate malignancies, detectable levels of PSMA are found in normal prostate tissue, brain tissue, salivary glands and the small intestine (Israeli et al., 1994). Protein expression is low in normal prostate epithelia and benign hyperplasia, but increased expression correlates with the aggressiveness of the disease, Gleason score and resistance to hormone therapy (Kawakami and Nakayama, 1997). In fact, PSMA expression in prostate tumours has been shown to increase following androgen deprivation therapy (Wright et al., 1996). The highest PSMA intensity is seen in metastases, making it a good marker for metastatic disease (Wright et al., 1995). Apart from prostate cancer tissue, PSMA is also a marker of neovasculature found in many common solid tumours. Renal cell, urothelial, colon, lung, breast, testicular, neuroendocrine, glioblastoma, melanoma, pancreatic and prostate carcinomas as well as soft tissue sarcoma have shown $PSMA^+$ vasculature that is not present in healthy tissue endothelium (Chang et al., 1999b, Liu et al., 1997, Silver et al., 1997). The selective expression in malignant tissues designates PSMA as a potential therapeutic target.

Since the discovery of PSMA, numerous therapeutic applications have been developed to exploit this tumour specific antigen. Clinical trials have been designed to test PSMA targeting therapies including dendritic cell vaccines, DNA or recombinant protein vaccines as well as naked or radio-/drug-conjugate antibodies (Olson et al., 2007). While many current clinical trials focused on PSMA entail the use of imaging modalities, one specific PSMA targeting radiopharmaceutical has progressed to a phase III trial. A lutetium-177 conjugated ligand specific for the catalytic region of PSMA demonstrated an acceptable toxicity profile in patients with metastatic castrate-resistant prostate cancer (Rahbar et al., 2018, Rahbar et al., 2017). As yet, no PSMA targeting drugs have been FDA approved for cancer treatment and one indium labelled version of the αPSMA antibody implicated in its discovery has been approved for prostate cancer imaging in patients (Bander, 2006).

Good xenograft models of metastatic prostate cancer do not currently exist. To address this limitation, the castrate resistant cell line PC3 was orthotopically implanted in the prostate of immune-compromised mice and draining lymph node metastases were harvested and re-implanted with the development of the derivative cell line PC3-LN3 (PL) (Sanderson et al., 2006). This generated an aggressive prostate cancer cell line with metastatic potential. Thus, PL was selected for this project along with a more indolent established castrate resistant line DU145. Both of these cell lines are PSMA negative and were engineered to express PSMA for this project.

4.1.2 P4 CAR development

Following the discovery of PSMA, using the 7E11 monoclonal antibody which targeted the cytoplasmic tail of the protein (Horoszewicz et al., 1987), additional extracellular domain binding antibodies were developed. The J591 antibody was produced through

hybridomas generated following LNCaP and primary prostate cancer cell immunisation in mice. This antibody binds to permeabilised sections of prostate cancer and vasculature of other solid tumours similar to 7E11, but also stains viable $PSMA^+$ cells unlike 7E11 (Liu et al., 1997). The scFv portion of the antibody was used to generate a 1st generation CAR construct that demonstrated cytotoxicity towards patient derived cells and cell lines expressing PSMA *in vitro* and *in vivo* (Gong et al., 1999). Secretion of IL-2 by J591 CAR T cells was significantly increased when the target cell line co-expresses PSMA and CD80, resulting in co-stimulation of the T cells (Gade et al., 2005, Gong et al., 1999). The CAR was developed into a 2nd generation construct, P28z, that exhibits superior IL-2 secretion, CD8 and CD4 subset expansion and restimulation capacity compared to the 1st generation CAR (Maher et al., 2002). Further engineering to incorporate an alternative 4-1BB co-stimulation region into the CAR construct resulted in even greater cytokine secretion, T cell activation and persistence in mouse tumour models as well as efficacy against $PSMA^+$ vasculature of primary ovarian tumours (Santoro et al., 2015, Zhong et al., 2010). The J591 scFv has been used to demonstrate proof of concept for delivering activation and co-stimulation through separate constructs targeting different antigens, with a PSCA-specific CAR alone delivering a suboptimal T cell activation signal. Due to a lack of strictly tumour specific antigens, this new type of dual targeted CAR demonstrates enhanced tumour discernment as it requires two points of tumour associated antigen recognition for effective T cell activation (Kloss et al., 2013). The 2nd generation CAR P28z is used in the present study and co-expressed with 4αβ for CAR T cell specific enrichment (Wilkie et al., 2010), giving rise to the nomenclature 'P4'. Phase I trials are ongoing with different PSMA targeting CAR motifs, including P28z, for metastatic castration resistant prostate cancer and two trials for bladder and cervical cancer (clinicaltrials.gov NCT04053062, NCT03356795, NCT03089203, NCT03185468, NCT01140373, and NCT03692663; accessed on 23rd August 2019).

To recapitulate the stromal compartment in prostate cancer for *in vitro* and *in vivo* investigation of the immunocytokine with P4 CAR T cells, the cell lines MRC5 and PS1 were utilised. Shown in this chapter, these mesenchymal lines both express endogenous FAP, rendering them suitable to evaluate FAP-dependent immunocytokine targeting. Previous investigations performed by members of our lab indicated no murine stromal recruitment for PLP prostate cancer xenograft models. This suggested that endogenous FAP expression within the murine stroma was not a reliable target for the immunocytokine, which crosses the species barrier. For this reason, we moved to develop a human stroma/prostate cancer model and characterise the growth patterns, antigen expression and efficacy of the therapy *in vitro* for subsequent *in vivo* studies.

4.1.3 Specific aims

1. Develop and characterise reporter gene engineered PCa and stromal cell lines.
2. Establish an *in vitro* PCa/stroma model for drug development.
3. Validate P4 CAR T cell efficacy against PCa cell lines and co-cultures with MRC5hT.
4. Establish signalling capabilities of eFAP-4 through the 4αβ receptor expressed on human T cells.
5. Analyse the effects of eFAP-4 on CAR T cells during killing assays *in vitro*.

4.2 Results

4.2.1 Development and characterisation of cell lines *in vitro*

Two castrate resistant prostate cancer cell lines were used in this project: PC3-LN3 (PL), a derivative of PC3, and DU145. Both are $PSMA^-$ and were retrovirally transduced to express PSMA along with the reporter gene ffLuciferase-tdTomato (LT). The PL line stably expressed LT at around 95%. When transduced to express both PSMA and LT

(PLP), the double positive population reached 100% [Figure 4.1A]. DU145 also highly expressed the LT reporter with 95.7% positivity, but the PSMA$^+$ population (DU145P) had a decreased proportion of LT$^+$ cells, at around 87% [Figure 4.1B]. The LT negative DU145P percentage remained constant throughout the project and never outgrew the LT expressing cells [data not shown].

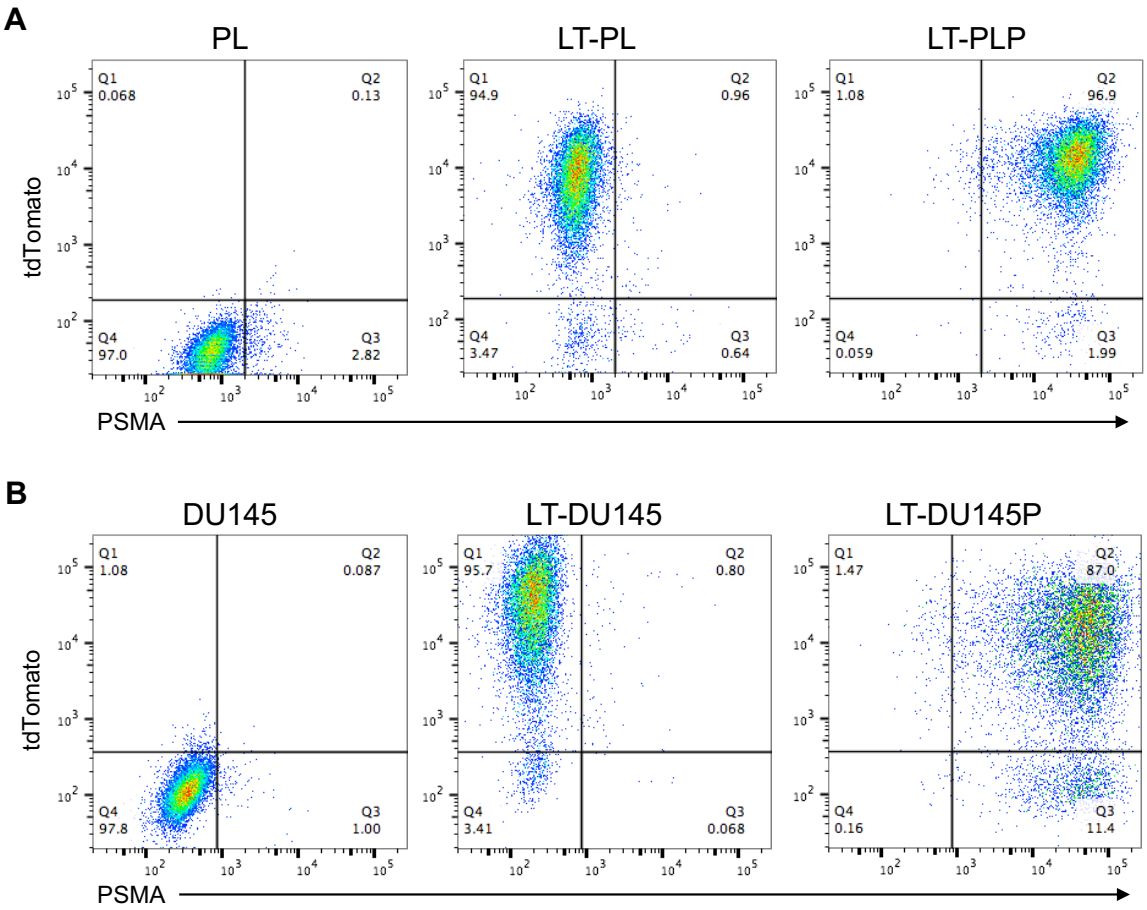

Figure 4.1 Transduction of PCa cell lines with LT and PSMA.
Retroviral vectors encoding the LT reporter and/ or PSMA were transduced into the cell lines A) PL and B) DU145. The parental double negative cell lines were stained with an isotype control for the αPSMA antibody and used to set the gate. A commercially available antibody was used to stain PSMA. The LT reporter was detected through tdTomato expression in the PE channel.

The newly generated prostate cancer cell lines were then analysed for specific antigen expression and growth kinetics. No FAP expression was detected in any of the cell lines and PSMA expression was restricted to the transduced LT-PLP and LT-DU145P cells [Figure 4.2A]. When seeded in culture and assessed over a 96-hour period, there was no

difference in growth rates between these derivatives of the same cell lines. However, the sublines of PL and DU145 showed a significant difference in expansion [Figure 4.2B]. LT-PL and LT-PLP cells underwent more rapid proliferation than LT-DU145 and LT-DU145P cells, suggesting that PL could be used to model more aggressive prostate cancer and DU145 could reflect a more indolent malignancy.

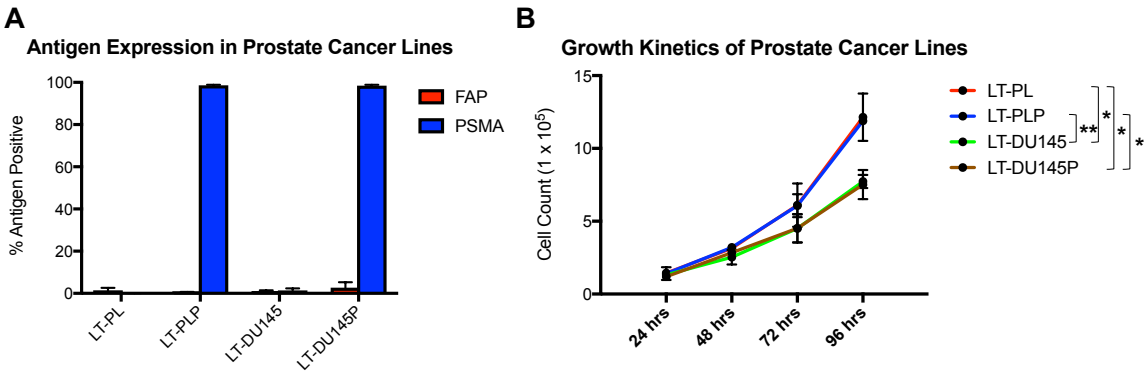

Figure 4.2 Characterisation of PCa lines.
PL and DU145 derivatives LT-PL, LT-PLP, LT-DU145 and LT-DU145P were characterised in terms of A) FAP and PSMA expression by flow cytometry and B) growth kinetics in D10 media. Significant differences between groups were determined using a two-way ANOVA (mean $\pm$ SEM, n=3) (* = $p < 0.05$; ** = $p < 0.01$).

For differential imaging of cell lines, the far-red reporter gene mNeptune was used for stroma identification. The cDNA was cloned into an SFG vector by GenScript and was visualised on an agarose gel after restriction digestion [Figure 4.3A]. The mNeptune insert was seen with a predicted band size of 737 bp and the SFG backbone at 6334 bp. This plasmid was then used to engineer a stable retroviral packaging cell line 293vec-RD114 (RD114). This resulted in a 65.6% population expression of mNeptune [Figure 4.3B]. The RD114 pseudotyped virus derived from these packaging cell lines was used to transduce stromal cells.

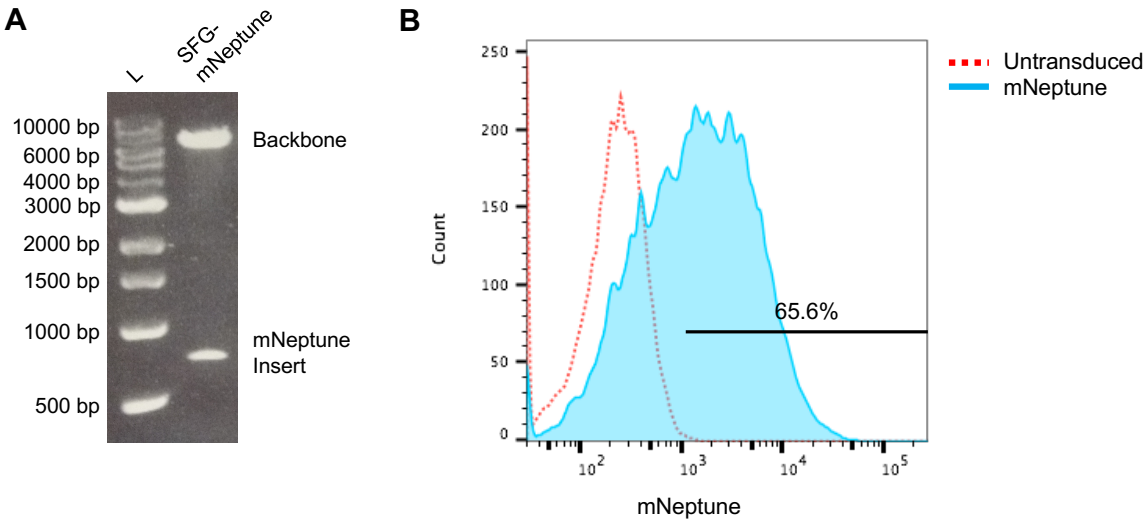

Figure 4.3 Development of an mNeptune packaging cell line.

The reporter gene mNeptune was cloned into an SFG retroviral backbone. A) Successful cloning was confirmed by electrophoresis. The plasmid was digested using the restriction enzymes NcoI and XhoI that flank the insert. A 1 kb ladder was used. B) This plasmid was transduced into the 293vec-RD114 pseudotyped retroviral packaging cell line. The untransduced parental cells were used to set the gate. Expression of mNeptune was detected in the APC channel.

Two stromal cell lines were used for this project, namely human telomerase transduced MRC5hT cells and the pancreatic stromal cell line, PS1. Both were transduced to express the mNeptune reporter. MRC5hT showed a positive population of 70.6% after one addition of viral supernatant. This increased to 94.5% mNeptune positive after an additional round of transduction [Figure 4.4A]. The PS1 cells were initially transduced to express 29.4% mNeptune and were sorted using FACS to yield a 90.7% positive population [Figure 4.4B]. These percentages remained stable throughout this project.

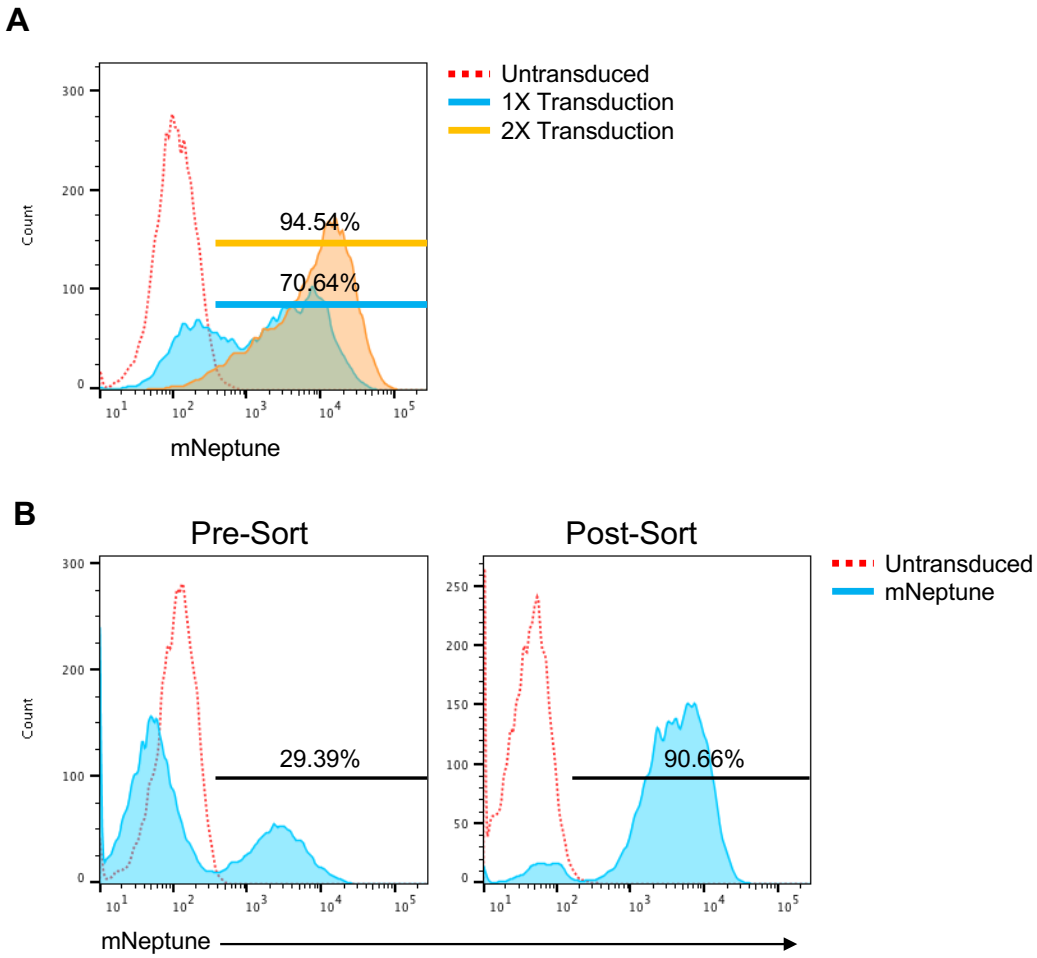

Figure 4.4 Transduction of stromal cells with mNeptune.
A) MRC5hT and B) PS1 were transduced with SFG mNeptune. MRC5hT were transduced with viral supernatant twice to achieve a strongly positive population. PS1 were transduced once and then flow sorted on a BD FACSAria I sorter. The untransduced parental lines were used to set the indicated gates.

Expression of FAP in the mNeptune expressing stromal cell lines was assessed using flow cytometry. Both the mN-MRC5hT and the mN-PS1 expressed 76% and 81% FAP respectively [Figure 4.5A]. Both cell lines were then stained for PSMA and FAP to demonstrate antigen expression in the stroma. As expected, neither cell line expressed PSMA, but consistently showed high levels of FAP [Figure 4.5B].

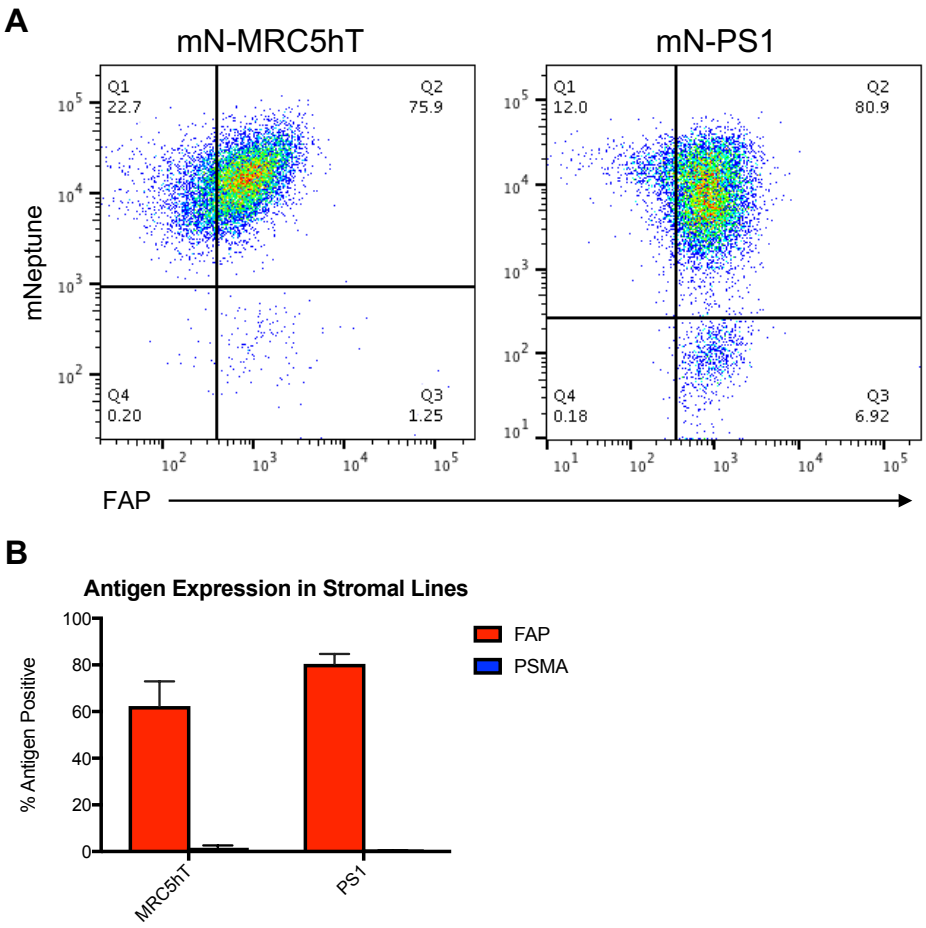

Figure 4.5 Antigen expression in stromal cell lines.

mN-MRC5hT and mN-PS1 cells were assessed for A) mNeptune and FAP dual expression and B) FAP and PSMA expression (mean ± SEM, n=3). An isotype control was used to set the gate for FAP and PSMA expression. Commercially available antibodies were used to detect FAP and PSMA.

4.2.2 Influence of prostate cancer and stromal cells on one another

In order to ultimately test the immunocytokine/ CAR T cell immunotherapy approach, I wished to establish cell models whereby PCa and stromal cells were co-cultured, both *in vitro* and *in vivo*. First, the growth kinetics of the PCa cell lines were analysed when cultured in conditioned media (CM) derived from the stromal cell lines. When PL/PLP and DU145/DU145P cells were cultured in 100% MRC5hT CM, 50% MRC5hT CM or fresh D10 for 96 hours, no significant difference in expansion was observed [Figure 4.6A-B]. When the same experiment was conducted using PS1 CM there was a significant decrease in expansion of the PL and PLP cells when cultured in either 100% or 50% PS1 CM, when compared to D10 [Figure 4.7A]. Co-cultures of DU145 and DU145P cells

with stromal cells showed a similar trend, but this did not reach significance [Figure 4.7B].

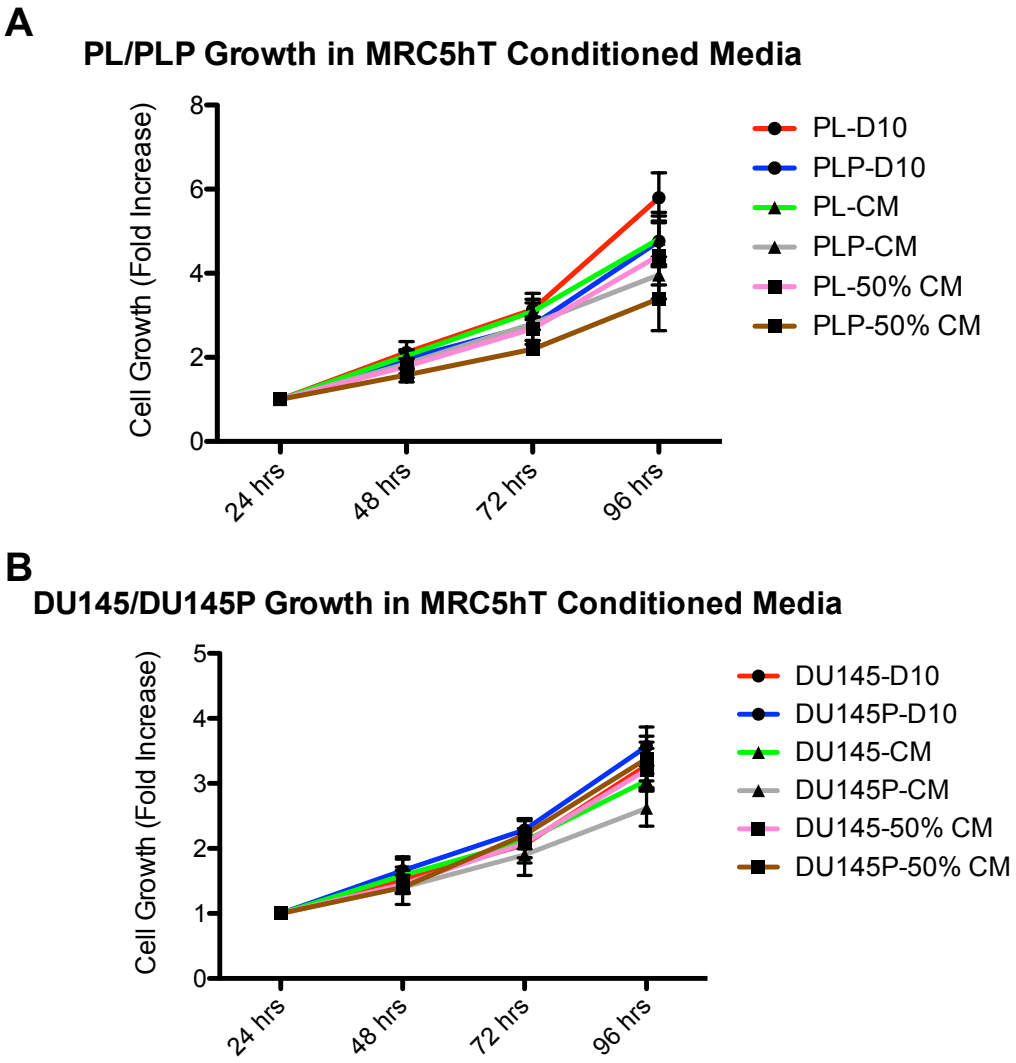

Figure 4.6 PCa growth kinetics in stromal cell conditioned media.

The impact of MRC5hT CM on *in vitro* expansion was assessed in A) PL/PLP cultures and B) DU145/DU145P cultures. The cell line is listed followed by the media conditions in the key to each panel. Significance was determined using a two-way ANOVA (mean ± SEM, n=3).

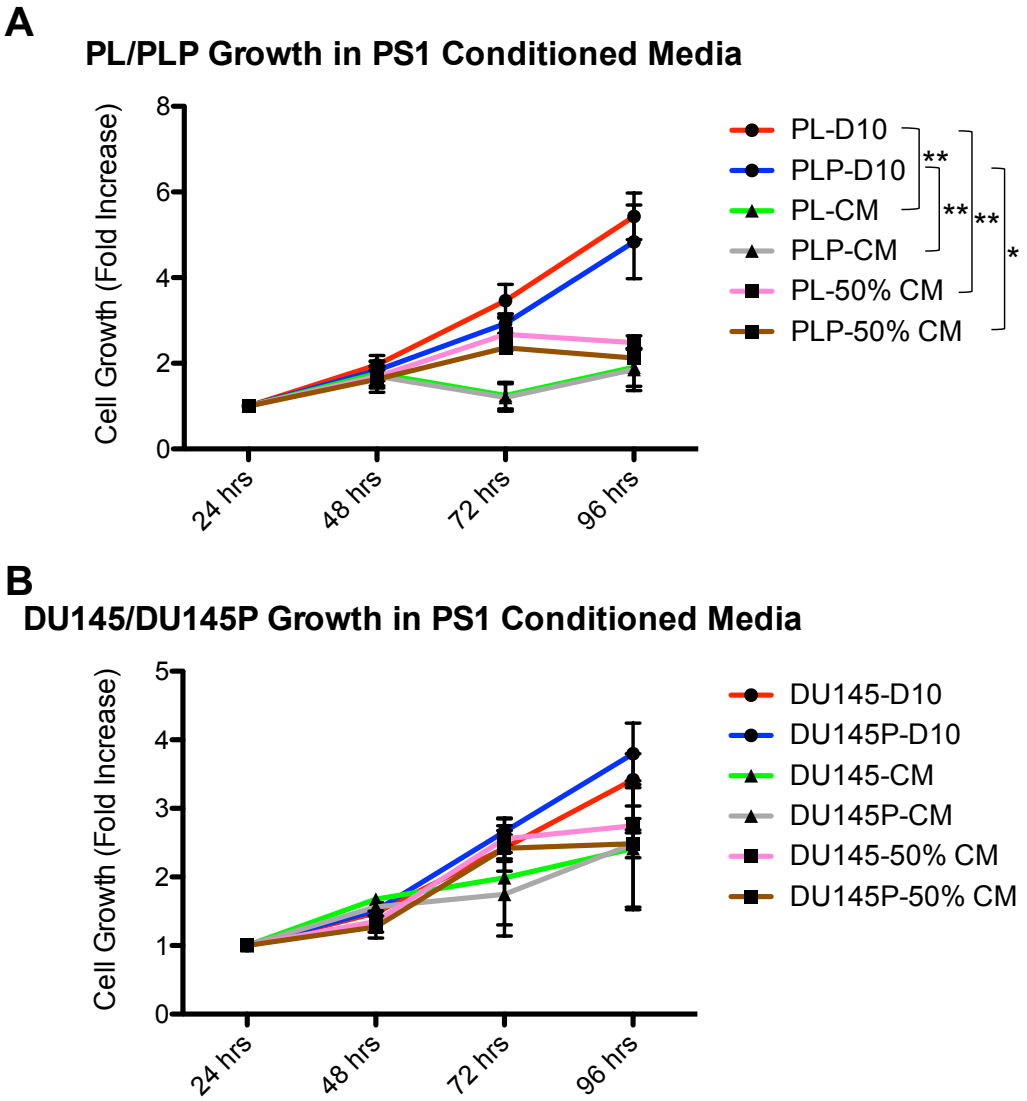

Figure 4.7 PCa growth kinetics in stromal cell conditioned media.
The impact of PS1 CM on *in vitro* expansion was assessed in A) PL/PLP and B) DU145/DU145P cultures. The cell line is listed followed by the media conditions in the key to each panel. Significance was determined using a two-way ANOVA (mean ± SEM, n=3) (* = $p < 0.05$; ** = $p < 0.01$).

Stromal cell growth was also investigated when these cells were cultured in the presence of CM derived from PCa cell lines. Expansion of MRC5hT cells did not seem to be affected by any of the PCa CM, whether added at 100% or 50% CM [Figure 4.8A-B]. By contrast, PS1 growth was slowed in response to the addition of both 100% and 50% CM from PL/PLP and DU145/DU145P cells [Figure 4.9A-B]. None of the growth kinetic variations that affected the stromal cell lines reached significance.

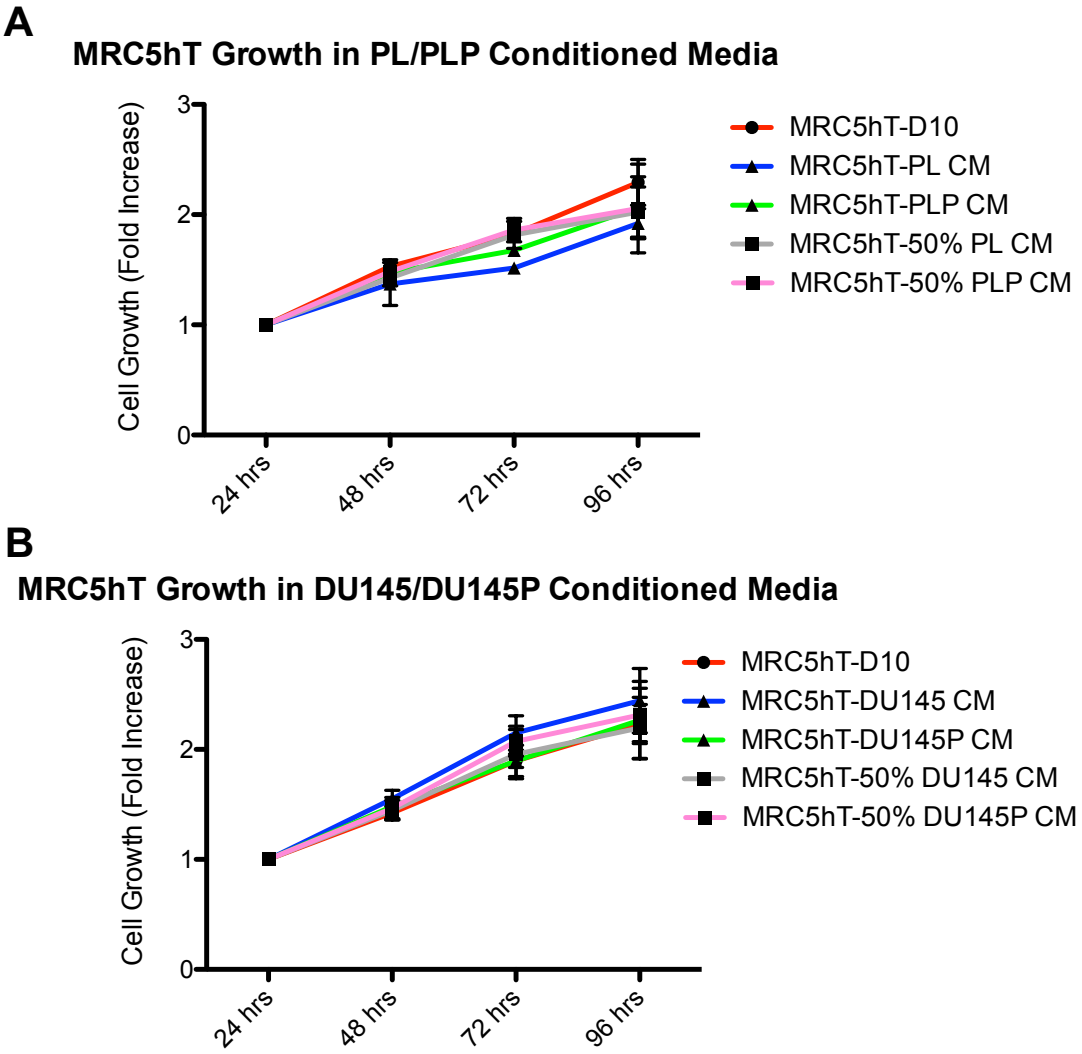

Figure 4.8 Stromal cell growth kinetics in PCa conditioned media.

MRC5hT growth rate was evaluated in A) PL/PLP CM and B) DU145/DU145P CM. The cell line is listed followed by the media conditions in the key to each panel. Significance was determined using a two-way ANOVA (mean ± SEM, n=3).

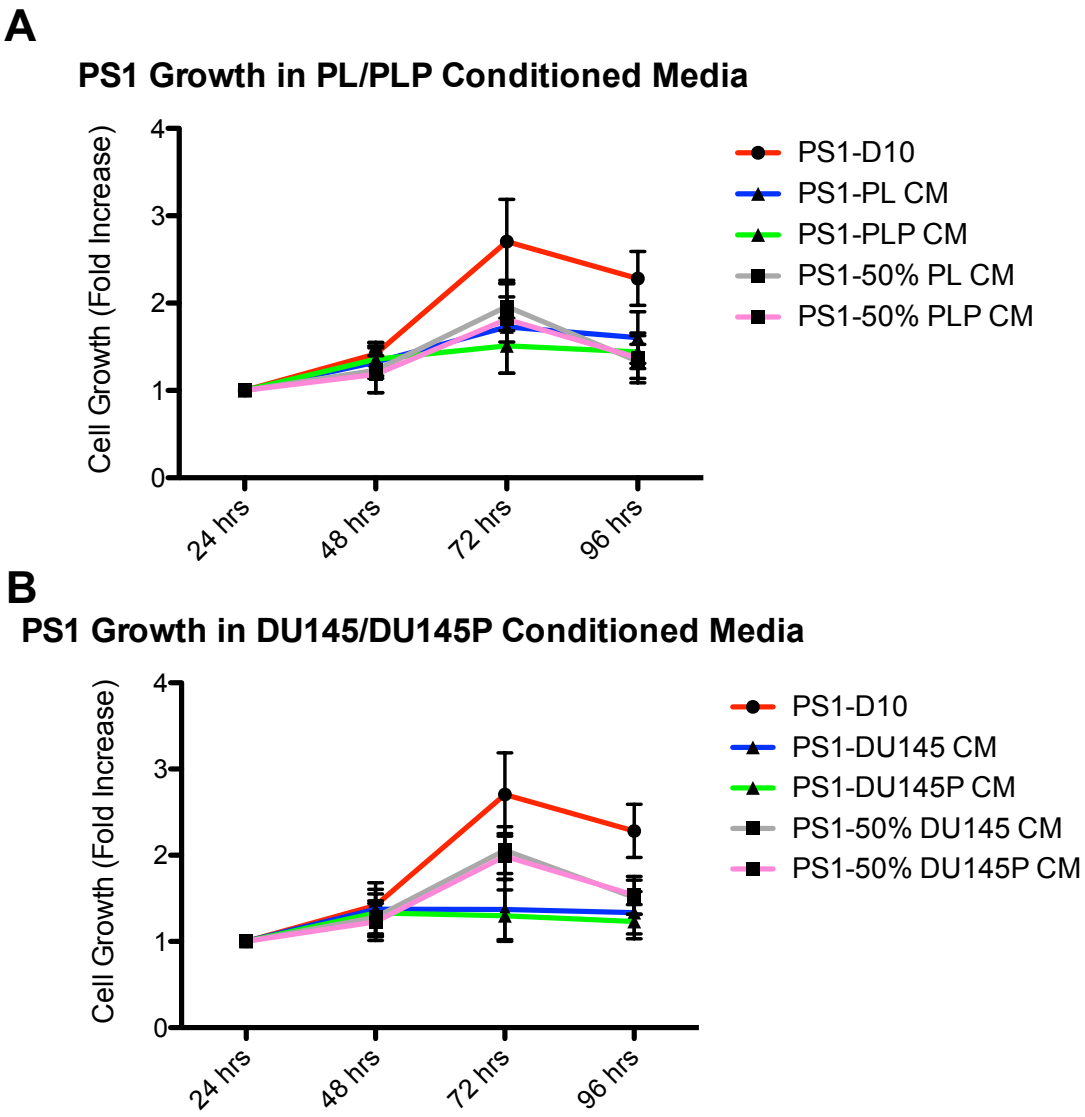

Figure 4.9 Stromal cell growth kinetics in PCa conditioned media.
PS1 growth was seen in A) PL/PLP CM and B) DU145/DU145P CM. The cell line is listed followed by the media conditions in the key to each panel. Significance was determined using a two-way ANOVA (mean ± SEM, n=3).

Next, I investigated FAP expression in stromal cells, when cultured in PCa conditioned media. While FAP expression in MRC5hT cells proved relatively consistent across these experiments [Figure 4.10A-B], expression of FAP on PS1 cells was more variable [Figure 4.10C-D]. There was an observed decrease in FAP expression in PS1 cells when cultured in PLP CM while an increase was noted in the presence of DU145 and DU145P CM at 72-hours. Nonetheless, these changes did not reach statistical significance.

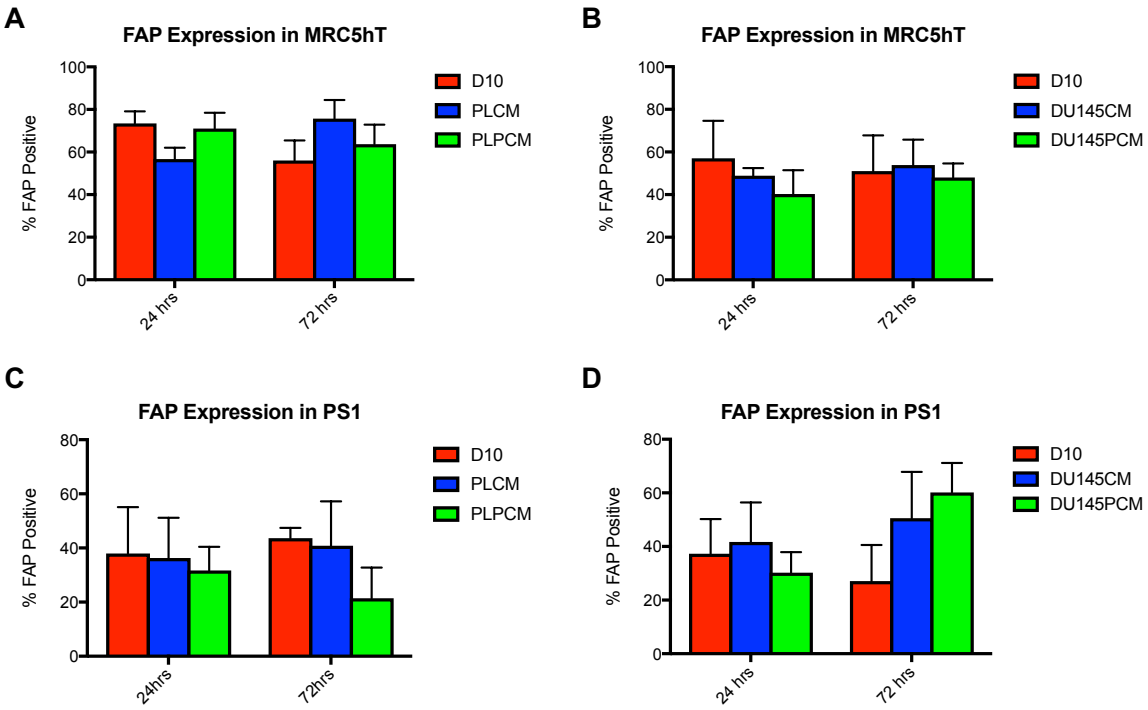

Figure 4.10 FAP expression in stromal cell lines in PCa conditioned media.

FAP expression on MRC5hT cultured in A) PL/PLP CM (n=3) and B) DU145/DU145P CM (n=3). FAP expression on PS1 cultured in C) PL/PLP CM (n=2-3) and D) DU145/DU145P CM (n=4) (mean ± SEM). A commercially available αFAP antibody was used to stain FAP and an isotype was used to set the gate on each condition. Statistical analysis was performed using a student's t-test.

Because of the distinctive growth patterns of each cell line it was necessary to establish an optimal co-culture ratio of stroma:PCa to avoid PCa outgrowth. At various plated ratios of PS1:PL, PL tended to moderately outgrow PS1 at 96-hours when compared to 24-hours [Figure 4.11A-B]. A similar pattern was seen with co-cultures of PS1 and PLP [Figure 4.11C-D]. At 96-hours, the PS1:PL/PLP plating ratio of 4:1 resulted in the stroma occupying around 70% of the co-culture. This ratio was chosen for future experiments. The same ratio plating determination was performed for PS1:DU145/DU145P. Although DU145 and DU145P did not outgrow PS1 as efficiently, they still became the predominant cell in co-cultures at the 1:1 plating ratio at 96-hours [Figure 4.11E-H]. The 4:1 PS1:DU145/DU145P ratio also yielded a co-culture that was around 70% stromal at 96-hours. Thus, this plating ratio was chosen for future evaluation.

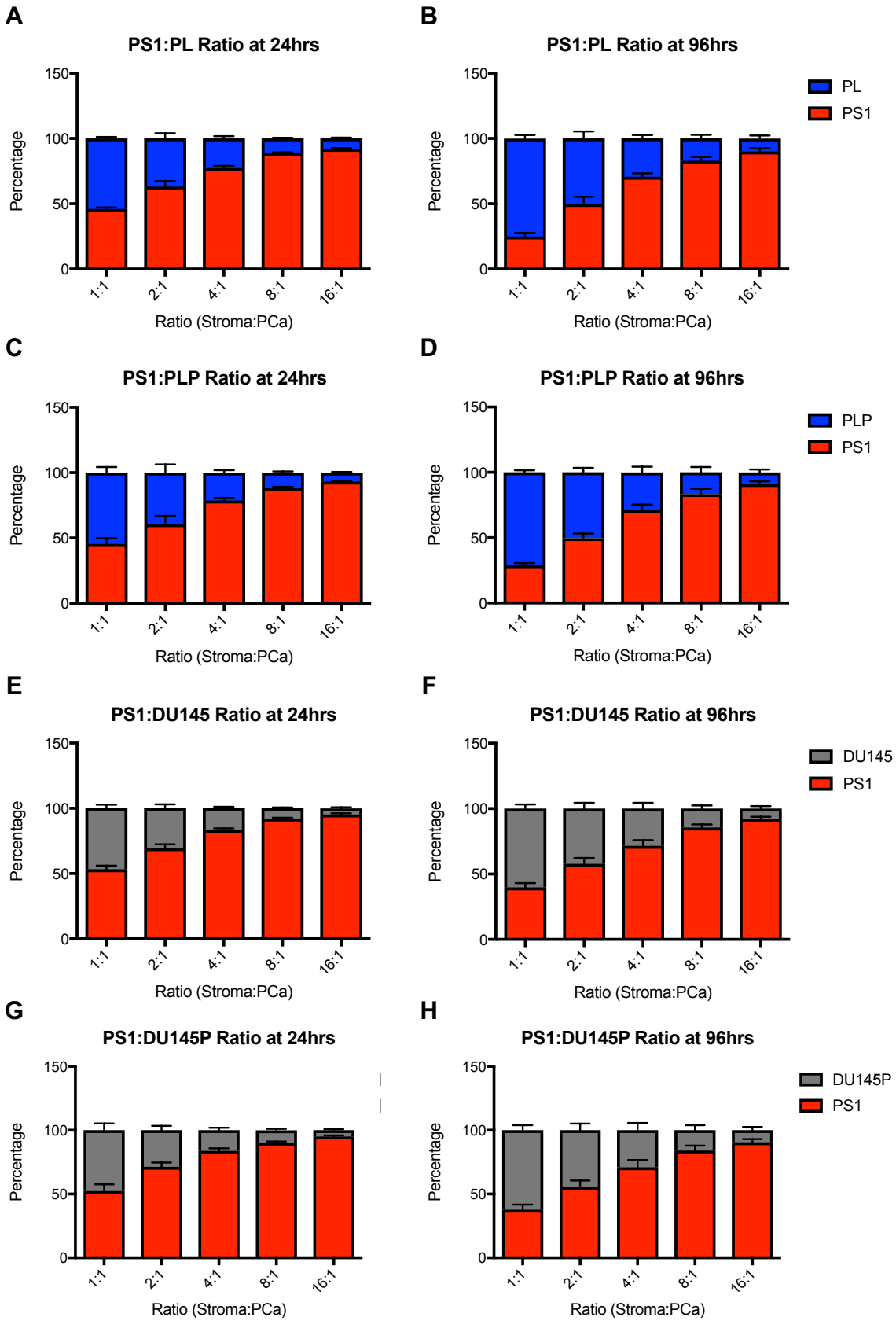

Figure 4.11 Co-culture ratio determination of PS1 and PCa lines.

Various plating ratios were observed for PS1:PL at A) 24-hours and B) 96-hours. The same was done for PS1:PLP at C) 24-hours and D) 96-hours, PS1:DU145 at E) 24-hours and F) 96-hours and PS1:DU145P at G) 24-hours and H) 96-hours. The resulting proportions of each cell line were determined by flow cytometry and are represented as percentages of the whole co-culture (mean ± SEM, n=3).

MRC5hT is a slower growing cell line than PS1 [data not shown]. Both PL and PLP cells overgrew the co-culture by 96-hours at a 1:1 seeding ratio leaving MRC5hT making up only around 4% of the total cell content [Figure 4.12A-D]. At an 8:1 plating density of MRC5hT:PL/PLP, the proportion of stromal cells at 96-hours was around 60%. This ratio was chosen for future analysis. The optimal plating ratio for MRC5hT and DU145/DU145P was determined in a similar manner. As seen previously, DU145/DU145P does not expand as rapidly as PL/PLP and did not take over the co-culture with MRC5hT as extensively [Figure 4.12E-G]. At 96-hours, all ratios above 4:1 resulted in the stromal cells comprising at least 50% of the co-culture with DU145 and DU145P. However, to ensure that stroma was the predominant cell type in the culture, an 8:1 seeding ratio was chosen. This produced a culture that was approximately 70% MRC5hT cells at the 96-hour time point.

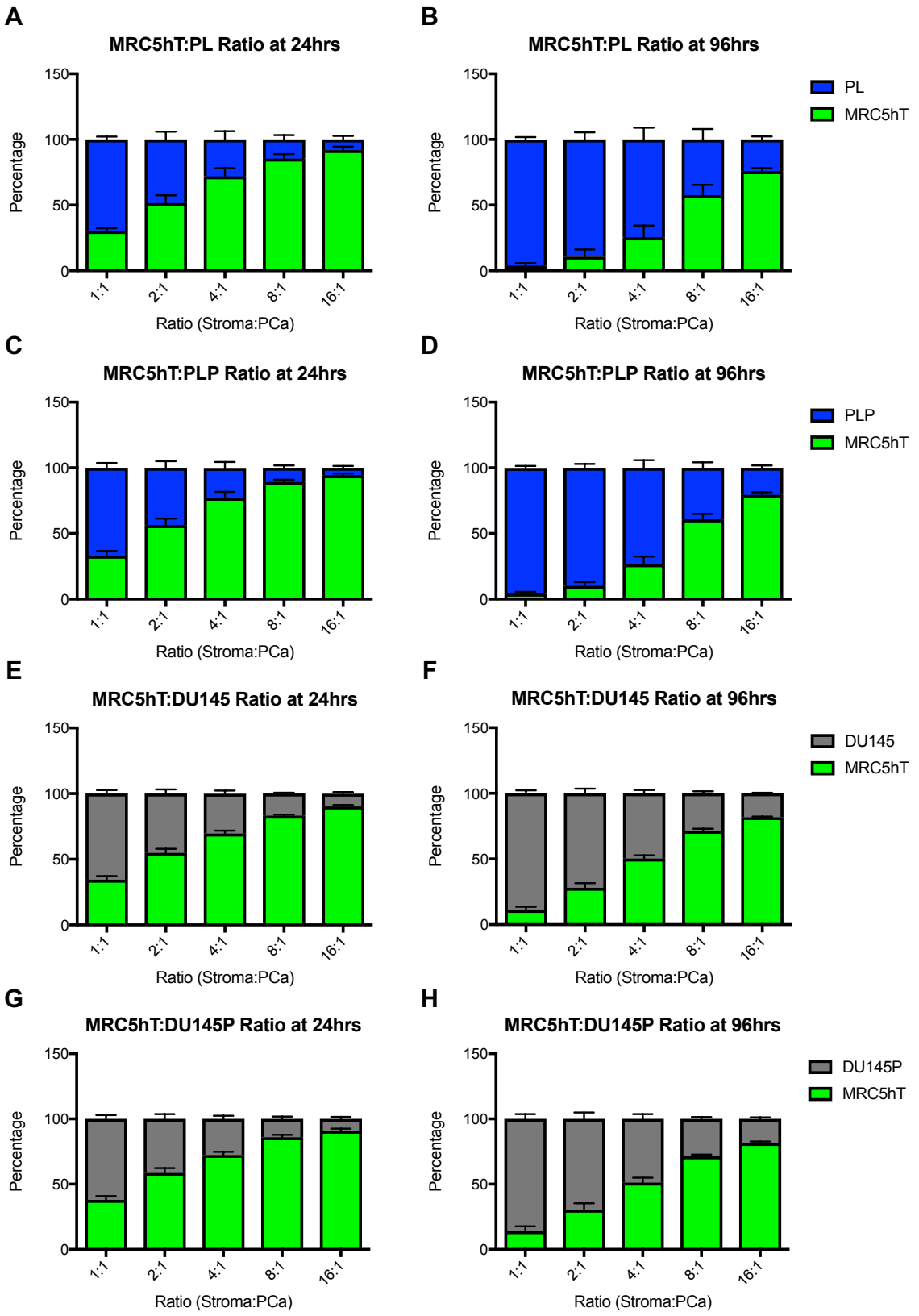

Figure 4.12 Co-culture ratio determination of MRC5hT and PCa lines.

Different plating ratios were observed for MRC5hT:PL at A) 24-hours and B) 96-hours. The same was done for MRC5hT:PLP at C) 24-hours and D) 96-hours, MRC5hT:DU145 at E) 24-hours and F) 96-hours and MRC5hT:DU145P at G) 24-hours and H) 96-hours. The resulting proportions of each cell line were determined by flow cytometry and are represented as percentages of the whole co-culture (mean ± SEM, n=3).

At the pre-determined optimal PS1:PCa plating ratio of 4:1, the effect of co-culture on the growth of both tumour and stromal cells was measured. PS1 stromal cells and PL/PLP tumour cells were plated at $4x10^4$ cells/well either as a mono-culture of either PS1 or the tumour cell line, or as a co-culture comprising 3.2×10^4 PS1 cells mixed with 0.8×10^4 PL or PLP cells. Control cells were plated alone but at their co-culture seeding densities (e.g. 3.2×10^4 PS1 cells alone or 0.8×10^4 PL or PLP cells alone) to determine the true effect of the other cell line on growth kinetics and thereby establish the impact of cell confluency. Cell growth was monitored each day over 4 days. The presence of PS1 cells did not alter the growth rate of PL or PLP cells, when compared to the corresponding tumour cell monocultures that had been plated at co-culture densities ($0.8x10^4$ cells). Nonetheless, when PS1 cells were established in co-culture with PL or PLP tumour cells, a small trend was noted (statistically not significant) whereby the stromal cells expanded more quickly [Figure 4.13A-B]. The possibility that this was an artefact of confluency and not due to PCa cell influence was ruled out by the demonstration that $4x10^4$ PS1 cells plated in mono-culture exhibited similar growth to PS1 cells that had been plated alone at co-culture density ($3.2x10^4$).

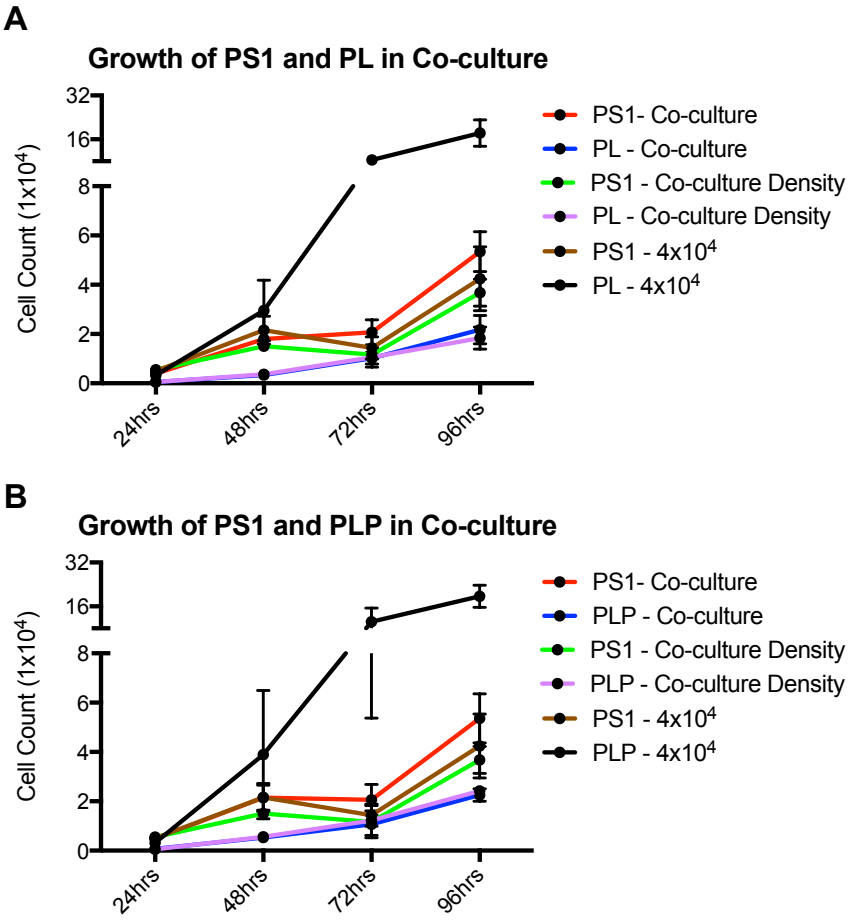

Figure 4.13 Growth kinetics of PS1 and PL/PLP in co-culture.

Co-cultures were established in which 3.2 x 10^4 PS1 cells were mixed with 0.8 x 10^4 PL cells A) or PLP cells B). Growth rates of PCa and stromal cells were monitored by flow cytometry. The key to each panel indicates the particular cell line followed by the condition in which the growth was observed (mono-cultures lines = green, purple, brown and black; co-culture lines = red and blue) (mean $\pm$ SEM, n=3).

The presence of DU145 and DU145P did not have an effect on PS1 growth rate in co-culture [Figure 4.14A-B]. All mono-cultures and co-cultures of PS1 with DU145/DU145P expanded equivalently. Additionally, DU145 and DU145P cells did not proliferate differently based on culture composition.

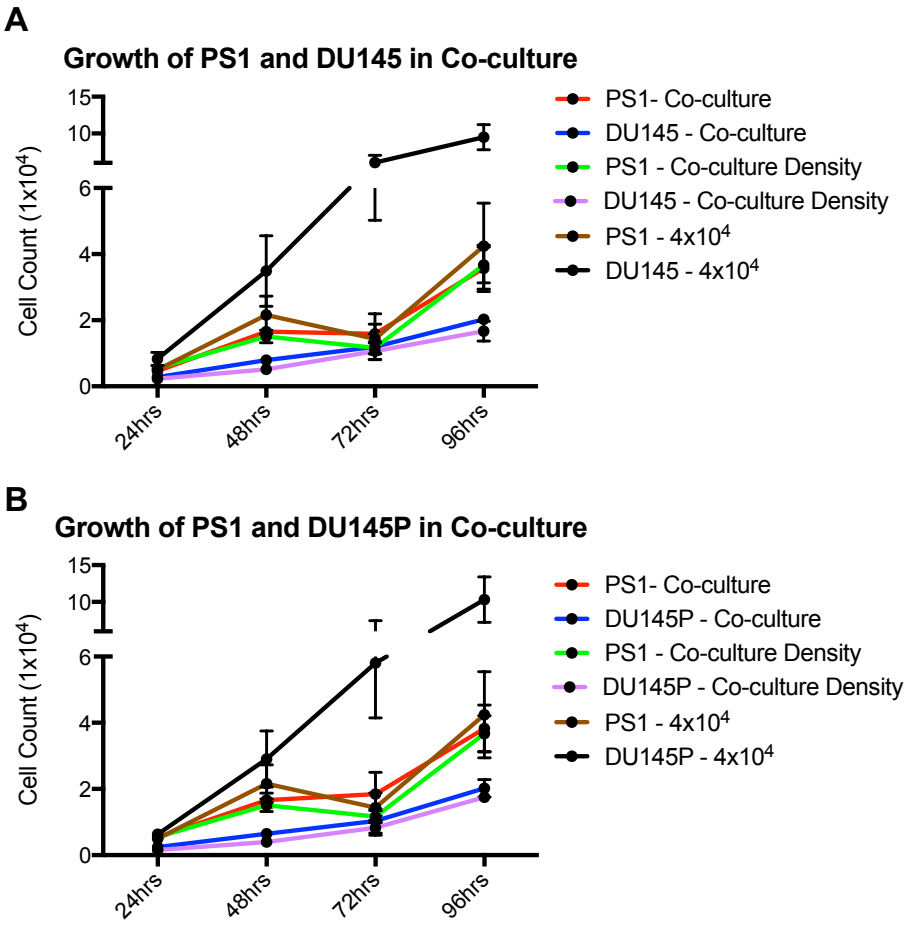

Figure 4.14 Growth kinetics of PS1 and DU145/DU145P in co-culture.

Co-cultures were established in which 3.2 x 10^4 PS1 cells were mixed with 0.8 x 10^4 DU145 cells A) or DU145P cells B). Growth rates of PCa and stromal cells in co-culture were monitored by flow cytometry. The key to each panel indicates the particular cell line followed by the condition in which the growth was observed (mono-cultures lines = green, purple, brown and black; co-culture lines = red and blue) (mean $\pm$ SEM, n=3).

When seeded at a stroma:PCa ratio of 8:1, the presence of PL or PLP tumour cells significantly increased the expansion rate of MRC5hT cells [Figure 4.15A-B]. This effect was evident by 72-hours in culture. However, neither PL or PLP growth was affected by co-culture with MRC5hT cells.

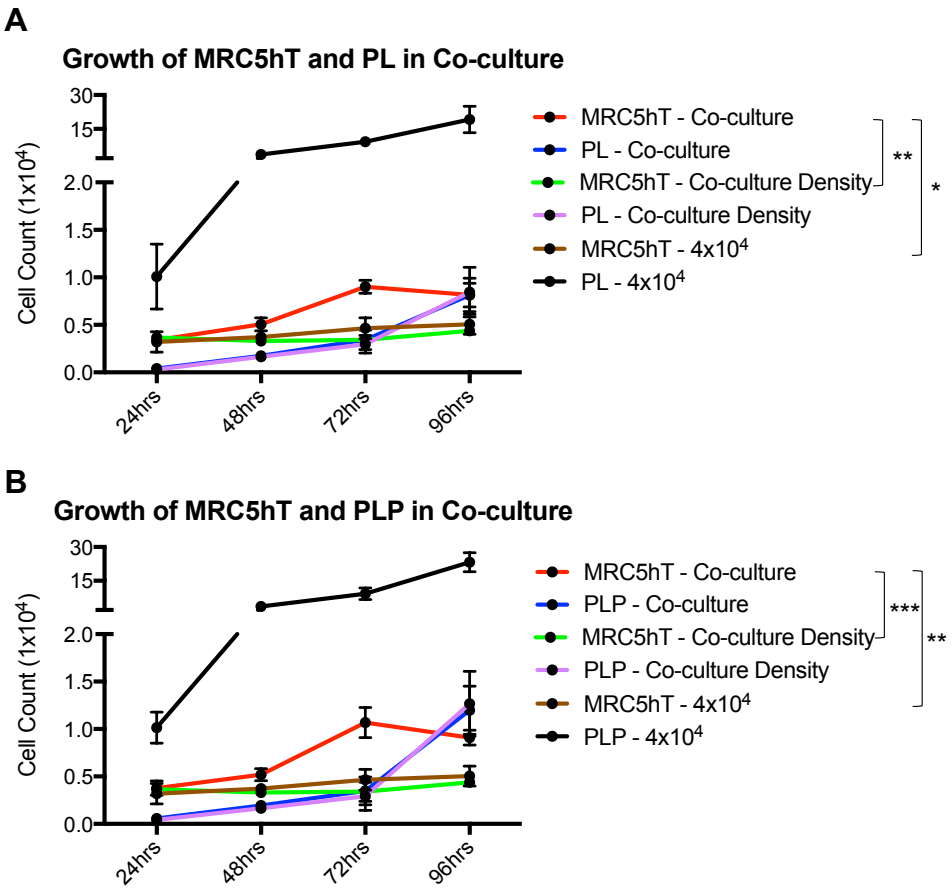

Figure 4.15 Growth kinetics of MRC5hT and PL/PLP in co-culture.

Co-cultures were established in which 3.2 x 10^4 MRC5hT cells were mixed with 0.8 x 10^4 PL cells A) or PLP cells B). Growth rates of PCa and stromal cells in co-culture were monitored by flow cytometry. The key to each panel indicates the particular cell line followed by the condition in which the growth was observed (mono-cultures lines = green, purple, brown and black; co-culture lines = red and blue). Significance was determined using a two-way ANOVA (mean $\pm$ SEM, n=3) (* = $p < 0.05$; ** = $p < 0.01$; *** = $p < 0.001$).

Analysis of DU145/DU145P cells in co-culture with MRC5hT cells also showed a significant growth advantage for MRC5hT cells in these co-cultures [Figure 4.16A-B]. DU145P tumour cells also demonstrated a significant increase in expansion when cultured with MRC5hT cells, when compared to a mono-culture of these stromal cells that had been plated at the same seeding density [Figure 4.16B].

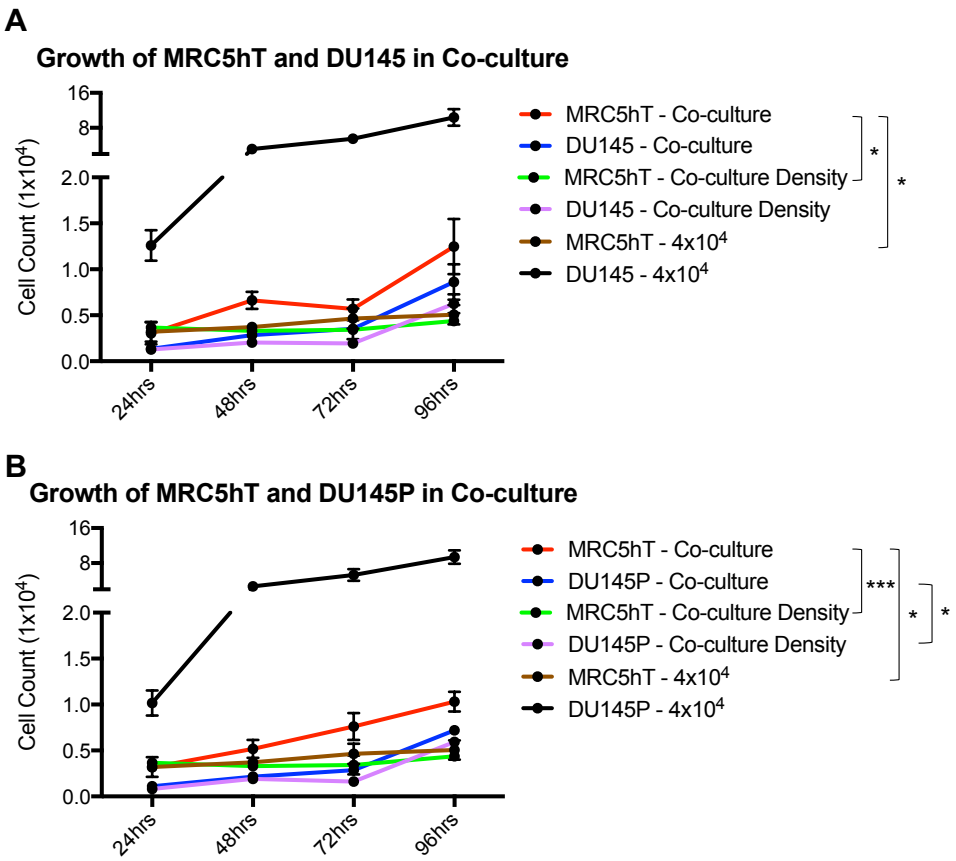

Figure 4.16 Growth kinetics of MRC5hT and DU145/DU145P in co-culture.
Co-cultures were established in which 3.2 x 10^4 MRC5hT cells were mixed with 0.8 x 10^4 DU145 cells A) or DU145P cells B). Growth rates of PCa and stromal cells in co-culture were monitored by flow cytometry. The key to each panel indicates the particular cell line followed by the condition in which the growth was observed (mono-cultures lines = green, purple, brown and black; co-culture lines = red and blue). Significance was determined using a two-way ANOVA (mean $\pm$ SEM, n=3) (* = $p < 0.05$; *** = $p < 0.001$).

Expression of FAP was analysed in the stromal cells when co-cultured with PCa cells, making comparison with stromal cell mono-cultures. PS1 cells showed a time-dependent decrease in the expression of FAP in every culture condition [Figure 4.17A-B], although this difference was only significant at 72-hours for the mono-cultures of PS1 seeded at co-culture density. This difference was only noted when measuring the percentage of FAP^+ cells [Figure 4.17A].

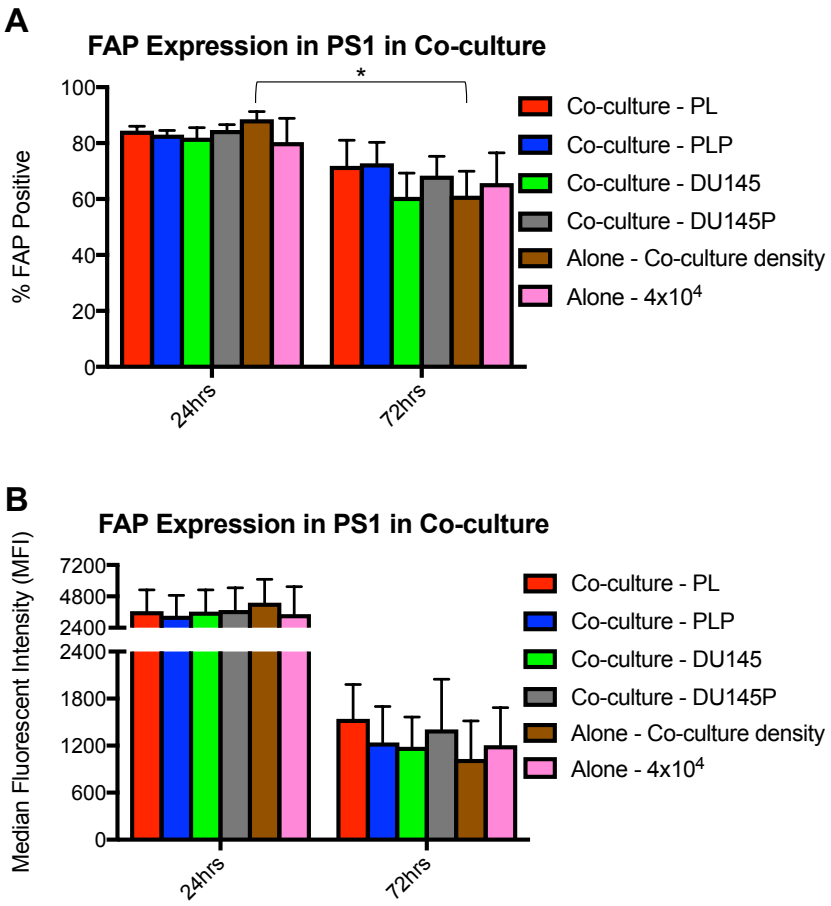

Figure 4.17 FAP expression in PS1 cells in PCa co-culture.

Expression of FAP was analysed in the different PS1 culture conditions by flow cytometry. Data are expressed as A) percentage of positive cells and B) median fluorescence intensity. Commercially available antibodies were used to stain FAP and an isotype control was used to set the gate. The key to each panel indicates whether PS1 was co-cultured with tumour cells or cultured alone and whether cells were seeded at monoculture or co-culture density. Statistical significance was determined using a student's t-test (mean $\pm$ SEM, n=3) (* = $p < 0.05$).

Expression of FAP in MRC5hT cells was not influenced by time or co-culture with the PL or PLP PCa cell lines [Figure 4.18A-B]. Cells remained between 40-60% FAP positive under all conditions. The MRC5hT stromal line was chosen for further drug development because of the increased stability of FAP expression and growth kinetics in co-cultures compared to PS1.

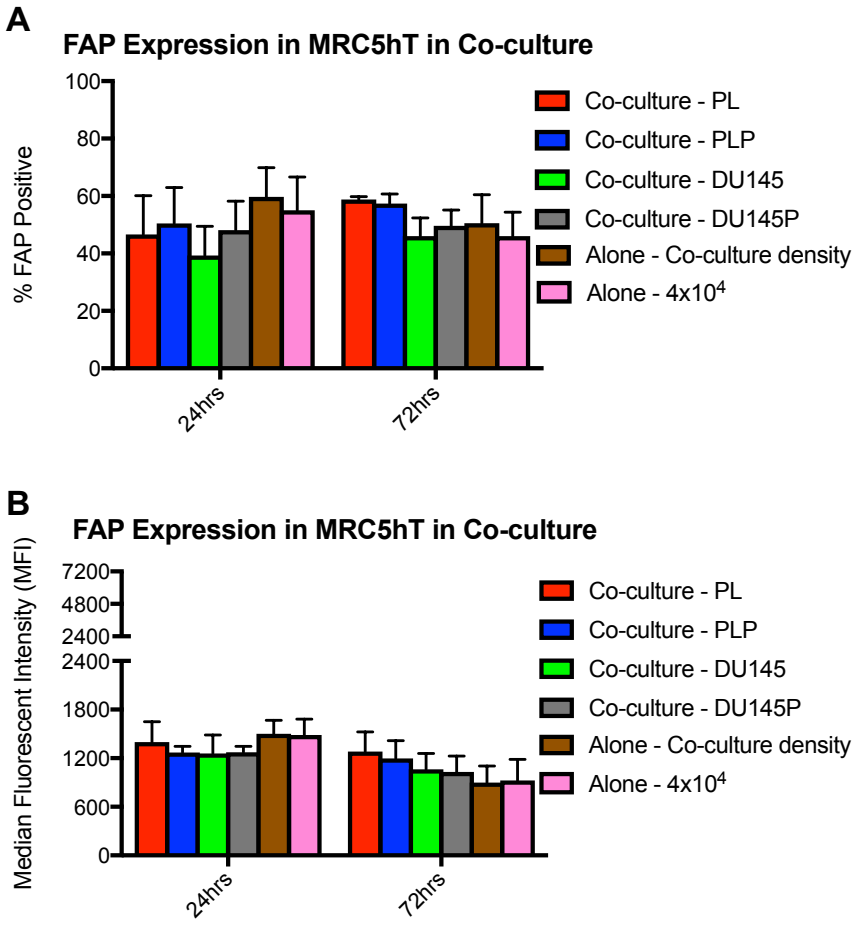

Figure 4.18 FAP expression in MRC5hT cells in PCa co-culture.

Expression of FAP was analysed in the different culturing conditions of MRC5hT by flow cytometry. Data are expressed as A) percentage of positive cells and B) median fluorescence intensity. Commercially available antibodies were used to stain FAP and an isotype control was used to set the gate. The key to each panel indicates whether MRC5hT was co-cultured with tumour cells or cultured alone and whether cells were seeded at monoculture or co-culture density (mean ± SEM, n=3).

4.2.3 Functional validation of eFAP-4 signalling through the 4αβ in human CAR T cells

After validation of eFAP-4 signalling through the 4αβ chimeric receptor in a murine leukaemia cell line CTLL2 [Figure 3.17], function was assessed in human T cells expressing P4 or the truncated control P4Tr construct in which P28z lacks an intracellular signalling domain. The expansion of P4 or P4Tr CAR T cells was similar in the presence of IL-4 or eFAP-4. With the P4 construct, both IL-4 and eFAP-4 elicited a greater degree of cell expansion than IL-2 and significantly more expansion than CAR T cells when cultured without cytokine [Figure 4.19A]. P4Tr CAR T cells expanded less well overall,

but once again, significantly more proliferation was seen in cultures with IL-4 or eFAP-4 compared to IL-2 or no cytokine over a 10-day period [Figure 4.19B].

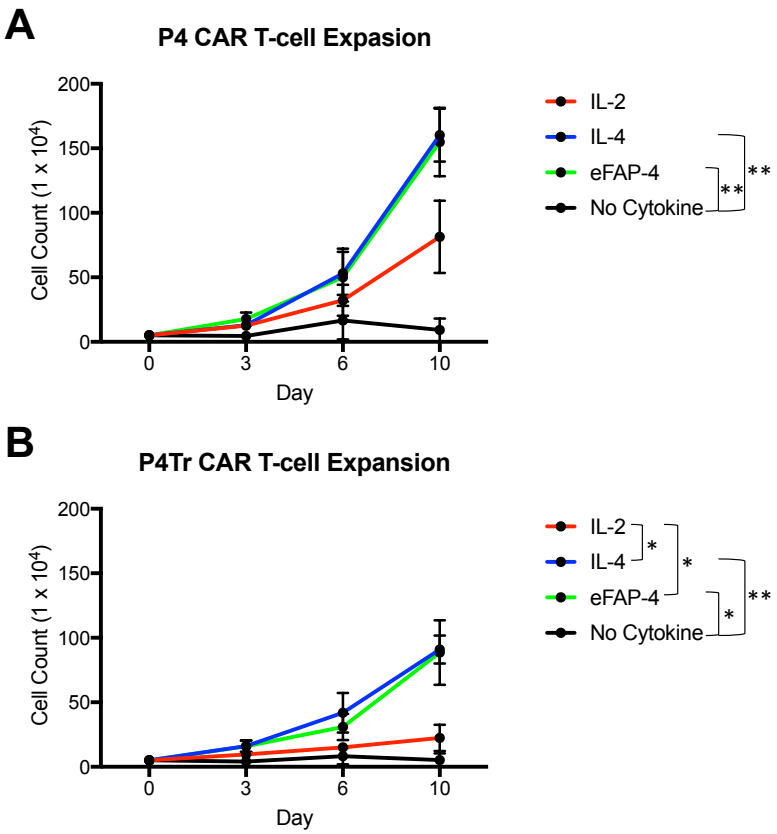

Figure 4.19 CAR T cell expansion with different cytokines.
Human T cells were engineered by retroviral transduction to express the P28z or PTr CARs together with the 4αβ chimeric cytokine receptor, known as P4 (A) or P4Tr (B) respectively. T cells were then cultured in 100 IU/mL IL-2, 2 nM IL-4 or 2 nM eFAP-4, which was repeatedly added every 2 days. Cell number was evaluated by trypan exclusion at the indicated time points (mean ± SEM, n=4). Significance was determined using a two-way ANOVA (* = $p < 0.05$; ** = $p < 0.01$).

These expansion cultures were also analysed for variations in the $CD8^+$:$CD4^+$ T cell ratio over 10-days. Although there was donor variability, there was a trend for P4 cells cultured in IL-2 to shift towards a higher CD8:CD4 ratio over the 10-day culture period [Figure 4.20A]. For the P4Tr CAR T cells the only visible change was a decrease in the CD8:CD4 ratio in IL-4 [Figure 4.20B].

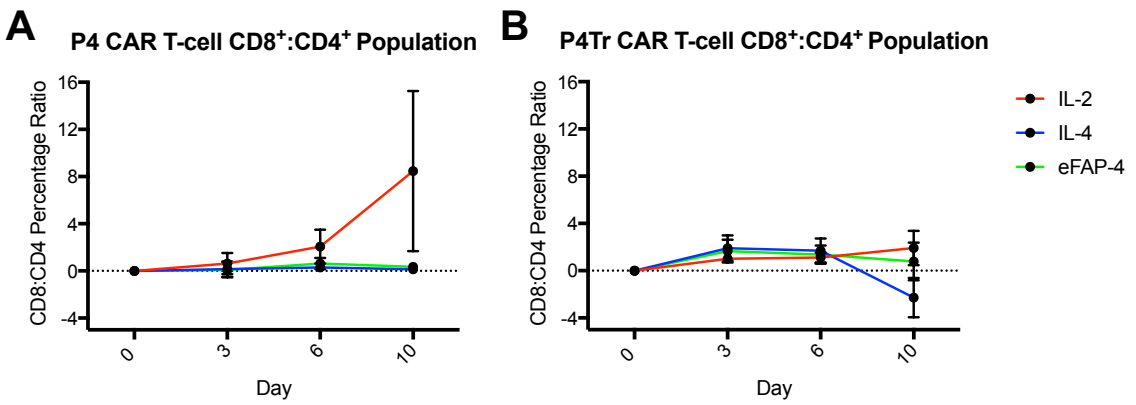

Figure 4.20 CD8$^+$:CD4$^+$ T cell ratio in different cytokine conditions.

The ratio of CD8$^+$:CD4$^+$ CAR T cells expanded with IL-2, IL-4 and eFAP-4 as described in Figure 4.17 was observed in T cell cultures expressing the A) P4 construct, or the B) P4Tr construct (mean ± SEM, n=4). Commercially available antibodies were used to stain CD8 and CD4 prior to analysis by flow cytometry. Baseline CD8:CD4 ratios were determined at day 0 and deviations were recorded as an increase or decrease of that ratio.

Next, *in vitro* P4 CAR T cell cytotoxicity was quantified in co-cultures with newly established PCa/MRC5hT monolayers. MRC5hT+PCa cells, PCa alone, or MRC5hT cells alone were co-cultured with P4 or P4Tr expressing CAR T cells for 24 hours at an effector to target ratio of one T cell to two target cells (combining tumour and stromal cells). PSMA-dependent tumour cell killing by P4-engineered T cells was observed [Figure 4.21A]. Some antigen independent 'bystander killing' of MRC5hT cells was also seen in the PSMA expressing MRC5hT+PCa co-cultures. A small amount of bystander killing of MRC5hT was also seen for P4Tr in the MRC5hT alone culture [Figure 4.21B]. Activation of P4 CAR T cells was associated with antigen-specific secretion of IFN-γ and IL-2 [Figure 4.21C-D]. There was a statistically significant reduction in cell viability for DU145 in the presence of the P4 CAR but this was modest in comparison to the PSMA expressing cell lines and was not associated with cytokine secretion by the CAR T cells [Figure 4.21A and C-D].

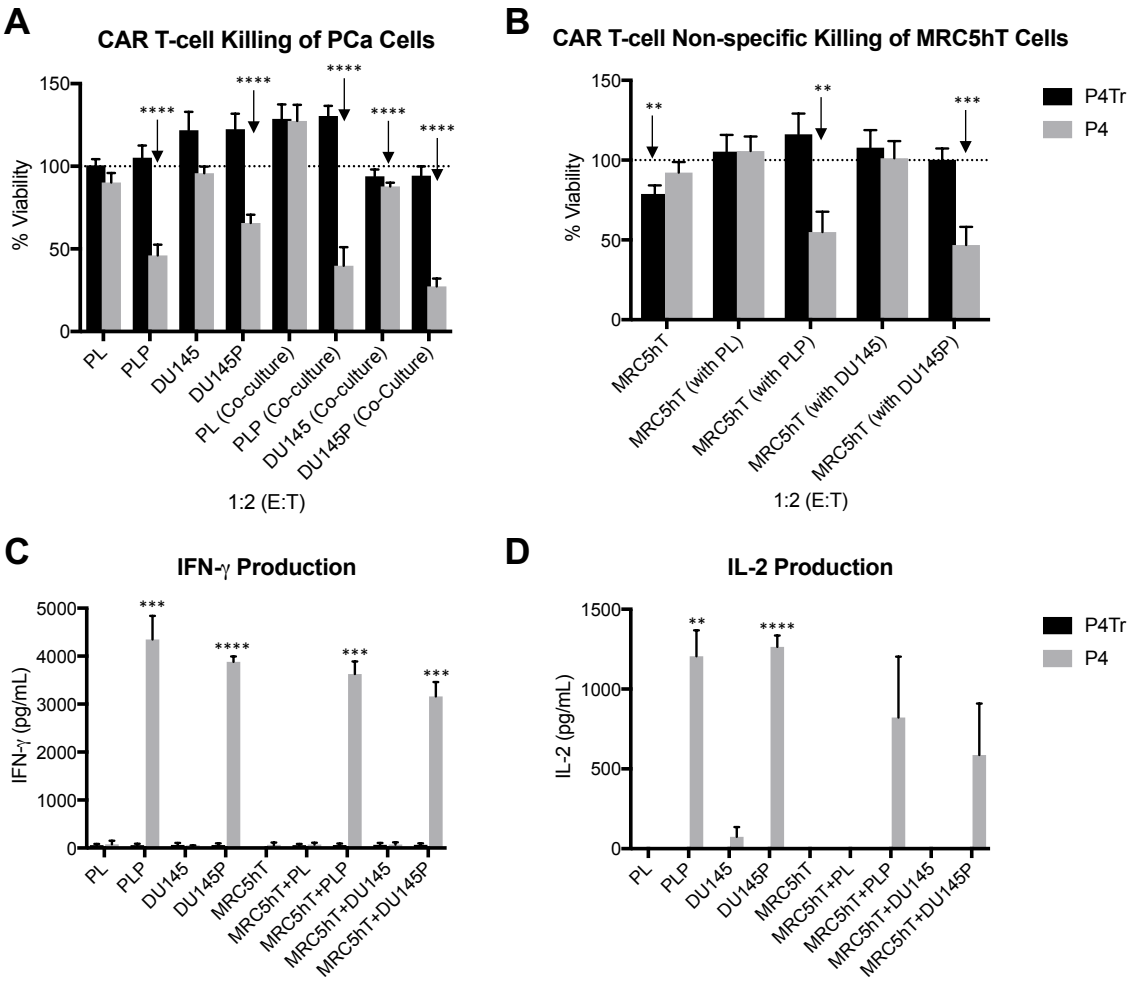

Figure 4.21 CAR T cell killing of PCa/MRC5hT monolayers.
Cell viability of monolayers following co-cultivation with either P4 or P4Tr CAR T cells (E:T ratio 1:2) was determined by flow cytometry at 24-hours as A) PCa cell line death, or B) MRC5hT cell death (n=3). PCa cell lines that were co-cultured are labelled (co-culture). MRC5hT that were co-cultured with specific PCa cell lines are specified in parentheses. Cytokine production by P4 and P4Tr CAR T cells was quantified for C) IFN-γ and D) IL-2. All data show mean ± SEM of n=3 independent biological replicates. All cultures had an effector to target (E:T) ratio of 1:2. Significant cell death compared to baseline was determined using a student's t-test (** = $p < 0.01$; *** = $p < 0.001$; **** = $p < 0.0001$).

4.2.4 Effect of eFAP-4 addition on restimulated co-cultures of P4 CAR T cells with PCa/stroma monolayers

To ensure that IL-4 and eFAP-4 did not have intrinsic anti-cancer characteristics, PCa and MRC5hT cells were cultured with these cytokines and cell viability was measured. No reduction in cell viability at 72-hours was observed for mono-cultures, or MRC5hT+PCa combined cultures when either IL-4, or eFAP-4 was added to the culture,

when compared to cultures without IL-4 or eFAP-4[Figure 4.22A-B]. DU145P cells cultured alone expanded more than other conditions in IL-4 alone [Figure 4.22B].

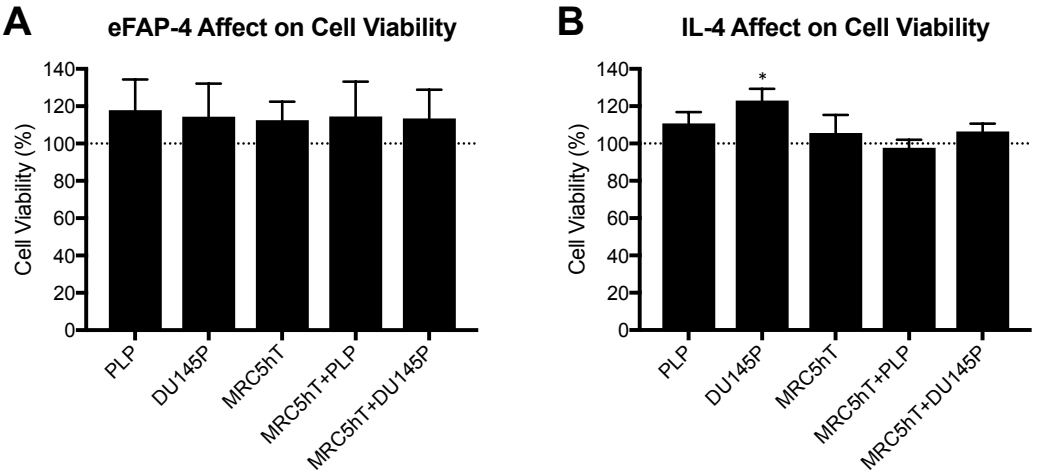

Figure 4.22 eFAP-4 and IL-4 influence on viability of monolayers.
Cell viability was determined by MTT assay after 72-hours of culture of 1 x 10^5 cells with A) 2 nM eFAP-4, or B) 2 nM IL-4 (mean $\pm$ SEM, n=3). Viability was compared to cultures without eFAP-4 or IL-4, which was considered 100% cell viability. Significance was determined using a student's t-test (* = $p < 0.05$).

CAR T cells were added to monolayers of either PCa cells, MRC5hT or MRC5hT+PCa combined cultures (comprising stromal and tumour cells at the predetermined optimal ratio of 8:1 respectively). T cell/monolayer cultures were initiated at an effector to target ratio of 1:2 and cultures were supplemented with 2 nM of IL-4, eFAP-4 or no cytokine. Cytotoxicity was evaluated after 72-96 hours by MTT assay in a re-stimulation co-culture experiment, whereby T cells were transferred to a new monolayer every 72-96 hours. When P4 CAR T cells were co-cultured with PLP alone, the presence of IL-4 or eFAP-4 resulted in sustained elimination of the PCa cells over 17 restimulations. Cytotoxicity was lost between the 4^{th} and 6^{th} restimulation when P4 CAR T cells were restimulated in this manner, but without cytokine supplementation [Figure 4.23A]. When MRC5hT cells were present in the monolayer, a similar pattern was seen. However, the magnitude of monolayer eradication was reduced when compared to the PLP alone condition,

presumably because the MRC5hT cells were surviving to a greater degree, given their PSMA negative status [Figure 4.23B].

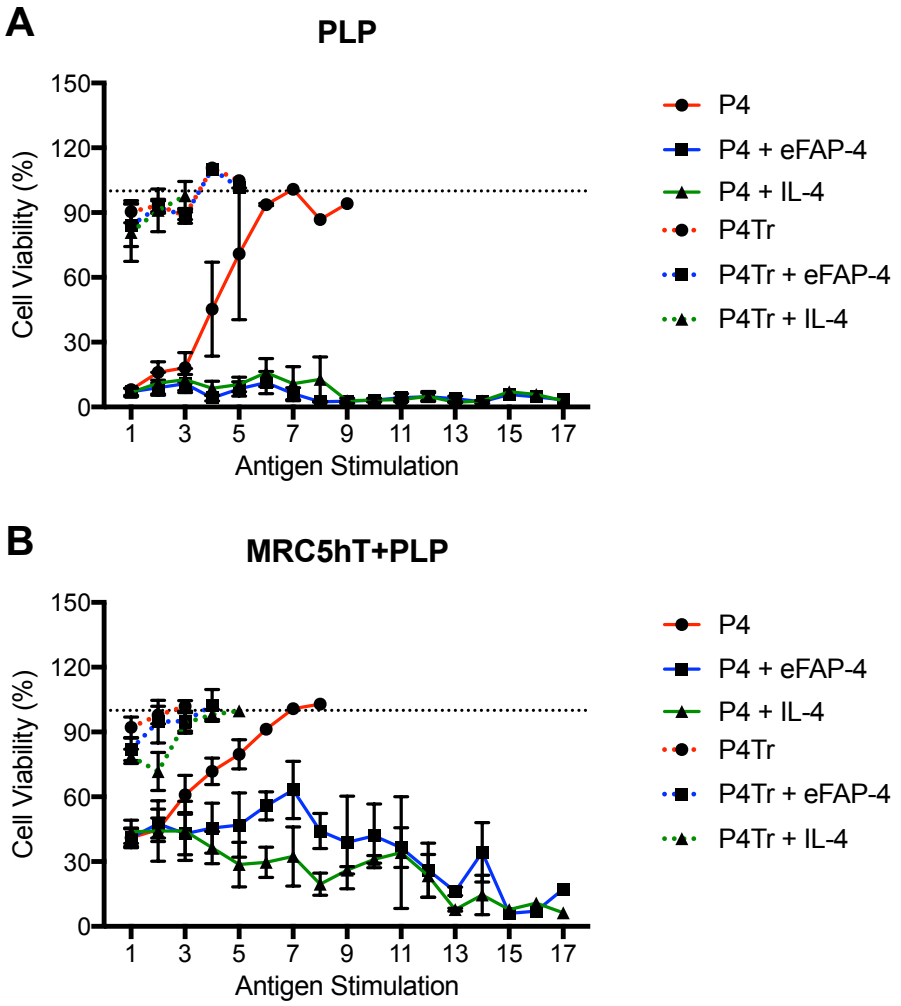

Figure 4.23 CAR T cell killing of PLP and MRC5hT+PLP monolayers.
P4 and P4Tr CAR T cells were added to monolayers at an initial E:T ratio of 1:2. Tumour cell viability was measured after 72-96 hours by MTT assay and T cells were restimulated on a new monolayer. Cell viability was compared to monolayers not receiving CAR T cells or cytokine supplementation (considered 100%; dotted black line). Efficacy was assessed alone or with either 2 nM eFAP-4 or IL-4 on monolayers of A) PLP, or B) MRC5hT+PLP (mean ± SEM, n=4). Dotted coloured lines in the legend represent the P4Tr counterpart for each condition.

Similar restimulation assays were established between CAR T cells and DU145P tumour cells, cultured alone or with MRC5hT stromal cells. For co-cultures of P4 CAR T cells with DU145P alone, the same pattern of improved killing with IL-4 and eFAP-4 was seen, albeit with an ameliorated depth of repeat monolayer elimination compared to PLP

containing cultures [Figure 4.24A]. For MRC5hT+DU145P antigen specific killing was seen, and IL-4 or eFAP-4 supplementation enhanced depth and duration of restimulation cytotoxicity. Ultimately though, the presence of the stromal cells conferred significant protection from CAR T cell mediated killing of the PSMA expressing tumour cells manifested by a marked reduction in the number of restimulations the CAR T cells sustained [Figure 4.24B].

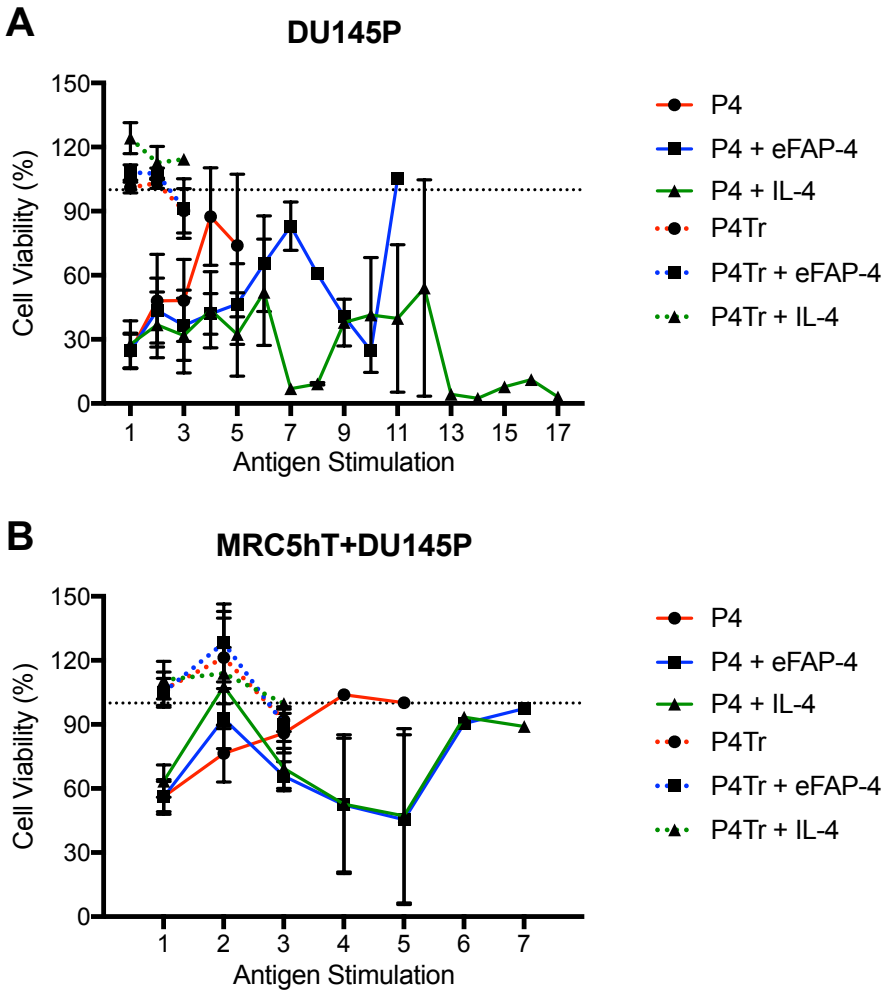

Figure 4.24 CAR T cell killing of DU145P and MRC5hT+DU145P monolayers.
P4 and P4Tr CAR T cells were added to monolayers at an initial E:T ratio of 1:2. Tumour cell viability was measured after 72-96 hours by MTT assay and T cells were restimulated on a new monolayer. Cell viability was compared to monolayers not receiving CAR T cells or cytokine supplementation (considered 100%; dotted black line). Efficacy was assessed alone or with either 2 nM eFAP-4 or IL-4 on monolayers of A) DU145P, or B) MRC5hT+DU145P (mean ± SEM, n=4). Dotted coloured lines in the legend represent the P4Tr counterpart for each condition.

When CAR T cells were cultured with monolayers that contained only MRC5hT cells, non-specific killing of these stromal cells was not seen in any culture conditions [Figure 4.25]. Moreover, as expected, P4Tr CAR T cells were unable to kill in any given condition [Figure 4.23-4.25].

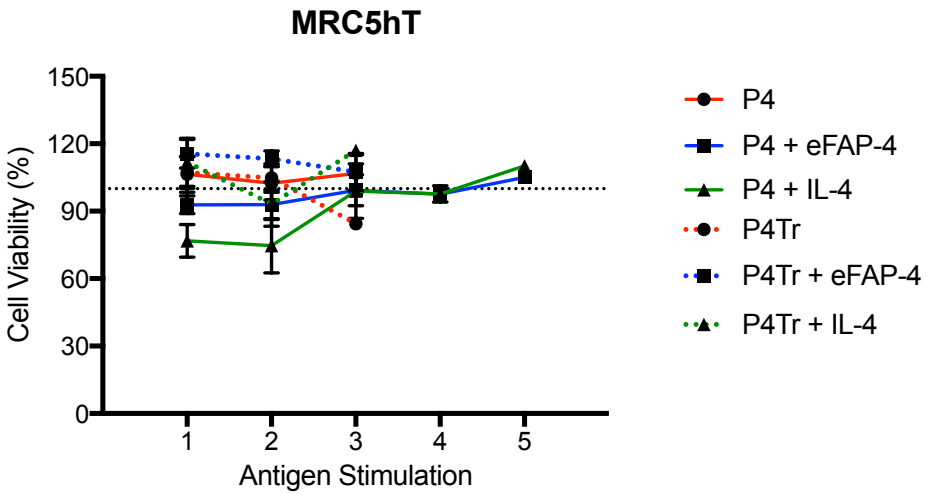

Figure 4.25 CAR T cell non-specific killing of MRC5hT monolayers.
P4 and P4Tr CAR T cells were added to monolayers at an initial E:T ratio of 1:2. Tumour cell viability was measured after 72-96 hours by MTT assay and T cells were restimulated on a new monolayer. Cell viability was compared to monolayers not receiving CAR T cells or cytokine supplementation (considered 100%; dotted black line). Efficacy was assessed alone or with either 2 nM eFAP-4 or IL-4 on monolayers of MRC5hT (mean ± SEM, n=4). Dotted coloured lines in the legend represent the P4Tr counterpart for each condition.

Cytokine production in the co-culture assays described above was quantified by ELISA. Production of IFN-γ was consistent with observed patterns of cytotoxicity [Figure 4.26A-E]. No IFN-γ was produced by P4 CAR T cells when co-cultured with MRC5hT monolayers [Figure 4.26E].

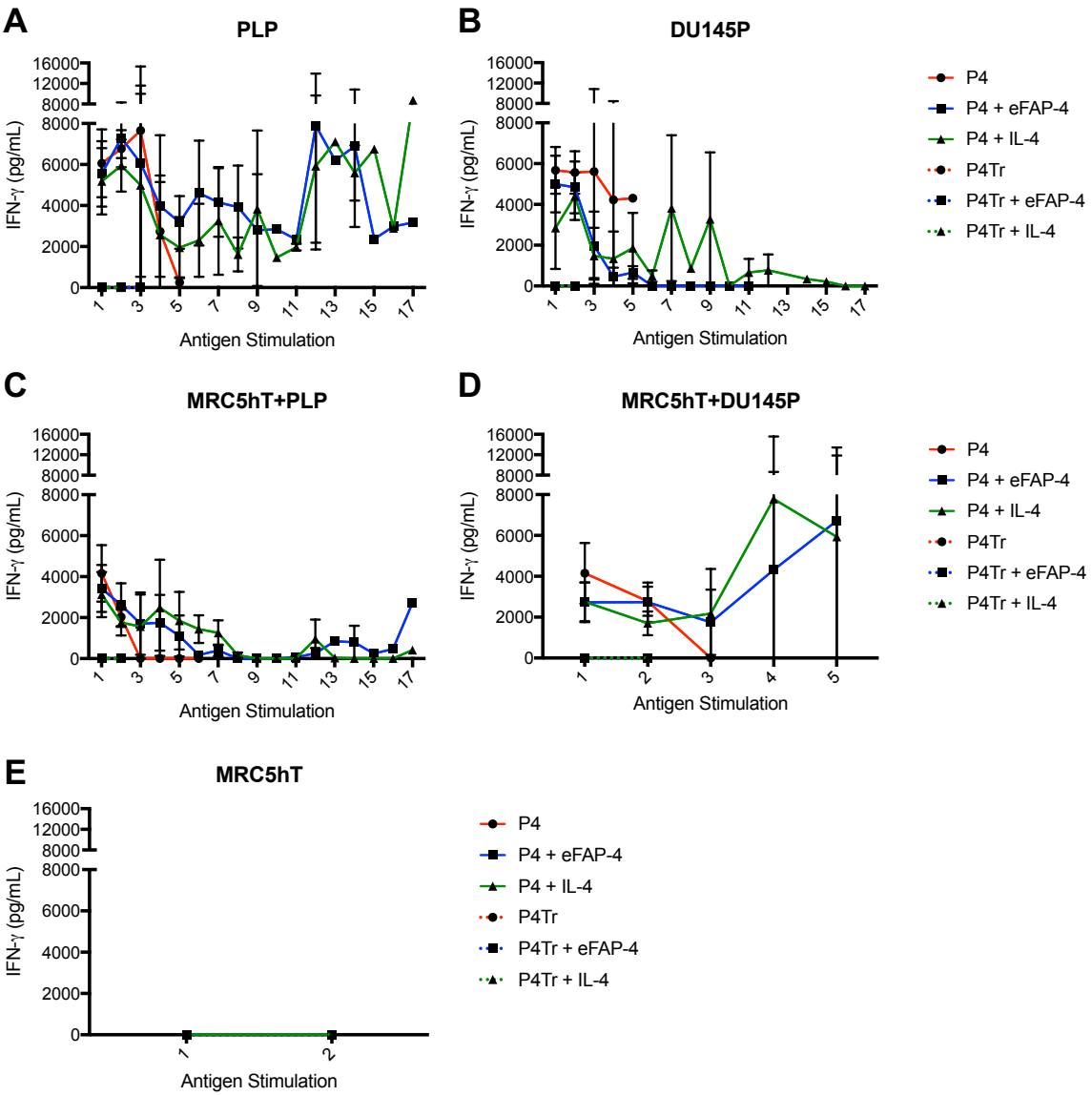

Figure 4.26 IFN-γ production by CAR T cells in PCa/MRC5hT cultures.

P4 and P4Tr CAR T cells were restimulated on A) PLP, B) DU145P tumour monolayers or C) MRC5hT+PLP, D) MRC5hT+DU145P stroma/tumour monolayers as described in Figure 4.21-23. Stimulation on E) MRC5hT monolayers served as negative control. IFN-γ secretion was assessed by ELISA in cultures without cytokine support or supplemented with either 2 nM eFAP-4 or IL-4. Dotted coloured lines represent the P4Tr counterpart for each condition (mean ± SEM, n=4).

Production of IL-2 by CAR T cells was also quantified by ELISA. High levels were seen at 72-hours after co-culture of P4 T cells with DU145P, MRC5hT+PLP and MRC5hT+DU145P cells during the 1st antigen stimulation in every cytokine condition. Levels tapered and became undetectable after the 3rd stimulation [Figure 4.27A-D]. Cultures with PLP exhibited peaks of IL-2 production in the P4+eFAP-4 condition at late stimulation points [Figure 4.27A]. P4Tr CAR T cells never produced detectable IL-2.

Additionally, there was no IL-2 production by P4 on MRC5hT monolayers [Figure 4.27E].

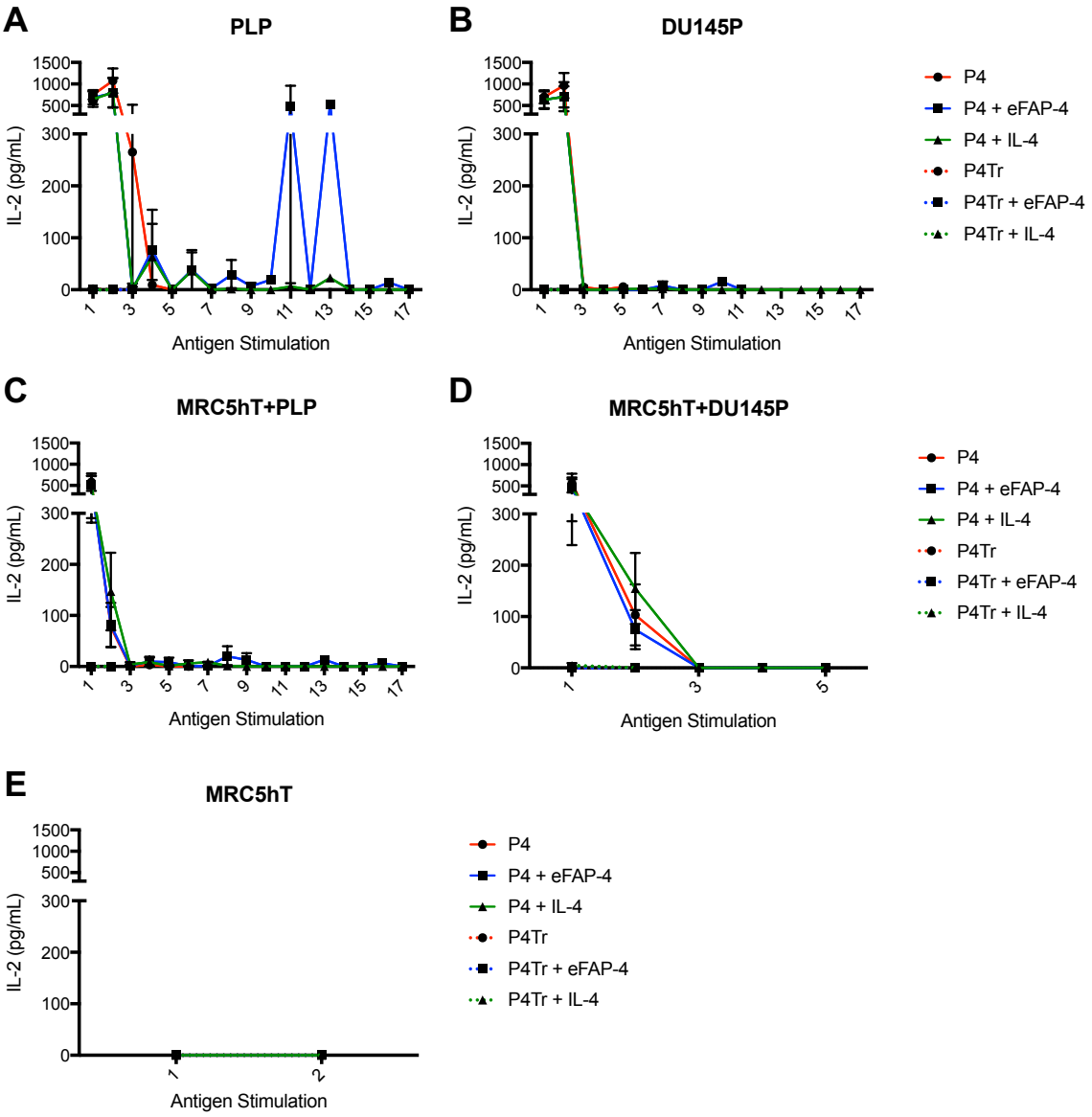

Figure 4.27 IL-2 production by CAR T cells in PCa/MRC5hT cultures.
P4 and P4Tr CAR T cells were restimulated on A) PLP, B) DU145P tumour monolayers or C) MRC5hT+PLP, D) MRC5hT+DU145P stroma/tumour monolayers as described in Figure 4.21-23. Stimulation on E) MRC5hT monolayers served as negative control. IL-2 secretion was assessed by ELISA in cultures without cytokine support or supplemented with either 2 nM eFAP-4 or IL-4. Dotted coloured lines represent the P4Tr counterpart for each condition (mean ± SEM, n=4).

Expansion of P4 T cells was significantly enhanced in co-culture with PLP target cells over multiple restimulations when IL-4 or eFAP-4 supplementation was present. In the MRC5hT+PLP monolayer restimulations this was also seen, but IL-4 was superior to

eFAP-4 in supporting expansion [Figure 4.28A&C]. In the P4 DU145P cultures, only IL-4 supplementation resulted in expansion [Figure 4.28B]. For MRC5hT+DU145P and MRC5hT alone very minimal expansion was seen [Figure 4.28D-E]. There was no proliferation of P4Tr CAR T cells.

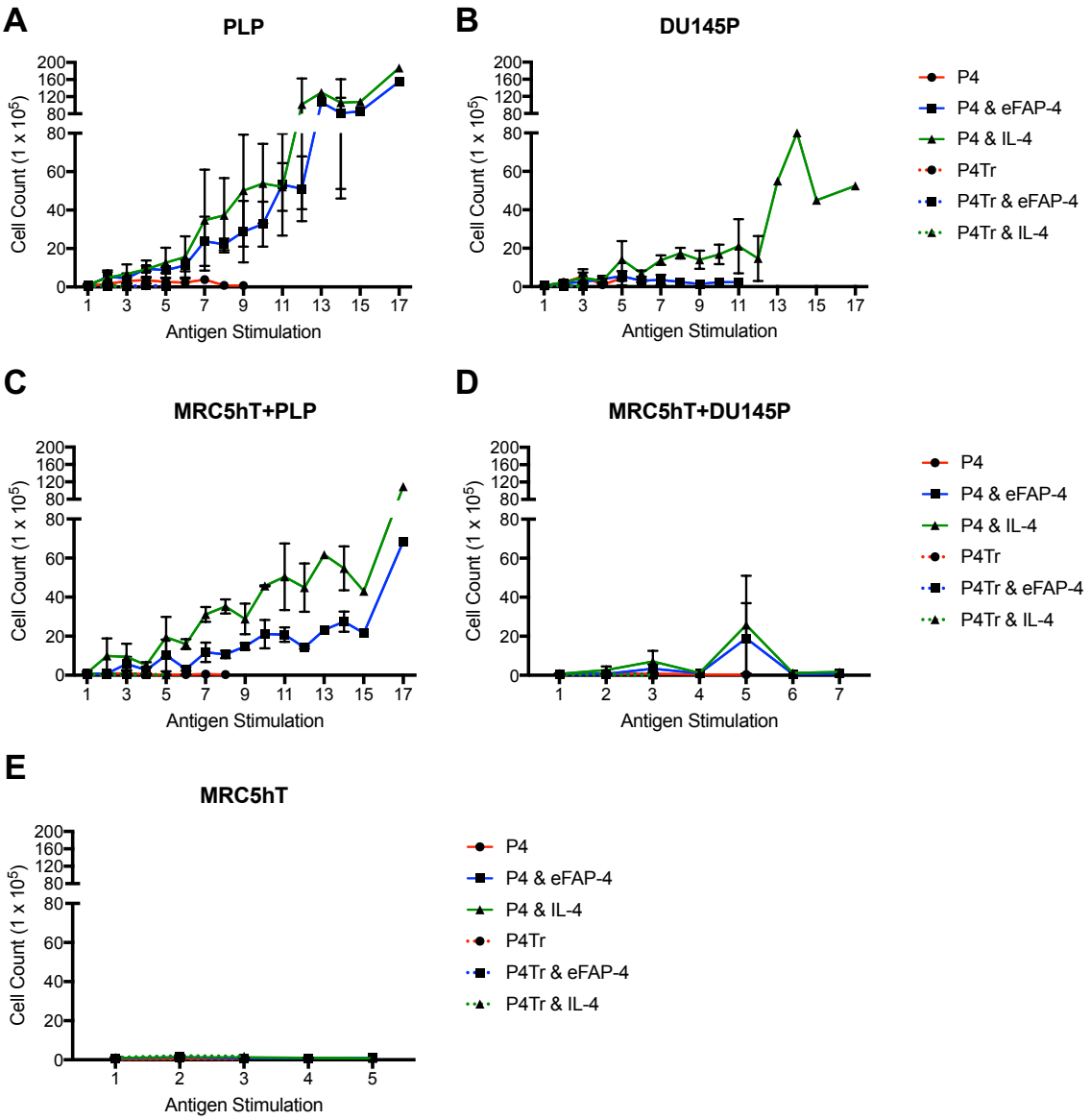

Figure 4.28 Proliferation of CAR T cells on PCa/MRC5hT monolayers.

P4 and P4Tr CAR T cells were restimulated on A) PLP, B) DU145P tumour monolayers or C) MRC5hT+PLP, D) MRC5hT+DU145P stroma/tumour monolayers as described in Figure 4.21-23. Stimulation on E) MRC5hT monolayers served as negative control. CAR T cell proliferation was assessed in cultures without cytokine support or supplemented with either 2 nM eFAP-4 or IL-4. Dotted coloured lines represent the P4Tr counterpart for each condition (mean ± SEM, n=4).

When $CD8^+$:$CD4^+$ ratios were studied by flow cytometry at baseline, antigen stimulation 3 and, where possible, at the time of the last stimulation there was a suggestion that the presence of IL-4 or eFAP-4 in the co-culture may increase the proportion of $CD4^+$ cells. Significant donor variability was observed [Figure 4.29A-E]. The decrease in the $CD8^+$:$CD4^+$ ratio was statistically significant at the 3rd antigen stimulation on monolayers of MRC5hT+PLP. This significance was seen between cultures of P4 and P4 supplemented with eFAP-4 or IL-4 [Figure 4.29C].

The expression of exhaustion marker PD-1 was analysed on P4 CAR T cells. Again, high donor variability was observed. No significant differences were seen [Figure 4.30A-D].

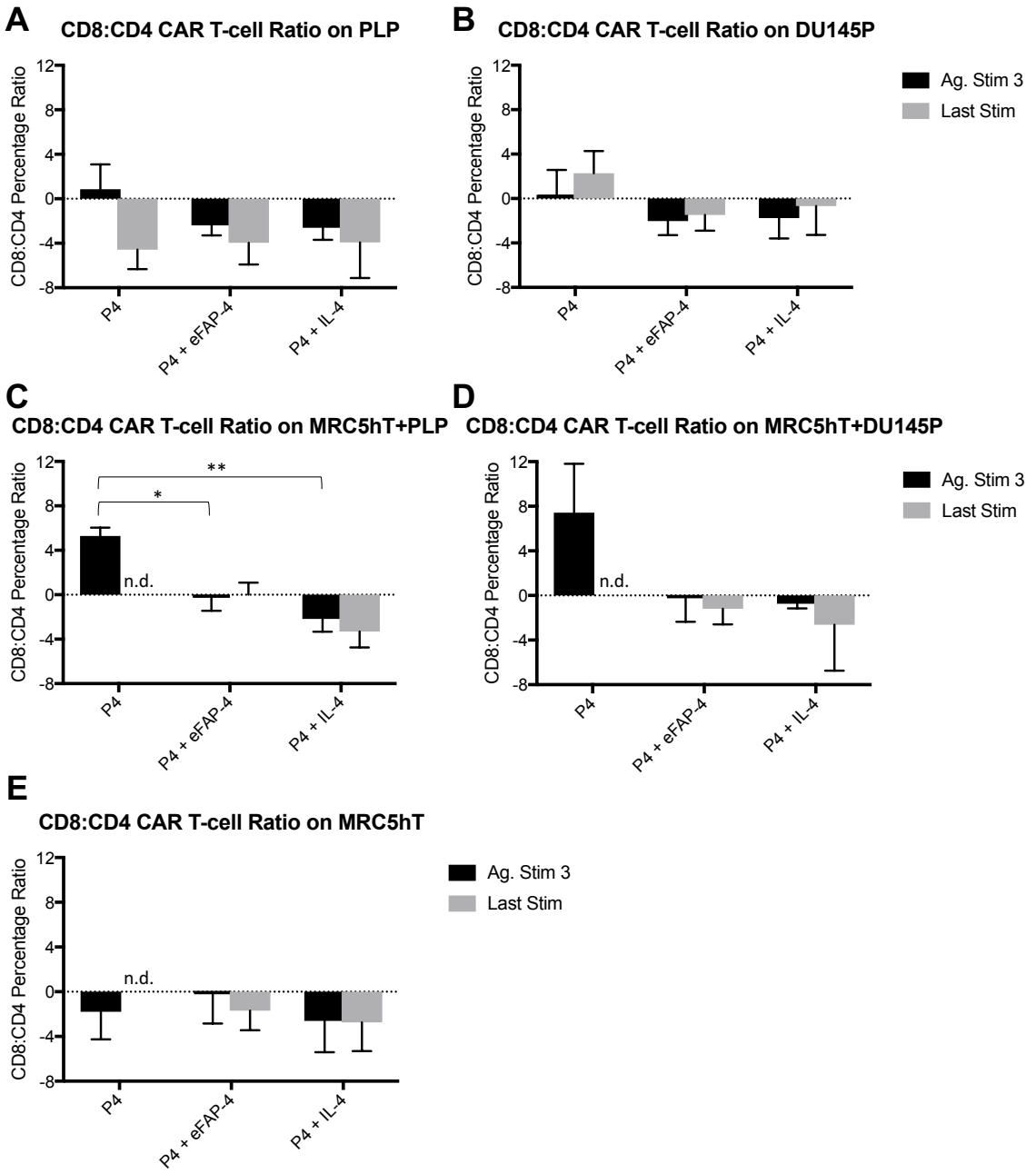

Figure 4.29 CD8$^+$:CD4$^+$ T cell ratio in different cytokine conditions during killing assays.

P4 and P4Tr CAR T cells were restimulated on A) PLP, B) DU145P tumour monolayers or C) MRC5hT+PLP, D) MRC5hT+DU145P stroma/tumour monolayers as described in Figure 4.21-22. Stimulation on E) MRC5hT monolayers served as negative control. Flow cytometry was used to determine the ratio of CD8$^+$:CD4$^+$ P4 CAR T cells in cultures without cytokine support or supplemented with either eFAP-4 or IL-4. Commercially available antibodies were used for CD8 and CD4. Baseline CD8:CD4 ratios were determined before antigen stimulation and deviations were recorded as an increase or decrease of that ratio. This was assessed after 3 antigen stimulations (Ag. Stim 3) and after the last stimulation (Last Stim). A no data (n.d.) point is noted when there were only 3 antigen stimulations in a given condition or there were not enough cells to analyse the last stimulation. Statistical significance was determined using a student's t-test (* = $p < 0.05$; ** = $p < 0.01$; mean $\pm$ SEM, n=2-4).

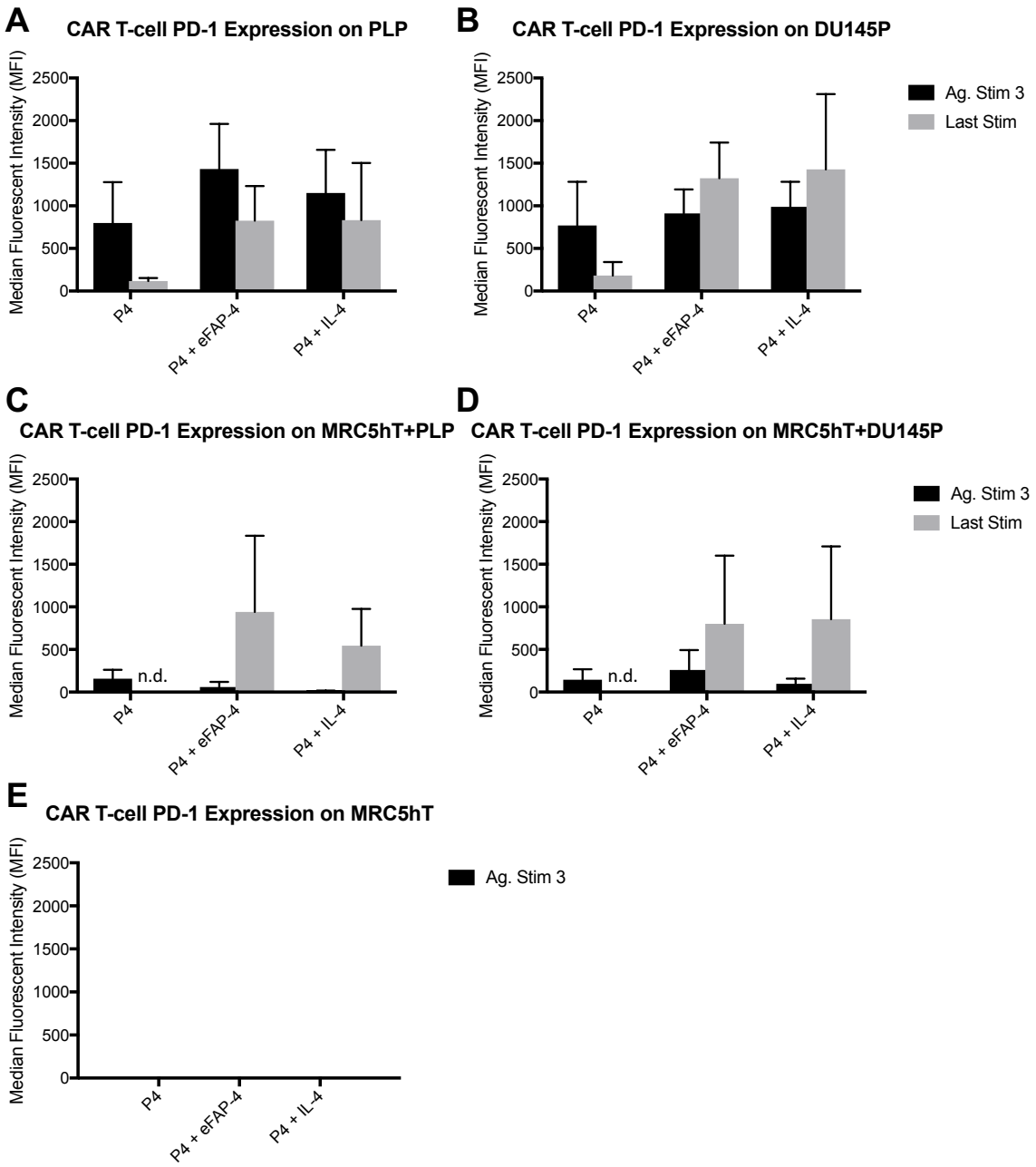

Figure 4.30 PD-1 expression in P4 CAR T cells during killing assays.

P4 and P4Tr CAR T cells were restimulated on A) PLP, B) DU145P tumour monolayers or C) MRC5hT+PLP, D) MRC5hT+DU145P stroma/tumour monolayers as described in Figure 4.21-22. Stimulation on E) MRC5hT monolayers served as negative control. Flow cytometry was used to determine the expression of PD-1 on P4 CAR T cells in cultures without cytokine support or supplemented with either eFAP-4 or IL-4. An isotype control was used to set the gate and a commercially available antibody was used to stain PD-1. This was assessed after 3 antigen stimulations (Ag. Stim 3) and after the last stimulation (Last Stim). A no data (n.d.) point is noted when there were only 3 antigen stimulations in a given condition or there were not enough cells to analyse the last stimulation (mean $\pm$ SEM, n=2-4). E) there is no data for the last stim condition.

Expression of the activation marker CD44 was analysed [Figure 4.31A-E] (Forster-Horvath et al., 2001, Kmieciak et al., 2009). CD44 expression increased on P4 CAR T

cells in the presence of eFAP-4 between the 3rd and final restimulation of MRC5hT+PLP. At the last stimulation, CD44 levels were higher on the P4 CAR T cells co-cultured with MRC5hT+PLP supplemented with eFAP-4 when compared to IL-4 [Figure 4.31C]. MRC5hT cultures were only assessed at the 3rd antigen stimulation and while CD44 expression appears higher in P4+eFAP-4 and P4+IL-4 conditions compared to P4 alone, this did not reach significance [Figure 4.31E].

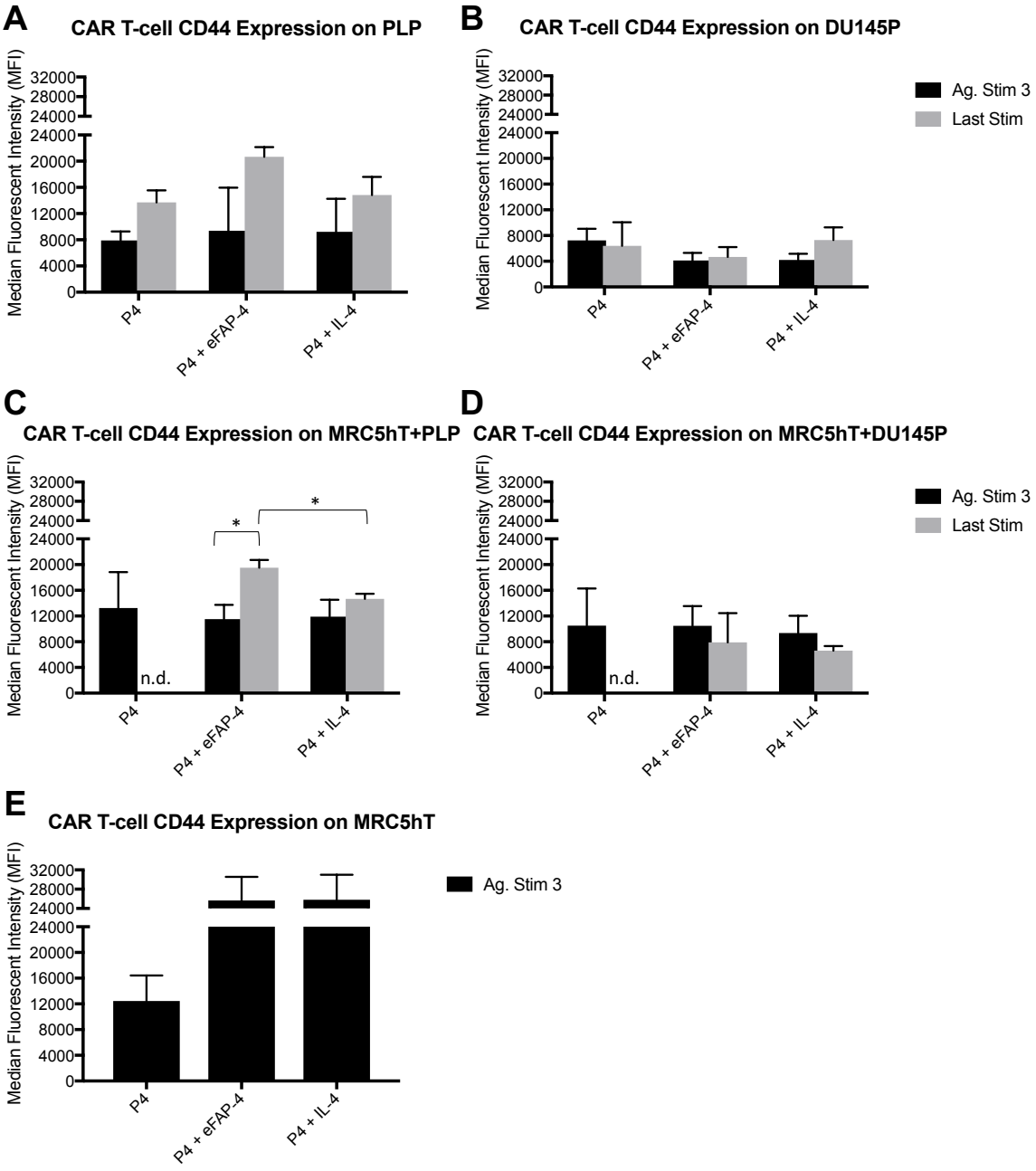

Figure 4.31 CD44 expression in P4 CAR T cells during killing assays.

P4 and P4Tr CAR T cells were restimulated on A) PLP, B) DU145P tumour monolayers or C) MRC5hT+PLP, D) MRC5hT+DU145P stroma/tumour monolayers as described in Figure 4.21-22. Stimulation on E) MRC5hT monolayers served as negative control. Flow cytometry was used to determine the expression of CD44 on P4 CAR T cells in cultures without cytokine support or supplemented with either eFAP-4 or IL-4. An isotype control was used to set the gate and a commercially available antibody was used to stain CD44. This was assessed after 3 antigen stimulations (Ag. Stim 3) and after the last stimulation (Last Stim). A no data (n.d.) point is noted when there were only 3 antigen stimulations in a given condition or there were not enough cells to analyse the last stimulation (mean $\pm$ SEM, n=2-4). E) there is no data for the last stim condition.

A pilot analysis of cytokine dependence was undertaken. In a single experiment, cultures that were on-going at restimulation cycle 15 were split into two groups. In group 1

cytokine supplementation continued and in group 2 no further IL-4 or eFAP-4 was given. Disruption of the PLP monolayer remained consistent across all conditions while CAR T cell expansion continued in the cytokine supplemented cultures, but not when eFAP-4 or IL-4 was removed [Figure 4.32A-B]. P4 killing of DU145P was completely abrogated within 2 stimulations after IL-4 removal [Figure 4.32C] and expansion was flat in group 1 and 2 [Figure 4.32D]. P4 CAR T cells on MRC5hT+PLP cultures continued to kill over 80% of the monolayers regardless of cytokine supplementation [Figure 4.32E]. Removal of cytokine support from MRC5hT+PLP cultures resulted in loss of expansion [Figure 4.32F]. This pilot experiment suggests an ongoing dependence of the presence of cytokine/immunocytokine with implications for dosing *in vivo.*

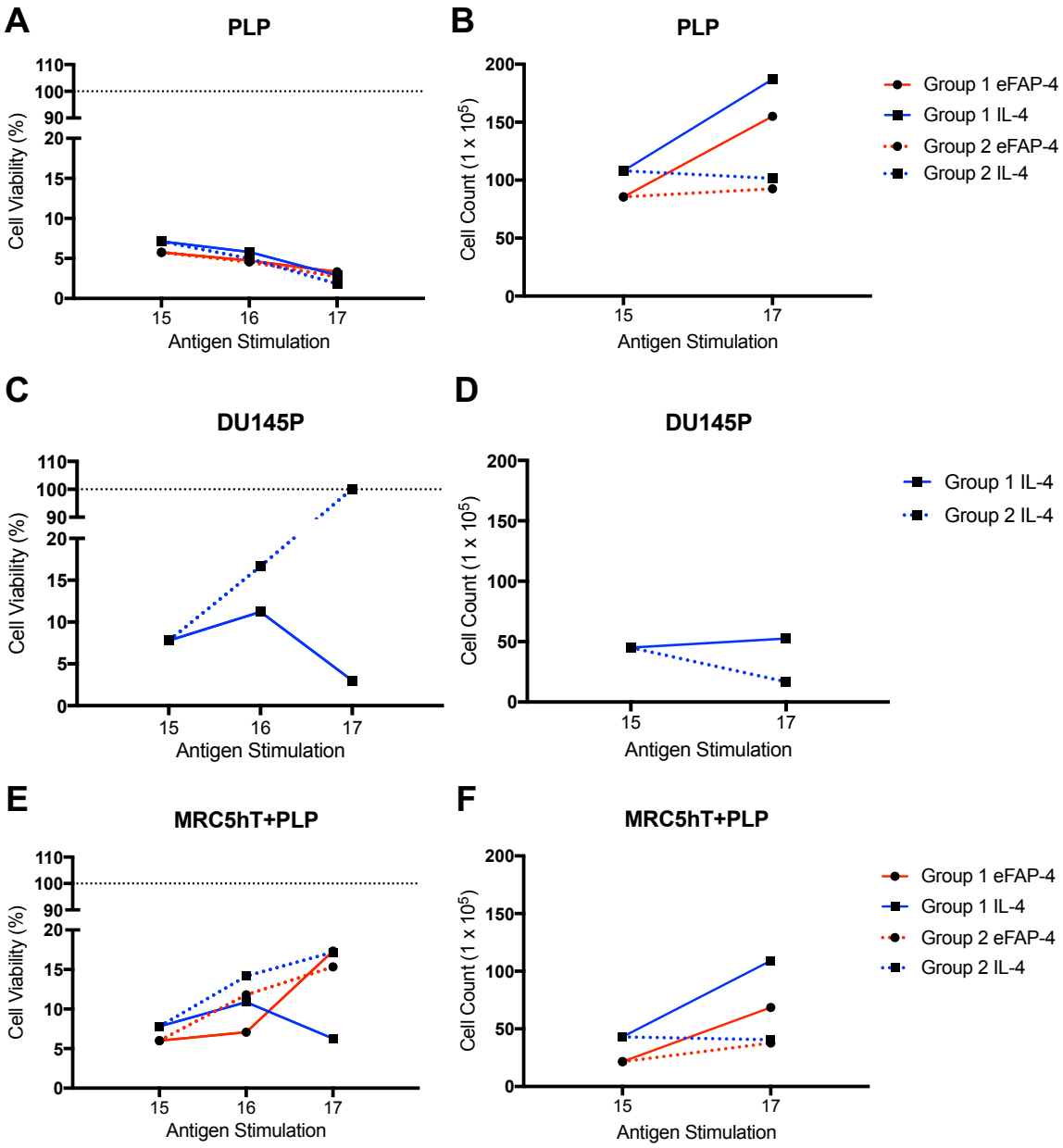

Figure 4.32 P4 CAR T cell killing and expansion after cytokine removal.

After 15 restimulation cycles, P4 CAR T cells killing and proliferation were assessed with eFAP-4 or IL-4 and assessed upon removal of the cytokine in cultures of A-B) PLP, C-D) DU145P and E-F) MRC5hT+PLP (n=1). Solid lines represent group 1 with continued supplementation of either 2 nM eFAP-4 or IL-4 and dotted lines represent cultures in group 2 in which all cytokine support was deprived from these cultures. Subsequent restimulations were carried out as described in Figure 4.21-4.23 and MTT assays were used to observe cell viability (A, C, E). T cell number was counted at each restimulation (B,D,F).

$CD8^+$:$CD4^+$ CAR T cell ratio was analysed in cultures for which the cytokine had been withdrawn. There did not appear to be an effect of cytokine removal on the CD8:CD4 ratio in cultures of PLP [Figure 4.33A]. The CD8:CD4 ratio decreased upon removal of IL-4 in DU145P cultures indicating an outgrowth of $CD4^+$ cells [Figure 4.33B]. In the

eFAP-4 condition on MRC5hT+PLP, removal of eFAP-4 showed a decrease in the CD8:CD4 ratio by more than half [Figure 4.33C].

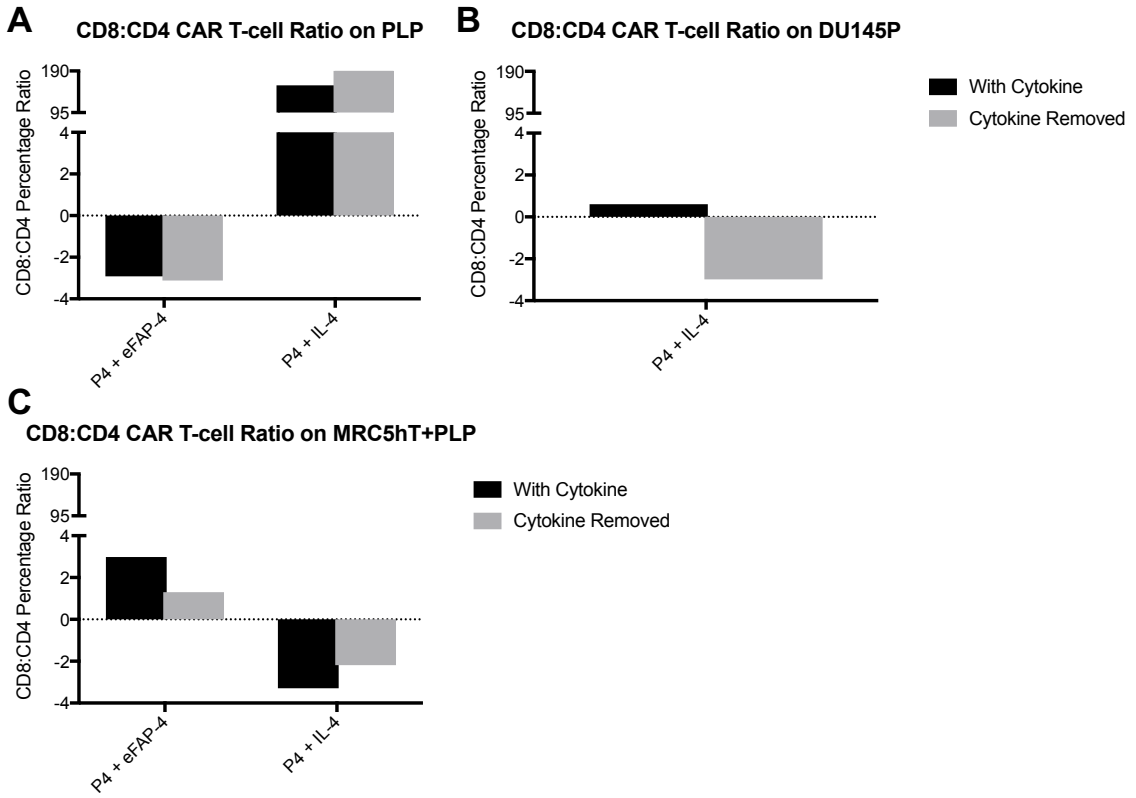

Figure 4.33 CD8$^+$:CD4$^+$ P4 CAR T cell ratio after cytokine removal.
P4 CAR T cell CD8:CD4 ratio was assessed with eFAP-4 or IL-4 and assessed upon removal of the cytokine in cultures of A) PLP, C) DU145P and E) MRC5hT+PLP (n=1). Commercially available antibodies were used for CD8 and CD4. Baseline CD8:CD4 ratios were determined before antigen stimulation and deviations were recorded as an increase or decrease of that ratio. This data was collected after the last stimulation.

The exhaustion and activation markers PD-1 and CD44 were examined on P4 CAR T cells after cytokine removal. Expression of PD-1 and CD44 increased in CAR T cells upon removal of either eFAP-4 or IL-4 from PLP cultures [Figure 4.34A-B]. Both markers remained relatively consistent on T cells in DU145P cultures with and without IL-4 [Figure 4.34C-D]. PD-1 expression was upregulated on P4 CAR T cells in MRC5hT+PLP cultures that had eFAP-4 removed compared to supplementation. There was no difference in CAR T cell PD-1 expression for IL-4 supplemented MRC5hT+PLP

cultures [Figure 4.34E]. Expression levels of CD44 on CAR T cells in these co-cultures were not affected by cytokine/immunocytokine removal [Figure 4.34F].

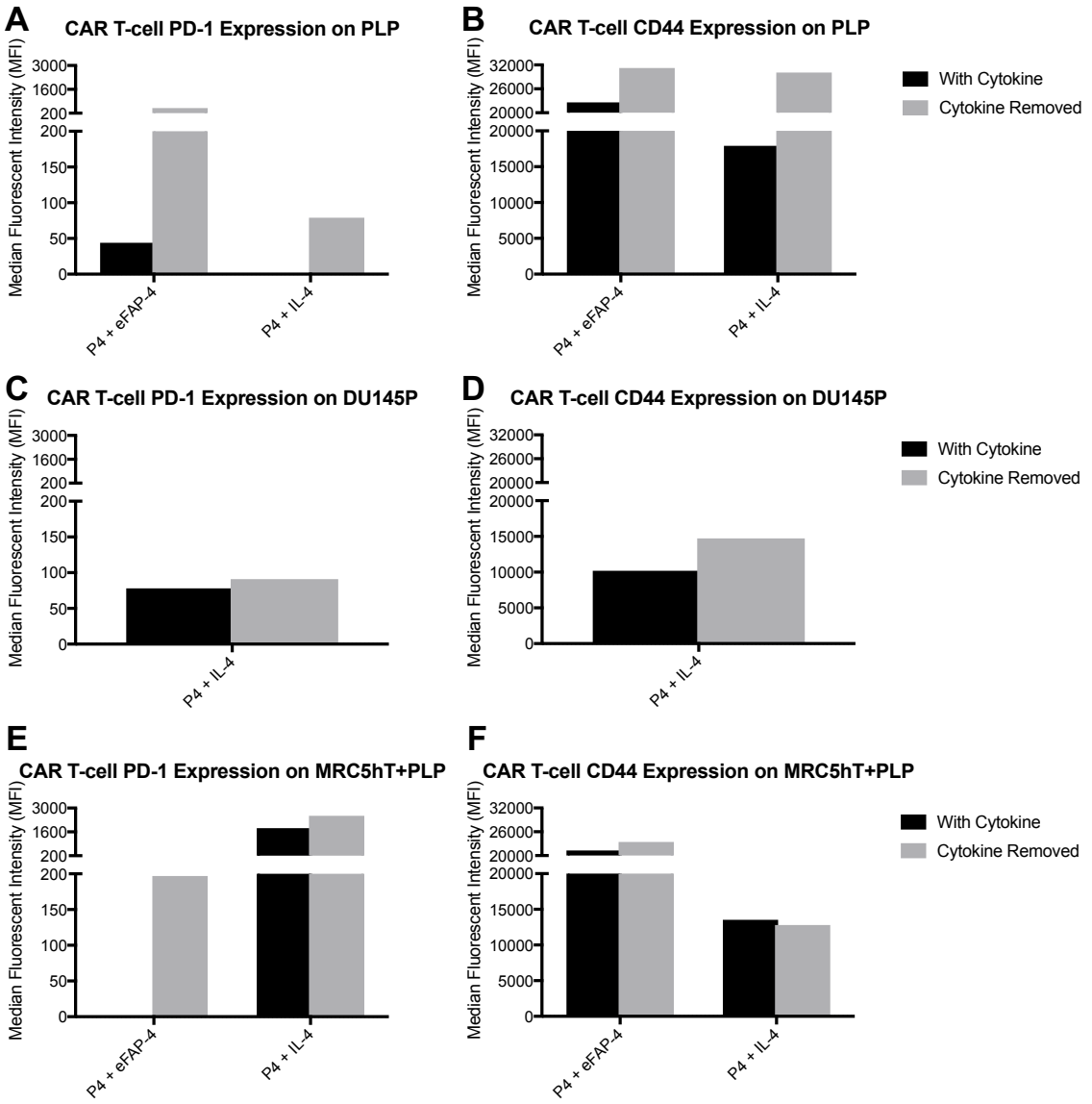

Figure 4.34 PD-1 and CD44 expression in P4 CAR T cells after cytokine removal.
P4 CAR T cell expression of PD-1 and CD44 was assessed with eFAP-4 or IL-4 and assessed upon removal of the cytokine in cultures of A-B) PLP, C-D) DU145P and E-F) MRC5hT+PLP (n=1). An isotype was used to set the gate and a commercially available antibody was used to stain CD44 and PD-1. This data was collected after the last stimulation.

4.3 Discussion

This chapter explored the development of human prostate cancer/stroma models for *in vitro* and *in vivo* experimentation. Two prostate cancer cell lines PL and DU145 were

engineered to express PSMA and the reporter gene LT for *in vitro* and *in vivo* tracking. Two stromal cell lines, MRC5hT and PS1, were engineered to express a far-red reporter gene, mNeptune. These reporters showed utility in flow cytometric analysis through identification of distinct cell populations in co-cultures. All the cell lines were characterised for their growth kinetics and FAP/PSMA expression in mono-cultures, PCa or stroma condition media, or in co-cultures. These investigations led to selection of an *in vitro* PCa/stroma model for further analysis of the CAR^+ T cells with the eFAP-4 immunocytokine.

The ability of eFAP-4 to sustain human CAR T cell expansion through the expression of the 4αβ receptor was confirmed. P4 CAR T cell mediated specific killing of $PSMA^+$ cells was established. Culture of cell lines with eFAP-4 and IL-4 alone did not result in tumour cell cytotoxicity. When in culture with P4 CAR T cells, eFAP-4 and IL-4 increased the expansion and persistence of the T cells and augmented their potential to kill PCa/stroma monolayers. These cytokines did not enhance the CAR T cell non-specific killing of MRC5hT monolayers alone.

A significant decrease in the CD8:CD4 ratio was seen in P4 CAR T cells on MRC5hT+PLP monolayers when supplemented with eFAP-4 or IL-4. This indicates skewing towards a $CD4^+$ T cell enriched population in cytokine supplemented cultures. A recent study demonstrated a similar enrichment of $CD4^+$ CAR T cells co-expressing an IL-4 chimeric receptor that recognises IL-4 and delivers an IL-7 signal. The $CD4^+$ population in IL-4 containing cultures secreted higher levels of IL-2 and exhibited elevated mitochondrial activity compared to the $CD8^+$ CAR T cells, but did not express regulatory markers. However, both populations were necessary to achieve tumour abrogation (Sukumaran et al., 2018). While $CD8^+$ T cells are the main effector cell

populations, it is widely accepted that long-lived memory immunity is dependent on the $CD4^+$ subset. $CD4^+$ T cells help generate $CD8^+$ memory T cells through interactions with CD40 (Rocha and Tanchot, 2004). An HIV envelope-specific CAR demonstrated increased persistence of the transgenic T cells when $CD4^+$ and $CD8^+$ arms were co-injected versus $CD8^+$ CAR T cells alone (Mitsuyasu et al., 2000). Against leukaemia cells, $CD4^+$ CAR T cell proliferate faster and produce more IFN-γ, IL-2 and TNF-α while the $CD8^+$ subset is more cytotoxic *in vitro* (Sommermeyer et al., 2016). There is evidence that a mixture of subsets has higher anti-tumour effects. When naïve $CD4^+$ and central memory $CD8^+$ CAR T cells are combined, they have a synergistic effect in *in vivo* leukaemia models compared to injection of only one of the subsets (Sommermeyer et al., 2016). In a second model system, intrapleural injection of a mesothelin targeting CAR shows an expansion of the $CD4^+$ subset and prolonged efficacy is dependent on early activation of $CD4^+$ T cells. In this model, complete tumour regression is accomplished and maintained with $CD4^+$ CAR T cells alone and less than 50% elimination after treatment with the pure $CD8^+$ CAR T cell subset. Once again, a combination of $CD4^+$ and $CD8^+$ CAR T cells demonstrated the greatest anti-tumour potential (Adusumilli et al., 2014). Even signalling through the endogenous TCR increases exhaustion in $CD8^+$ CAR T cells that is not detectable in $CD4^+$ CAR T cells (Yang et al., 2017). These observations have led one group clinically developing specified CD4:CD8 ratios for CAR T cells as opposed to the widely donor variable CD8:CD4 ratio initially seen in transduced PBMCs (Turtle et al., 2016). Therefore, it is potentially beneficial that eFAP-4 addition increases the $CD4^+$ CAR T cell population in our PCa/stroma model and could partially explain the increased persistence of the T cells.

Effects of eFAP-4 and IL-4 on CD44 and PD-1 expression, CD8:CD4 ratio, monolayer destruction and expansion of P4 CAR T cells are all comparable on PLP containing

cultures in this study, suggesting similar signalling capabilities through the 4αβ receptor. However, IL-4 outperformed eFAP-4 on DU145P cultures. DU145P cell lines were more resistant to treatment in general with P4 CAR T cells as evident by the decrease in T cell expansion, cytokine secretion and destruction of DU145P containing monolayers. There was an even greater resistance to cell death when cultured with MRC5hT. The decrease in cell death for monolayers containing MRC5hT might be explained by the survival of these cells due to their $PSMA^-$ negative status. While bystander killing of the MRC5hT was observed in $PSMA^+$ monolayers co-cultured with P4, it was incomplete and approximately 50% of the MRC5hT survived [Figure 4.21]. Future experiments could aim to delineate which cell population is surviving in these PCa/stroma monolayers. This could be accomplished through luciferase assays instead of MTT assays as this would be specific for the viability of the LT-PCa cells only. Removal of each cytokine from cultures resulted in a continuation of monolayer disruption for PLP and MRC5hT+PLP cultures, but a complete reversal of cytotoxicity for DU145P. In all cases, removal of cytokine decreased T cell expansion.

4.4 Summary

- FAP^+ MRC5hT and PS1 cells were engineered to express mNeptune.
- PL and DU145 were engineered to express PSMA and LT.
- *In vitro* co-cultures PCa/ stromal co-culture models were established.
- eFAP-4 elicits a proliferation signal similar to IL-4 in human T cells expressing 4αβ.
- eFAP-4 and IL-4 increase expansion, cytokine release and cytotoxicity of CAR T cells against PCa/MRC5hT cultures.
- eFAP-4 and IL-4 comparatively decreased the CD8:CD4 ratio in MRC5hT+PLP cultures.

- Removal of cytokines reverse T cell expansion in all cultures and killing of DU145P monolayers.

Chapter 5: Efficacy of eFAP-4 and P4 CAR T cells *in vivo*

5.1 Introduction

5.1.1 Current *in vivo* models for prostate cancer

Preclinical prostate cancer research relies heavily on models using immortalized cell lines. The repertoire of human prostate cancer cell lines available is limited, with the majority of studies utilising PC3, DU145 and LNCaP. This panel is clearly not representative of the diversity of human prostate cancer given the heterogeneity of patient derived samples and xenografts (Namekawa et al., 2019). Xenografts are useful for translational drug development, offering humanised models that enable the evaluation of drugs designed to target human antigens and cells. Unfortunately, this type of *in vivo* model overlooks the immune system's influence on drug efficacy because of the immune-deficiency of the mice. Syngeneic and transgenic models provide a means to incorporating the host's immunity into the prostate cancer model. Nonetheless, there is a lack of murine prostate cancer cell lines and transgenic models are expensive, technically challenging and tumour development is unreliable. Patient-derived xenograft (PDX) models of prostate cancer offer a further alternative solution in which some degree of tumour heterogeneity is maintained. Organoids derived from PDX cultures can engraft in immunocompromised mice and retain the histology seen in the original biopsy (Gao et al., 2014a). Counterbalancing this however, PDX models are difficult to culture, establish *in vivo* and reproduce (Russell et al., 2015). Incorporation of stromal components of the tumour microenvironment into organoids could greatly enrich the experimental yields of these models for cancer immunotherapy development (Neal et al., 2018).

The establishment of prostate cancer xenografts in the extremely immune-deficient mouse model NOD-SCID-IL2Rγ-/- (NSG) has been well documented. NSG mice have an improved rate of engraftment for human cell lines (malignant and hematopoietic) and,

despite their immune compromised nature, they have been used widely for selected immunotherapy studies (Shultz et al., 2014). These mouse models of PCa have a particular value in the assessment of metastases as the lack of a functional immune system aids in tumour cell dissemination (Hudson et al., 2015, Mussawy et al., 2018, Vormoor et al., 2014). Moreover, humanised models based on NSG mice can provide additional insights into disease biology. Illustrating this, one study showed that the ability of prostate cancer cell lines to metastasise can partially be explained by overexpression of CD47 on tumour cells, enabling them to avoid phagocytosis in a reconstituted innate immune system (Rivera et al., 2015). The NSG mouse is also used to model bone metastases (common in human prostate cancer) and the effect of drug intervention on lesions in the bone marrow (Eswaraka et al., 2014). Additionally, without the host immune system's influence on the tumour, such models offer a means to test cellular therapies and their specific effects on progression (Nada et al., 2017, Roth and Harui, 2015).

5.1.2 Stroma compartment *in vivo*

The tumour microenvironment plays an important role in disease progression. Non-cancerous cells of the stroma often assist in immune evasion and metastasis. The tumour stroma is both a focus for targeted therapy development and enhanced understanding of interactions between cancer cells and their surroundings. Recapitulating this environment *in vivo* is crucial and has been approached in different ways. PDX models are often implanted with endogenous human stromal cells from the tumour, but over time and passage this is replaced with host murine stroma. Murine stromal elements have been detected in different carcinoma xenografts, including prostate cancer, indicating an ability for the mouse stroma to partially support the human tumour growth (Bradford et al., 2016, Delitto et al., 2015, Mo et al., 2018). Stromal FAP expression is often found in these models and has shown to be of mouse origin (Niedermeyer et al., 1997). Accordingly,

NSG mice are also able to recruit host stromal cells to the site of human PDX tumours and replace the human fibroblasts completely after multiple passages *in vivo* (Maykel et al., 2014, Braekeveldt et al., 2016).

Xenografts in NSG mice derived from the human PC3 and DU145 PCa cell lines have been shown to recruit murine stroma. Establishment of a stroma is inversely correlated with *SOCS1* expression in the prostate cancer cells (Villalobos-Hernandez et al., 2017). However, initial studies of PCa xenografts in our lab showed a lack of murine stroma recruitment. To ensure the presence of the stromal compartment and to observe stroma-tumour interactions that do not cross the species barrier, fibroblasts can be co-administered. Reactive prostate stromal cell lines and cancer-associated fibroblasts taken from patients express a different gene signature compared to normal prostatic tissue fibroblasts and are able to promote prostate cancer engraftment, vascularisation and growth *in vivo* (Dakhova et al., 2014, Minciacchi et al., 2017, Tuxhorn et al., 2002b, Wilkinson et al., 2013). Non-prostatic stromal cells have been used to represent the prostate tumour microenvironment, including the murine fibroblast line NIH3T3 and the bone marrow derived stromal cells Hs5 via a co-culture injection (Bruzzese et al., 2014, Chen et al., 2013a). Bone marrow-derived mesenchymal stem cells have also been shown to be recruited to the prostate tumour in both transgenic and xenograft models (Placencio et al., 2010). In this project, I aimed to create a model of the tumour microenvironment in which human stromal FAP expression is seen, as is the case in human prostate cancer (Tuxhorn et al., 2002a). The human foetal lung fibroblast cell line MRC5 is a reactive fibroblast that naturally expresses endogenous FAP. Co-injection of MRC5 cells with malignant cells has been successfully demonstrated in *in vivo* models leading to its use in this study (Chen et al., 2013b, Jiang et al., 2005, Kanaji et al., 2017, Wang et al., 2012).

5.1.3 Specific aims

1. Establish an *in vivo* PCa/stroma model for drug development.
2. Test the anti-tumour efficacy of eFAP-4 when combined with P4 CAR T cells *in vivo*.

5.2 Results

5.2.1 Establishment of prostate cancer/stroma co-culture *in vivo*

The results presented above indicate that the PCa/MRC5hT combination provides a useful *in vitro* PCa/stroma model in which both PSMA (tumour) and FAP (stroma) co-expression are maintained. Consequently, an *in vivo* model was next established using these cells. Given the *in vitro* results, cells were mixed at an 8:1 cell (MRC5hT:PCa) ratio such that a total of $9x10^5$ of MRC5hT+PL, MRC5hT+PLP, MRC5hT+DU145 or MRC5hT+DU145P cells were administered to NSG mice by subcutaneous injection. Ratios of PCa and stromal cell types were analysed by flow cytometry before subcutaneous administration and it was observed that the injected cultures contained between 12-15% of respective PCa cells and between 83-86% MRC5hT cells, in keeping with the 8:1 stromal to tumour cell target ratio [Figure 5.1A-B].

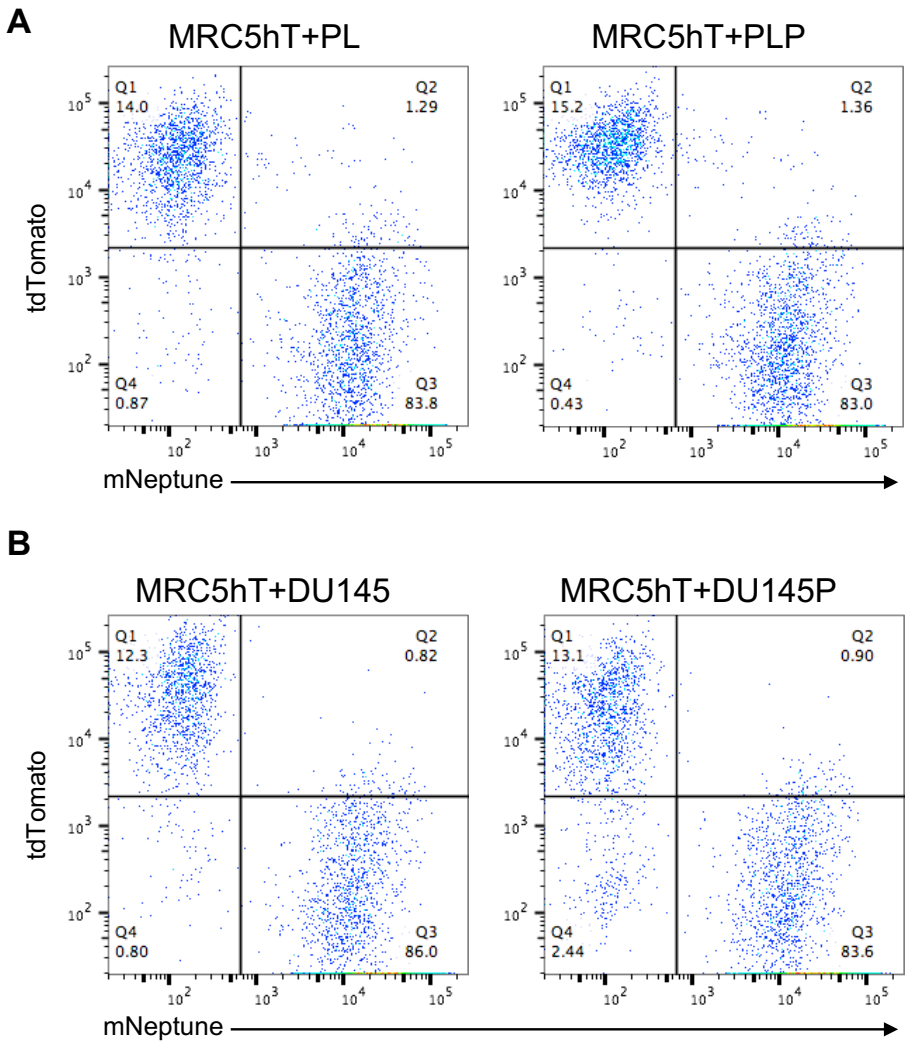

Figure 5.1 Ratio confirmation of injected MRC5hT:PCa co-cultures.

The indicated tumour/ stromal cell mixtures were analysed by flow cytometry prior to injection in NSG mice. Ratios were determined by detection of the PCa cells through tdTomato expression and MRC5hT through mNeptune expression in A) MRC5hT+PL, MRC5hT+PLP, B) MRC5hT+DU145 and MRC5hT+DU145P.

Tumour growth was imaged *in vivo* using bioluminescence of the luciferase expressing PCa cells. A clear demarcation between the PL and DU145 sublines can be seen at day 10 and result in *in vivo* tumour models with distinctive growth kinetics [Figure 5.2A]. The PL/PLP tumours present a rapidly growing model of disease, requiring sacrifice at day 21 due to tumour size. The DU145/DU145P tumours, in keeping with the kinetics observed *in vitro*, are more indolent with the model extending out to 43 days. The weight of the mice was monitored at each imaging time point [Figure 5.2B].

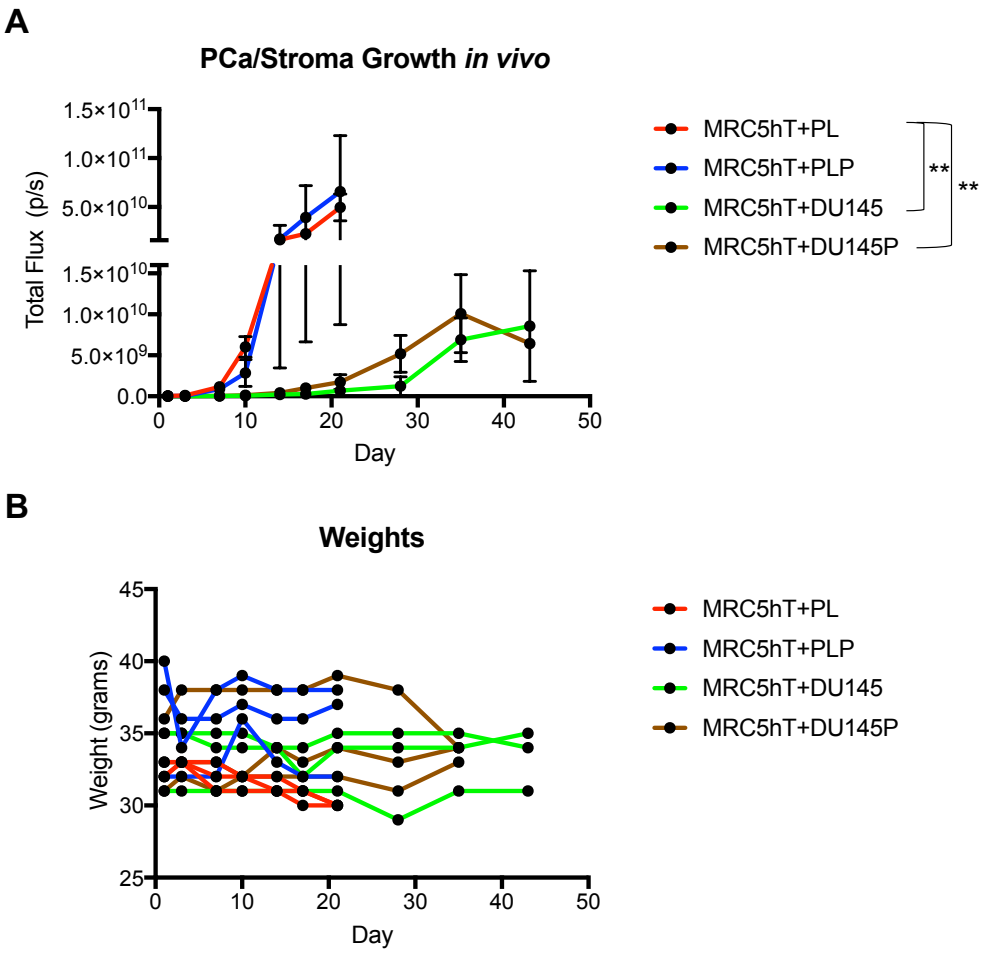

Figure 5.2 *In vivo* establishment of PCa/stroma tumour.

Indicated MRC5hT+PCa combinations were injected subcutaneously. A) BLI was performed to track tumour growth (mean ± SEM, n=3 mice per group). B) Weight of the mice was recorded at each imaging time point. Statistical significance was determined using a two-way ANOVA (** = $p < 0.01$).

Tumours harvested from the mice described above were analysed for the presence of both PCa cells and MRC5hT using flow cytometry. This was carried out using the gating strategy in Figure 5.3. Zombie Green™ dye was used to stain dead cells and a single cell suspension was selected [Figure 5.3A-B]. A control containing LT-PL + PL cells was used to set the gate for tdTomato$^+$ cells and a second control with mNeptune-MRC5hT + MRC5hT was used to set the gate for mNeptune$^+$ cells [Figure 5.3C-D].

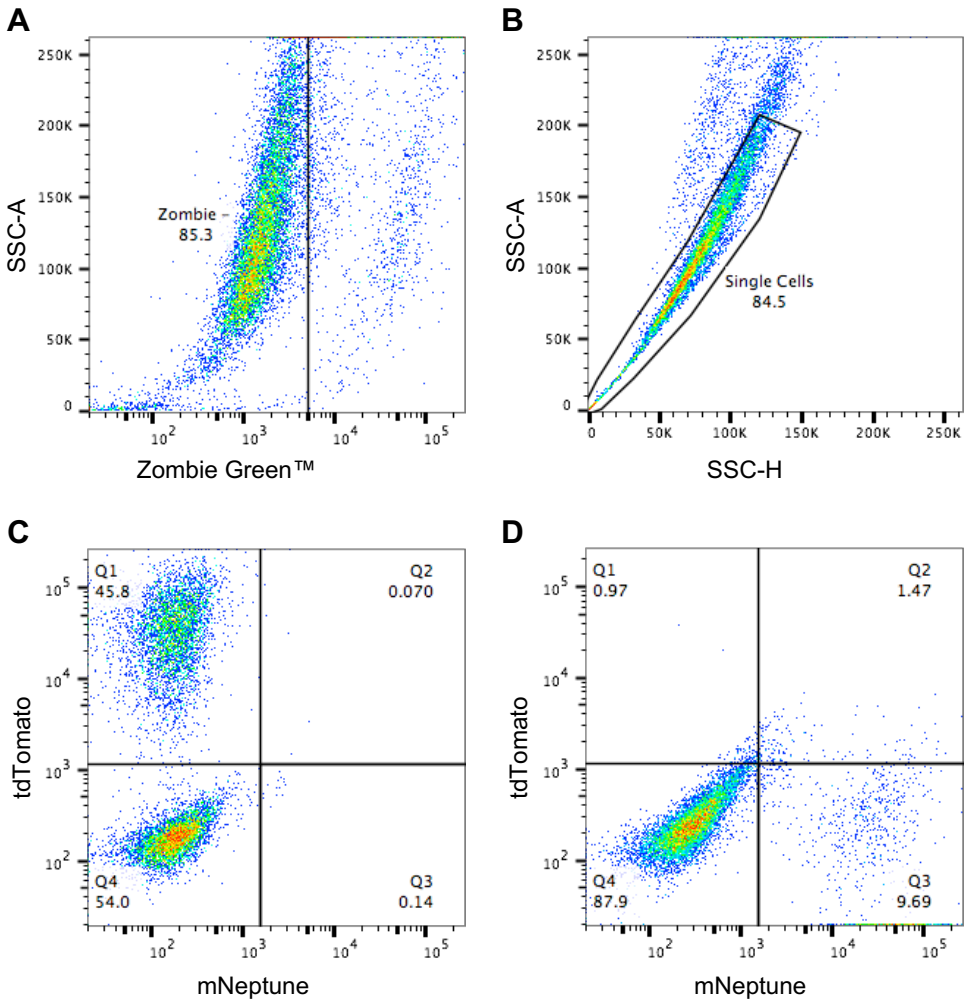

Figure 5.3 Gating strategy for flow cytometric analysis of tumours.
Harvested tumours were analysed by A) dead cell stain with Zombie Green™, gated on the negative population and B) single cell suspension was gated for using side scatter area (SSC-A) and side scatter height (SSC-H). C) LT-PL+PL controls were used to gate for tdTomato$^+$ cells and D) mNeptune-MRC5hT+MRC5hT controls were used to set the parameter for mNeptune$^+$ cells. This strategy was applied to all subsequent flow cytometric analysis.

Mice with PL/PLP tumours were sacrificed at day 21 and animals with DU145/DU145P tumours were culled at between day 37 and 43. Tumours were harvested and half was processed into a single cell suspension and half was snap-frozen. The fresh single cell suspension was analysed for the presence of both PCa and stromal cells. In the case of MRC5hT+PL-injected mice, a tdTomato$^+$ population was detected in all three tumours. No mNeptune MRC5hT cells were detected [Figure 5.4A]. When stained for human PSMA and FAP, neither antigen was present [Figure 5.4B].

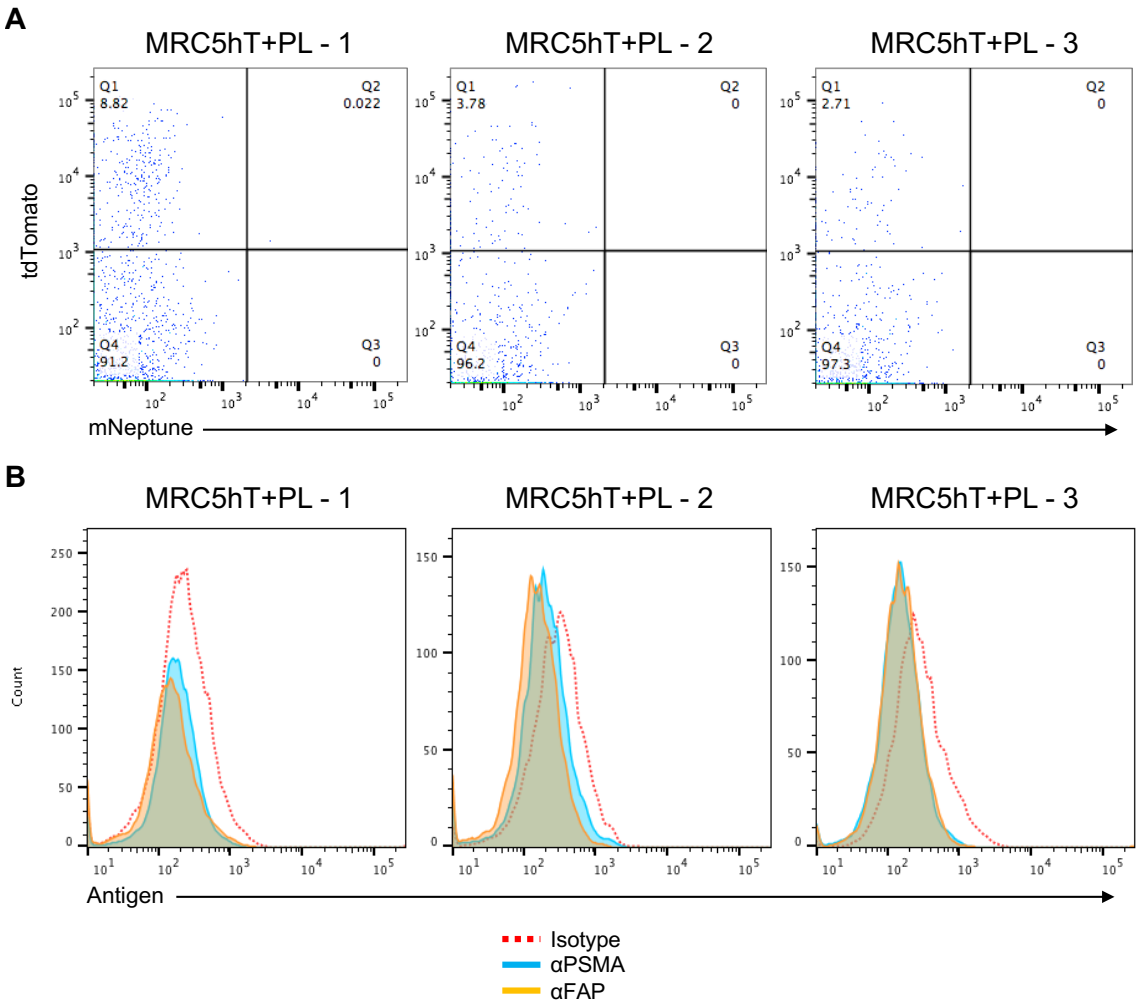

Figure 5.4 MRC5hT+PL tumour analysis.

MRC5hT+PL tumour cells collected from the mice were evaluated for A) presence of both cell types through tdTomato and mNeptune expression and B) FAP and PSMA expression. Commercially available antibodies were used for FAP and PSMA and an isotype was used to set the gate. Data shown is from each mouse in the group (n=3).

For the day 21 MRC5hT+PLP tumours, none of the animals had detectable mNeptune signal and 2 of 3 had low levels of tdTomato [Figure 5.5A]. The third animal had a very distinct tdTomato^{+} population of 13.9%. This animal differed from the other 2 in the group as significant intra-abdominal ascites had developed. This was harvested and analysed [Figure 5.5, MRC5hT+PLP - 3]. The single cell preparation was much more rapid for this animal and as such, cell death/loss in preparation was attenuated. No FAP expression was seen. PSMA was detected [Figure 5.5B]. Mouse 3 had a non-specific peak in the FAP detection channel that mimicked the isotype control.

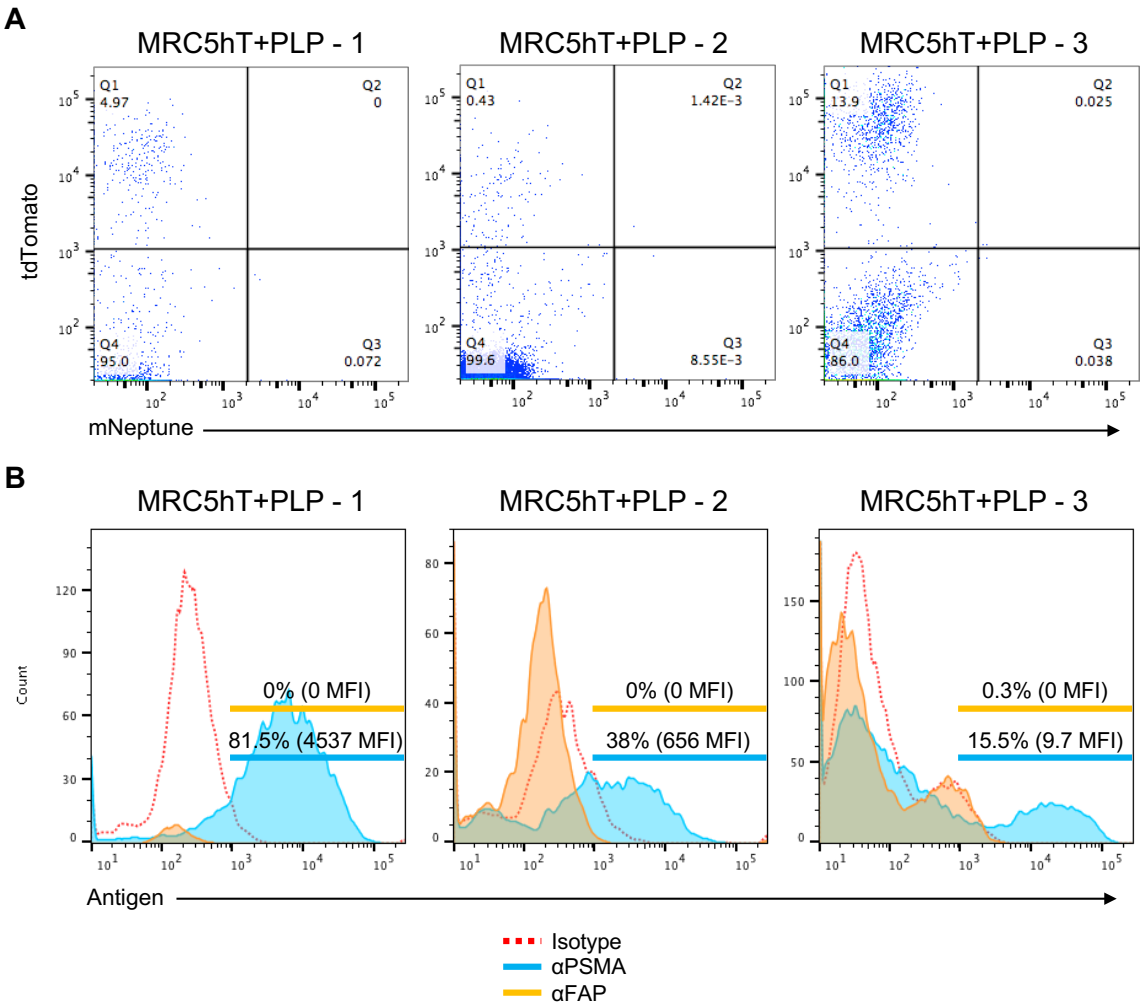

Figure 5.5 MRC5hT+PLP tumour analysis.

MRC5hT+PLP tumour cells collected from the mice were evaluated for A) presence of both cell types through tdTomato and mNeptune expression and B) FAP and PSMA expression. Commercially available antibodies were used for FAP and PSMA and an isotype was used to set the gate. Data shown is from each mouse in the group (n=3).

In light of the difficulty in establishing a good yield of live cells for flow cytometry with the PL/PLP+MRC5hT model, a different method was used to prepare a single cell suspension from harvested MRC5hT+DU145 and MRC5hT+DU145P tumours. This included a tissue digestion step which improved the live cell yield for analysis. Only 2 of 3 mice had visible tumours at day 43 in the MRC5hT+DU145 group and 2 of 3 mice had no tissue collected in the MRC5hT+DU145P group due to an unexpected death and illness before day 43. From the tumours collected, a tdTomato$^+$ cell population was seen in each case, but no definitive mNeptune population [Figure 5.6A]. No FAP was detected

in any tumour. A PSMA^{+} population was clearly visible in the MRC5hT+DU145P tumour preparation [Figure 5.6B]

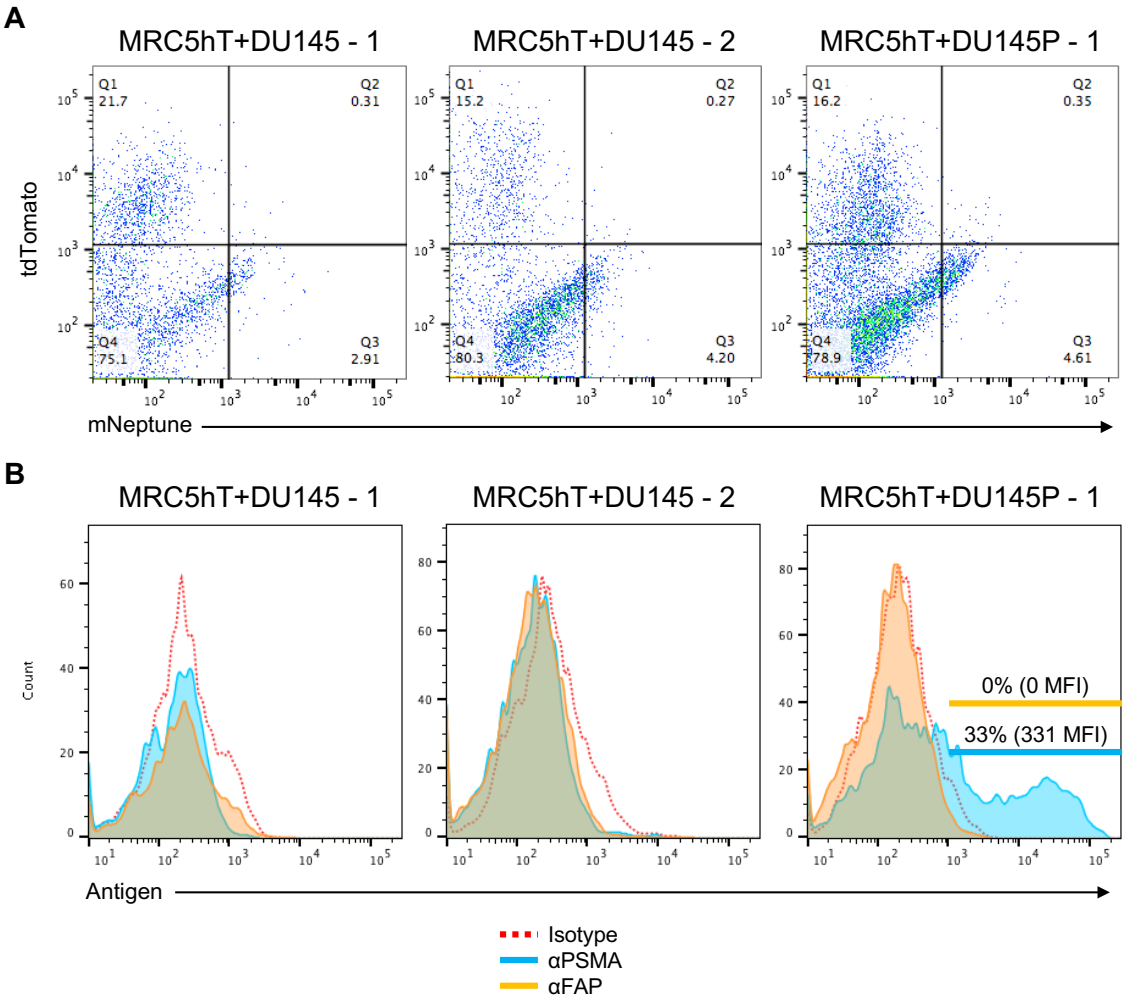

Figure 5.6 MRC5hT+DU145 and MRC5hT+DU145P tumour analysis.
MRC5hT+DU145/DU145P tumour cells collected from the mice were evaluated for A) presence of both cell types through tdTomato and mNeptune expression and B) FAP and PSMA expression. Commercially available antibodies were used for FAP and PSMA and an isotype was used to set the gate. Data shown is from collected tumours from the group (MRC5hT+DU145: n=2; MRC5hT+DU145P: n=1).

The frozen tumours were sectioned for further investigation. Haematoxylin and Eosin (H&E) staining of day 21 MRC5hT+PLP and day 43 MRC5hT+DU145P tumour sections showed the presence of the cuboidal PCa cells, but exhibited poor stromal inclusion in the tissue [Figure 5.7A-B].

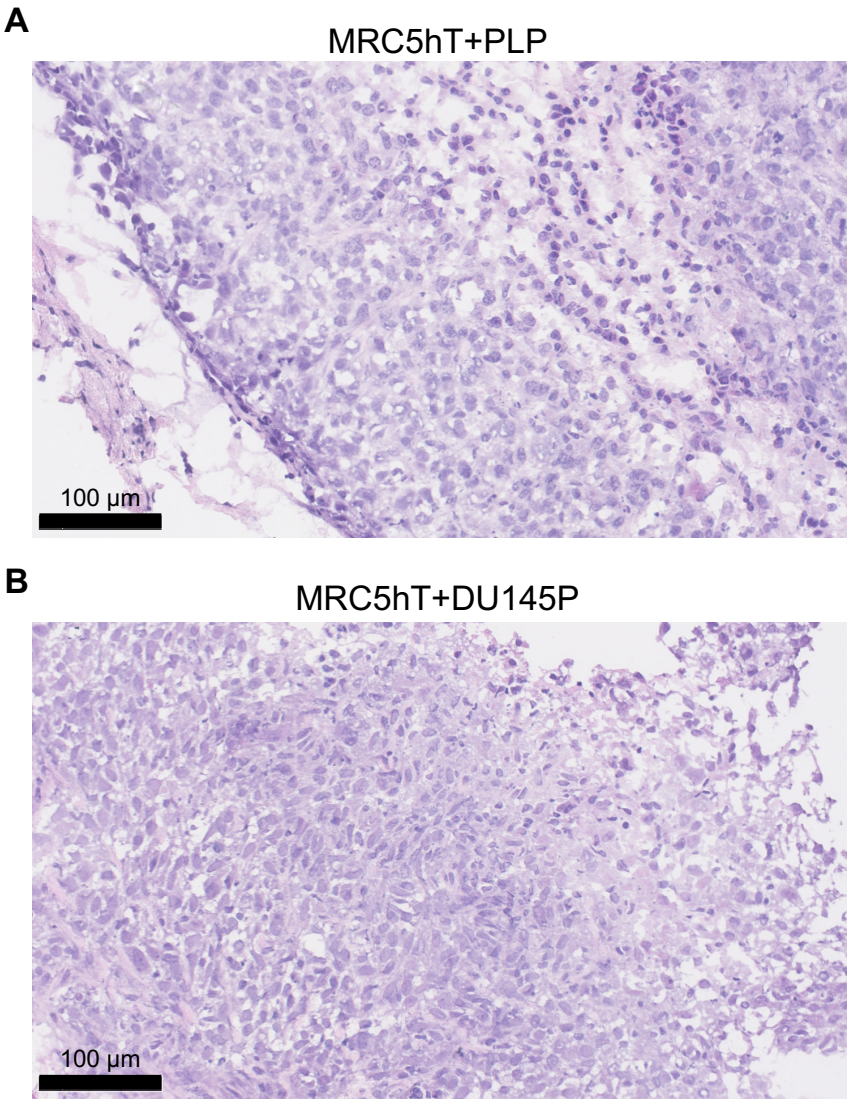

Figure 5.7 H&E stain of tumour sections

An H&E stain was performed on tumour sections for A) MRC5hT+PLP and B) MRC5hT+DU145P. Representative images are shown together with a scale bar.

Fluorescence microscopy was performed on MRC5hT+PLP tumours in order to detect MRC5hT stromal cells and PLP tumour cells by virtue of their expression of the mNeptune and tdTomato fluorescence reporter genes respectively. DAPI was used to visualise cell nuclei. Although signal was detected in the mNeptune channel, this appeared to overlap completely with the tdTomato^{+} area [Figure 5.8]. It was assumed that this phenomenon was due to spectral overlap of tdTomato and mNeptune. This bleeding effect from tdTomato was not seen during flow cytometry due to compensation controls that could not be applied to microscopy.

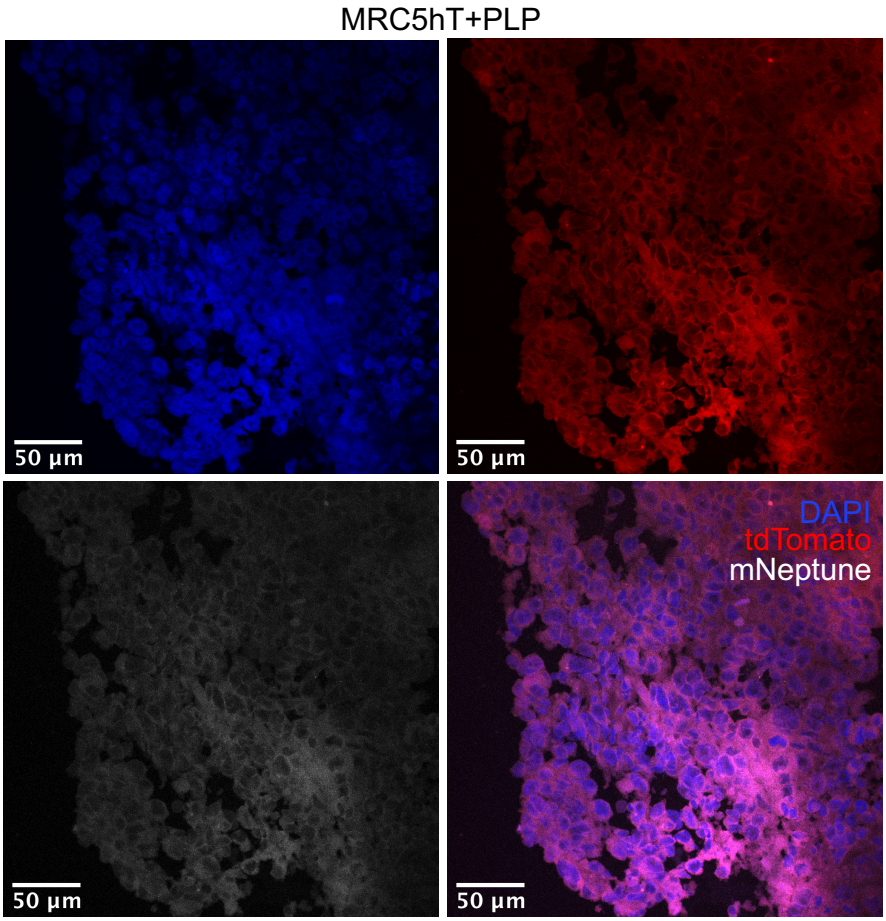

Figure 5.8 Fluorescence microscopy of the MRC5hT+PLP tumour.
The fluorescent reporter tdTomato (red) and mNeptune (white) were visualised. DAPI (blue) was used to locate the cell nuclei. Image was taken on a Nikon A1R inverted confocal microscope. The 405nm laser was used for DAPI excitation. The 561nm laser was used for tdTomato and mNeptune excitation. DAPI, tdTomato and mNeptune were detected in the ranges 450/50, 525/50 and 595/50 nm respectively. Representative images are shown together with a scale bar.

Fluorescence microscopy was also undertaken on a single MRC5hT+DU145P tumour. A similar pattern was seen to the MRC5hT+PLP tumours with clear DAPI staining and an overlapping detection signal of tdTomato and mNeptune in the tissue most likely due to tdTomato bleed through into the mNeptune detection filter [Figure 5.9].

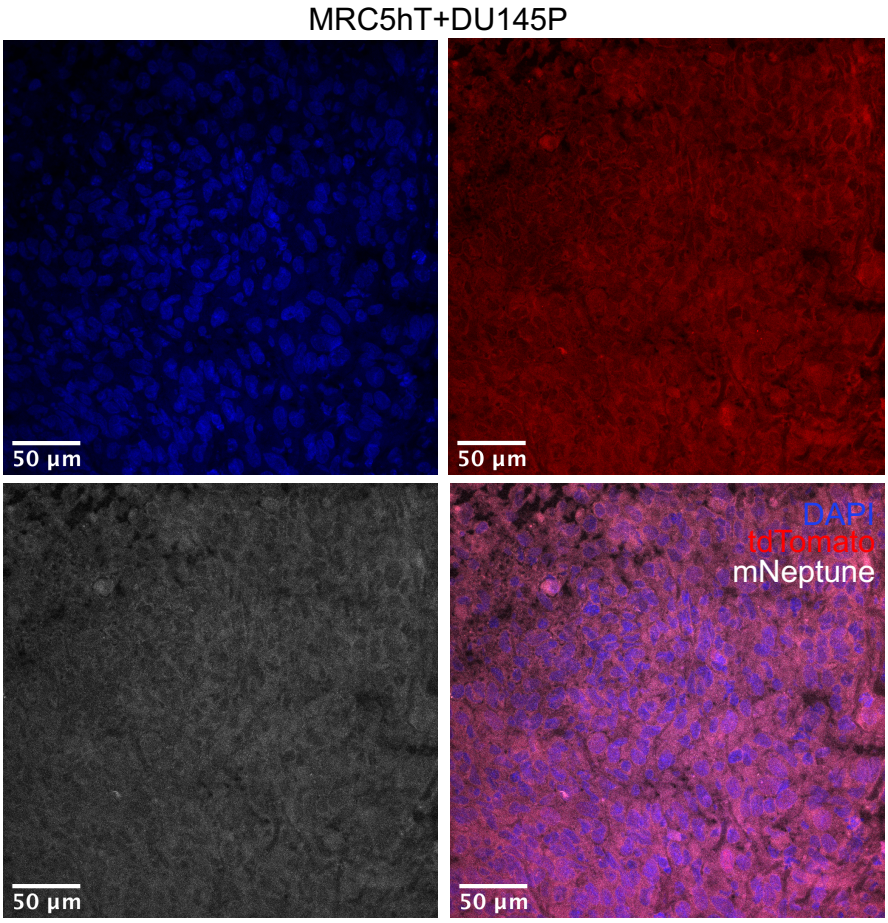

Figure 5.9 Fluorescence microscopy of the MRC5hT+DU145P tumour.
The fluorescent reporter tdTomato (red) and mNeptune (white) were visualised. DAPI (blue) was used to locate the cell nuclei. Image was taken on a Nikon A1R inverted confocal microscope. The 405nm laser was used for DAPI excitation. The 561nm laser was used for tdTomato and mNeptune excitation. DAPI, tdTomato and mNeptune were detected in the ranges 450/50, 525/50 and 595/50 nm respectively. Representative images are shown together with a scale bar.

Using both flow cytometry and fluorescence microscopy for mNeptune emission and flow cytometry for human FAP expression, no definite evidence of persistence of mNeptune expressing cells in tumours was apparent. I concluded therefore that the MRC5hT stromal cells had not survived in these tumour models. A new *in vivo* experiment was undertaken in which MRC5hT+PL and MRC5hT+PLP cells were embedded in matrigel to facilitate stroma engraftment. Once again, subcutaneous tumour xenograft engraftment was demonstrated by bioluminescence [Figure 5.10A]. Mice were sacrificed at day 18 and weights were monitored across the experimental timeline [Figure 5.10B].

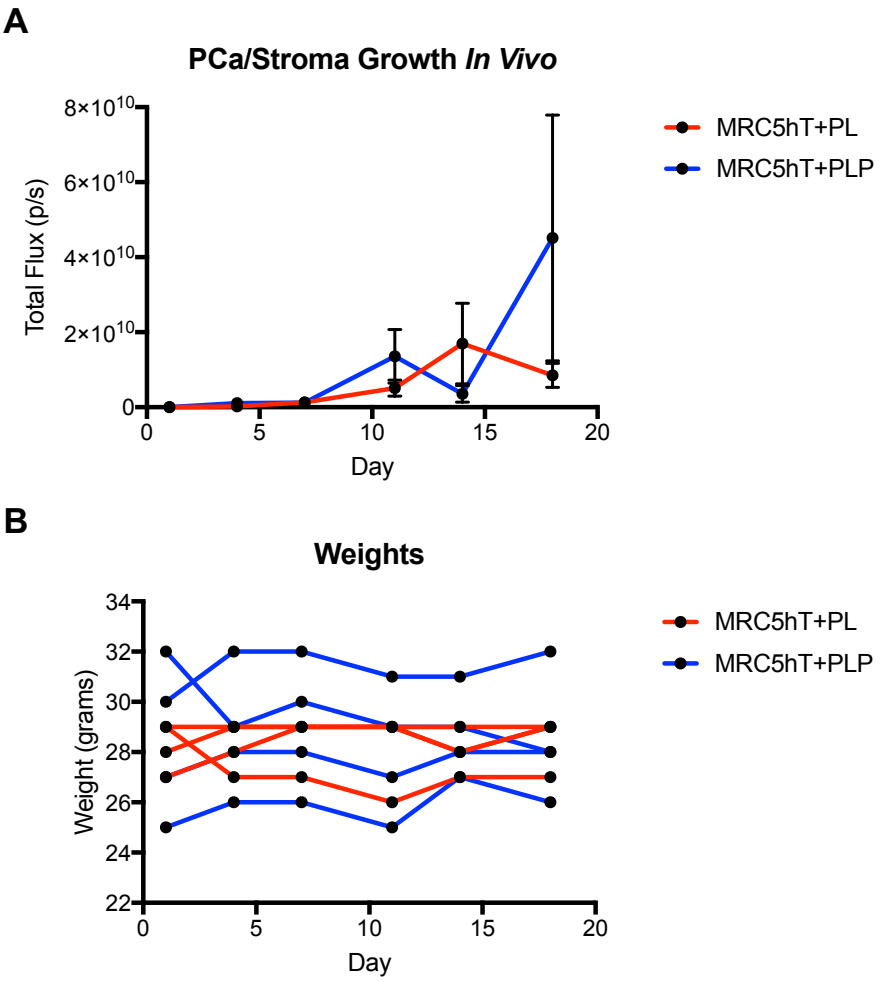

Figure 5.10 *In vivo* imaging of MRC5hT+PL/PLP tumour progression in matrigel. Mixtures of MRC5hT+PL and MRC5hT+PLP cells were suspended in matrigel and injected in NSG mice using the subcutaneous route. A) Tumour growth was assessed using bioluminescence imaging (mean ± SEM, n=4). B) The weight of the mice was recorded throughout the experiment.

Three of four mice had visible tumours, which were collected from the MRC5hT+PL matrigel group and revealed high levels of tdTomato expression between 53% and 62%. No mNeptune expression was detected by flow cytometry [Figure 5.11A]. When stained for FAP and PSMA, all 3 tumours were negative for both [Figure 5.11B].

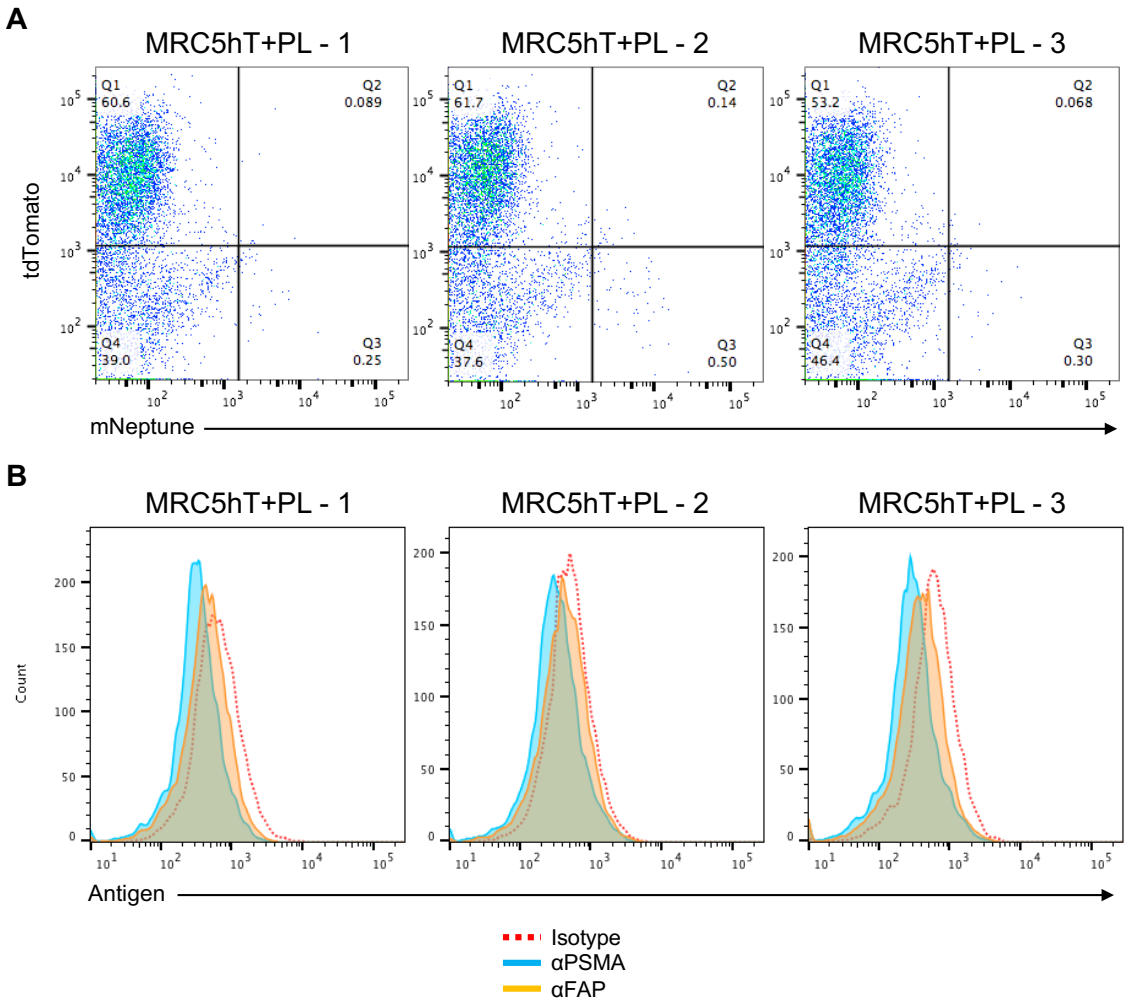

Figure 5.11 Flow cytometric analysis of MRC5hT+PL tumours established in matrigel.
Single cell suspensions were prepared from three subcutaneous MRC5hT+PL tumours following engraftment in NSG mice. Flow cytometry was performed to evaluate A) the presence of tumour and stromal cells through tdTomato and mNeptune expression; B) FAP and PSMA expression. Commercially available antibodies were used to detect FAP and PSMA and an isotype control was used to set the gate. Data shown is from collected tumours from the group (n=3).

All 4 tumours were harvested from the MRC5hT+PLP in matrigel group although mouse 2 had only ascites. Again, high levels of tdTomato was detected in the 4 tumours but no mNeptune expression was seen [Figure 5.12A]. Staining showed no expression of human FAP in the tumour, but high levels of PSMA were found in tumour cells [Figure 5.12B].

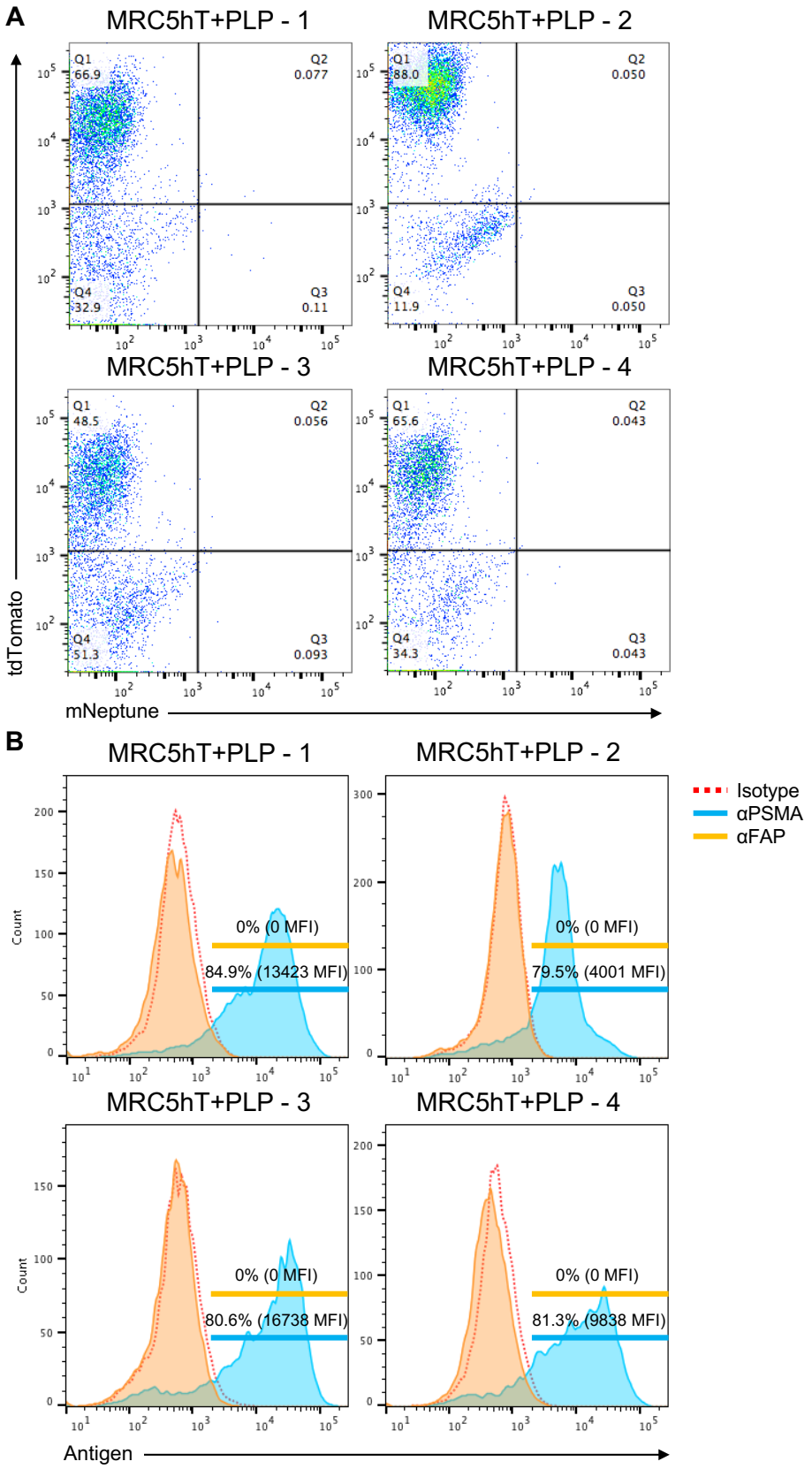

Figure 5.12 MRC5hT+PLP in matrigel tumour analysis.

MRC5hT+PLP tumour cells were collected and evaluated for A) presence of both cell types through tdTomato and mNeptune expression and B) FAP and PSMA expression. Commercially available antibodies were used for FAP and PSMA and an isotype was used to set the gate. Data shown is from collected tumours from the group (n=4).

Haematoxylin and Eosin staining and fluorescence microscopy were used to visualise the cells in sections prepared from MRC5hT+PLP tumours that had been established in matrigel. The H&E stain showed the presence of the PLP cells in the tissue and no apparent stroma [Figure 5.13A]. Applying the same detection filters as before, fluorescence microscopy showed a clear staining of the cell nucleus with DAPI. The signal for both tdTomato and mNeptune again was overlapping indicating the possibility of spectral overlap and a false positive signal for mNeptune [Figure 5.13B].

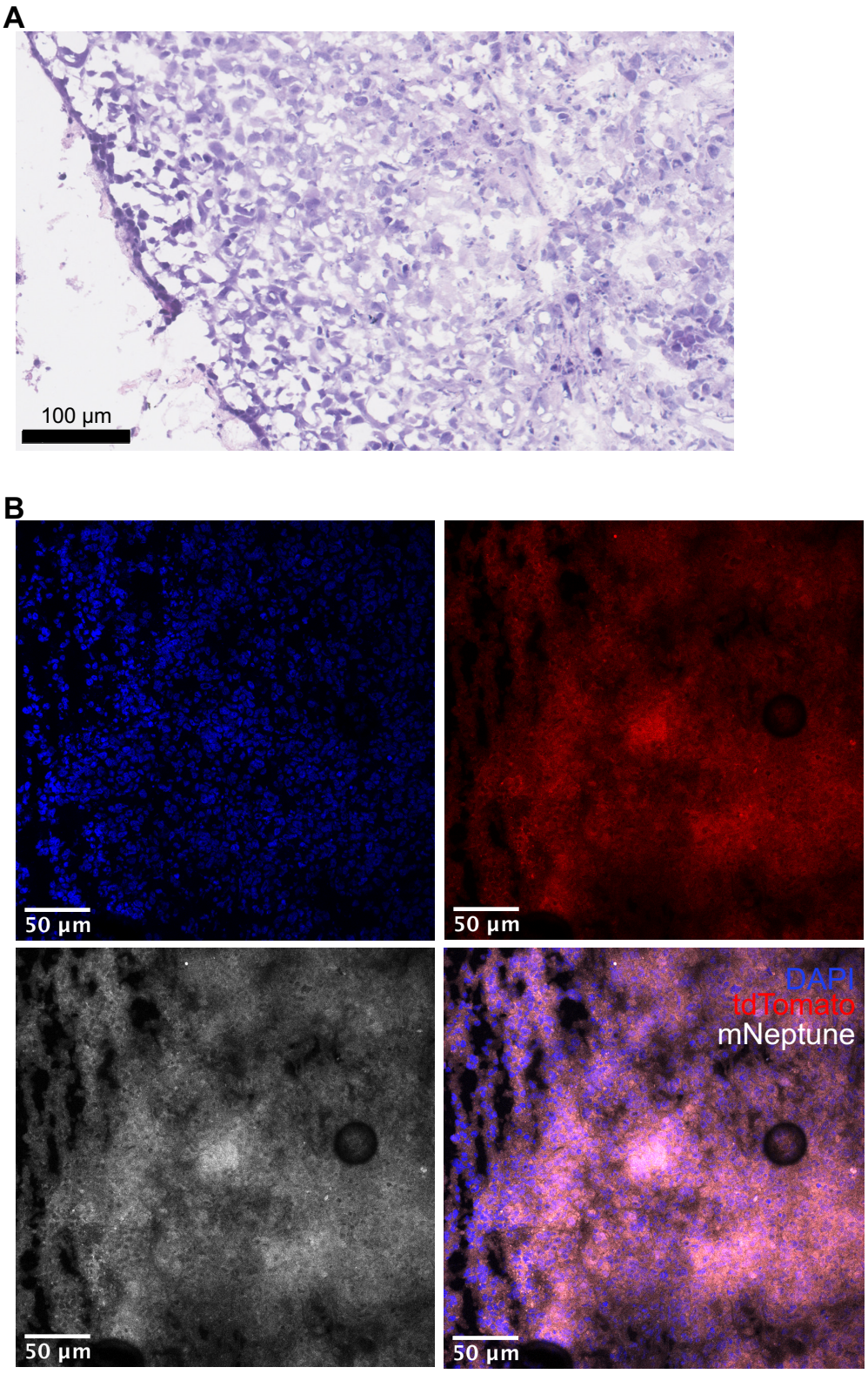

Figure 5.13 H&E stain and fluorescence microscopy of the MRC5hT+PLP tumour in matrigel.
The MRC5hT+PLP matrigel tumour section was visualised with A) H&E staining and B) fluorescence microscopy for tdTomato (red), mNeptune (white) and DAPI (blue). Images were taken on a Nikon A1R inverted confocal microscope. The 405nm laser was used for DAPI excitation. The 561nm laser was used for tdTomato and mNeptune excitation. DAPI, tdTomato and mNeptune were detected in the ranges 450/50, 525/50 and 595/50 nm respectively. Representative images are shown together with a scale bar.

To determine whether the MRC5hT cells were engrafting in these subcutaneous tumours, live fluorescence imaging of the mNeptune reporter was conducted alongside bioluminescence imaging of the PCa cells. MRC5hT+DU145 and MRC5hT+DU145P cells were injected in matrigel and bioluminescence imaging showed tumour growth for both groups with MRC5hT+DU145 tumours progressing more quickly after day 29 [Figure 5.14A-B]. *In vivo* fluorescence imaging detected signal in the mNeptune channel and showed a significant increase in signal in the two MRC5hT+PCa groups compared to MRC5hT injected alone, suggesting further bleed through from the tdTomato into the mNeptune detection channel [Figure 5.14C-D]. The signal was taken from a region of interest drawn around the injection site. Throughout the imaging sessions, weight of the mice was monitored [Figure 5.14E].

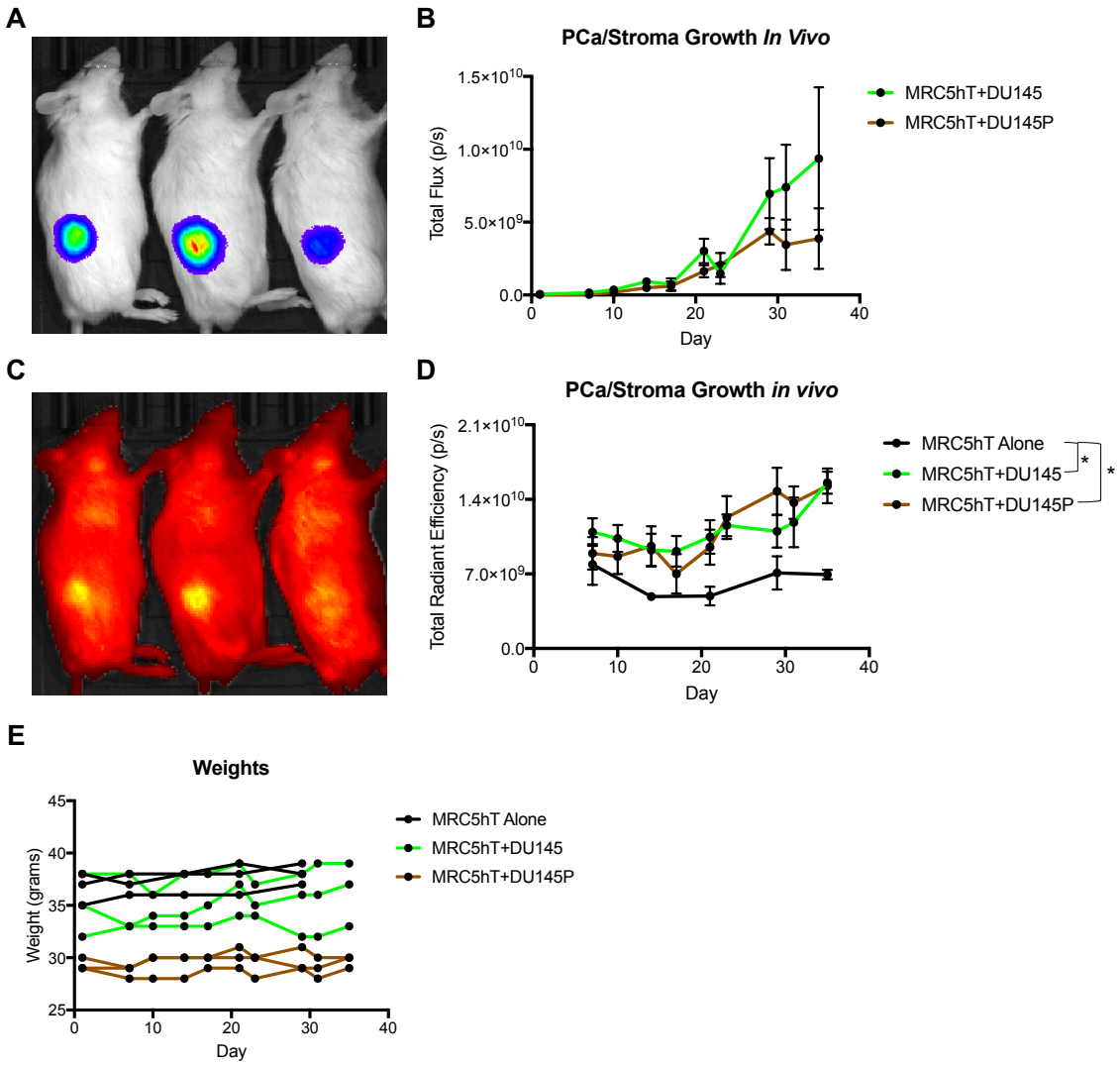

Figure 5.14 *In vivo* imaging of MRC5hT+DU145 and MRC5hT+DU145P tumours in matrigel.
Subcutaneous tumours comprising MRC5hT+DU145 and MRC5hT+DU145P cells were established in matrigel and were monitored using A-B) Bioluminescence and C-D) far-red fluorescence imaging. A) and C) are representative images at day 28. E) Weights of the mice were monitored throughout the experiment. B) and D) statistical significance was determined using a two-way ANOVA (mean ± SEM, n=3) (* = $p < 0.05$).

Tumours were collected at day 35 and H&E staining of the MRC5hT+DU145P matrigel tumour sections once again showed the PCa cells, but no morphologically stromal cells [Figure 5.15A]. Fluorescence microscopy detected tdTomato and only background noise in the mNeptune channel [Figure 5.15B]. This differs from the mNeptune bleed through previously seen perhaps due to a lower tdTomato signal and images acquired at a lower magnification (10x).

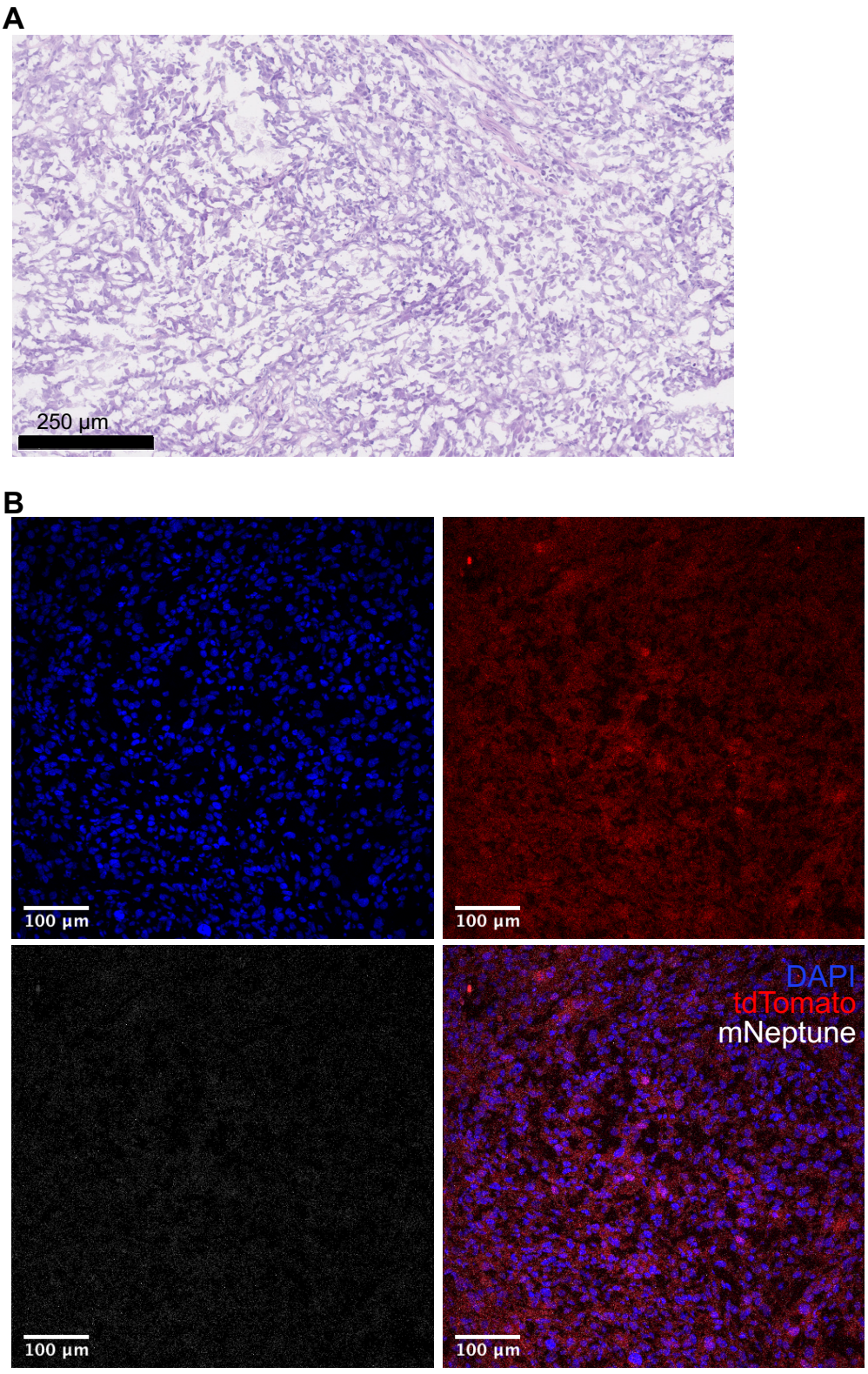

Figure 5.15 H&E stain and fluorescence microscopy of the MRC5hT+DU145P tumour in matrigel.
The MRC5hT+DU145P matrigel tumour section was visualised with A) H&E staining and B) fluorescence microscopy for tdTomato (red), mNeptune (white) and DAPI (blue). Images were taken on a Nikon A1R inverted confocal microscope. The 405nm laser was used for DAPI excitation. The 561nm laser was used for tdTomato and mNeptune excitation. DAPI, tdTomato and mNeptune were detected in the ranges 450/50, 525/50 and 595/50 nm respectively. Representative images are shown together with a scale bar.

Tissues from the previous *in vivo* experiments were analysed for murine stroma recruitment and intratumoural presence of FAP by immunohistochemistry. Tumours consisting of MRC5hT+PLP cells exhibited areas positive for the murine stromal marker α smooth muscle actin (αSMA) suggesting that these tumours were able to recruit murine stroma [Figure 5.16A]. There was also positive staining for FAP in the tissue although there were high levels of background in the FAP stain [Figure 5.16B]. Because the FAP antibody crosses the species barrier, this could be either human FAP expressed in the MRC5hT or murine FAP from recruited stroma.

Another section of MRC5hT+PLP tumours exhibited murine αSMA at low levels and mostly on the fringe of the tissue [Figure 5.17A]. There were higher levels of FAP staining throughout the section [Figure 5.17B].

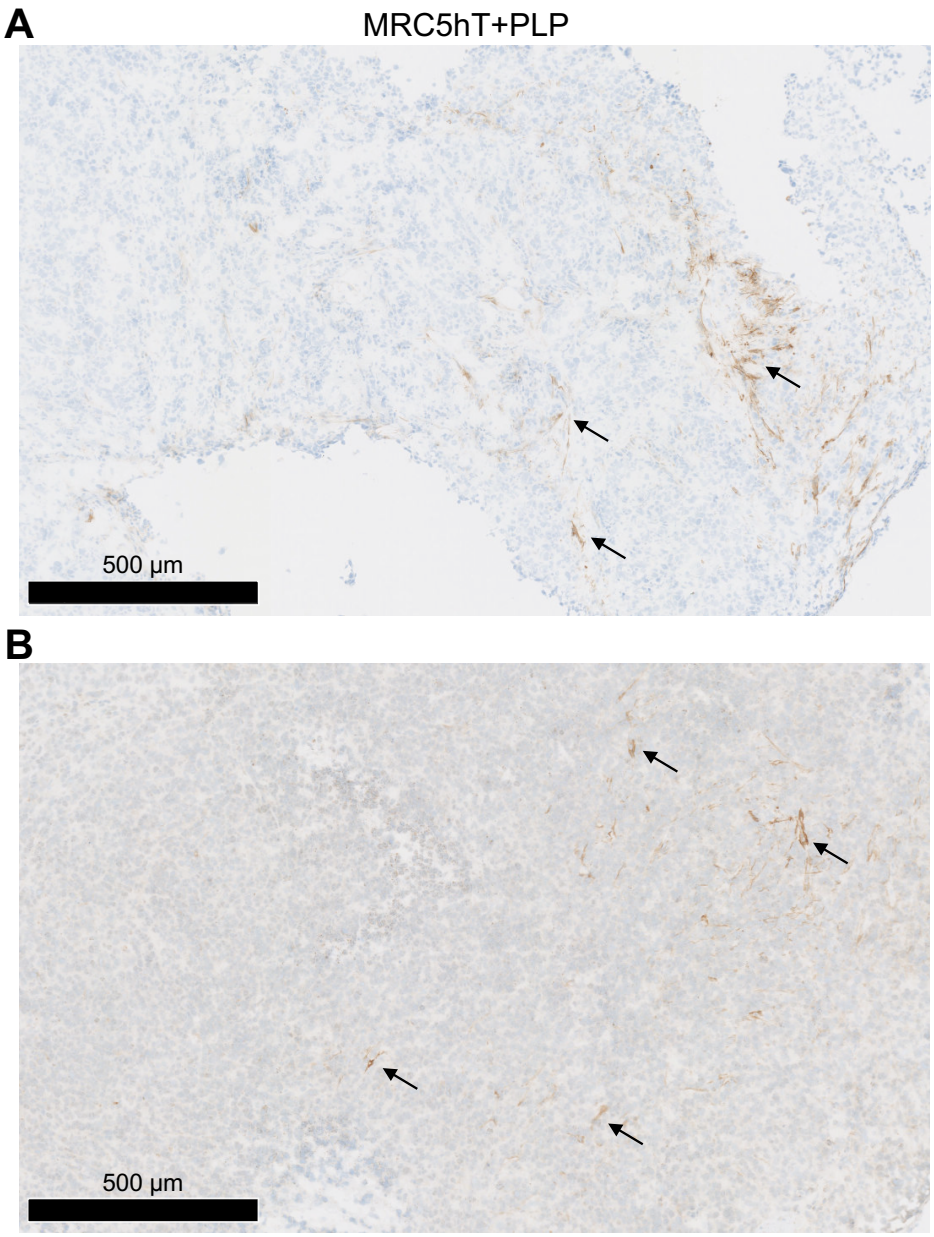

Figure 5.16 Immunohistochemical detection of stromal markers in MRC5hT+PLP tumours.
Tumour sections were stained for A) murine αSMA, or B) murine/human FAP to visualise stromal tissue. A counterstain was used to visualise the nuclei (blue). A section is shown for 1 of 2 tumours. Arrows indicate areas positive for relevant antigen detection (brown). Images are shown together with a scale bar.

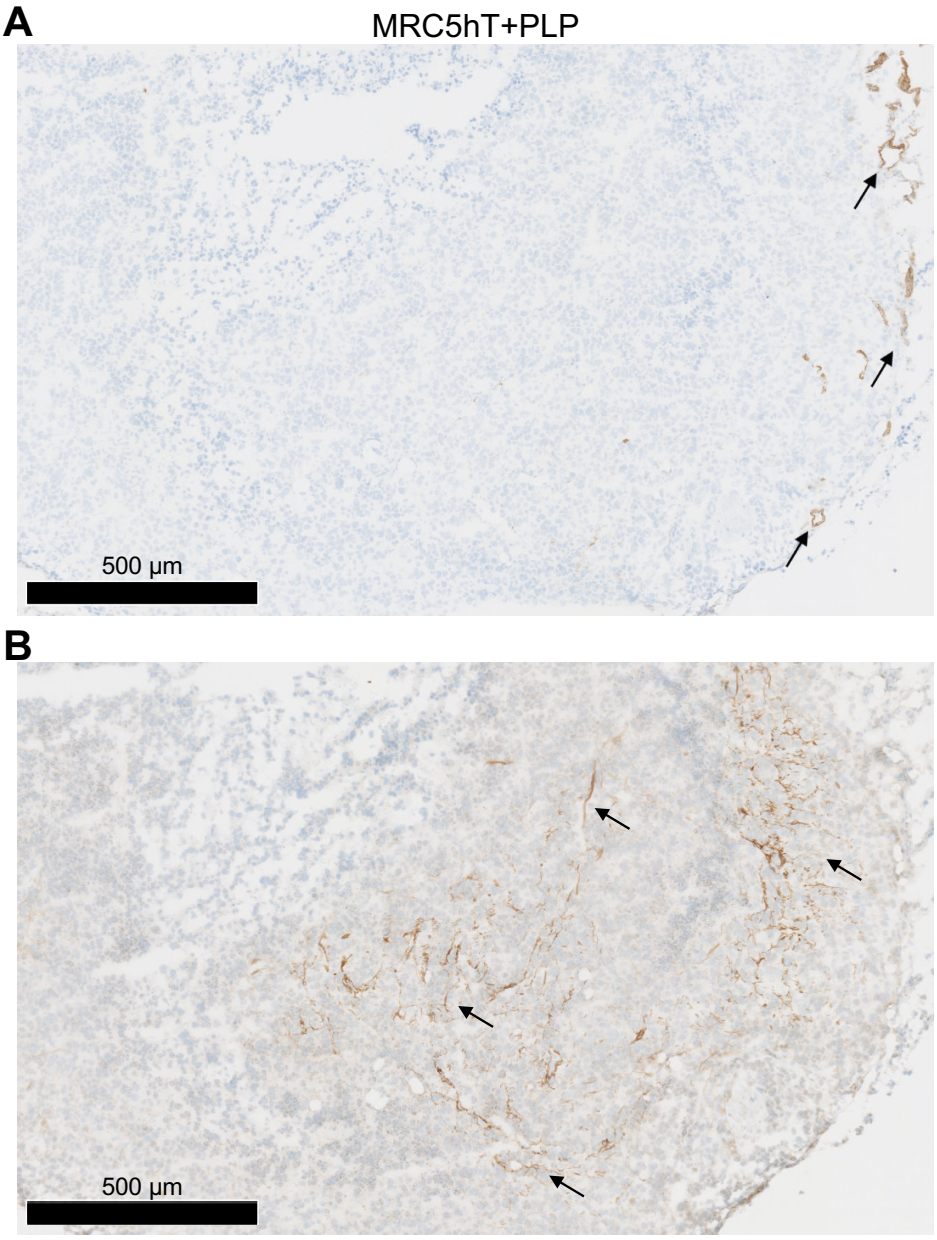

Figure 5.17 Immunohistochemical detection of stromal markers in MRC5hT+PLP tumours.
Tumour sections were stained for A) murine αSMA, or B) murine/human FAP to visualise stromal tissue. A counterstain was used to visualise the nuclei (blue). A section is shown for 2 of 2 tumours. Arrows indicate areas positive for relevant antigen detection (brown). Images are shown together with a scale bar.

Finally, a sample of MRC5hT+DU145P tumour tissue was probed for αSMA and FAP. The MRC5hT+DU145P tissue demonstrated murine αSMA, suggesting endogenous stroma recruitment *in vivo* [Figure 5.18A]. In contrast to the MRC5hT+PLP tumours, the MRC5hT+DU145P sections exhibited non-specific background staining for FAP, with a low FAP^+ area overlapping with αSMA [Figure 5.18A-B].

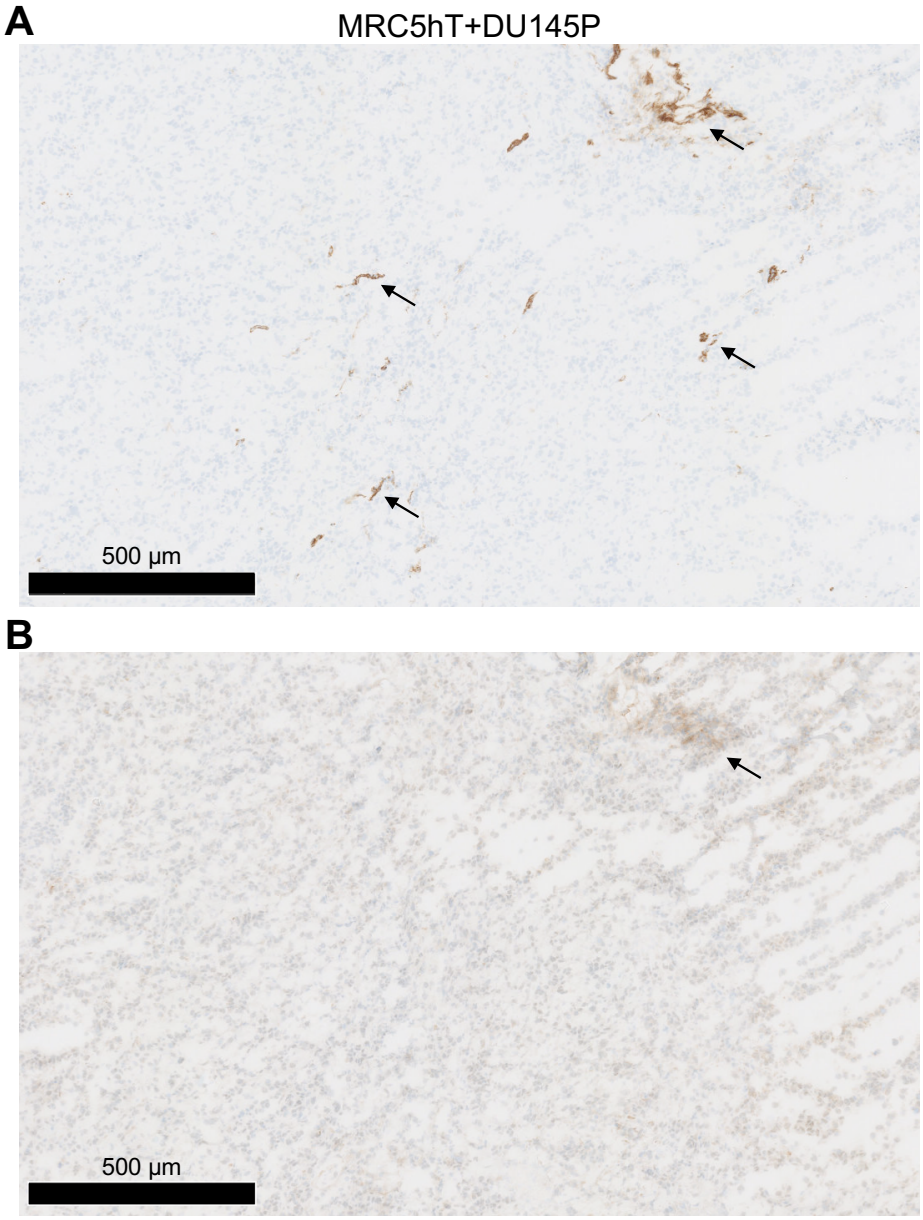

Figure 5.18 Immunohistochemical detection of stromal markers in MRC5hT+DU145P tumours.
Tumour sections were stained for A) murine αSMA, or B) murine/human FAP to visualise stromal tissue. A counterstain was used to visualise the nuclei (blue). A single tumour was investigated. Arrows indicate areas positive for relevant antigen detection (brown). Images are shown together with a scale bar.

An *in vivo* experiment was carried out in an attempt to confidently detect mNeptune and thus the engraftment of the stromal cells in these PCa/stroma tumour models without potential bleed through from the tdTomato reporter. A mono-culture of mNeptune^{+} MRC5hT cells or a co-culture also containing PLP or DU145P that had not been transduced with the tdTomato-encoding LT vector were injected in matrigel. Tumours

were monitored using *in vivo* fluorescence imaging. There was an increase in fluorescence signal in all of the groups including the background mice that were not injected with anything [Figure 5.19A]. The signal was taken from a region of interest drawn around the injection site. The weights of the mice were recorded during imaging sessions [Figure 5.19B].

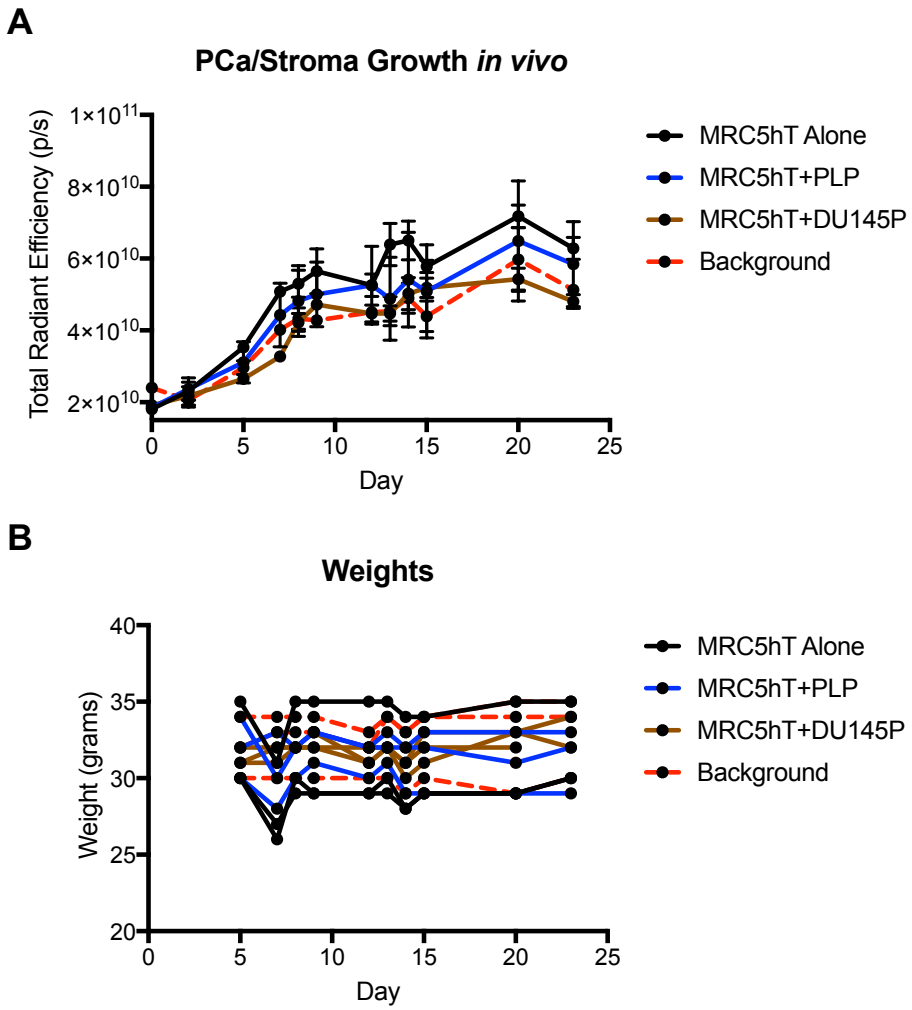

Figure 5.19 Fluorescence *in vivo* imaging of tumour progression in matrigel.
Engraftment of MRC5hT alone, MRC5hT+PLP and MRC5hT+DU145P in matrigel were assessed with A) fluorescence imaging of mNeptune (mean ± SEM, n=3). B) The weight of the mice was recorded throughout the experiment.

At day 23, tumours were harvested, sectioned and imaged for mNeptune expression. MRC5hT+PLP tumours showed sections of high mNeptune signal that corresponded with increased DAPI staining [Figure 5.20A]. mNeptune signal was detected in

MRC5hT+DU145P tumour sections at lower levels [Figure 5.20B]. However, there was a lack of a negative control comprising of fluorescently negative tumour tissue and therefore high autofluorescence from the tumour in areas of dense cellularity could be the source of signal in the mNeptune detection channel. The mNeptune reporter was not informative for *in vivo* imaging of engraftment and tumour growth and sufficient MRC5hT presence could not be definitively detected.

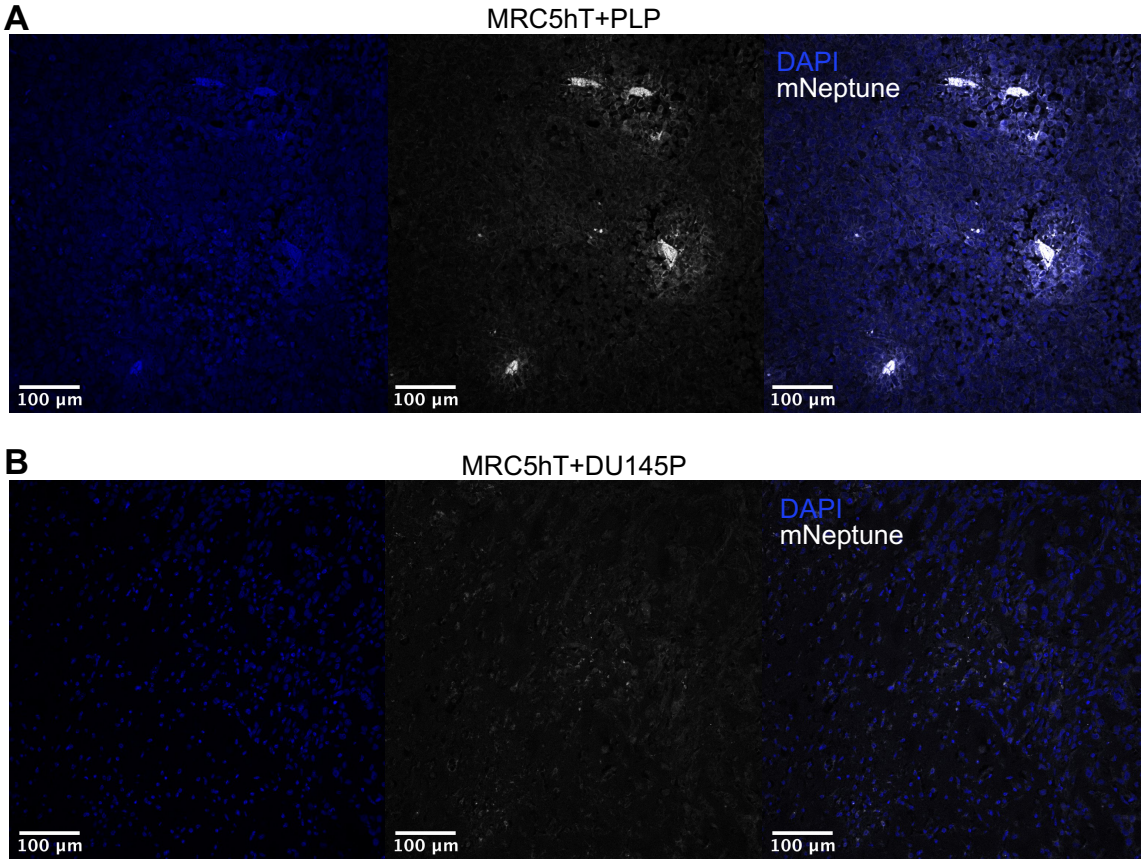

Figure 5.20 Fluorescence microscopy of the MRC5hT+PCa tumour in matrigel. Tumour sections of A) MRC5hT+PLP and B) MRC5hT+DU145P were visualised with using fluorescence microscopy for mNeptune (white) and DAPI (blue). Representative image of 3 tumours/group. Images were taken on a Nikon A1R inverted confocal microscope. The 405nm laser was used for DAPI excitation. The 561nm laser was used for mNeptune excitation. DAPI and mNeptune were detected in the ranges 450/50 and 595/50 nm respectively. Images are shown together with a scale bar.

5.2.2 *In vivo* efficacy of P4 CAR T cells with eFAP-4

The core hypothesis underlying this thesis is that PSMA-targeted CAR T cell immunotherapy of prostate cancer can be potentiated by a stromal targeted immunocytokine that delivers a selective growth signal to the CAR T cells at that location. However, the data presented in the preceding sections of this chapter demonstrate that engraftment of MRC5hT cells in subcutaneous tumours is inefficient to allow testing of this hypothesis using an *in vivo* model. To circumvent this issue, I elected to express FAP in the LT-PLP tumour cell line. The 293vec-RD114 cell line was transduced with a FAP-SFG retroviral plasmid at high levels [Figure 5.21A]. The virus-containing supernatant from these cells was used to successfully transduce LT-PLP cells. Expression of FAP was detectable in the transduced cells with a commercial antibody [Figure 5.21B]. In addition, when the eFAP-4 immunocytokine was added to these cells, binding could be detected using anti-IL-4 antibody [Figure 5.21B]. Expression of FAP had no effect on *in vitro* cell growth over a 72-hour period [Figure 5.21C].

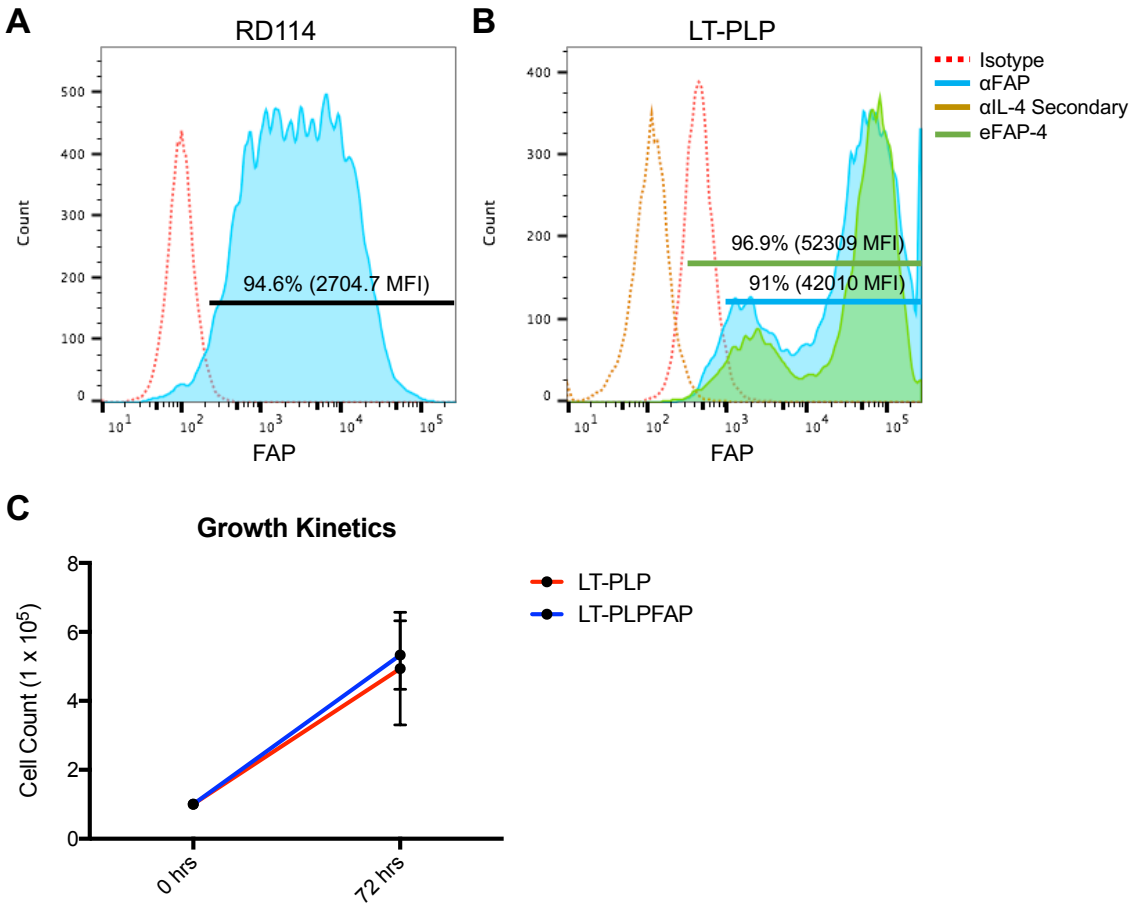

Figure 5.21 Generation of LT-PLPFAP.
A) A FAP-SFG RD114 pseudotyped retrovirus was produced in the 293vec-RD114 packaging line. B) The LT$^+$ and PSMA$^+$ prostate cancer cell line LT-PLP was transduced with FAP-SFG. Expression of FAP was detected using a commercially available αFAP antibody and with eFAP-4 followed by αIL-4-PE secondary antibody. C) The growth of parental LT-PLP and LT-PLPFAP cells was compared over 72 hours in D10 media. Cells were quantified using trypan blue exclusion and haemocytometer (mean + SEM, n=3).

LT-PLPFAP cells were used in an *in vivo* pilot study to assess anti-tumour activity of eFAP-4 when combined with P4 CAR T cells [Figure 5.22A]. LT-PLPFAP cells demonstrated expression of the CAR target antigen PSMA and the immunocytokine target antigen FAP before injection. These cells also demonstrated high expression of the reporter gene LT [Figure 5.22B]. Human T cells transduced with P4 or P4Tr showed high levels of CAR expression through detection of the CAR scFv using a polyclonal PE-conjugated goat anti-mouse immunoglobulin (GAM-PE), or detection of 4αβ expression with αCD124 [Figure 5.22C]. The CD124 expression percentage was used to define CAR

expression and calculate what number of T cells was required to deliver 1x10^6 CAR$^+$ T cells for treatment.

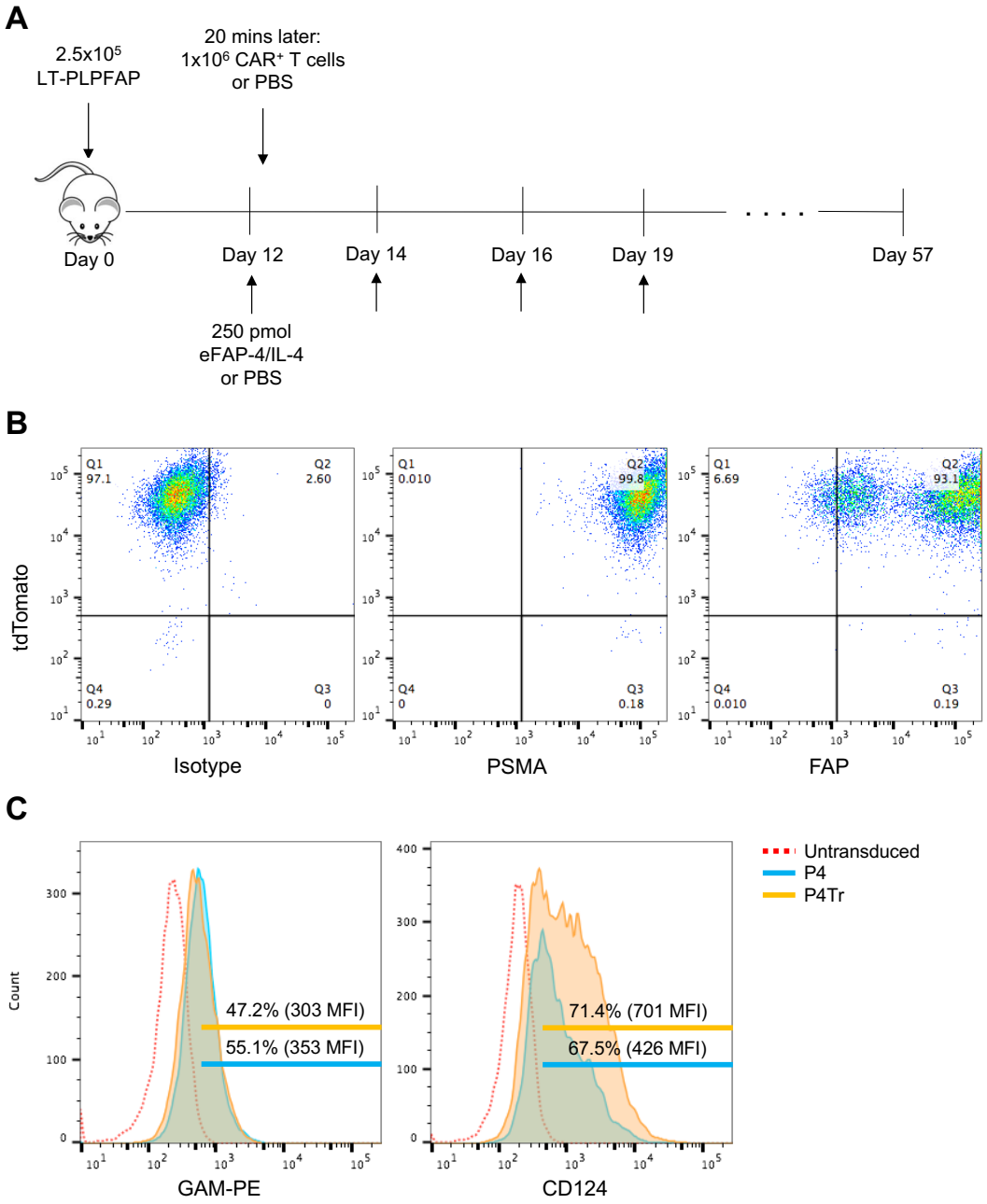

Figure 5.22 Pilot eFAP-4 efficacy study plan and cell analysis.
A) Male NSG mice received a subcutaneous injection of LT-PLPFAP cells in the right flank on day 0. On day 12, either eFAP-4, IL-4 or PBS was injected IP and, 20 minutes later, CAR T cells were administered IV. Upward pointing arrows indicate time-points of eFAP-4/IL-4 or PBS injection. Mice were monitored for tumour growth (BLI) and toxicity until the end of the study at day 57. B) LT-PLPFAP tumour cells injected on day 0 were positive for the reporter gene tdTomato, PSMA and FAP. C) Expression of the P4 and P4Tr CARs were detected on the surface of human T cells by staining with goat anti mouse-PE (GAM-PE – detects anti-PSMA scFv) or αCD124 (detects 4αβ) before injection. Untransduced cells were used to set all gates as appropriate.

Pooled bioluminescence data from the treatment groups showed that tumours progressed at similar rates [Figure 5.23A]. Individual mice in the P4 + eFAP-4 and P4Tr + IL-4 survived until termination of the study at day 57 and displayed lower tumour burden. Weight was monitored throughout the experiment and no toxicity was seen in any of the mice [Figure 5.23B].

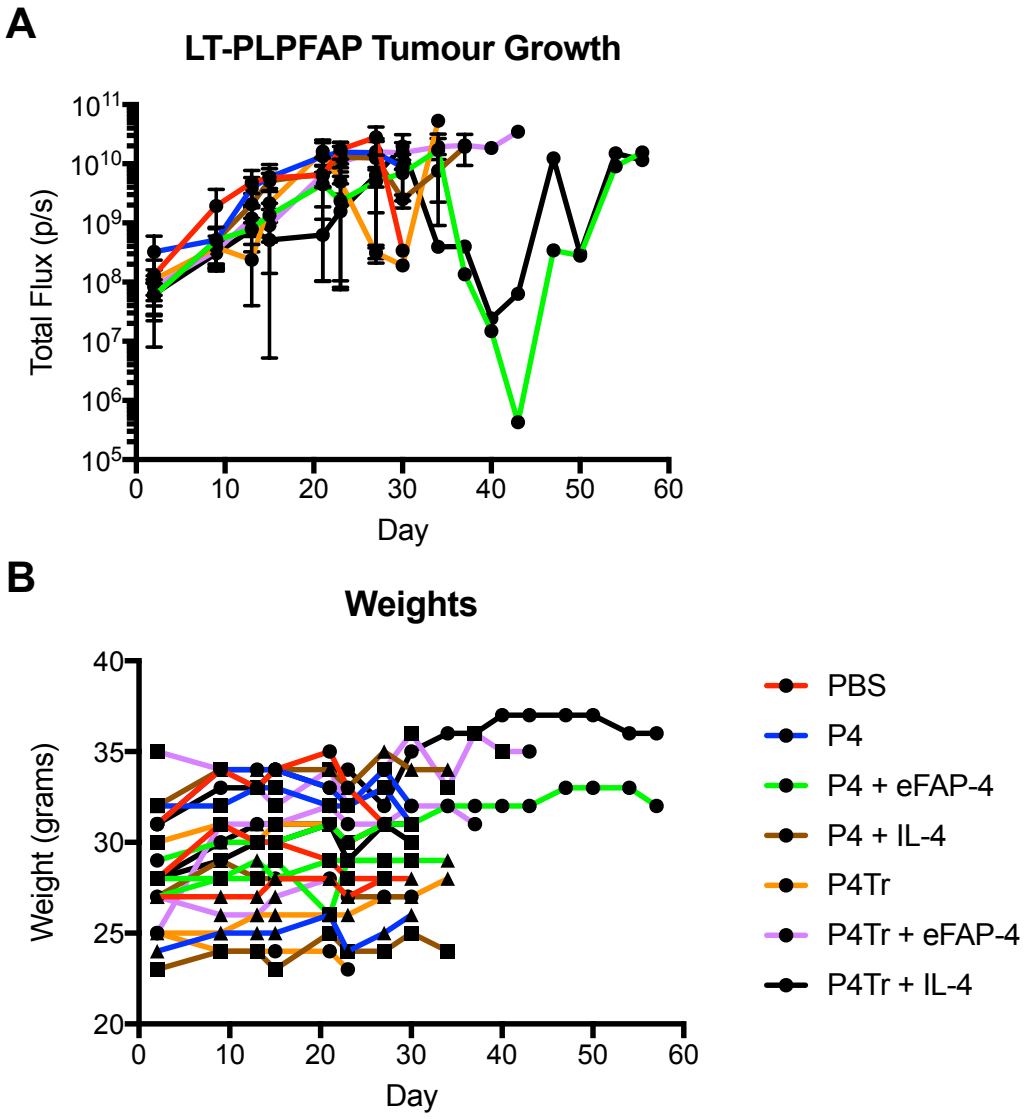

Figure 5.23 *In vivo* imaging of tumour progression and weight assessment. Treatments groups were monitored for A) tumour growth using bioluminescence (mean ± SEM, n=3). B) The weight of the mice was recorded at each imaging time point.

Individual mice in each treated group are represented [Figure 5.24A-G]. The bioluminescence signal did not always correspond with tumour volume measured with

callipers at the end point. There was an apparent decrease in signal at time points that mice were sacrificed (due to the tumour size reaching home office limits). This was evident for mice in the PBS and P4Tr groups [Figure 5.24A&E]. One mouse in the P4 + eFAP-4 group exhibited tumour regression dropping below the limit of detection (10^6 p/s) on day 43 and showing no palpable tumour. There was subsequent tumour progression afterwards until the termination of the study at day 57 [Figure 5.24C]. One mouse in the P4Tr + IL-4 demonstrated low bioluminescence signal and no palpable tumour until day 47. However, this individual presented with 2 logs lower signal compared to the other two mice in the group at the first imaging session. This suggests a miss-injection of lower tumour cell count [Figure 5.24G].

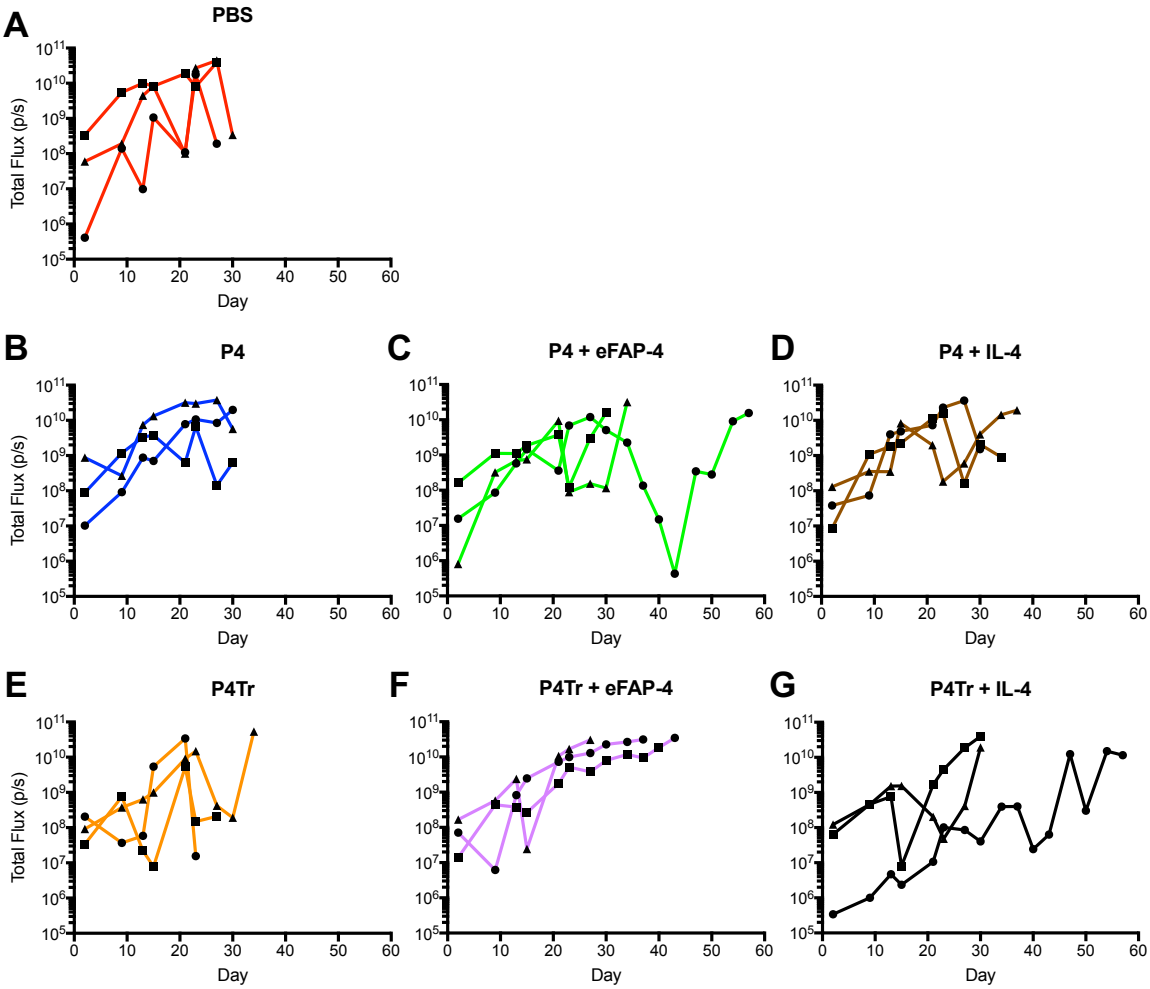

Figure 5.24 Individual *in vivo* imaging of tumour progression.
Tumour growth in mice was monitored via bioluminescence imaging and individual values are shown for A) PBS, B) P4, C) P4 + eFAP-4, D) P4 + IL-4, E) P4Tr, F) P4Tr + eFAP-4 and G) P4Tr + IL-4 (n=3).

Bioluminescence images show the progression of the individual tumours up until day 40 for groups treated with P4 CAR T cells with/without eFAP-4 or IL-4 [Figure 5.25]. The P4 + eFAP-4 treated mouse that survived until the end of the experiment showed an increase in tumour burden followed by a regression starting at day 27, 15-days post CAR T cell administration. There was an absence of detectable tumour at day 40.

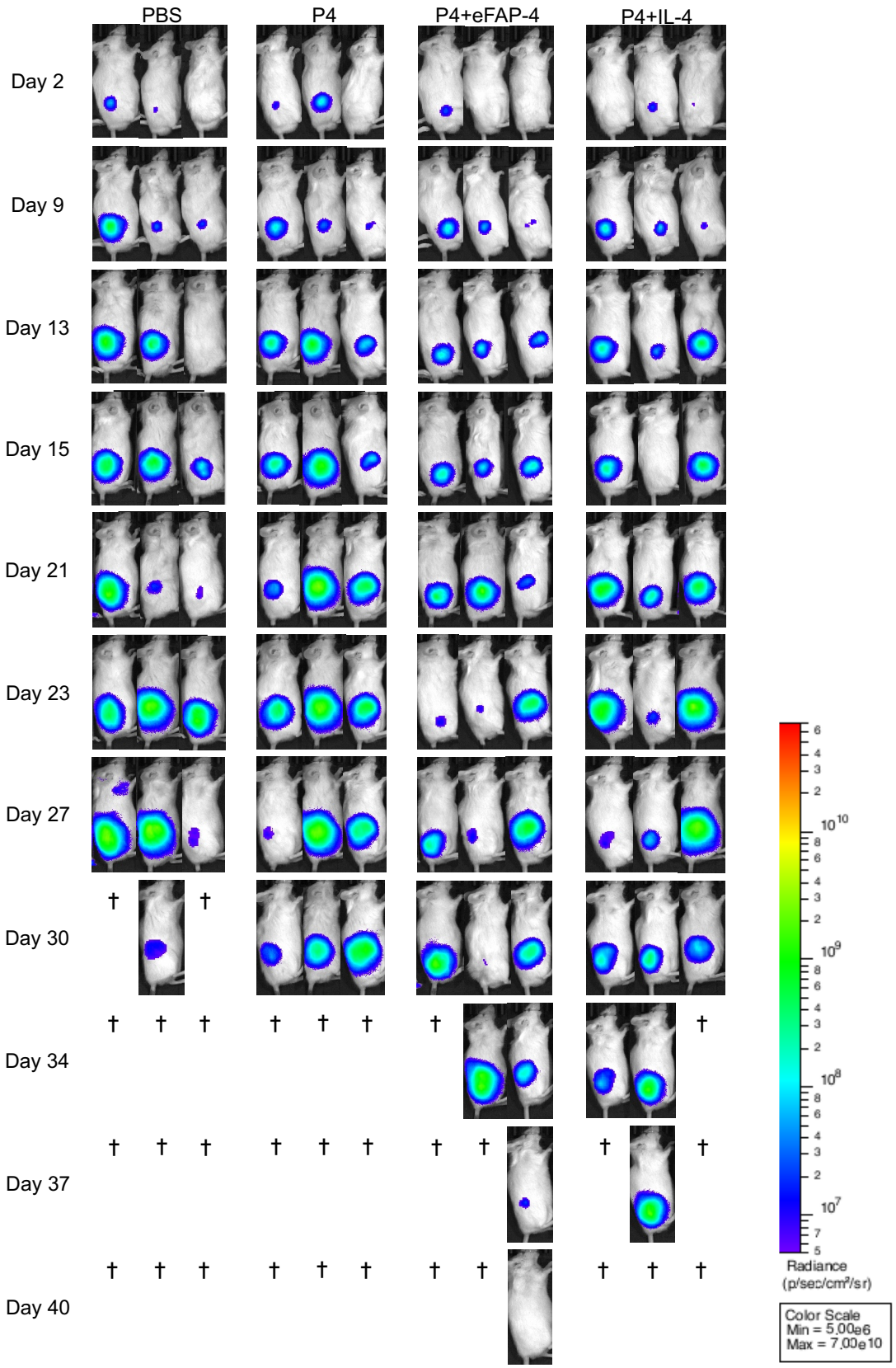

Figure 5.25 Individual bioluminescence images of P4 CAR T cell treated groups. Bioluminescence images of mice in the PBS, P4, P4 + eFAP-4 and P4 + IL-4 groups are shown from day 2 to day 40 after LT-PLPFAP inoculation. The scale bar indicates a logarithmic scale for radiance ranging from $5x10^6$ – $7x10^{10}$. Crosses indicate the loss of the animal due to reaching home office limits on tumour volume or approaching ulceration.

Bioluminescence images show the progression of the individual tumours up until day 40 for control groups treated with P4Tr CAR T cells with/without eFAP-4 or IL-4 [Figure 5.26]. The P4Tr + IL-4 treated mouse that survived until the end of the experiment had no/low tumour burden signal until day 23. This signal remained low until day 40 indicating an error in tumour cell inoculation.

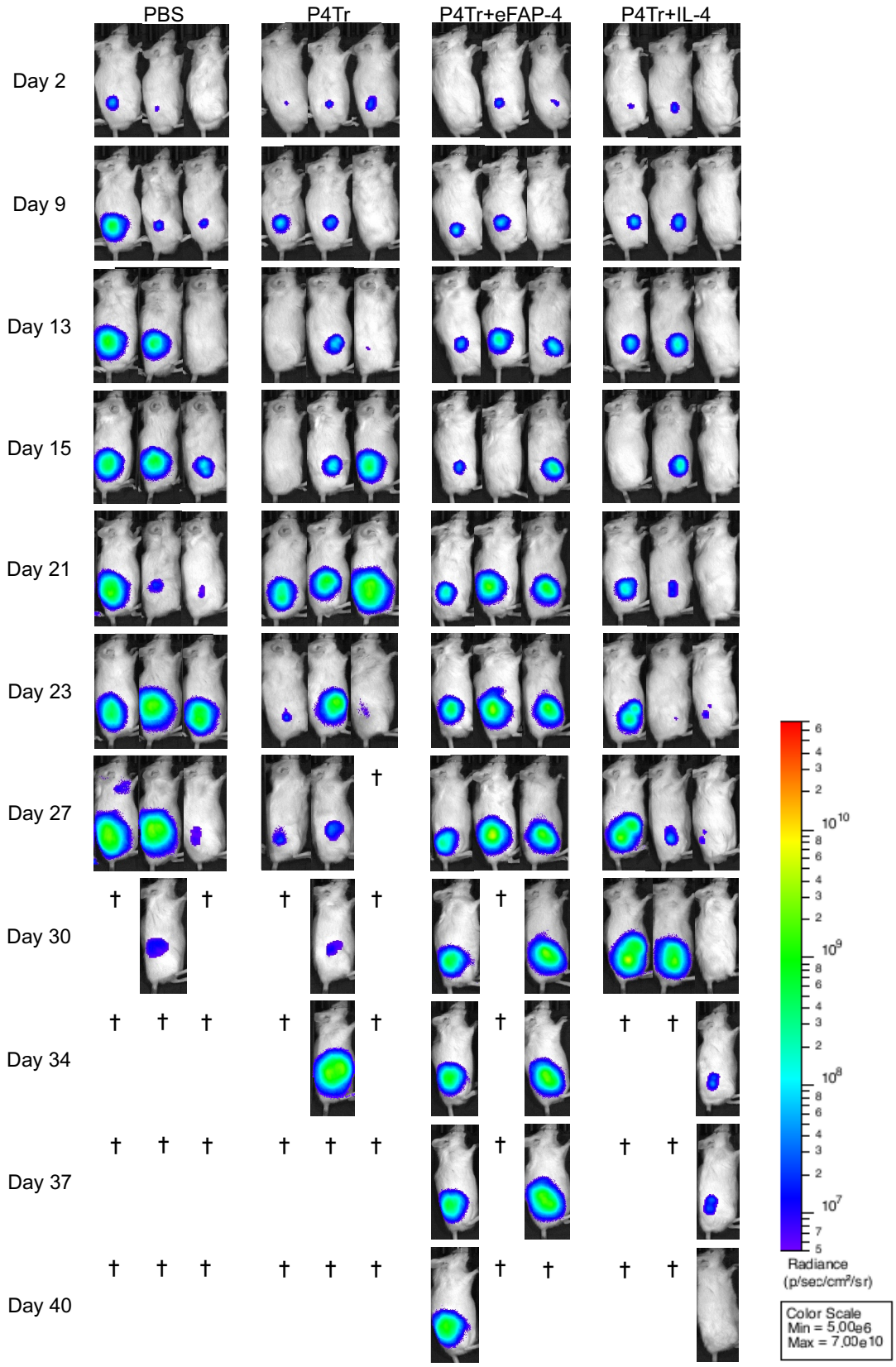

Figure 5.26 Individual bioluminescence images of P4Tr CAR T cell treated groups. Bioluminescence images of mice in the PBS, P4Tr, P4Tr + eFAP-4 and P4Tr + IL-4 groups are shown from day 2 to day 40 after LT-PLPFAP inoculation. The scale bar indicates a logarithmic scale for radiance ranging from $5x10^6$ – $7x10^{10}$. Crosses indicate the loss of the animal due to reaching home office limits on tumour volume or approaching ulceration.

The final two weeks of imaging in this pilot study showed the increasing tumour growth in the remaining mice [Figure 5.27A]. The last mouse in the P4Tr + eFAP-4 group was culled on day 43 due to tumour size. Both mice in the P4 + eFAP-4 and P4Tr + IL-4 groups exhibited tumour progression until day 57 when they were sacrificed because of tumour size. A survival curve of the treatment groups shows a tend towards survival benefit for the P4 + eFAP-4 and P4Tr + IL-4 groups [Figure 5.27B]. This benefit did not reach significance in this cohort.

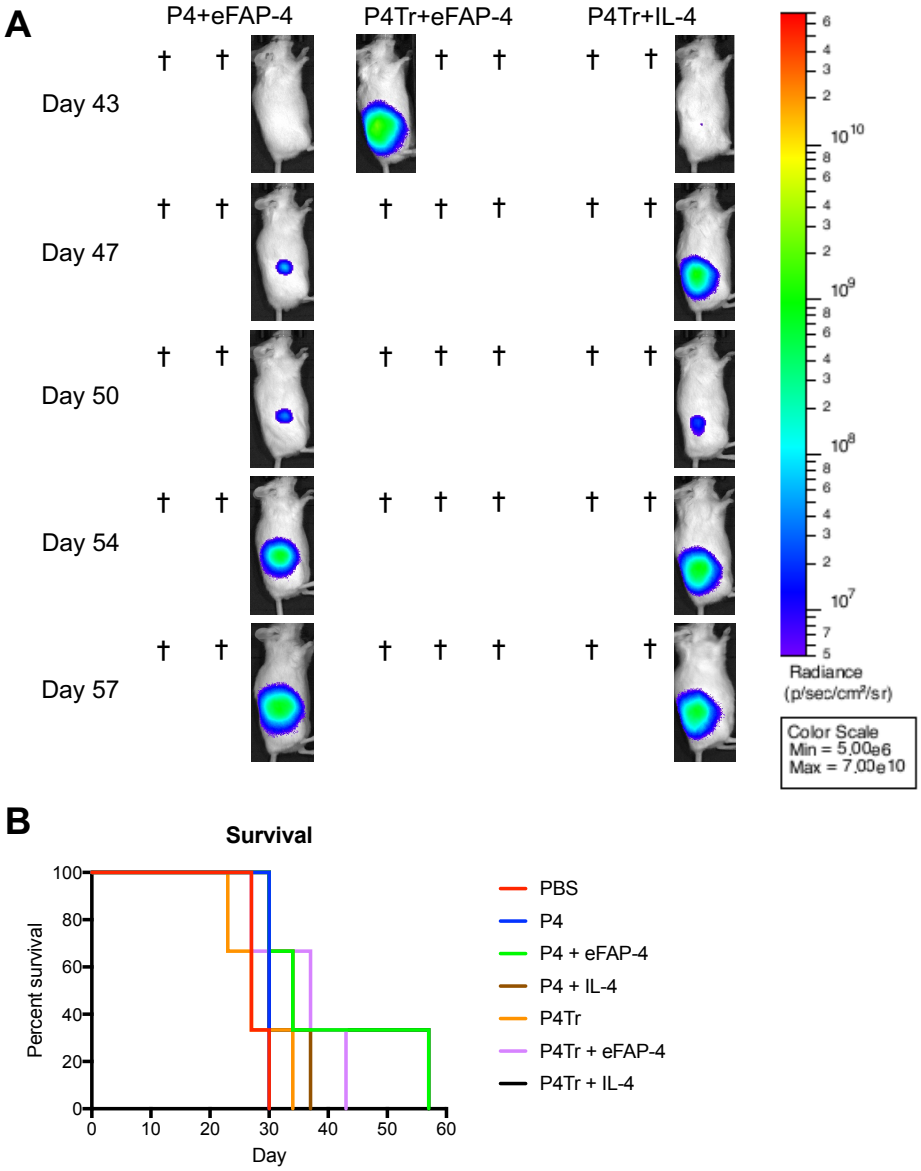

Figure 5.27 Individual bioluminescence images from day 43-57 and survival data. A) Bioluminescence images of surviving mice in the P4 + eFAP-4, P4Tr + eFAP-4 and P4Tr + IL-4 groups are shown from day 43 to day 57 after LT-PLPFAP inoculation. The scale bar indicates a logarithmic scale for radiance ranging from $5x10^6$ – $7x10^{10}$. Crosses indicate the loss of the animal due to reaching home office limits on tumour volume or close to ulceration. B) Survival is represented as a Kaplan-Meier curve. Log-rank and Gehan-Wilcoxon statistical tests were used to determine non-significance (n=3).

5.3 Discussion

Establishment of a human PCa/stroma xenograft in NSG mice proved challenging as the engraftment of the MRC5hT was not definitively shown. While scattered mNeptune signal was detected using fluorescence microscopy imaging of some tumour sections, this might have been an artefact of tdTomato expression in the PCa cells. While the peak emission of tdTomato is 581 nm, it is a comparatively bright protein at 595 nm with an

emission that continually decreases up to around 700 nm (Shaner et al., 2004). The mNeptune variant that was used in this study has a brightness of 17.5 and an emission peak at 652 nm and ranging up to 800 nm (Li et al., 2014b). Therefore, tdTomato could have bled into the mNeptune channel during *in vivo* fluorescent imaging and microscopy causing a false positive. This overlap was not an issue for flow cytometry because compensation was applied. Additionally, mNeptune signal could have been an artefact of autofluorescence of the tumour tissue. Tumour H&E stains did not indicate the presence of stroma. Immunohistochemistry analysis indicated that there were low levels of FAP expression in the MRC5hT+PLP tumours. Because the antibody used to detect FAP crosses the species barrier, it is unknown if the source was human or murine in these tumours. The MRC5hT+PLP and MRC5hT+DU145P tumours also showed low level expression of murine αSMA, further suggesting the recruitment of some murine stroma. Because of the low level of FAP expression, this recruitment was not considered to be sufficient to test the P4+eFAP-4 therapy (the ESC11 scFv having specificity for both human and murine FAP).

To monitor mNeptune^{+} MRC5hT engraftment in the absence of any possible contamination by tdTomato-derived fluorescence, I co-injected these stromal cells with tdTomato^{-} PCa cells and undertook *in vivo* fluorescence imaging. While there was an increase in signal throughout the experiment, there was also an increase in fluorescence of the background mice. Indeed, the MRC5hT alone group had the highest signal, but no tumour was visible for excision. Further analysis of sectioned tumours showed signal in the mNeptune detection channel for MRC5hT+PLP tumours using fluorescent microscopy. Because there was no negative control tissue, it is unclear whether this was autofluorescence from the tumour tissue. A limitation of the fluorescence microscopy used in this study was the lack of a negative control tissue. A sufficient control would

have been a resected xenograft tumour of the untransduced cell lines, and thus negative for all fluorescent reports. Because the aim of mNeptune expression was for *in vivo* detection, no animals were used for mNeptune$^-$ MRC5hT injection. Future *in vivo* experiments could utilise a different reporter gene for conclusive detection of MRC5hT engraftment. This could be done by putting the firefly luciferase reporter into the MRC5hT cells instead of the PCa cells, or using a different bioluminescence reporter such as renilla luciferase, allowing for dual bioluminescent *in vivo* imaging of the cell types (Wendt et al., 2011).

It is unclear why the MRC5hT cells were not detectable in the digested tumours when examining either mNeptune-derived fluorescence or FAP expression. In my hands, these cells were very sensitive to handling and it is possible that the MRC5hT did not survive the digestion. However, the lack of conclusive evidence of the MRC5hT presence *in vivo* or in the retrieved tumours suggests an initial engraftment issue or poor persistence/expansion. While the MRC5 cell line has previously been established in NSG mice, issues with engraftment have been noted using senescent MRC5 (da Silva et al., 2019). In my study, MRC5 cells transduced to express human telomerase (hT) were used to circumvent senescence although they had not been validated for *in vivo* engraftment potential previously (Ahmed et al., 2008). Additionally, MRC5hT cultures have shown variability in their ability to continue proliferating with growth arrest occurring in G1 phase and/or phases of "growth crisis" in which rate of cell death matches cell doubling (MacKenzie et al., 2000). Alternative cell lines could be used to recapitulate the stroma. PS1 were not selected for *in vivo* study because of perceived unsatisfactory *in vitro* growth kinetics. The *in vivo* use of these stromal cells could be revisited to assess their utility in the PCa/stroma model. Additionally, a prostate cancer stromal cell line could be used to model a more physiological microenvironment as these cells have shown to

engraft and promote tumour growth with PCa cells *in vivo* (Tuxhorn et al., 2002b). One of the prostate stromal cell lines, HPS-19I, generated by the Rowley group was FAP^+ and was targeted by a FAP-specific CAR (Kakarla et al., 2013).

As FAP expression is the key defining factor of stroma in this study, an *in vivo* model of FAP and PSMA co-expressing LT-PLPFAP cells was used for a pilot efficacy study of eFAP-4 with P4 CAR T-cells. The cells successfully expressed both antigens and did not exhibit differential growth kinetics from the parental line. A higher tumour burden model, in which the rapidly expanding xenograft could not be controlled by P4 CAR T cells, was used to allow for demonstration of improved efficacy (Emami-Shahri et al., 2018). This was indeed the case in my pilot study. Interleukin-4 did not seem to improve P4 CAR T cell efficacy at the dosage administered. One mouse receiving eFAP-4 and P4 CAR T cells demonstrated partial tumour regression and prolonged survival. The LT-PLPFAP tumour ultimately progressed owing to incomplete eradication. One study showed anti-tumour activity with an IL-4 based immunocytokine at a dosage of 568 pmol every 48-hours for 8 injections (Hemmerle and Neri, 2014). The dosage of eFAP-4 in my pilot study was administered at less than half this concentration and half the number of injections. Administration of a higher dose given more consistently in the LT-PLPFAP prostate cancer model might lead to a greater anti-tumour efficacy for eFAP-4 with P4 CAR T cells. Future *in vivo* experiments should optimise the treatment protocol by establishing a dose response curve for the immunocytokine administered with $1x10^6$ CAR^+ T cells. This could determine a therapeutic window for eFAP-4 with P4 CAR T cells. Additionally, a larger cohort of mice might help distinguish any significant improvement in survival or tumour control between the different treatment groups. A biodistribution study would also confirm the ability of eFAP-4 to traffic to the tumour.

5.4 Summary

- Engraftment of MRC5hT stromal cells *in vivo* in PCa/stroma xenograft models proved inadequate, leading to the establishment of a tumour model in which PSMA and FAP were co-expressed in LT-PLP cells.
- A pilot efficacy study of eFAP-4 with P4 CAR T cells demonstrated the safety of this approach, with a small trend towards improved survival and tumour control.

Chapter 6: Discussion

6.1 Overview of findings

The aim of this thesis was to develop an IL-4 immunocytokine targeted to FAP in order to increase P4 CAR T cell proliferation in the tumour microenvironment and thereby enhance *in vivo* efficacy against castrate resistant prostate cancer.

Targeted delivery of cytokines using the immunocytokine format has been shown to increase their therapeutic efficacy and to reduce systemic toxicity (Borsi et al., 2003, Liu et al., 2006). In this project, development of the immunocytokine was first addressed through generation and screening of hybridomas for FAP specificity. Fibroblast activation protein is commonly upregulated in the stroma of epithelial tumours and was chosen as the target for the scFv employed in the immunocytokine (Garin-Chesa et al., 1990). Antibodies derived from several hybridoma clones demonstrated FAP-specificity upon screening of unpurified supernatant. However, selected subclones produced antibodies that exhibited marked instability and a rapid loss of FAP-binding after purification and manipulation. To overcome this, I designed an scFv derived from a FAP-specific antibody with a published nucleotide sequence available in the literature (Fischer et al., 2012). This was engineered into a scFv-Fc format which showed comparable binding to FAP as that seen with a commercially available antibody. This scFv was developed into an IL-4 immunocytokine, termed eFAP-4. Testing of both the scFv and cytokine components of this fusion molecule confirmed that both FAP-specificity and IL-4 functionality were retained.

Interleukin-4 was chosen as the delivered cytokine to enable specific enrichment of CAR T cells co-expressing the 4αβ receptor. The 4αβ receptor couples the IL-4 ectodomain to the transmembrane and endodomain of IL-2/IL-15 receptor β. Addition of IL-4 to T cells

that express this chimeric cytokine receptor enables the selective enrichment and expansion of these cells (Wilkie et al., 2010), an approach that is currently in use in a Phase I clinical trial. The cytokine signalling capabilities of the eFAP-4 fusion proved comparable to that of an equimolar amount of unmodified recombinant human IL-4. When the 4αβ chimeric receptor is introduced into the IL-2 dependent murine T cell line, CTLL-2, these cells proliferate in response to IL-4. Culturing CTLL-4αβ with recombinant IL-4, eFAP-4 or IL-2 allowed robust validation of the IL-4 component of the immunocytokine, which promoted comparable expansion of these cells to that seen with IL-4 or IL-2. Donor human PBMCs engineered to express a CAR and the 4αβ receptor also proliferated in response to eFAP-4 in a manner comparable with IL-4 and IL-2. Consequently, I concluded that these investigations demonstrate a functional FAP-targeting IL-4 immunocytokine.

In order to test the efficacy of eFAP-4 in combination with CAR T cells, the PSMA-targeted P4 vector was selected. P4 comprises a second generation PSMA-targeting CAR co-expressed 4αβ. P4 CAR T cells proliferate in response to IL-4 and demonstrate anti-tumour efficacy *in vitro* and *in vivo* against $PSMA^+$ prostate cancer cell lines (Emami-Shahri et al., 2018, Maher et al., 2002, Wilkie et al., 2010, Zhong et al., 2010).

To generate a model for *in vitro* and *in vivo* testing of P4 and eFAP-4, I set out to develop a co-culture system that includes both $PSMA^+$ malignant and FAP^+ stromal components. The prostate cancer cell lines DU145 and a PC3 derivative named PL were selected. The PC3 derived sub-line PL was previously developed as a line with a more aggressive phenotype (Sanderson et al., 2006). The DU145 line is more indolent *in vitro* and as a xenograft. In contrast to naturally occurring prostate cancer in man, neither of these cell lines expressed endogenous PSMA. Consequently, both cell lines were successfully

transduced with retroviral vectors to co-express PSMA and the firefly luciferase-tdTomato (LT) bioluminescence and fluorescence reporter genes. Similarly, the stromal cell lines MRC5hT and PS1 were transduced successfully with the far-red fluorescence reporter mNeptune. Maintained expression of endogenous FAP was confirmed in these cells after this intervention. MRC5hT cells had been transduced with human telomerase by another group, to allow for extended passage time (Ahmed et al., 2008). Growth kinetics, antigen expression and optimised co-culture ratios were characterised for these PCa:stromal cell combinations *in vitro*. Prostate cancer/MRC5hT monolayers were advanced for further therapeutic investigation.

P4 transduced T cells demonstrated PSMA specific cytotoxicity in MRC5hT+PCa mixed co-cultures. Bystander killing of the MRC5hT cells was seen in the presence of $PSMA^+$ but not $PSMA^-$ tumour cells. Dual targeting of the stroma and the malignant cells of tumours has demonstrated superior efficacy for CAR T cell therapy compared to the targeting of stroma or tumour cells alone (Kakarla et al., 2013). Therefore, this bystander killing effect of the stroma could be beneficial for P4 CAR T cell therapy. When P4 CAR T cells were co-cultured with either IL-4 or eFAP-4 on PCa or MRC5hT+PCa monolayers cytotoxicity, proliferation and cytokine secretion was enhanced over multiple restimulation cycles when compared to CAR T cells alone. The increase in anti-tumour efficacy was greater for PLP-containing compared to DU145P cultures. Studies have shown a greater cell death resistance in DU145 compared to PC3 from serum deprivation, CAR T cell treatment, or treatment with doxorubicin and tumour necrosis factor-related apoptosis-inducing ligand (TRAIL) (Sanchez et al., 2013, Tang et al., 1998, Voelkel-Johnson et al., 2002). The *in vitro* efficacy data seen in this project correlates with the observation of reduced susceptibility to cell death for DU145 compared to PC3 and thus PC3-derived PLP was selected for further studies.

Supplementation of MRC5hT+PLP+P4 co-cultures with both IL-4 and eFAP-4 resulted in a shift towards a lower CD8:CD4 ratio over time. The immunocytokine eFAP-4 upregulated the activation marker CD44 on P4 CAR T cells co-cultured with MRC5hT+PLP monolayers. Altogether, eFAP-4 enhances P4 CAR T cell anti-tumour activity *in vitro* in a manner broadly comparable to IL-4.

The MRC5hT:PCa co-culture model was taken *in vivo* for further characterisation and therapeutic development of eFAP-4. Using *in vivo* fluorescence imaging, flow cytometric analysis and fluorescence microscopy, I was unable to demonstrate convincing evidence of engraftment of the MRC5hT stromal cell line *in vivo*. Difficulty establishing the MRC5 cell line *in vivo* has been demonstrated by others (da Silva et al., 2019). Tissue autofluorescence limited the utility of mNeptune as a live imaging fluorescence reporter gene in this project. This could be overcome by using a different reporting gene such as firefly or renilla luciferase to offer a definitive analysis of MRC5hT engraftment. There was evidence of murine stroma recruitment in the MRC5hT+PLP tumours and FAP expression at low levels. Future *in vivo* investigation could rely on FAP expression from murine stroma for further eFAP-4 development as the scFv crosses the species barrier (Renner et al., 2012).

In order to set up a pilot efficacy study to evaluate eFAP-4 in combination with P4 CAR T cells, LT-PLP cells were engineered to co-express the FAP target. The resulting LT-PLPFAP tumours were established *in vivo* and growth was observed using bioluminescence imaging. A higher tumour burden model was used based on previous reports of P4 efficacy in low but not high tumour burden models of PLP (Emami-Shahri et al., 2018). In this pilot study, P4 CAR T cells alone were insufficient to control tumour growth. The eFAP-4 immunocytokine was administered at a modest dosage of 4

intraperitoneal injections of 250 pmols. At this dose, there was a suggestion of a delayed tumour progression compared to P4 CAR T cells alone or with the equivalent dose of IL-4. There was anti-tumour activity indicated by a partial regression seen in one of the P4 + eFAP-4 treated mice. Tumour bioluminescence fell below the limit of detection before relapsing. No dose limiting toxicities were seen. An improved survival trend was also seen with P4 + eFAP-4 compared to other treatment groups, although this did not reach significance. Further *in vivo* work with larger cohorts is needed to establish an optimised dose and treatment schedule for the eFAP-4 immunocytokine with P4 CAR T cells in prostate cancer models.

6.2 Limitations

There is increasing evidence that interactions between different cell types within the tumour microenvironment are crucial for disease progression. Therapeutic investigation utilising *in vitro* monolayers and *in vivo* tumours of solely cancer cells may not reflect the activity of the drug in patients. Here, this limitation was partially addressed through the co-culture of prostate cancer cells with stromal cell lines, although ultimately it proved difficult to translate this model *in vivo*. Additionally, drug efficacy against monolayers has shown to be superior when compared to efficacy against cancer spheroids (Lal-Nag et al., 2017, Shan et al., 2018). Three-dimensional *in vitro* cancer cell cultures are more representative of the histology, gene expression and architecture of *in vivo* tumours (Lee et al., 2013). These 3D models have been used to assess CAR T cell efficacy (Dillard et al., 2018). Multicellular spheroids incorporate a variety of cell types present in the tumour and recapitulate the cell-cell interactions within the microenvironment (Lazzari et al., 2018). These multicellular spheroids could be used as representative xenografts in immunodeficient mice that lack many cell types found in tumours. In order to better

model the tumour microenvironment, future directions for this project could utilise spheroids in CAR T cell drug development.

The cell line used in the *in vivo* pilot efficacy investigation constituted forced expression of the target antigens PSMA and FAP. This may result in higher levels of protein expression compared to endogenously expressing cell lines. Higher antigen expression in the tumour would theoretically enable greater targeting and efficacy of the eFAP-4 immunocytokine and P4 CAR T cells. Cell lines that endogenously express the target antigens could be used in co-cultures to represent physiological levels such as the prostate cancer cell line LNCaP. Patient-derived xenografts would produce a model most similar to primary tumours, but are known to be difficult to culture and reproduce for drug development (Russell et al., 2015).

Due to time constraints of this project, approximately 1 mg of eFAP-4 was produced for experimental analysis. The 250 pmol dose used in the pilot efficacy study therefore was determined by resource availability. Suggestion of an increase in efficacy in the P4 + eFAP-4 treated group warrants further investigation to establish an optimal dosing concentration. Immunocytokine studies *in vivo* vary widely in effective dosages and thus it was difficult to predict the concentration needed for the pilot study (Bauer et al., 2004, Borsi et al., 2003, Carnemolla et al., 2002, Hemmerle and Neri, 2014, Kawalkowska et al., 2016, Kermer et al., 2012, Muller et al., 2008, Quattrone et al., 2015). A study utilising a CD20-targeting IL-2 immunocytokine co-injected with CD19-specific CAR T cells observed efficacy at doses of 7 x 30 pmol/injections spanning 3 weeks and 10^7 CAR^+ T cells (Singh et al., 2007). For further *in vivo* analysis, more eFAP-4 should be generated and biodistribution/pharmacokinetic studies utilised to assess the *in vivo* activity of eFAP-4 and influence dosing frequency. Additionally, a dose curve and treatment schedule

should be established to assess a therapeutic window for co-administration with P4 CAR T cells.

6.3 Conclusions

There is an unmet clinical need to improve the efficacy and safety of CAR T cell immunotherapy for solid tumours. This project aimed to address this need by developing a system for intratumoural CAR T cell enrichment, with the support of a tumour-specific immunocytokine. To achieve this, I developed a stable FAP-specific IL-4 immunocytokine, designated eFAP-4, which exhibited comparable signalling capabilities to IL-4 in primary human CAR T cells expressing the 4αβ chimeric receptor. Addition of eFAP-4 resulted in increased persistence/enrichment of P4 CAR T cells in restimulation killing assays of prostate cancer and stroma cell lines *in vitro*. The prolongation of this effect suggested dependence on continued immunocytokine supplementation. Translation of this therapy to an *in vivo* pilot study indicated a potential increase in survival and tumour growth control for P4 + eFAP-4 treated mice. The implications of this therapy in the clinic could provide a dose dependent and reversible strategy to increase CAR T cell efficacy. Additional investigations are needed to assess the true potential of CAR T cell combination therapy with eFAP-4.

References

ABAD, J. D., WRZENSINSKI, C., OVERWIJK, W., DE WITTE, M. A., JORRITSMA, A., HSU, C., GATTINONI, L., COHEN, C. J., PAULOS, C. M., PALMER, D. C., HAANEN, J. B., SCHUMACHER, T. N., ROSENBERG, S. A., RESTIFO, N. P. & MORGAN, R. A. 2008. T-cell receptor gene therapy of established tumors in a murine melanoma model. *J Immunother,* 31**,** 1-6.

ABKEN, H., HOMBACH, A., HEUSER, C., SIRCAR, R., POHL, C. & REINHOLD, U. 1997. Chimeric T-cell receptors: highly specific tools to target cytotoxic T-lymphocytes to tumour cells. *Cancer Treat Rev,* 23**,** 97-112.

ADACHI, K., KANO, Y., NAGAI, T., OKUYAMA, N., SAKODA, Y. & TAMADA, K. 2018. IL-7 and CCL19 expression in CAR-T cells improves immune cell infiltration and CAR-T cell survival in the tumor. *Nat Biotechnol,* 36**,** 346-351.

ADUSUMILLI, P. S., CHERKASSKY, L., VILLENA-VARGAS, J., COLOVOS, C., SERVAIS, E., PLOTKIN, J., JONES, D. R. & SADELAIN, M. 2014. Regional delivery of mesothelin-targeted CAR T cell therapy generates potent and long-lasting CD4-dependent tumor immunity. *Sci Transl Med,* 6**,** 261ra151.

ADUSUMILLI, P. S., ZAUDERER, M. G., RUSCH, V. W., O'CEARBHAILL, R., ZHU, A., NGAI, D., MCGEE, E., CHINTALA, N., MESSINGER, J., CHEEMA, W., HALTON, E., DIAMONTE, C., PINEDA, J., VINCENT, A., MODI, S., SOLOMON, S. B., JONES, D. R., BRENTJENS, R. J., RIVIERE, I. & SADELAIN, M. 2019. Regional delivery of mesothelin-targeted CAR T cells for pleural cancers: Safety and preliminary efficacy in combination with anti-PD-1 agent. *Journal of Clinical Oncology,* 37**,** 2511-2511.

AERTGEERTS, K., LEVIN, I., SHI, L., SNELL, G. P., JENNINGS, A., PRASAD, G. S., ZHANG, Y., KRAUS, M. L., SALAKIAN, S., SRIDHAR, V., WIJNANDS, R. & TENNANT, M. G. 2005. Structural and kinetic analysis of the substrate specificity of human fibroblast activation protein alpha. *J Biol Chem,* 280**,** 19441-4.

AHMADZADEH, M., ROSENBERG, S.A., 2005. TGF-beta 1 attenuates the acquisition and expression of effector function by tumor antigen-specific human memory CD8 T cells. J. Immunol. Baltim. Md 1950 174, 5215–5223. https://doi.org/10.4049/jimmunol.174.9.521

AHMED, S., PASSOS, J. F., BIRKET, M. J., BECKMANN, T., BRINGS, S., PETERS, H., BIRCH-MACHIN, M. A., VON ZGLINICKI, T. & SARETZKI, G. 2008. Telomerase does not counteract telomere shortening but protects mitochondrial function under oxidative stress. *J Cell Sci,* 121**,** 1046-53.

ALBERTINI, M. R., HANK, J. A., GADBAW, B., KOSTLEVY, J., HALDEMAN, J., SCHALCH, H., GAN, J., KIM, K., EICKHOFF, J., GILLIES, S. D. & SONDEL, P. M. 2012. Phase II trial of hu14.18-IL2 for patients with metastatic melanoma. *Cancer Immunol Immunother,* 61**,** 2261-71.

ALBERTINI, M. R., YANG, R. K., RANHEIM, E. A., HANK, J. A., ZULEGER, C. L., WEBER, S., NEUMAN, H., HARTIG, G., WEIGEL, T., MAHVI, D., HENRY, M. B., QUALE, R., MCFARLAND, T., GAN, J., CARMICHAEL, L., KIM, K., LOIBNER, H., GILLIES, S. D. & SONDEL, P. M. 2018. Pilot trial of the hu14.18-IL2 immunocytokine in patients with completely resectable recurrent stage III or stage IV melanoma. *Cancer Immunology, Immunotherapy,* 67**,** 1647-1658.

ALEMOZAFFAR, M., REGAN, M. M., COOPERBERG, M. R., WEI, J. T., MICHALSKI, J. M., SANDLER, H. M., HEMBROFF, L., SADETSKY, N., SAIGAL, C. S., LITWIN, M. S., KLEIN, E., KIBEL, A. S., HAMSTRA, D. A., PISTERS, L. L., KUBAN, D. A., KAPLAN, I. D., WOOD, D. P., CIEZKI, J.,

DUNN, R. L., CARROLL, P. R. & SANDA, M. G. 2011. Prediction of erectile function following treatment for prostate cancer. *Jama,* 306**,** 1205-14.

ALLAOUI, R., BERGENFELZ, C., MOHLIN, S., HAGERLING, C., SALARI, K., WERB, Z., ANDERSON, R.L., ETHIER, S.P., JIRSTROM, K., PAHLMAN, S., BEXELL, D., TAHIN, B., JOHANSSON, M.E., LARSSON, C., LEANDERSSON, K., 2016. Cancer-associated fibroblast-secreted CXCL16 attracts monocytes to promote stroma activation in triple-negative breast cancers. Nat. Commun. 7, 13050. https://doi.org/10.1038/ncomms13050

ALSAAB, H. O., SAU, S., ALZHRANI, R., TATIPARTI, K., BHISE, K., KASHAW, S. K. & IYER, A. K. 2017. PD-1 and PD-L1 Checkpoint Signaling Inhibition for Cancer Immunotherapy: Mechanism, Combinations, and Clinical Outcome. *Front Pharmacol,* 8**,** 561.

ALTENSCHMIDT, U., KAHL, R., MORITZ, D., SCHNIERLE, B. S., GERSTMAYER, B., WELS, W. & GRONER, B. 1996. Cytolysis of tumor cells expressing the Neu/erbB-2, erbB-3, and erbB-4 receptors by genetically targeted naive T lymphocytes. *Clin Cancer Res,* 2**,** 1001-8.

ALVAREZ-VALLINA, L. & HAWKINS, R. E. 1996. Antigen-specific targeting of CD28-mediated T cell co-stimulation using chimeric single-chain antibody variable fragment-CD28 receptors. *Eur J Immunol,* 26**,** 2304-9.

AMAN, M. J., TAYEBI, N., OBIRI, N. I., PURI, R. K., MODI, W. S. & LEONARD, W. J. 1996. cDNA cloning and characterization of the human interleukin 13 receptor alpha chain. *J Biol Chem,* 271**,** 29265-70.

ANDERSON, B. D., NAKAMURA, T., RUSSELL, S. J. & PENG, K. W. 2004. High CD46 receptor density determines preferential killing of tumor cells by oncolytic measles virus. *Cancer Res,* 64**,** 4919-26.

ANDTBACKA, R. H., KAUFMAN, H. L., COLLICHIO, F., AMATRUDA, T., SENZER, N., CHESNEY, J., DELMAN, K. A., SPITLER, L. E., PUZANOV, I., AGARWALA, S. S., MILHEM, M., CRANMER, L., CURTI, B., LEWIS, K., ROSS, M., GUTHRIE, T., LINETTE, G. P., DANIELS, G. A., HARRINGTON, K., MIDDLETON, M. R., MILLER, W. H., JR., ZAGER, J. S., YE, Y., YAO, B., LI, A., DOLEMAN, S., VANDERWALDE, A., GANSERT, J. & COFFIN, R. S. 2015. Talimogene Laherparepvec Improves Durable Response Rate in Patients With Advanced Melanoma. *J Clin Oncol,* 33**,** 2780-8.

ANDTBACKA, R. H., ROSS, M., PUZANOV, I., MILHEM, M., COLLICHIO, F., DELMAN, K. A., AMATRUDA, T., ZAGER, J. S., CRANMER, L., HSUEH, E., CHEN, L., SHILKRUT, M. & KAUFMAN, H. L. 2016. Patterns of Clinical Response with Talimogene Laherparepvec (T-VEC) in Patients with Melanoma Treated in the OPTiM Phase III Clinical Trial. *Ann Surg Oncol,* 23**,** 4169-4177.

ANTONY, P. A., PICCIRILLO, C. A., AKPINARLI, A., FINKELSTEIN, S. E., SPEISS, P. J., SURMAN, D. R., PALMER, D. C., CHAN, C. C., KLEBANOFF, C. A., OVERWIJK, W. W., ROSENBERG, S. A. & RESTIFO, N. P. 2005. CD8+ T cell immunity against a tumor/self-antigen is augmented by CD4+ T helper cells and hindered by naturally occurring T regulatory cells. *J Immunol,* 174**,** 2591-601.

ARORA, V. K., SCHENKEIN, E., MURALI, R., SUBUDHI, S. K., WONGVIPAT, J., BALBAS, M. D., SHAH, N., CAI, L., EFSTATHIOU, E., LOGOTHETIS, C., ZHENG, D. & SAWYERS, C. L. 2013. Glucocorticoid receptor confers resistance to antiandrogens by bypassing androgen receptor blockade. *Cell,* 155**,** 1309-22.

ASCIERTO, P. A., MELERO, I., BHATIA, S., BONO, P., SANBORN, R. E., LIPSON, E. J., CALLAHAN, M. K., GAJEWSKI, T., GOMEZ-ROCA, C. A., HODI, F. S., CURIGLIANO, G., NYAKAS, M., PREUSSER, M., KOGUCHI, Y., MAURER, M., CLYNES, R., MITRA, P., SURYAWANSHI, S. & MUÑOZ-

COUSELO, E. 2017. Initial efficacy of anti-lymphocyte activation gene-3 (anti–LAG-3; BMS-986016) in combination with nivolumab (nivo) in pts with melanoma (MEL) previously treated with anti–PD-1/PD-L1 therapy. *Journal of Clinical Oncology,* 35**,** 9520-9520.

AU, G. G., BEAGLEY, L. G., HALEY, E. S., BARRY, R. D. & SHAFREN, D. R. 2011. Oncolysis of malignant human melanoma tumors by Coxsackieviruses A13, A15 and A18. *Virol J,* 8**,** 22.

BAE, S., PARK, C. W., SON, H. K., JU, H. K., PAIK, D., JEON, C. J., KOH, G. Y., KIM, J. & KIM, H. 2008. Fibroblast activation protein alpha identifies mesenchymal stromal cells from human bone marrow. *Br J Haematol,* 142**,** 827-30.

BAIER, P. K., WOLFF-VORBECK, G., EGGSTEIN, S., BAUMGARTNER, U. & HOPT, U. T. 2005. Cytokine expression in colon carcinoma. *Anticancer Res,* 25**,** 2135-9.

BAIRD, S. K., ALLAN, L., RENNER, C., SCOTT, F. E. & SCOTT, A. M. 2015. Fibroblast activation protein increases metastatic potential of fibrosarcoma line HT1080 through upregulation of integrin-mediated signaling pathways. *Clin Exp Metastasis,* 32**,** 507-16.

BANDER, N. H. 2006. Technology insight: monoclonal antibody imaging of prostate cancer. *Nat Clin Pract Urol,* 3**,** 216-25.

BARRIE, S. E., HAYNES, B. P., POTTER, G. A., CHAN, F. C., GODDARD, P. M., DOWSETT, M. & JARMAN, M. 1997. Biochemistry and pharmacokinetics of potent non-steroidal cytochrome P450(17alpha) inhibitors. *J Steroid Biochem Mol Biol,* 60**,** 347-51.

BARTOSCHEK, M., OSKOLKOV, N., BOCCI, M., LOVROT, J., LARSSON, C., SOMMARIN, M., MADSEN, C.D., LINDGREN, D., PEKAR, G., KARLSSON, G., RINGNER, M., BERGH, J., BJORKLUND, A., PIETRAS, K., 2018. Spatially and functionally distinct subclasses of breast cancer-associated fibroblasts revealed by single cell RNA sequencing. Nat. Commun. 9, 5150. https://doi.org/10.1038/s41467-018-07582-3

BAUER, S., ADRIAN, N., WILLIAMSON, B., PANOUSIS, C., FADLE, N., SMERD, J., FETTAH, I., SCOTT, A. M., PFREUNDSCHUH, M. & RENNER, C. 2004. Targeted Bioactivity of Membrane-Anchored TNF by an Antibody-Derived TNF Fusion Protein. *The Journal of Immunology,* 172**,** 3930-3939.

BAVIK, C., COLEMAN, I., DEAN, J.P., KNUDSEN, B., PLYMATE, S., NELSON, P.S., 2006. The gene expression program of prostate fibroblast senescence modulates neoplastic epithelial cell proliferation through paracrine mechanisms. Cancer Res. 66, 794–802. https://doi.org/10.1158/0008-5472.CAN-05-1716

BECHTEL, W., MCGOOHAN, S., ZEISBERG, E.M., MULLER, G.A., KALBACHER, H., SALANT, D.J., MULLER, C.A., KALLURI, R., ZEISBERG, M., 2010. Methylation determines fibroblast activation and fibrogenesis in the kidney. Nat. Med. 16, 544–550. https://doi.org/10.1038/nm.2135

BECKER, M. L., NEAR, R., MUDGETT-HUNTER, M., MARGOLIES, M. N., KUBO, R. T., KAYE, J. & HEDRICK, S. M. 1989. Expression of a hybrid immunoglobulin-T cell receptor protein in transgenic mice. *Cell,* 58**,** 911-21.

BEER, T. M., KWON, E. D., DRAKE, C. G., FIZAZI, K., LOGOTHETIS, C., GRAVIS, G., GANJU, V., POLIKOFF, J., SAAD, F., HUMANSKI, P., PIULATS, J. M., MELLA, P. G., NG, S. S., JAEGER, D., PARNIS, F. X., FRANKE, F. A., PUENTE, J., CARVAJAL, R., SENGELØV, L., MCHENRY, M. B., VARMA, A., EERTWEGH, A. J. V. D. & GERRITSEN, W. 2017. Randomized, Double-Blind, Phase III Trial of Ipilimumab Versus Placebo in Asymptomatic or

Minimally Symptomatic Patients With Metastatic Chemotherapy-Naive Castration-Resistant Prostate Cancer. *Journal of Clinical Oncology,* 35**,** 40-47.

BEHRING, E. V. 1890. Über das zustandekommen der diphtherie-immunität und der tetanus-immunität bei thieren.

BERNT, K. M., NI, S., TIEU, A. T. & LIEBER, A. 2005. Assessment of a combined, adenovirus-mediated oncolytic and immunostimulatory tumor therapy. *Cancer Res,* 65**,** 4343-52.

BHOME, R., AL SAIHATI, H. A., GOH, R. W., BULLOCK, M. D., PRIMROSE, J. N., THOMAS, G. J., SAYAN, A. E. & MIRNEZAMI, A. H. 2016. Translational aspects in targeting the stromal tumour microenvironment: from bench to bedside. *New Horiz Transl Med,* 3**,** 9-21.

BIGGAR, R. J., HORM, J., GOEDERT, J. J. & MELBYE, M. 1987. Cancer in a group at risk of acquired immunodeficiency syndrome (AIDS) through 1984. *Am J Epidemiol,* 126**,** 578-86.

BIRKELAND, S. A., STORM, H. H., LAMM, L. U., BARLOW, L., BLOHME, I., FORSBERG, B., EKLUND, B., FJELDBORG, O., FRIEDBERG, M., FRODIN, L. & ET AL. 1995. Cancer risk after renal transplantation in the Nordic countries, 1964-1986. *Int J Cancer,* 60**,** 183-9.

BOCCA, P., DI CARLO, E., CARUANA, I., EMIONITE, L., CILLI, M., DE ANGELIS, B., QUINTARELLI, C., PEZZOLO, A., RAFFAGHELLO, L., MORANDI, F., LOCATELLI, F., PISTOIA, V. & PRIGIONE, I. 2017. Bevacizumab-mediated tumor vasculature remodelling improves tumor infiltration and antitumor efficacy of GD2-CAR T cells in a human neuroblastoma preclinical model. *Oncoimmunology,* 7**,** e1378843.

BONINI, C., FERRARI, G., VERZELETTI, S., SERVIDA, P., ZAPPONE, E., RUGGIERI, L., PONZONI, M., ROSSINI, S., MAVILIO, F., TRAVERSARI, C. & BORDIGNON, C. 1997. HSV-TK gene transfer into donor lymphocytes for control of allogeneic graft-versus-leukemia. *Science,* 276**,** 1719-24.

BONINI, C. & MONDINO, A. 2015. Adoptive T-cell therapy for cancer: The era of engineered T cells. *Eur J Immunol,* 45**,** 2457-69.

BORSI, L., BALZA, E., CARNEMOLLA, B., SASSI, F., CASTELLANI, P., BERNDT, A., KOSMEHL, H., BIRO, A., SIRI, A., ORECCHIA, P., GRASSI, J., NERI, D. & ZARDI, L. 2003. Selective targeted delivery of TNFalpha to tumor blood vessels. *Blood,* 102**,** 4384-92.

BOSTWICK, D. G., PACELLI, A., BLUTE, M., ROCHE, P. & MURPHY, G. P. 1998. Prostate specific membrane antigen expression in prostatic intraepithelial neoplasia and adenocarcinoma: a study of 184 cases. *Cancer,* 82**,** 2256-61.

BOZOKY, B., SAVCHENKO, A., CSERMELY, P., KORCSMAROS, T., DUL, Z., PONTEN, F., SZEKELY, L., KLEIN, G., 2013. Novel signatures of cancer-associated fibroblasts. Int. J. Cancer 133, 286–293. https://doi.org/10.1002/ijc.28035

BRADFORD, J. R., WAPPETT, M., BERAN, G., LOGIE, A., DELPUECH, O., BROWN, H., BOROS, J., CAMP, N. J., MCEWEN, R., MAZZOLA, A. M., D'CRUZ, C. & BARRY, S. T. 2016. Whole transcriptome profiling of patient-derived xenograft models as a tool to identify both tumor and stromal specific biomarkers. *Oncotarget,* 7**,** 20773-87.

BRAEKEVELDT, N., WIGERUP, C., TADEO, I., BECKMAN, S., SANDEN, C., JONSSON, J., ERJEFALT, J. S., BERBEGALL, A. P., BORJESSON, A., BACKMAN, T., ORA, I., NAVARRO, S., NOGUERA, R., GISSELSSON, D., PAHLMAN, S. & BEXELL, D. 2016. Neuroblastoma patient-derived orthotopic

xenografts reflect the microenvironmental hallmarks of aggressive patient tumours. *Cancer Lett,* 375**,** 384-389.

BRAHMER, J. R., DRAKE, C. G., WOLLNER, I., POWDERLY, J. D., PICUS, J., SHARFMAN, W. H., STANKEVICH, E., PONS, A., SALAY, T. M., MCMILLER, T. L., GILSON, M. M., WANG, C., SELBY, M., TAUBE, J. M., ANDERS, R., CHEN, L., KORMAN, A. J., PARDOLL, D. M., LOWY, I. & TOPALIAN, S. L. 2010. Phase I study of single-agent anti-programmed death-1 (MDX-1106) in refractory solid tumors: safety, clinical activity, pharmacodynamics, and immunologic correlates. *J Clin Oncol,* 28**,** 3167-75.

BRAIDWOOD, L., LEARMONTH, K., GRAHAM, A. & CONNER, J. 2014. Potent efficacy signals from systemically administered oncolytic herpes simplex virus (HSV1716) in hepatocellular carcinoma xenograft models. *J Hepatocell Carcinoma,* 1**,** 149-61.

BREITBACH, C. J., ARULANANDAM, R., DE SILVA, N., THORNE, S. H., PATT, R., DANESHMAND, M., MOON, A., ILKOW, C., BURKE, J., HWANG, T. H., HEO, J., CHO, M., CHEN, H., ANGARITA, F. A., ADDISON, C., MCCART, J. A., BELL, J. C. & KIRN, D. H. 2013. Oncolytic vaccinia virus disrupts tumor-associated vasculature in humans. *Cancer Res,* 73**,** 1265-75.

BROCKER, T. & KARJALAINEN, K. 1995. Signals through T cell receptor-zeta chain alone are insufficient to prime resting T lymphocytes. *J Exp Med,* 181**,** 1653-9.

BROWN, C. E., BADIE, B., BARISH, M. E., WENG, L., OSTBERG, J. R., CHANG, W. C., NARANJO, A., STARR, R., WAGNER, J., WRIGHT, C., ZHAI, Y., BADING, J. R., RESSLER, J. A., PORTNOW, J., D'APUZZO, M., FORMAN, S. J. & JENSEN, M. C. 2015. Bioactivity and Safety of IL13Ralpha2-Redirected Chimeric Antigen Receptor CD8+ T Cells in Patients with Recurrent Glioblastoma. *Clin Cancer Res,* 21**,** 4062-72.

BRUNET, J. F., DENIZOT, F., LUCIANI, M. F., ROUX-DOSSETO, M., SUZAN, M., MATTEI, M. G. & GOLSTEIN, P. 1987. A new member of the immunoglobulin superfamily--CTLA-4. *Nature,* 328**,** 267-70.

BRUZZESE, F., HAGGLOF, C., LEONE, A., SJOBERG, E., ROCA, M. S., KIFLEMARIAM, S., SJOBLOM, T., HAMMARSTEN, P., EGEVAD, L., BERGH, A., OSTMAN, A., BUDILLON, A. & AUGSTEN, M. 2014. Local and systemic protumorigenic effects of cancer-associated fibroblast-derived GDF15. *Cancer Res,* 74**,** 3408-17.

BUNSE, M., BENDLE, G. M., LINNEMANN, C., BIES, L., SCHULZ, S., SCHUMACHER, T. N. & UCKERT, W. 2014. RNAi-mediated TCR knockdown prevents autoimmunity in mice caused by mixed TCR dimers following TCR gene transfer. *Mol Ther,* 22**,** 1983-91.

CALDEMEYER, L. E., AKARD, L. P., EDWARDS, J. R., TANDRA, A., WAGENKNECHT, D. R. & DUGAN, M. J. 2017. Donor Lymphocyte Infusions Used to Treat Mixed-Chimeric and High-Risk Patient Populations in the Relapsed and Nonrelapsed Settings after Allogeneic Transplantation for Hematologic Malignancies Are Associated with High Five-Year Survival if Persistent Full Donor Chimerism Is Obtained or Maintained. *Biol Blood Marrow Transplant,* 23**,** 1989-1997.

CAO, M., CAO, P., YAN, H., LU, W., REN, F., HU, Y. & ZHANG, S. 2009. Construction, purification, and characterization of anti-BAFF scFv-Fc fusion antibody expressed in CHO/dhfr- cells. *Appl Biochem Biotechnol,* 157**,** 562-74.

CARDENAS, D. M., SANCHEZ, A. C., ROSAS, D. A., RIVERO, E., PAPARONI, M. D., CRUZ, M. A., SUAREZ, Y. P. & GALVIS, N. F. 2018. Preliminary analysis of single-nucleotide polymorphisms in IL-10, IL-4, and IL-4Ralpha genes and

profile of circulating cytokines in patients with gastric Cancer. *BMC Gastroenterol,* 18**,** 184.

CARNEMOLLA, B., BORSI, L., BALZA, E., CASTELLANI, P., MEAZZA, R., BERNDT, A., FERRINI, S., KOSMEHL, H., NERI, D. & ZARDI, L. 2002. Enhancement of the antitumor properties of interleukin-2 by its targeted delivery to the tumor blood vessel extracellular matrix. *Blood,* 99**,** 1659-65.

CARPENITO, C., MILONE, M. C., HASSAN, R., SIMONET, J. C., LAKHAL, M., SUHOSKI, M. M., VARELA-ROHENA, A., HAINES, K. M., HEITJAN, D. F., ALBELDA, S. M., CARROLL, R. G., RILEY, J. L., PASTAN, I. & JUNE, C. H. 2009. Control of large, established tumor xenografts with genetically retargeted human T cells containing CD28 and CD137 domains. *Proc Natl Acad Sci U S A,* 106**,** 3360-5.

CARTELLIERI, M., FELDMANN, A., KORISTKA, S., ARNDT, C., LOFF, S., EHNINGER, A., VON BONIN, M., BEJESTANI, E. P., EHNINGER, G. & BACHMANN, M. P. 2016. Switching CAR T cells on and off: a novel modular platform for retargeting of T cells to AML blasts. *Blood Cancer J,* 6**,** e458.

CARTER, L. L. & CARRENO, B. M. 2003. Cytotoxic T-lymphocyte antigen-4 and programmed death-1 function as negative regulators of lymphocyte activation. *Immunol Res,* 28**,** 49-59.

CARTER, R. E., FELDMAN, A. R. & COYLE, J. T. 1996. Prostate-specific membrane antigen is a hydrolase with substrate and pharmacologic characteristics of a neuropeptidase. *Proc Natl Acad Sci U S A,* 93**,** 749-53.

CATANIA, C., MAUR, M., BERARDI, R., ROCCA, A., GIACOMO, A. M., SPITALERI, G., MASINI, C., PIERANTONI, C., GONZALEZ-IGLESIAS, R., ZIGON, G., TASCIOTTI, A., GIOVANNONI, L., LOVATO, V., ELIA, G., MENSSEN, H. D., NERI, D., CASCINU, S., CONTE, P. F. & BRAUD, F. 2015. The tumor-targeting immunocytokine F16-IL2 in combination with doxorubicin: dose escalation in patients with advanced solid tumors and expansion into patients with metastatic breast cancer. *Cell Adh Migr,* 9**,** 14-21.

CAZET, A.S., HUI, M.N., ELSWORTH, B.L., WU, S.Z., RODEN, D., CHAN, C.-L., SKHINAS, J.N., COLLOT, R., YANG, J., HARVEY, K., JOHAN, M.Z., COOPER, C., NAIR, R., HERRMANN, D., MCFARLAND, A., DENG, N., RUIZ-BORREGO, M., ROJO, F., TRIGO, J.M., BEZARES, S., CABALLERO, R., LIM, E., TIMPSON, P., O'TOOLE, S., WATKINS, D.N., COX, T.R., SAMUEL, M.S., MARTIN, M., SWARBRICK, A., 2018. Targeting stromal remodeling and cancer stem cell plasticity overcomes chemoresistance in triple negative breast cancer. Nat. Commun. 9, 2897. https://doi.org/10.1038/s41467-018-05220-6

CESARETTI, J. A., KAO, J., STONE, N. N. & STOCK, R. G. 2007. Effect of low dose-rate prostate brachytherapy on the sexual health of men with optimal sexual function before treatment: analysis at > or = 7 years of follow-up. *BJU Int,* 100**,** 362-7.

CHANG, S. S., BOORJIAN, S. A., CHOU, R., CLARK, P. E., DANESHMAND, S., KONETY, B. R., PRUTHI, R., QUALE, D. Z., RITCH, C. R., SEIGNE, J. D., SKINNER, E. C., SMITH, N. D. & MCKIERNAN, J. M. 2016. Diagnosis and Treatment of Non-Muscle Invasive Bladder Cancer: AUA/SUO Guideline. *J Urol,* 196**,** 1021-9.

CHANG, S. S., O'KEEFE, D. S., BACICH, D. J., REUTER, V. E., HESTON, W. D. & GAUDIN, P. B. 1999a. Prostate-specific membrane antigen is produced in tumor-associated neovasculature. *Clin Cancer Res,* 5**,** 2674-81.

CHANG, S. S., REUTER, V. E., HESTON, W. D., BANDER, N. H., GRAUER, L. S. & GAUDIN, P. B. 1999b. Five different anti-prostate-specific membrane antigen (PSMA) antibodies confirm PSMA expression in tumor-associated neovasculature. *Cancer Res,* 59**,** 3192-8.

CHANG, H.Y., CHI, J.-T., DUDOIT, S., BONDRE, C., VAN DE RIJN, M., BOTSTEIN, D., BROWN, P.O., 2002. Diversity, topographic differentiation, and positional memory in human fibroblasts. Proc. Natl. Acad. Sci. U. S. A. 99, 12877–12882. https://doi.org/10.1073/pnas.16248859

CHAUHAN, V.P., MARTIN, J.D., LIU, H., LACORRE, D.A., JAIN, S.R., KOZIN, S.V., STYLIANOPOULOS, T., MOUSA, A.S., HAN, X., ADSTAMONGKONKUL, P., POPOVIC, Z., HUANG, P., BAWENDI, M.G., BOUCHER, Y., JAIN, R.K., 2013. Angiotensin inhibition enhances drug delivery and potentiates chemotherapy by decompressing tumour blood vessels. Nat. Commun. 4, 2516. https://doi.org/10.1038/ncomms3516

CHEN, H., YANG, W. W., WEN, Q. T., XU, L. & CHEN, M. 2009. TGF-beta induces fibroblast activation protein expression; fibroblast activation protein expression increases the proliferation, adhesion, and migration of HO-8910PM [corrected]. *Exp Mol Pathol,* 87**,** 189-94.

CHEN, X., LIU, B., LI, Q., HONORIO, S., LIU, X., LIU, C., MULTANI, A. S., CALHOUN-DAVIS, T. & TANG, D. G. 2013a. Dissociated primary human prostate cancer cells coinjected with the immortalized Hs5 bone marrow stromal cells generate undifferentiated tumors in NOD/SCID-gamma mice. *PLoS One,* 8**,** e56903.

CHEN, X., ZHOU, J. Y., ZHAO, J., CHEN, J. J., MA, S. N. & ZHOU, J. Y. 2013b. Crizotinib overcomes hepatocyte growth factor-mediated resistance to gefitinib in EGFR-mutant non-small-cell lung cancer cells. *Anticancer Drugs,* 24**,** 1039-46.

CHHEDA, Z. S., KOHANBASH, G., OKADA, K., JAHAN, N., SIDNEY, J., PECORARO, M., YANG, X., CARRERA, D. A., DOWNEY, K. M., SHRIVASTAV, S., LIU, S., LIN, Y., LAGISETTI, C., CHUNTOVA, P., WATCHMAKER, P. B., MUELLER, S., POLLACK, I. F., RAJALINGAM, R., CARCABOSO, A. M., MANN, M., SETTE, A., GARCIA, K. C., HOU, Y. & OKADA, H. 2018. Novel and shared neoantigen derived from histone 3 variant H3.3K27M mutation for glioma T cell therapy. *J Exp Med,* 215**,** 141-157.

CHMIELEWSKI, M. & ABKEN, H. 2017. CAR T Cells Releasing IL-18 Convert to T-Bet(high) FoxO1(low) Effectors that Exhibit Augmented Activity against Advanced Solid Tumors. *Cell Rep,* 21**,** 3205-3219.

CHMIELEWSKI, M., KOPECKY, C., HOMBACH, A. A. & ABKEN, H. 2011. IL-12 release by engineered T cells expressing chimeric antigen receptors can effectively Muster an antigen-independent macrophage response on tumor cells that have shut down tumor antigen expression. *Cancer Res,* 71**,** 5697-706.

CHODON, T., COMIN-ANDUIX, B., CHMIELOWSKI, B., KOYA, R. C., WU, Z., AUERBACH, M., NG, C., AVRAMIS, E., SEJA, E., VILLANUEVA, A., MCCANNEL, T. A., ISHIYAMA, A., CZERNIN, J., RADU, C. G., WANG, X., GJERTSON, D. W., COCHRAN, A. J., CORNETTA, K., WONG, D. J., KAPLAN-LEFKO, P., HAMID, O., SAMLOWSKI, W., COHEN, P. A., DANIELS, G. A., MUKHERJI, B., YANG, L., ZACK, J. A., KOHN, D. B., HEATH, J. R., GLASPY, J. A., WITTE, O. N., BALTIMORE, D., ECONOMOU, J. S. & RIBAS, A. 2014. Adoptive transfer of MART-1 T-cell receptor transgenic lymphocytes and dendritic cell vaccination in patients with metastatic melanoma. *Clin Cancer Res,* 20**,** 2457-65.

CHOMARAT, P., BANCHEREAU, J., DAVOUST, J., PALUCKA, A.K., 2000. IL-6 switches the differentiation of monocytes from dendritic cells to macrophages. Nat. Immunol. 1, 510–514. https://doi.org/10.1038/82763

CLARK, W. H., JR., ELDER, D. E., GUERRY, D. T., BRAITMAN, L. E., TROCK, B. J., SCHULTZ, D., SYNNESTVEDT, M. & HALPERN, A. C. 1989. Model predicting survival in stage I melanoma based on tumor progression. *J Natl Cancer Inst,* 81**,** 1893-904.

CLAY, T. M., CUSTER, M. C., SACHS, J., HWU, P., ROSENBERG, S. A. & NISHIMURA, M. I. 1999. Efficient transfer of a tumor antigen-reactive TCR to human peripheral blood lymphocytes confers anti-tumor reactivity. *J Immunol,* 163**,** 507-13.

CLEMENTE, C. G., MIHM, M. C., JR., BUFALINO, R., ZURRIDA, S., COLLINI, P. & CASCINELLI, N. 1996. Prognostic value of tumor infiltrating lymphocytes in the vertical growth phase of primary cutaneous melanoma. *Cancer,* 77**,** 1303-10.

COHEN, N., SHANI, O., RAZ, Y., SHARON, Y., HOFFMAN, D., ABRAMOVITZ, L., EREZ, N., 2017. Fibroblasts drive an immunosuppressive and growth-promoting microenvironment in breast cancer via secretion of Chitinase 3-like 1. Oncogene 36, 4457–4468. https://doi.org/10.1038/onc.2017.65

COLE, D. J., WEIL, D. P., SHILYANSKY, J., CUSTER, M., KAWAKAMI, Y., ROSENBERG, S. A. & NISHIMURA, M. I. 1995. Characterization of the functional specificity of a cloned T-cell receptor heterodimer recognizing the MART-1 melanoma antigen. *Cancer Res,* 55**,** 748-52.

COLEY, W. B. 1891. II. Contribution to the Knowledge of Sarcoma. *Ann Surg,* 14**,** 199-220.

COLEY, W. B. 1893. The treatment of malignant tumors by repeated inoculations of erysipelas. With a report of ten original cases. 1893. *Am J Med Sci,* 105**,** 487-511.

CONNOR, J. P., CRISTEA, M. C., LEWIS, N. L., LEWIS, L. D., KOMARNITSKY, P. B., MATTIACCI, M. R., FELDER, M., STEWART, S., HARTER, J., HENSLEE-DOWNEY, J., KRAMER, D., NEUGEBAUER, R. & STUPP, R. 2013. A phase 1b study of humanized KS-interleukin-2 (huKS-IL2) immunocytokine with cyclophosphamide in patients with EpCAM-positive advanced solid tumors. *BMC Cancer,* 13**,** 20.

CONTICELLO, C., PEDINI, F., ZEUNER, A., PATTI, M., ZERILLI, M., STASSI, G., MESSINA, A., PESCHLE, C. & DE MARIA, R. 2004. IL-4 Protects Tumor Cells from Anti-CD95 and Chemotherapeutic Agents via Up-Regulation of Antiapoptotic Proteins. *The Journal of Immunology,* 172**,** 5467-5477.

CRADDOCK, J. A., LU, A., BEAR, A., PULE, M., BRENNER, M. K., ROONEY, C. M. & FOSTER, A. E. 2010. Enhanced tumor trafficking of GD2 chimeric antigen receptor T cells by expression of the chemokine receptor CCR2b. *J Immunother,* 33**,** 780-8.

CROSS, A. H., GIRARD, T. J., GIACOLETTO, K. S., EVANS, R. J., KEELING, R. M., LIN, R. F., TROTTER, J. L. & KARR, R. W. 1995. Long-term inhibition of murine experimental autoimmune encephalomyelitis using CTLA-4-Fc supports a key role for CD28 costimulation. *J Clin Invest,* 95**,** 2783-9.

CULIG, Z., HOBISCH, A., CRONAUER, M. V., RADMAYR, C., TRAPMAN, J., HITTMAIR, A., BARTSCH, G. & KLOCKER, H. 1994. Androgen receptor activation in prostatic tumor cell lines by insulin-like growth factor-I, keratinocyte growth factor, and epidermal growth factor. *Cancer Res,* 54**,** 5474-8.

CURRAN, K. J., SEINSTRA, B. A., NIKHAMIN, Y., YEH, R., USACHENKO, Y., VAN LEEUWEN, D. G., PURDON, T., PEGRAM, H. J. & BRENTJENS, R. J.

2015. Enhancing antitumor efficacy of chimeric antigen receptor T cells through constitutive CD40L expression. *Mol Ther,* 23**,** 769-78.

DA SILVA, P. F. L., OGRODNIK, M., KUCHERYAVENKO, O., GLIBERT, J., MIWA, S., CAMERON, K., ISHAQ, A., SARETZKI, G., NAGARAJA-GRELLSCHEID, S., NELSON, G. & VON ZGLINICKI, T. 2019. The bystander effect contributes to the accumulation of senescent cells in vivo. *Aging Cell,* 18**,** e12848.

DAKHOVA, O., ROWLEY, D. & ITTMANN, M. 2014. Genes upregulated in prostate cancer reactive stroma promote prostate cancer progression in vivo. *Clin Cancer Res,* 20**,** 100-9.

DANIELLI, R., PATUZZO, R., DI GIACOMO, A. M., GALLINO, G., MAURICHI, A., DI FLORIO, A., CUTAIA, O., LAZZERI, A., FAZIO, C., MIRACCO, C., GIOVANNONI, L., ELIA, G., NERI, D., MAIO, M. & SANTINAMI, M. 2015. Intralesional administration of L19-IL2/L19-TNF in stage III or stage IVM1a melanoma patients: results of a phase II study. *Cancer Immunol Immunother,* 64**,** 999-1009.

DARCY, P. K., KERSHAW, M. H., TRAPANI, J. A. & SMYTH, M. J. 1998. Expression in cytotoxic T lymphocytes of a single-chain anti-carcinoembryonic antigen antibody. Redirected Fas ligand-mediated lysis of colon carcinoma. *Eur J Immunol,* 28**,** 1663-72.

DELITTO, D., PHAM, K., VLADA, A. C., SAROSI, G. A., THOMAS, R. M., BEHRNS, K. E., LIU, C., HUGHES, S. J., WALLET, S. M. & TREVINO, J. G. 2015. Patient-derived xenograft models for pancreatic adenocarcinoma demonstrate retention of tumor morphology through incorporation of murine stromal elements. *Am J Pathol,* 185**,** 1297-303.

DENG, Z., WU, Y., MA, W., ZHANG, S. & ZHANG, Y. Q. 2015. Adoptive T-cell therapy of prostate cancer targeting the cancer stem cell antigen EpCAM. *BMC Immunol,* 16**,** 1.

DI STASI, A., TEY, S. K., DOTTI, G., FUJITA, Y., KENNEDY-NASSER, A., MARTINEZ, C., STRAATHOF, K., LIU, E., DURETT, A. G., GRILLEY, B., LIU, H., CRUZ, C. R., SAVOLDO, B., GEE, A. P., SCHINDLER, J., KRANCE, R. A., HESLOP, H. E., SPENCER, D. M., ROONEY, C. M. & BRENNER, M. K. 2011. Inducible apoptosis as a safety switch for adoptive cell therapy. *N Engl J Med,* 365**,** 1673-83.

DIGHE, A. S., RICHARDS, E., OLD, L. J. & SCHREIBER, R. D. 1994. Enhanced in vivo growth and resistance to rejection of tumor cells expressing dominant negative IFN gamma receptors. *Immunity,* 1**,** 447-56.

DILLARD, P., KOKSAL, H., INDERBERG, E. M. & WALCHLI, S. 2018. A Spheroid Killing Assay by CAR T Cells. *J Vis Exp*.

DISPENZIERI, A., TONG, C., LAPLANT, B., LACY, M. Q., LAUMANN, K., DINGLI, D., ZHOU, Y., FEDERSPIEL, M. J., GERTZ, M. A., HAYMAN, S., BUADI, F., O'CONNOR, M., LOWE, V. J., PENG, K. W. & RUSSELL, S. J. 2017. Phase I trial of systemic administration of Edmonston strain of measles virus genetically engineered to express the sodium iodide symporter in patients with recurrent or refractory multiple myeloma. *Leukemia,* 31**,** 2791-2798.

DOAN, A. & PULSIPHER, M. A. 2018. Hypogammaglobulinemia due to CAR T-cell therapy. *Pediatr Blood Cancer,* 65.

DONG, H., STROME, S. E., SALOMAO, D. R., TAMURA, H., HIRANO, F., FLIES, D. B., ROCHE, P. C., LU, J., ZHU, G., TAMADA, K., LENNON, V. A., CELIS, E. & CHEN, L. 2002. Tumor-associated B7-H1 promotes T-cell apoptosis: a potential mechanism of immune evasion. *Nat Med,* 8**,** 793-800.

DREICER, R., JONES, R., OUDARD, S., EFSTATHIOU, E., SAAD, F., WIT, R. D., BONO, J. S. D., SHI, Y., TEJURA, B., AGUS, D. B., BORGSTEIN, N. G., BELLMUNT, J. & FIZAZI, K. 2014. Results from a phase 3, randomized, double-blind, multicenter, placebo-controlled trial of orteronel (TAK-700) plus prednisone in patients with metastatic castration-resistant prostate cancer (mCRPC) that has progressed during or following docetaxel-based therapy (ELM-PC 5 trial). *Journal of Clinical Oncology,* 32**,** 7-7.

DUBLIN, E. A., BARNES, D. M., WANG, D. Y., KING, R. J. & LEVISON, D. A. 1993. TGF alpha and TGF beta expression in mammary carcinoma. *J Pathol,* 170**,** 15-22.

DUDLEY, M. E., WUNDERLICH, J. R., ROBBINS, P. F., YANG, J. C., HWU, P., SCHWARTZENTRUBER, D. J., TOPALIAN, S. L., SHERRY, R., RESTIFO, N. P., HUBICKI, A. M., ROBINSON, M. R., RAFFELD, M., DURAY, P., SEIPP, C. A., ROGERS-FREEZER, L., MORTON, K. E., MAVROUKAKIS, S. A., WHITE, D. E. & ROSENBERG, S. A. 2002. Cancer regression and autoimmunity in patients after clonal repopulation with antitumor lymphocytes. *Science,* 298**,** 850-4.

DUNN, G. P., BRUCE, A. T., IKEDA, H., OLD, L. J. & SCHREIBER, R. D. 2002. Cancer immunoediting: from immunosurveillance to tumor escape. *Nat Immunol,* 3**,** 991-8.

DWYER, C. J., KNOCHELMANN, H. M., SMITH, A. S., WYATT, M. M., RANGEL RIVERA, G. O., ARHONTOULIS, D. C., BARTEE, E., LI, Z., RUBINSTEIN, M. P. & PAULOS, C. M. 2019. Fueling Cancer Immunotherapy With Common Gamma Chain Cytokines. *Front Immunol,* 10**,** 263.

EBBELL, B. 1937. *The Papyrus Ebers: the greatest Egyptian medical document*, Levin & Munksgaard.

EGUCHI, J., HIROISHI, K., ISHII, S., BABA, T., MATSUMURA, T., HIRAIDE, A., OKADA, H. & IMAWARI, M. 2005. Interleukin-4 gene transduced tumor cells promote a potent tumor-specific Th1-type response in cooperation with interferon-alpha transduction. *Gene Ther,* 12**,** 733-41.

EIGENTLER, T. K., WEIDE, B., DE BRAUD, F., SPITALERI, G., ROMANINI, A., PFLUGFELDER, A., GONZALEZ-IGLESIAS, R., TASCIOTTI, A., GIOVANNONI, L., SCHWAGER, K., LOVATO, V., KASPAR, M., TRACHSEL, E., MENSSEN, H. D., NERI, D. & GARBE, C. 2011. A dose-escalation and signal-generating study of the immunocytokine L19-IL2 in combination with dacarbazine for the therapy of patients with metastatic melanoma. *Clin Cancer Res,* 17**,** 7732-42.

EMAMI-SHAHRI, N., FOSTER, J., KASHANI, R., GAZINSKA, P., COOK, C., SOSABOWSKI, J., MAHER, J. & PAPA, S. 2018. Clinically compliant spatial and temporal imaging of chimeric antigen receptor T-cells. *Nat Commun,* 9**,** 1081.

ENBLAD, G., KARLSSON, H., GAMMELGARD, G., WENTHE, J., LOVGREN, T., AMINI, R. M., WIKSTROM, K. I., ESSAND, M., SAVOLDO, B., HALLBOOK, H., HOGLUND, M., DOTTI, G., BRENNER, M. K., HAGBERG, H. & LOSKOG, A. 2018. A Phase I/IIa Trial Using CD19-Targeted Third-Generation CAR T Cells for Lymphoma and Leukemia. *Clin Cancer Res,* 24**,** 6185-6194.

ENGEL, J., BASTIAN, P. J., BAUR, H., BEER, V., CHAUSSY, C., GSCHWEND, J. E., OBERNEDER, R., ROTHENBERGER, K. H., STIEF, C. G. & HOLZEL, D. 2010. Survival benefit of radical prostatectomy in lymph node-positive patients with prostate cancer. *Eur Urol,* 57**,** 754-61.

EPSTEIN, J. I., EGEVAD, L., AMIN, M. B., DELAHUNT, B., SRIGLEY, J. R. & HUMPHREY, P. A. 2016. The 2014 International Society of Urological Pathology (ISUP) Consensus Conference on Gleason Grading of Prostatic

Carcinoma: Definition of Grading Patterns and Proposal for a New Grading System. *Am J Surg Pathol,* 40**,** 244-52.

EPSTEIN, N. A. & FATTI, L. P. 1976. Prostatic carcinoma: some morphological features affecting prognosis. *Cancer,* 37**,** 2455-65.

ERARD, F., WILD, M. T., GARCIA-SANZ, J. A. & LE GROS, G. 1993. Switch of CD8 T cells to noncytolytic CD8-CD4- cells that make TH2 cytokines and help B cells. *Science,* 260**,** 1802-5.

ERDOGAN, B., AO, M., WHITE, L.M., MEANS, A.L., BREWER, B.M., YANG, L., WASHINGTON, M.K., SHI, C., FRANCO, O.E., WEAVER, A.M., HAYWARD, S.W., LI, D., WEBB, D.J., 2017. Cancer-associated fibroblasts promote directional cancer cell migration by aligning fibronectin. United States.

ESHHAR, Z. & GROSS, G. 1990. Chimeric T cell receptor which incorporates the anti-tumour specificity of a monoclonal antibody with the cytolytic activity of T cells: a model system for immunotherapeutical approach. *Br J Cancer Suppl,* 10**,** 27-9.

ESHHAR, Z., WAKS, T., GROSS, G. & SCHINDLER, D. G. 1993. Specific activation and targeting of cytotoxic lymphocytes through chimeric single chains consisting of antibody-binding domains and the gamma or zeta subunits of the immunoglobulin and T-cell receptors. *Proc Natl Acad Sci U S A,* 90**,** 720-4.

ESWARAKA, J., GIDDABASAPPA, A., HAN, G., LALWANI, K., EISELE, K., FENG, Z., AFFOLTER, T., CHRISTENSEN, J. & LI, G. 2014. Axitinib and crizotinib combination therapy inhibits bone loss in a mouse model of castration resistant prostate cancer. *BMC Cancer,* 14**,** 742.

FAHMY, O., KHAIRUL-ASRI, M. G., HADI, S., GAKIS, G. & STENZL, A. 2017. The Role of Radical Prostatectomy and Radiotherapy in Treatment of Locally Advanced Prostate Cancer: A Systematic Review and Meta-Analysis. *Urol Int,* 99**,** 249-256.

FARASSATI, F., YANG, A. D. & LEE, P. W. 2001. Oncogenes in Ras signalling pathway dictate host-cell permissiveness to herpes simplex virus 1. *Nat Cell Biol,* 3**,** 745-50.

FEDOROV, V. D., THEMELI, M. & SADELAIN, M. 2013. PD-1- and CTLA-4-based inhibitory chimeric antigen receptors (iCARs) divert off-target immunotherapy responses. *Sci Transl Med,* 5**,** 215ra172.

FELDMAN, S. A., ASSADIPOUR, Y., KRILEY, I., GOFF, S. L. & ROSENBERG, S. A. 2015. Adoptive Cell Therapy--Tumor-Infiltrating Lymphocytes, T-Cell Receptors, and Chimeric Antigen Receptors. *Semin Oncol,* 42**,** 626-39.

FELDMANN, A., ARNDT, C., BERGMANN, R., LOFF, S., CARTELLIERI, M., BACHMANN, D., ALIPERTA, R., HETZENECKER, M., LUDWIG, F., ALBERT, S., ZILLER-WALTER, P., KEGLER, A., KORISTKA, S., GARTNER, S., SCHMITZ, M., EHNINGER, A., EHNINGER, G., PIETZSCH, J., STEINBACH, J. & BACHMANN, M. 2017. Retargeting of T lymphocytes to PSCA- or PSMA positive prostate cancer cells using the novel modular chimeric antigen receptor platform technology "UniCAR". *Oncotarget,* 8**,** 31368-31385.

FINNEY, H. M., AKBAR, A. N. & LAWSON, A. D. 2004. Activation of resting human primary T cells with chimeric receptors: costimulation from CD28, inducible costimulator, CD134, and CD137 in series with signals from the TCR zeta chain. *J Immunol,* 172**,** 104-13.

FINNEY, H. M., LAWSON, A. D., BEBBINGTON, C. R. & WEIR, A. N. 1998. Chimeric receptors providing both primary and costimulatory signaling in T cells from a single gene product. *J Immunol,* 161**,** 2791-7.

FISCHER, E., CHAITANYA, K., WUEST, T., WADLE, A., SCOTT, A. M., VAN DEN BROEK, M., SCHIBLI, R., BAUER, S. & RENNER, C. 2012.

Radioimmunotherapy of fibroblast activation protein positive tumors by rapidly internalizing antibodies. *Clin Cancer Res,* 18**,** 6208-18.

FORSTER-HORVATH, C., BOCSI, J., RASO, E., ORBAN, T. I., OLAH, E., TIMAR, J. & LADANYI, A. 2001. Constitutive intracellular expression and activation-induced cell surface up-regulation of CD44v3 in human T lymphocytes. *Eur J Immunol,* 31**,** 600-8.

FOSSA, S. D., WIKLUND, F., KLEPP, O., ANGELSEN, A., SOLBERG, A., DAMBER, J. E., HOYER, M. & WIDMARK, A. 2016. Ten- and 15-yr Prostate Cancer-specific Mortality in Patients with Nonmetastatic Locally Advanced or Aggressive Intermediate Prostate Cancer, Randomized to Lifelong Endocrine Treatment Alone or Combined with Radiotherapy: Final Results of The Scandinavian Prostate Cancer Group-7. *Eur Urol,* 70**,** 684-691.

FRAIETTA, J. A., BECKWITH, K. A., PATEL, P. R., RUELLA, M., ZHENG, Z., BARRETT, D. M., LACEY, S. F., MELENHORST, J. J., MCGETTIGAN, S. E., COOK, D. R., ZHANG, C., XU, J., DO, P., HULITT, J., KUDCHODKAR, S. B., COGDILL, A. P., GILL, S., PORTER, D. L., WOYACH, J. A., LONG, M., JOHNSON, A. J., MADDOCKS, K., MUTHUSAMY, N., LEVINE, B. L., JUNE, C. H., BYRD, J. C. & MAUS, M. V. 2016. Ibrutinib enhances chimeric antigen receptor T-cell engraftment and efficacy in leukemia. *Blood,* 127**,** 1117-27.

FRANCINI, E., GRAY, K. P., SHAW, G. K., EVAN, C. P., HAMID, A. A., PERRY, C. E., KANTOFF, P. W., TAPLIN, M. E. & SWEENEY, C. J. 2019. Impact of new systemic therapies on overall survival of patients with metastatic castration-resistant prostate cancer in a hospital-based registry. *Prostate Cancer Prostatic Dis*.

FREEMAN, A. I., ZAKAY-RONES, Z., GOMORI, J. M., LINETSKY, E., RASOOLY, L., GREENBAUM, E., ROZENMAN-YAIR, S., PANET, A., LIBSON, E., IRVING, C. S., GALUN, E. & SIEGAL, T. 2006. Phase I/II trial of intravenous NDV-HUJ oncolytic virus in recurrent glioblastoma multiforme. *Mol Ther,* 13**,** 221-8.

FREEMAN, G. J., LONG, A. J., IWAI, Y., BOURQUE, K., CHERNOVA, T., NISHIMURA, H., FITZ, L. J., MALENKOVICH, N., OKAZAKI, T., BYRNE, M. C., HORTON, H. F., FOUSER, L., CARTER, L., LING, V., BOWMAN, M. R., CARRENO, B. M., COLLINS, M., WOOD, C. R. & HONJO, T. 2000. Engagement of the PD-1 immunoinhibitory receptor by a novel B7 family member leads to negative regulation of lymphocyte activation. *J Exp Med,* 192**,** 1027-34.

FREY, N. V., SHAW, P. A., HEXNER, E. O., GILL, S., MARCUCCI, K., LUGER, S. M., MANGAN, J. K., GRUPP, S. A., MAUDE, S. L., ERICSON, S., LEVINE, B., LACEY, S. F., MELENHORST, J. J., JUNE, C. H. & PORTER, D. L. 2016. Optimizing chimeric antigen receptor (CAR) T cell therapy for adult patients with relapsed or refractory (r/r) acute lymphoblastic leukemia (ALL). *Journal of Clinical Oncology,* 34**,** 7002-7002.

FRIESS, H., YAMANAKA, Y., BUCHLER, M., EBERT, M., BEGER, H. G., GOLD, L. I. & KORC, M. 1993. Enhanced expression of transforming growth factor beta isoforms in pancreatic cancer correlates with decreased survival. *Gastroenterology,* 105**,** 1846-56.

FRIGAULT, M. J., LEE, J., BASIL, M. C., CARPENITO, C., MOTOHASHI, S., SCHOLLER, J., KAWALEKAR, O. U., GUEDAN, S., MCGETTIGAN, S. E., POSEY, A. D., JR., ANG, S., COOPER, L. J., PLATT, J. M., JOHNSON, F. B., PAULOS, C. M., ZHAO, Y., KALOS, M., MILONE, M. C. & JUNE, C. H. 2015. Identification of chimeric antigen receptors that mediate constitutive or inducible proliferation of T cells. *Cancer Immunol Res,* 3**,** 356-67.

FRISCH, M., BIGGAR, R. J., ENGELS, E. A. & GOEDERT, J. J. 2001. Association of cancer with AIDS-related immunosuppression in adults. *Jama,* 285**,** 1736-45.

FROELING, F.E.M., FEIG, C., CHELALA, C., DOBSON, R., MEIN, C.E., TUVESON, D.A., CLEVERS, H., HART, I.R., KOCHER, H.M., 2011. Retinoic acid-induced pancreatic stellate cell quiescence reduces paracrine Wnt-beta-catenin signaling to slow tumor progression. Gastroenterology 141, 1486–1497, 1497.e1–14. https://doi.org/10.1053/j.gastro.2011.06.047

GABRILOVICH, D., ISHIDA, T., OYAMA, T., RAN, S., KRAVTSOV, V., NADAF, S., CARBONE, D.P., 1998. Vascular Endothelial Growth Factor Inhibits the Development of Dendritic Cells and Dramatically Affects the Differentiation of Multiple Hematopoietic Lineages In Vivo: Presented in part at the Keystone Symposium "Cellular and Molecular Biology of Dendritic Cells," Santa Fe, NM, March 3-9, 1998, and at the annual meeting of the American Association for Cancer Research, March 28-April 1, 1998. Blood 92, 4150–4166. https://doi.org/10.1182/blood.V92.11.4150

GADE, T. P., HASSEN, W., SANTOS, E., GUNSET, G., SAUDEMONT, A., GONG, M. C., BRENTJENS, R., ZHONG, X. S., STEPHAN, M., STEFANSKI, J., LYDDANE, C., OSBORNE, J. R., BUCHANAN, I. M., HALL, S. J., HESTON, W. D., RIVIERE, I., LARSON, S. M., KOUTCHER, J. A. & SADELAIN, M. 2005. Targeted elimination of prostate cancer by genetically directed human T lymphocytes. *Cancer Res,* 65**,** 9080-8.

GAGGIOLI, C., HOOPER, S., HIDALGO-CARCEDO, C., GROSSE, R., MARSHALL, J.F., HARRINGTON, K., SAHAI, E., 2007. Fibroblast-led collective invasion of carcinoma cells with differing roles for RhoGTPases in leading and following cells. Nat. Cell Biol. 9, 1392–1400. https://doi.org/10.1038/ncb1658

GAO, D., VELA, I., SBONER, A., IAQUINTA, P. J., KARTHAUS, W. R., GOPALAN, A., DOWLING, C., WANJALA, J. N., UNDVALL, E. A., ARORA, V. K., WONGVIPAT, J., KOSSAI, M., RAMAZANOGLU, S., BARBOZA, L. P., DI, W., CAO, Z., ZHANG, Q. F., SIROTA, I., RAN, L., MACDONALD, T. Y., BELTRAN, H., MOSQUERA, J. M., TOUIJER, K. A., SCARDINO, P. T., LAUDONE, V. P., CURTIS, K. R., RATHKOPF, D. E., MORRIS, M. J., DANILA, D. C., SLOVIN, S. F., SOLOMON, S. B., EASTHAM, J. A., CHI, P., CARVER, B., RUBIN, M. A., SCHER, H. I., CLEVERS, H., SAWYERS, C. L. & CHEN, Y. 2014a. Organoid cultures derived from patients with advanced prostate cancer. *Cell,* 159**,** 176-187.

GAO, J., WU, Y., SU, Z., AMOAH BARNIE, P., JIAO, Z., BIE, Q., LU, L., WANG, S. & XU, H. 2014b. Infiltration of alternatively activated macrophages in cancer tissue is associated with MDSC and Th2 polarization in patients with esophageal cancer. *PLoS One,* 9**,** e104453.

GARCIA-CARBONERO, R., SALAZAR, R., DURAN, I., OSMAN-GARCIA, I., PAZ-ARES, L., BOZADA, J. M., BONI, V., BLANC, C., SEYMOUR, L., BEADLE, J., ALVIS, S., CHAMPION, B., CALVO, E. & FISHER, K. 2017. Phase 1 study of intravenous administration of the chimeric adenovirus enadenotucirev in patients undergoing primary tumor resection. *J Immunother Cancer,* 5**,** 71.

GARGETT, T. & BROWN, M. P. 2015. Different cytokine and stimulation conditions influence the expansion and immune phenotype of third-generation chimeric antigen receptor T cells specific for tumor antigen GD2. *Cytotherapy,* 17**,** 487-95.

GARIN-CHESA, P., OLD, L. J. & RETTIG, W. J. 1990. Cell surface glycoprotein of reactive stromal fibroblasts as a potential antibody target in human epithelial cancers. *Proc Natl Acad Sci U S A,* 87**,** 7235-9.

GARRIDO, F., RUIZ-CABELLO, F., CABRERA, T., PEREZ-VILLAR, J. J., LOPEZ-BOTET, M., DUGGAN-KEEN, M. & STERN, P. L. 1997. Implications for immunosurveillance of altered HLA class I phenotypes in human tumours. *Immunol Today,* 18**,** 89-95.

GASSER, S., CORTHESY, P., BEERMAN, F., MACDONALD, H. R. & NABHOLZ, M. 2000. Constitutive Expression of a Chimeric Receptor That Delivers IL-2/IL-15 Signals Allows Antigen-Independent Proliferation of CD8+CD44high But Not Other T Cells. *The Journal of Immunology,* 164**,** 5659-5667.

GASSER, S., LIM, L. H. K. & CHEUNG, F. S. G. 2017. The role of the tumour microenvironment in immunotherapy. *Endocr Relat Cancer,* 24**,** T283-t295.

GATTINONI, L., FINKELSTEIN, S. E., KLEBANOFF, C. A., ANTONY, P. A., PALMER, D. C., SPIESS, P. J., HWANG, L. N., YU, Z., WRZESINSKI, C., HEIMANN, D. M., SURH, C. D., ROSENBERG, S. A. & RESTIFO, N. P. 2005. Removal of homeostatic cytokine sinks by lymphodepletion enhances the efficacy of adoptively transferred tumor-specific CD8+ T cells. *J Exp Med,* 202**,** 907-12.

GHASSEMI, S., NUNEZ-CRUZ, S., O'CONNOR, R. S., FRAIETTA, J. A., PATEL, P. R., SCHOLLER, J., BARRETT, D. M., LUNDH, S. M., DAVIS, M. M., BEDOYA, F., ZHANG, C., LEFEROVICH, J., LACEY, S. F., LEVINE, B. L., GRUPP, S. A., JUNE, C. H., MELENHORST, J. J. & MILONE, M. C. 2018. Reducing Ex Vivo Culture Improves the Antileukemic Activity of Chimeric Antigen Receptor (CAR) T Cells. *Cancer Immunol Res,* 6**,** 1100-1109.

GILLEECE, M. H., SCARFFE, J. H., GHOSH, A., HEYWORTH, C. M., BONNEM, E., TESTA, N., STERN, P. & DEXTER, T. M. 1992. Recombinant human interleukin 4 (IL-4) given as daily subcutaneous injections--a phase I dose toxicity trial. *Br J Cancer,* 66**,** 204-10.

GILLESSEN, S., GNAD-VOGT, U. S., GALLERANI, E., BECK, J., SESSA, C., OMLIN, A., MATTIACCI, M. R., LIEDERT, B., KRAMER, D., LAURENT, J., SPEISER, D. E. & STUPP, R. 2013. A phase I dose-escalation study of the immunocytokine EMD 521873 (Selectikine) in patients with advanced solid tumours. *Eur J Cancer,* 49**,** 35-44.

GILLIS, S. & SMITH, K. A. 1977. Long term culture of tumour-specific cytotoxic T cells. *Nature,* 268**,** 154-6.

GLADKOV, O., RAMLAU, R., SERWATOWSKI, P., MILANOWSKI, J., TOMECZKO, J., KOMARNITSKY, P. B., KRAMER, D. & KRZAKOWSKI, M. J. 2015. Cyclophosphamide and tucotuzumab (huKS-IL2) following first-line chemotherapy in responding patients with extensive-disease small-cell lung cancer. *Anti-Cancer Drugs,* 26**,** 1061-1068.

GLEASON, D. F. 1966. Classification of prostatic carcinomas. *Cancer Chemother Rep,* 50**,** 125-8.

GOBIN, E., BAGWELL, K., WAGNER, J., MYSONA, D., SANDIRASEGARANE, S., SMITH, N., BAI, S., SHARMA, A., SCHLEIFER, R. & SHE, J. X. 2019. A pan-cancer perspective of matrix metalloproteases (MMP) gene expression profile and their diagnostic/prognostic potential. *BMC Cancer,* 19**,** 581.

GOCHEVA, V., WANG, H. W., GADEA, B. B., SHREE, T., HUNTER, K. E., GARFALL, A. L., BERMAN, T. & JOYCE, J. A. 2010. IL-4 induces cathepsin protease activity in tumor-associated macrophages to promote cancer growth and invasion. *Genes Dev,* 24**,** 241-55.

GOLDMAN, B. & DEFRANCESCO, L. 2009. The cancer vaccine roller coaster. *Nat Biotechnol,* 27**,** 129-39.

GOLDSTEIN, R., HANLEY, C., MORRIS, J., CAHILL, D., CHANDRA, A., HARPER, P., CHOWDHURY, S., MAHER, J. & BURBRIDGE, S. 2011. Clinical

investigation of the role of interleukin-4 and interleukin-13 in the evolution of prostate cancer. *Cancers (Basel),* 3**,** 4281-93.

GOLUMBEK, P. T., LAZENBY, A. J., LEVITSKY, H. I., JAFFEE, L. M., KARASUYAMA, H., BAKER, M. & PARDOLL, D. M. 1991. Treatment of established renal cancer by tumor cells engineered to secrete interleukin-4. *Science,* 254**,** 713-6.

GOMES DA SILVA, D., MUKHERJEE, M., SRINIVASAN, M., DAKHOVA, O., LIU, H., GRILLEY, B., GEE, A. P., NEELAPU, S. S., ROONEY, C. M., HESLOP, H. E., SAVOLDO, B., DOTTI, G., BRENNER, M. K., MAMONKIN, M. & RAMOS, C. A. 2016. Direct Comparison of In Vivo Fate of Second and Third-Generation CD19-Specific Chimeric Antigen Receptor (CAR)-T Cells in Patients with B-Cell Lymphoma: Reversal of Toxicity from Tonic Signaling. *Blood,* 128**,** 1851-1851.

GONG, M. C., LATOUCHE, J. B., KRAUSE, A., HESTON, W. D., BANDER, N. H. & SADELAIN, M. 1999. Cancer patient T cells genetically targeted to prostate-specific membrane antigen specifically lyse prostate cancer cells and release cytokines in response to prostate-specific membrane antigen. *Neoplasia,* 1**,** 123-7.

GOOCH, J. L., CHRISTY, B. & YEE, D. 2002. STAT6 mediates interleukin-4 growth inhibition in human breast cancer cells. *Neoplasia,* 4**,** 324-31.

GOVERMAN, J., GOMEZ, S. M., SEGESMAN, K. D., HUNKAPILLER, T., LAUG, W. E. & HOOD, L. 1990. Chimeric immunoglobulin-T cell receptor proteins form functional receptors: implications for T cell receptor complex formation and activation. *Cell,* 60**,** 929-39.

GROSS, G. & ESHHAR, Z. 1992. Endowing T cells with antibody specificity using chimeric T cell receptors. *Faseb j,* 6**,** 3370-8.

GROSS, G., WAKS, T. & ESHHAR, Z. 1989. Expression of immunoglobulin-T-cell receptor chimeric molecules as functional receptors with antibody-type specificity. *Proc Natl Acad Sci U S A,* 86**,** 10024-8.

GROZESCU, T. & POPA, F. 2017. Prostate cancer between prognosis and adequate/proper therapy. *J Med Life,* 10**,** 5-12.

GRUPP, S. A., KALOS, M., BARRETT, D., APLENC, R., PORTER, D. L., RHEINGOLD, S. R., TEACHEY, D. T., CHEW, A., HAUCK, B., WRIGHT, J. F., MILONE, M. C., LEVINE, B. L. & JUNE, C. H. 2013. Chimeric antigen receptor-modified T cells for acute lymphoid leukemia. *N Engl J Med,* 368**,** 1509-1518.

GUEDAN, S., CHEN, X., MADAR, A., CARPENITO, C., MCGETTIGAN, S. E., FRIGAULT, M. J., LEE, J., POSEY, A. D., JR., SCHOLLER, J., SCHOLLER, N., BONNEAU, R. & JUNE, C. H. 2014. ICOS-based chimeric antigen receptors program bipolar TH17/TH1 cells. *Blood,* 124**,** 1070-80.

GUEDAN, S., POSEY, A. D., JR., SHAW, C., WING, A., DA, T., PATEL, P. R., MCGETTIGAN, S. E., CASADO-MEDRANO, V., KAWALEKAR, O. U., URIBE-HERRANZ, M., SONG, D., MELENHORST, J. J., LACEY, S. F., SCHOLLER, J., KEITH, B., YOUNG, R. M. & JUNE, C. H. 2018. Enhancing CAR T cell persistence through ICOS and 4-1BB costimulation. *JCI Insight,* 3.

GUERRERO-JUAREZ, C.F., DEDHIA, P.H., JIN, S., RUIZ-VEGA, R., MA, D., LIU, Y., YAMAGA, K., SHESTOVA, O., GAY, D.L., YANG, Z., KESSENBROCK, K., NIE, Q., PEAR, W.S., COTSARELIS, G., PLIKUS, M.V., 2019. Single-cell analysis reveals fibroblast heterogeneity and myeloid-derived adipocyte progenitors in murine skin wounds. Nat. Commun. 10, 650. https://doi.org/10.1038/s41467-018-08247-x

HA, S., OU, Y., VLASAK, J., LI, Y., WANG, S., VO, K., DU, Y., MACH, A., FANG, Y. & ZHANG, N. 2011. Isolation and characterization of IgG1 with asymmetrical Fc glycosylation. *Glycobiology,* 21**,** 1087-96.

HALABI, S., LIN, C. Y., KELLY, W. K., FIZAZI, K. S., MOUL, J. W., KAPLAN, E. B., MORRIS, M. J. & SMALL, E. J. 2014. Updated prognostic model for predicting overall survival in first-line chemotherapy for patients with metastatic castration-resistant prostate cancer. *J Clin Oncol,* 32**,** 671-7.

HAMDY, F. C., DONOVAN, J. L., LANE, J. A., MASON, M., METCALFE, C., HOLDING, P., DAVIS, M., PETERS, T. J., TURNER, E. L., MARTIN, R. M., OXLEY, J., ROBINSON, M., STAFFURTH, J., WALSH, E., BOLLINA, P., CATTO, J., DOBLE, A., DOHERTY, A., GILLATT, D., KOCKELBERGH, R., KYNASTON, H., PAUL, A., POWELL, P., PRESCOTT, S., ROSARIO, D. J., ROWE, E. & NEAL, D. E. 2016. 10-Year Outcomes after Monitoring, Surgery, or Radiotherapy for Localized Prostate Cancer. *N Engl J Med,* 375**,** 1415-1424.

HANLEY, C.J., MELLONE, M., FORD, K., THIRDBOROUGH, S.M., MELLOWS, T., FRAMPTON, S.J., SMITH, D.M., HARDEN, E., SZYNDRALEWIEZ, C., BULLOCK, M., NOBLE, F., MOUTASIM, K.A., KING, E.V., VIJAYANAND, P., MIRNEZAMI, A.H., UNDERWOOD, T.J., OTTENSMEIER, C.H., THOMAS, G.J., 2018. Targeting the Myofibroblastic Cancer-Associated Fibroblast Phenotype Through Inhibition of NOX4. J. Natl. Cancer Inst. 110. https://doi.org/10.1093/jnci/djx121

HARPER, K., BALZANO, C., ROUVIER, E., MATTEI, M. G., LUCIANI, M. F. & GOLSTEIN, P. 1991. CTLA-4 and CD28 activated lymphocyte molecules are closely related in both mouse and human as to sequence, message expression, gene structure, and chromosomal location. *J Immunol,* 147**,** 1037-44.

HARRIS, D. T., HAGER, M. V., SMITH, S. N., CAI, Q., STONE, J. D., KRUGER, P., LEVER, M., DUSHEK, O., SCHMITT, T. M., GREENBERG, P. D. & KRANZ, D. M. 2018. Comparison of T Cell Activities Mediated by Human TCRs and CARs That Use the Same Recognition Domains. *J Immunol,* 200**,** 1088-1100.

HASSONA, Y., CIRILLO, N., HEESOM, K., PARKINSON, E.K., PRIME, S.S., 2014. Senescent cancer-associated fibroblasts secrete active MMP-2 that promotes keratinocyte dis-cohesion and invasion. Br. J. Cancer 111, 1230–1237. https://doi.org/10.1038/bjc.2014.438

HASSONA, Y., CIRILLO, N., LIM, K.P., HERMAN, A., MELLONE, M., THOMAS, G.J., PITIYAGE, G.N., PARKINSON, E.K., PRIME, S.S., 2013. Progression of genotype-specific oral cancer leads to senescence of cancer-associated fibroblasts and is mediated by oxidative stress and TGF-beta. Carcinogenesis 34, 1286–1295. https://doi.org/10.1093/carcin/bgt035

HAYNES, N. M., SNOOK, M. B., TRAPANI, J. A., CERRUTI, L., JANE, S. M., SMYTH, M. J. & DARCY, P. K. 2001. Redirecting mouse CTL against colon carcinoma: superior signaling efficacy of single-chain variable domain chimeras containing TCR-zeta vs Fc epsilon RI-gamma. *J Immunol,* 166**,** 182-7.

HECZEY, A., LOUIS, C. U., SAVOLDO, B., DAKHOVA, O., DURETT, A., GRILLEY, B., LIU, H., WU, M. F., MEI, Z., GEE, A., MEHTA, B., ZHANG, H., MAHMOOD, N., TASHIRO, H., HESLOP, H. E., DOTTI, G., ROONEY, C. M. & BRENNER, M. K. 2017. CAR T Cells Administered in Combination with Lymphodepletion and PD-1 Inhibition to Patients with Neuroblastoma. *Mol Ther,* 25**,** 2214-2224.

HEIDENREICH, A., BELLMUNT, J., BOLLA, M., JONIAU, S., MASON, M., MATVEEV, V., MOTTET, N., SCHMID, H. P., VAN DER KWAST, T., WIEGEL, T. & ZATTONI, F. 2011. EAU guidelines on prostate cancer. Part 1:

screening, diagnosis, and treatment of clinically localised disease. *Eur Urol,* 59**,** 61-71.

HEISE, C., SAMPSON-JOHANNES, A., WILLIAMS, A., MCCORMICK, F., VON HOFF, D. D. & KIRN, D. H. 1997. ONYX-015, an E1B gene-attenuated adenovirus, causes tumor-specific cytolysis and antitumoral efficacy that can be augmented by standard chemotherapeutic agents. *Nat Med,* 3**,** 639-45.

HEMMERLE, T., DOLL, F. & NERI, D. 2014a. Antibody-based delivery of IL4 to the neovasculature cures mice with arthritis. *Proc Natl Acad Sci U S A,* 111**,** 12008-12.

HEMMERLE, T. & NERI, D. 2014. The antibody-based targeted delivery of interleukin-4 and 12 to the tumor neovasculature eradicates tumors in three mouse models of cancer. *International Journal of Cancer,* 134**,** 467-477.

HEMMERLE, T., ZGRAGGEN, S., MATASCI, M., HALIN, C., DETMAR, M. & NERI, D. 2014b. Antibody-mediated delivery of interleukin 4 to the neovasculature reduces chronic skin inflammation. *J Dermatol Sci,* 76**,** 96-103.

HENRIKSSON, M. L., EDIN, S., DAHLIN, A. M., OLDENBORG, P. A., OBERG, A., VAN GUELPEN, B., RUTEGARD, J., STENLING, R. & PALMQVIST, R. 2011. Colorectal cancer cells activate adjacent fibroblasts resulting in FGF1/FGFR3 signaling and increased invasion. *Am J Pathol,* 178**,** 1387-94.

HILLERDAL, V., RAMACHANDRAN, M., LEJA, J. & ESSAND, M. 2014. Systemic treatment with CAR-engineered T cells against PSCA delays subcutaneous tumor growth and prolongs survival of mice. *BMC Cancer,* 14**,** 30.

HODI, F. S., O'DAY, S. J., MCDERMOTT, D. F., WEBER, R. W., SOSMAN, J. A., HAANEN, J. B., GONZALEZ, R., ROBERT, C., SCHADENDORF, D., HASSEL, J. C., AKERLEY, W., VAN DEN EERTWEGH, A. J., LUTZKY, J., LORIGAN, P., VAUBEL, J. M., LINETTE, G. P., HOGG, D., OTTENSMEIER, C. H., LEBBE, C., PESCHEL, C., QUIRT, I., CLARK, J. I., WOLCHOK, J. D., WEBER, J. S., TIAN, J., YELLIN, M. J., NICHOL, G. M., HOOS, A. & URBA, W. J. 2010. Improved survival with ipilimumab in patients with metastatic melanoma. *N Engl J Med,* 363**,** 711-23.

HODKINSON, P.S., ELLIOTT, T., WONG, W.S., RINTOUL, R.C., MACKINNON, A.C., HASLETT, C., SETHI, T., 2006. ECM overrides DNA damage-induced cell cycle arrest and apoptosis in small-cell lung cancer cells through beta1 integrin-dependent activation of PI3-kinase. Cell Death Differ. 13, 1776–1788. https://doi.org/10.1038/sj.cdd.4401849

HOFHEINZ, R. D., AL-BATRAN, S. E., HARTMANN, F., HARTUNG, G., JAGER, D., RENNER, C., TANSWELL, P., KUNZ, U., AMELSBERG, A., KUTHAN, H. & STEHLE, G. 2003. Stromal antigen targeting by a humanised monoclonal antibody: an early phase II trial of sibrotuzumab in patients with metastatic colorectal cancer. *Onkologie,* 26**,** 44-8.

HOMBACH, A., HEUSER, C., SIRCAR, R., TILLMANN, T., DIEHL, V., KRUIS, W., POHL, C. & ABKEN, H. 1997. T cell targeting of TAG72+ tumor cells by a chimeric receptor with antibody-like specificity for a carbohydrate epitope. *Gastroenterology,* 113**,** 1163-70.

HOMBACH, A. A., RAPPL, G. & ABKEN, H. 2013. Arming cytokine-induced killer cells with chimeric antigen receptors: CD28 outperforms combined CD28-OX40 "super-stimulation". *Mol Ther,* 21**,** 2268-77.

HONEGGER, A. 2008. Engineering antibodies for stability and efficient folding. *Handb Exp Pharmacol***,** 47-68.

HOOPER, J. A. 2015. The history and evolution of immunoglobulin products and their clinical indications. *LymphoSign Journal,* 2**,** 181-194.

HOROSZEWICZ, J. S., KAWINSKI, E. & MURPHY, G. P. 1987. Monoclonal antibodies to a new antigenic marker in epithelial prostatic cells and serum of prostatic cancer patients. *Anticancer Res,* 7**,** 927-35.

HOWLADER, N., NOONE, A. M., KRAPCHO, M., MILLER, D., BREST, A., YU, M., RUHL, J., TATALOVICH, Z., MARIOTTO, A., LEWIS, D. R., CHEN, H. S., FEUER, E. J. & CRONIN, K. A. E. 2019. SEER Cancer Statistics Review, 1975-2016, National Cancer Institute. Bethesda, MD, https://seer.cancer.gov/csr/1975_2016/, based on November 2018 SEER data submission, posted to the SEER web site, April 2019.

HOYOS, V., SAVOLDO, B., QUINTARELLI, C., MAHENDRAVADA, A., ZHANG, M., VERA, J., HESLOP, H. E., ROONEY, C. M., BRENNER, M. K. & DOTTI, G. 2010. Engineering CD19-specific T lymphocytes with interleukin-15 and a suicide gene to enhance their anti-lymphoma/leukemia effects and safety. *Leukemia,* 24**,** 1160-70.

HSU, Y.-L., HUNG, J.-Y., CHIANG, S.-Y., JIAN, S.-F., WU, C.-Y., LIN, Y.-S., TSAI, Y.-M., CHOU, S.-H., TSAI, M.-J., KUO, P.-L., 2016. Lung cancer-derived galectin-1 contributes to cancer associated fibroblast-mediated cancer progression and immune suppression through TDO2/kynurenine axis. Oncotarget 7, 27584–27598. https://doi.org/10.18632/oncotarget.8488

HUDSON, B. D., HUM, N. R., THOMAS, C. B., KOHLGRUBER, A., SEBASTIAN, A., COLLETTE, N. M., COLEMAN, M. A., CHRISTIANSEN, B. A. & LOOTS, G. G. 2015. SOST Inhibits Prostate Cancer Invasion. *PLoS One,* 10**,** e0142058.

HUGGINS, C. 1967. Endocrine-induced regression of cancers. *Cancer Res,* 27**,** 1925-30.

HUGGINS, C. & HODGES, C. V. 1941. Studies on Prostatic Cancer. I. The Effect of Castration, of Estrogen and of Androgen Injection on Serum Phosphatases in Metastatic Carcinoma of the Prostate. *Cancer Research,* 1**,** 293-297.

HUGHES, M. S., YU, Y. Y., DUDLEY, M. E., ZHENG, Z., ROBBINS, P. F., LI, Y., WUNDERLICH, J., HAWLEY, R. G., MOAYERI, M., ROSENBERG, S. A. & MORGAN, R. A. 2005. Transfer of a TCR gene derived from a patient with a marked antitumor response conveys highly active T-cell effector functions. *Hum Gene Ther,* 16**,** 457-72.

HWU, P., SHAFER, G. E., TREISMAN, J., SCHINDLER, D. G., GROSS, G., COWHERD, R., ROSENBERG, S. A. & ESHHAR, Z. 1993. Lysis of ovarian cancer cells by human lymphocytes redirected with a chimeric gene composed of an antibody variable region and the Fc receptor gamma chain. *J Exp Med,* 178**,** 361-6.

HWU, P., YANG, J. C., COWHERD, R., TREISMAN, J., SHAFER, G. E., ESHHAR, Z. & ROSENBERG, S. A. 1995. In vivo antitumor activity of T cells redirected with chimeric antibody/T-cell receptor genes. *Cancer Res,* 55**,** 3369-73.

IMAI, C., MIHARA, K., ANDREANSKY, M., NICHOLSON, I. C., PUI, C. H., GEIGER, T. L. & CAMPANA, D. 2004. Chimeric receptors with 4-1BB signaling capacity provoke potent cytotoxicity against acute lymphoblastic leukemia. *Leukemia,* 18**,** 676-84.

INFANTE, J. R., HANSEN, A. R., PISHVAIAN, M. J., CHOW, L. Q. M., MCARTHUR, G. A., BAUER, T. M., LIU, S. V., SANDHU, S. K., TSAI, F. Y.-C., KIM, J., STEFANICH, E., LI, C.-C., GILBERT, H., MCCALL, B., ANDERSON, M. S., HUSENI, M., RHEE, I. P., SIU, L. L. & GORDON, M. S. 2016. A phase Ib dose escalation study of the OX40 agonist MOXR0916 and the PD-L1 inhibitor atezolizumab in patients with advanced solid tumors. *Journal of Clinical Oncology,* 34**,** 101-101.

INO, Y., YAMAZAKI-ITOH, R., OGURO, S., SHIMADA, K., KOSUGE, T., ZAVADA, J., KANAI, Y., HIRAOKA, N., 2013. Arginase II expressed in cancer-associated fibroblasts indicates tissue hypoxia and predicts poor outcome in patients with pancreatic cancer. PloS One 8, e55146. https://doi.org/10.1371/journal.pone.0055146

ISHIDA, Y., AGATA, Y., SHIBAHARA, K. & HONJO, T. 1992. Induced expression of PD-1, a novel member of the immunoglobulin gene superfamily, upon programmed cell death. *Embo j,* 11**,** 3887-95.

ISRAELI, R. S., POWELL, C. T., CORR, J. G., FAIR, W. R. & HESTON, W. D. 1994. Expression of the prostate-specific membrane antigen. *Cancer Res,* 54**,** 1807-11.

ISRAELI, R. S., POWELL, C. T., FAIR, W. R. & HESTON, W. D. 1993. Molecular cloning of a complementary DNA encoding a prostate-specific membrane antigen. *Cancer Res,* 53**,** 227-30.

IULIUCCI, J. D., OLIVER, S. D., MORLEY, S., WARD, C., WARD, J., DALGARNO, D., CLACKSON, T. & BERGER, H. J. 2001. Intravenous safety and pharmacokinetics of a novel dimerizer drug, AP1903, in healthy volunteers. *J Clin Pharmacol,* 41**,** 870-9.

IWAI, Y., ISHIDA, M., TANAKA, Y., OKAZAKI, T., HONJO, T. & MINATO, N. 2002. Involvement of PD-L1 on tumor cells in the escape from host immune system and tumor immunotherapy by PD-L1 blockade. *Proc Natl Acad Sci U S A,* 99**,** 12293-7.

IZUHARA, K., MIYAJIMA, A. & HARADA, N. 1993. The chimeric receptor between interleukin-2 receptor beta chain and interleukin-4 receptor transduces interleukin-2 signal. *Biochem Biophys Res Commun,* 190**,** 992-1000.

JACOBS, J., DESCHOOLMEESTER, V., ZWAENEPOEL, K., FLIESWASSER, T., DEBEN, C., VAN DEN BOSSCHE, J., HERMANS, C., ROLFO, C., PEETERS, M., DE WEVER, O., LARDON, F., SIOZOPOULOU, V., SMITS, E., PAUWELS, P., 2018. Unveiling a CD70-positive subset of cancer-associated fibroblasts marked by pro-migratory activity and thriving regulatory T cell accumulation. Oncoimmunology 7, e1440167. https://doi.org/10.1080/2162402X.2018.1440167

JAGER, V., BUSSOW, K., WAGNER, A., WEBER, S., HUST, M., FRENZEL, A. & SCHIRRMANN, T. 2013. High level transient production of recombinant antibodies and antibody fusion proteins in HEK293 cells. *BMC Biotechnol,* 13**,** 52.

JAMES, J. R. 2018. Tuning ITAM multiplicity on T cell receptors can control potency and selectivity to ligand density. *Sci Signal,* 11.

JAMES, N. D., PIRRIE, S. J., POPE, A. M., BARTON, D., ANDRONIS, L., GORANITIS, I., COLLINS, S., DAUNTON, A., MCLAREN, D., O'SULLIVAN, J., PARKER, C., PORFIRI, E., STAFFURTH, J., STANLEY, A., WYLIE, J., BEESLEY, S., BIRTLE, A., BROWN, J., CHAKRABORTI, P., HUSSAIN, S., RUSSELL, M. & BILLINGHAM, L. J. 2016a. Clinical Outcomes and Survival Following Treatment of Metastatic Castrate-Refractory Prostate Cancer With Docetaxel Alone or With Strontium-89, Zoledronic Acid, or Both: The TRAPEZE Randomized Clinical Trial. *JAMA Oncol,* 2**,** 493-9.

JAMES, N. D., SYDES, M. R., CLARKE, N. W., MASON, M. D., DEARNALEY, D. P., SPEARS, M. R., RITCHIE, A. W., PARKER, C. C., RUSSELL, J. M., ATTARD, G., DE BONO, J., CROSS, W., JONES, R. J., THALMANN, G., AMOS, C., MATHESON, D., MILLMAN, R., ALZOUEBI, M., BEESLEY, S., BIRTLE, A. J., BROCK, S., CATHOMAS, R., CHAKRABORTI, P., CHOWDHURY, S., COOK, A., ELLIOTT, T., GALE, J., GIBBS, S., GRAHAM,

J. D., HETHERINGTON, J., HUGHES, R., LAING, R., MCKINNA, F., MCLAREN, D. B., O'SULLIVAN, J. M., PARIKH, O., PEEDELL, C., PROTHEROE, A., ROBINSON, A. J., SRIHARI, N., SRINIVASAN, R., STAFFURTH, J., SUNDAR, S., TOLAN, S., TSANG, D., WAGSTAFF, J. & PARMAR, M. K. 2016b. Addition of docetaxel, zoledronic acid, or both to first-line long-term hormone therapy in prostate cancer (STAMPEDE): survival results from an adaptive, multiarm, multistage, platform randomised controlled trial. *Lancet,* 387**,** 1163-77.

JIANG, W. G., DAVIES, G., MARTIN, T. A., PARR, C., WATKINS, G., MANSEL, R. E. & MASON, M. D. 2005. The potential lymphangiogenic effects of hepatocyte growth factor/scatter factor in vitro and in vivo. *Int J Mol Med,* 16**,** 723-8.

JOHANNSEN, M., SPITALERI, G., CURIGLIANO, G., ROIGAS, J., WEIKERT, S., KEMPKENSTEFFEN, C., ROEMER, A., KLOETERS, C., ROGALLA, P., PECHER, G., MILLER, K., BERNDT, A., KOSMEHL, H., TRACHSEL, E., KASPAR, M., LOVATO, V., GONZALEZ-IGLESIAS, R., GIOVANNONI, L., MENSSEN, H. D., NERI, D. & DE BRAUD, F. 2010. The tumour-targeting human L19-IL2 immunocytokine: preclinical safety studies, phase I clinical trial in patients with solid tumours and expansion into patients with advanced renal cell carcinoma. *Eur J Cancer,* 46**,** 2926-35.

JOHNSON, L. A., MORGAN, R. A., DUDLEY, M. E., CASSARD, L., YANG, J. C., HUGHES, M. S., KAMMULA, U. S., ROYAL, R. E., SHERRY, R. M., WUNDERLICH, J. R., LEE, C. C., RESTIFO, N. P., SCHWARZ, S. L., COGDILL, A. P., BISHOP, R. J., KIM, H., BREWER, C. C., RUDY, S. F., VANWAES, C., DAVIS, J. L., MATHUR, A., RIPLEY, R. T., NATHAN, D. A., LAURENCOT, C. M. & ROSENBERG, S. A. 2009. Gene therapy with human and mouse T-cell receptors mediates cancer regression and targets normal tissues expressing cognate antigen. *Blood,* 114**,** 535-46.

JUNGHANS, R. P., MA, Q., RATHORE, R., GOMES, E. M., BAIS, A. J., LO, A. S., ABEDI, M., DAVIES, R. A., CABRAL, H. J., AL-HOMSI, A. S. & COHEN, S. I. 2016. Phase I Trial of Anti-PSMA Designer CAR-T Cells in Prostate Cancer: Possible Role for Interacting Interleukin 2-T Cell Pharmacodynamics as a Determinant of Clinical Response. *Prostate,* 76**,** 1257-70.

KAGEYAMA, S., IKEDA, H., MIYAHARA, Y., IMAI, N., ISHIHARA, M., SAITO, K., SUGINO, S., UEDA, S., ISHIKAWA, T., KOKURA, S., NAOTA, H., OHISHI, K., SHIRAISHI, T., INOUE, N., TANABE, M., KIDOKORO, T., YOSHIOKA, H., TOMURA, D., NUKAYA, I., MINENO, J., TAKESAKO, K., KATAYAMA, N. & SHIKU, H. 2015. Adoptive Transfer of MAGE-A4 T-cell Receptor Gene-Transduced Lymphocytes in Patients with Recurrent Esophageal Cancer. *Clin Cancer Res,* 21**,** 2268-77.

KAITTANIS, C., ANDREOU, C., HIERONYMUS, H., MAO, N., FOSS, C. A., EIBER, M., WEIRICH, G., PANCHAL, P., GOPALAN, A., ZURITA, J., ACHILEFU, S., CHIOSIS, G., PONOMAREV, V., SCHWAIGER, M., CARVER, B. S., POMPER, M. G. & GRIMM, J. 2018. Prostate-specific membrane antigen cleavage of vitamin B9 stimulates oncogenic signaling through metabotropic glutamate receptors. *J Exp Med,* 215**,** 159-175.

KAKARLA, S., CHOW, K. K. H., MATA, M., SHAFFER, D. R., SONG, X.-T., WU, M.-F., LIU, H., WANG, L. L., ROWLEY, D. R., PFIZENMAIER, K. & GOTTSCHALK, S. 2013. Antitumor Effects of Chimeric Receptor Engineered Human T Cells Directed to Tumor Stroma. *Molecular Therapy,* 21**,** 1611-1620.

KANAJI, N., YOKOHIRA, M., NAKANO-NARUSAWA, Y., WATANABE, N., IMAIDA, K., KADOWAKI, N. & BANDOH, S. 2017. Hepatocyte growth factor

produced in lung fibroblasts enhances non-small cell lung cancer cell survival and tumor progression. *Respir Res,* 18**,** 118.

KANG, T. H., MAO, C. P., LA, V., CHEN, A., HUNG, C. F. & WU, T. C. 2013. Innovative DNA vaccine to break immune tolerance against tumor self-antigen. *Hum Gene Ther,* 24**,** 181-8.

KANTOFF, P. W., HIGANO, C. S., SHORE, N. D., BERGER, E. R., SMALL, E. J., PENSON, D. F., REDFERN, C. H., FERRARI, A. C., DREICER, R., SIMS, R. B., XU, Y., FROHLICH, M. W. & SCHELLHAMMER, P. F. 2010. Sipuleucel-T immunotherapy for castration-resistant prostate cancer. *N Engl J Med,* 363**,** 411-22.

KAO, R. L., TRUSCOTT, L. C., CHIOU, T. T., TSAI, W., WU, A. M. & DE OLIVEIRA, S. N. 2019. A Cetuximab-Mediated Suicide System in Chimeric Antigen Receptor-Modified Hematopoietic Stem Cells for Cancer Therapy. *Hum Gene Ther,* 30**,** 413-428.

KAPLAN, D. H., SHANKARAN, V., DIGHE, A. S., STOCKERT, E., AGUET, M., OLD, L. J. & SCHREIBER, R. D. 1998. Demonstration of an interferon gamma-dependent tumor surveillance system in immunocompetent mice. *Proc Natl Acad Sci U S A,* 95**,** 7556-61.

KAUFMAN, H. L., KOHLHAPP, F. J. & ZLOZA, A. 2015. Oncolytic viruses: a new class of immunotherapy drugs. *Nat Rev Drug Discov,* 14**,** 642-62.

KAWAKAMI, M. & NAKAYAMA, J. 1997. Enhanced expression of prostate-specific membrane antigen gene in prostate cancer as revealed by in situ hybridization. *Cancer Res,* 57**,** 2321-4.

KAWAKAMI, Y., ELIYAHU, S., DELGADO, C. H., ROBBINS, P. F., RIVOLTINI, L., TOPALIAN, S. L., MIKI, T. & ROSENBERG, S. A. 1994a. Cloning of the gene coding for a shared human melanoma antigen recognized by autologous T cells infiltrating into tumor. *Proc Natl Acad Sci U S A,* 91**,** 3515-9.

KAWAKAMI, Y., ELIYAHU, S., DELGADO, C. H., ROBBINS, P. F., SAKAGUCHI, K., APPELLA, E., YANNELLI, J. R., ADEMA, G. J., MIKI, T. & ROSENBERG, S. A. 1994b. Identification of a human melanoma antigen recognized by tumor-infiltrating lymphocytes associated with in vivo tumor rejection. *Proc Natl Acad Sci U S A,* 91**,** 6458-62.

KAWALEKAR, O. U., O'CONNOR, R. S., FRAIETTA, J. A., GUO, L., MCGETTIGAN, S. E., POSEY, A. D., JR., PATEL, P. R., GUEDAN, S., SCHOLLER, J., KEITH, B., SNYDER, N. W., BLAIR, I. A., MILONE, M. C. & JUNE, C. H. 2016. Distinct Signaling of Coreceptors Regulates Specific Metabolism Pathways and Impacts Memory Development in CAR T Cells. *Immunity,* 44**,** 380-90.

KAWALKOWSKA, J. Z., HEMMERLE, T., PRETTO, F., MATASCI, M., NERI, D. & WILLIAMS, R. O. 2016. Targeted IL-4 therapy synergizes with dexamethasone to induce a state of tolerance by promoting Treg cells and macrophages in mice with arthritis. *Eur J Immunol,* 46**,** 1246-57.

KEANE, F. M., NADVI, N. A., YAO, T. W. & GORRELL, M. D. 2011. Neuropeptide Y, B-type natriuretic peptide, substance P and peptide YY are novel substrates of fibroblast activation protein-alpha. *Febs j,* 278**,** 1316-32.

KERMER, V., BAUM, V., HORNIG, N., KONTERMANN, R. E. & MULLER, D. 2012. An antibody fusion protein for cancer immunotherapy mimicking IL-15 trans-presentation at the tumor site. *Mol Cancer Ther,* 11**,** 1279-88.

KEYES, M., MILLER, S., MORAVAN, V., PICKLES, T., MCKENZIE, M., PAI, H., LIU, M., KWAN, W., AGRANOVICH, A., SPADINGER, I., LAPOINTE, V., HALPERIN, R. & MORRIS, W. J. 2009. Predictive factors for acute and late

urinary toxicity after permanent prostate brachytherapy: long-term outcome in 712 consecutive patients. *Int J Radiat Oncol Biol Phys,* 73**,** 1023-32.

KICIELINSKI, K. P., CHIOCCA, E. A., YU, J. S., GILL, G. M., COFFEY, M. & MARKERT, J. M. 2014. Phase 1 clinical trial of intratumoral reovirus infusion for the treatment of recurrent malignant gliomas in adults. *Mol Ther,* 22**,** 1056-62.

KIENZLE, N., OLVER, S., BUTTIGIEG, K., GROVES, P., JANAS, M. L., BAZ, A. & KELSO, A. 2005. Progressive differentiation and commitment of CD8+ T cells to a poorly cytolytic CD8low phenotype in the presence of IL-4. *J Immunol,* 174**,** 2021-9.

KING, D. M., ALBERTINI, M. R., SCHALCH, H., HANK, J. A., GAN, J., SURFUS, J., MAHVI, D., SCHILLER, J. H., WARNER, T., KIM, K., EICKHOFF, J., KENDRA, K., REISFELD, R., GILLIES, S. D. & SONDEL, P. 2004. Phase I clinical trial of the immunocytokine EMD 273063 in melanoma patients. *J Clin Oncol,* 22**,** 4463-73.

KLOSS, C. C., CONDOMINES, M., CARTELLIERI, M., BACHMANN, M. & SADELAIN, M. 2013. Combinatorial antigen recognition with balanced signaling promotes selective tumor eradication by engineered T cells. *Nat Biotechnol,* 31**,** 71-5.

KLOSS, C. C., LEE, J., ZHANG, A., CHEN, F., MELENHORST, J. J., LACEY, S. F., MAUS, M. V., FRAIETTA, J. A., ZHAO, Y. & JUNE, C. H. 2018. Dominant-Negative TGF-beta Receptor Enhances PSMA-Targeted Human CAR T Cell Proliferation And Augments Prostate Cancer Eradication. *Mol Ther,* 26**,** 1855-1866.

KLOTZ, L., VESPRINI, D., SETHUKAVALAN, P., JETHAVA, V., ZHANG, L., JAIN, S., YAMAMOTO, T., MAMEDOV, A. & LOBLAW, A. 2015. Long-term follow-up of a large active surveillance cohort of patients with prostate cancer. *J Clin Oncol,* 33**,** 272-7.

KMIECIAK, M., GOWDA, M., GRAHAM, L., GODDER, K., BEAR, H. D., MARINCOLA, F. M. & MANJILI, M. H. 2009. Human T cells express CD25 and Foxp3 upon activation and exhibit effector/memory phenotypes without any regulatory/suppressor function. *J Transl Med,* 7**,** 89.

KNIPPING, F., OSBORN, M. J., PETRI, K., TOLAR, J., GLIMM, H., VON KALLE, C., SCHMIDT, M. & GABRIEL, R. 2017. Genome-wide Specificity of Highly Efficient TALENs and CRISPR/Cas9 for T Cell Receptor Modification. *Mol Ther Methods Clin Dev,* 4**,** 213-224.

KNOCHELMANN, H. M., SMITH, A. S., DWYER, C. J., WYATT, M. M., MEHROTRA, S. & PAULOS, C. M. 2018. CAR T Cells in Solid Tumors: Blueprints for Building Effective Therapies. *Front Immunol,* 9**,** 1740.

KO, Y. J., BUBLEY, G. J., WEBER, R., REDFERN, C., GOLD, D. P., FINKE, L., KOVAR, A., DAHL, T. & GILLIES, S. D. 2004. Safety, pharmacokinetics, and biological pharmacodynamics of the immunocytokine EMD 273066 (huKS-IL2): results of a phase I trial in patients with prostate cancer. *J Immunother,* 27**,** 232-9.

KOCHENDERFER, J. N., DUDLEY, M. E., FELDMAN, S. A., WILSON, W. H., SPANER, D. E., MARIC, I., STETLER-STEVENSON, M., PHAN, G. Q., HUGHES, M. S., SHERRY, R. M., YANG, J. C., KAMMULA, U. S., DEVILLIER, L., CARPENTER, R., NATHAN, D. A., MORGAN, R. A., LAURENCOT, C. & ROSENBERG, S. A. 2012. B-cell depletion and remissions of malignancy along with cytokine-associated toxicity in a clinical trial of anti-CD19 chimeric-antigen-receptor-transduced T cells. *Blood,* 119**,** 2709-20.

KOCHENDERFER, J. N., WILSON, W. H., JANIK, J. E., DUDLEY, M. E., STETLER-STEVENSON, M., FELDMAN, S. A., MARIC, I., RAFFELD, M., NATHAN,

D. A., LANIER, B. J., MORGAN, R. A. & ROSENBERG, S. A. 2010. Eradication of B-lineage cells and regression of lymphoma in a patient treated with autologous T cells genetically engineered to recognize CD19. *Blood,* 116**,** 4099-102.

KOEBEL, C. M., VERMI, W., SWANN, J. B., ZERAFA, N., RODIG, S. J., OLD, L. J., SMYTH, M. J. & SCHREIBER, R. D. 2007. Adaptive immunity maintains occult cancer in an equilibrium state. *Nature,* 450**,** 903.

KOHLER, G. & MILSTEIN, C. 2005. Continuous cultures of fused cells secreting antibody of predefined specificity. 1975. *J Immunol,* 174**,** 2453-5.

KOIVISTO, P., KONONEN, J., PALMBERG, C., TAMMELA, T., HYYTINEN, E., ISOLA, J., TRAPMAN, J., CLEUTJENS, K., NOORDZIJ, A., VISAKORPI, T. & KALLIONIEMI, O. P. 1997. Androgen receptor gene amplification: a possible molecular mechanism for androgen deprivation therapy failure in prostate cancer. *Cancer Res,* 57**,** 314-9.

KOJIMA, Y., ACAR, A., EATON, E.N., MELLODY, K.T., SCHEEL, C., BEN-PORATH, I., ONDER, T.T., WANG, Z.C., RICHARDSON, A.L., WEINBERG, R.A., ORIMO, A., 2010. Autocrine TGF-beta and stromal cell-derived factor-1 (SDF-1) signaling drives the evolution of tumor-promoting mammary stromal myofibroblasts. Proc. Natl. Acad. Sci. U. S. A. 107, 20009–20014. https://doi.org/10.1073/pnas.1013805107

KOLLER, F. L., HWANG, D. G., DOZIER, E. A. & FINGLETON, B. 2010. Epithelial interleukin-4 receptor expression promotes colon tumor growth. *Carcinogenesis,* 31**,** 1010-7.

KORISTKA, S., CARTELLIERI, M., FELDMANN, A., ARNDT, C., LOFF, S., MICHALK, I., ALIPERTA, R., VON BONIN, M., BORNHÄUSER, M., EHNINGER, A., EHNINGER, G. & BACHMANN, M. P. 2014. Flexible Antigen-Specific Redirection of Human Regulatory T Cells Via a Novel Universal Chimeric Antigen Receptor System. *Blood,* 124**,** 3494-3494.

KREMER, J. P., REISBACH, G., NERL, C. & DORMER, P. 1992. B-cell chronic lymphocytic leukaemia cells express and release transforming growth factor-beta. *Br J Haematol,* 80**,** 480-7.

KRENCIUTE, G., PRINZING, B. L., YI, Z., WU, M. F., LIU, H., DOTTI, G., BALYASNIKOVA, I. V. & GOTTSCHALK, S. 2017. Transgenic Expression of IL15 Improves Antiglioma Activity of IL13Ralpha2-CAR T Cells but Results in Antigen Loss Variants. *Cancer Immunol Res,* 5**,** 571-581.

KRUMMEL, M. F. & ALLISON, J. P. 1995. CD28 and CTLA-4 have opposing effects on the response of T cells to stimulation. *J Exp Med,* 182**,** 459-65.

KUMAI, T., LEE, S., CHO, H. I., SULTAN, H., KOBAYASHI, H., HARABUCHI, Y. & CELIS, E. 2017. Optimization of Peptide Vaccines to Induce Robust Antitumor CD4 T-cell Responses. *Cancer Immunol Res,* 5**,** 72-83.

KUMAR, S., SAINI, R. V. & MAHINDROO, N. 2017. Recent advances in cancer immunology and immunology-based anticancer therapies. *Biomed Pharmacother,* 96**,** 1491-1500.

KUWANA, Y., ASAKURA, Y., UTSUNOMIYA, N., NAKANISHI, M., ARATA, Y., ITOH, S., NAGASE, F. & KUROSAWA, Y. 1987. Expression of chimeric receptor composed of immunoglobulin-derived V regions and T-cell receptor-derived C regions. *Biochem Biophys Res Commun,* 149**,** 960-8.

LAL-NAG, M., MCGEE, L., TITUS, S. A., BRIMACOMBE, K., MICHAEL, S., SITTAMPALAM, G. & FERRER, M. 2017. Exploring Drug Dosing Regimens In Vitro Using Real-Time 3D Spheroid Tumor Growth Assays. *SLAS DISCOVERY: Advancing Life Sciences R&D,* 22**,** 537-546.

LAMERS, C. H., SLEIJFER, S., VAN STEENBERGEN, S., VAN ELZAKKER, P., VAN KRIMPEN, B., GROOT, C., VULTO, A., DEN BAKKER, M., OOSTERWIJK, E., DEBETS, R. & GRATAMA, J. W. 2013. Treatment of metastatic renal cell carcinoma with CAIX CAR-engineered T cells: clinical evaluation and management of on-target toxicity. *Mol Ther,* 21**,** 904-12.

LANITIS, E., POUSSIN, M., KLATTENHOFF, A. W., SONG, D., SANDALTZOPOULOS, R., JUNE, C. H. & POWELL, D. J., JR. 2013. Chimeric antigen receptor T Cells with dissociated signaling domains exhibit focused antitumor activity with reduced potential for toxicity in vivo. *Cancer Immunol Res,* 1**,** 43-53.

LATCHMAN, Y., WOOD, C. R., CHERNOVA, T., CHAUDHARY, D., BORDE, M., CHERNOVA, I., IWAI, Y., LONG, A. J., BROWN, J. A., NUNES, R., GREENFIELD, E. A., BOURQUE, K., BOUSSIOTIS, V. A., CARTER, L. L., CARRENO, B. M., MALENKOVICH, N., NISHIMURA, H., OKAZAKI, T., HONJO, T., SHARPE, A. H. & FREEMAN, G. J. 2001. PD-L2 is a second ligand for PD-1 and inhibits T cell activation. *Nat Immunol,* 2**,** 261-8.

LAZZARI, G., NICOLAS, V., MATSUSAKI, M., AKASHI, M., COUVREUR, P. & MURA, S. 2018. Multicellular spheroid based on a triple co-culture: A novel 3D model to mimic pancreatic tumor complexity. *Acta Biomater,* 78**,** 296-307.

LEACH, D. R., KRUMMEL, M. F. & ALLISON, J. P. 1996. Enhancement of antitumor immunity by CTLA-4 blockade. *Science,* 271**,** 1734-6.

LEE, D. W., GARDNER, R., PORTER, D. L., LOUIS, C. U., AHMED, N., JENSEN, M., GRUPP, S. A. & MACKALL, C. L. 2014. Current concepts in the diagnosis and management of cytokine release syndrome. *Blood,* 124**,** 188-195.

LEE, D. W., KOCHENDERFER, J. N., STETLER-STEVENSON, M., CUI, Y. K., DELBROOK, C., FELDMAN, S. A., FRY, T. J., ORENTAS, R., SABATINO, M., SHAH, N. N., STEINBERG, S. M., STRONCEK, D., TSCHERNIA, N., YUAN, C., ZHANG, H., ZHANG, L., ROSENBERG, S. A., WAYNE, A. S. & MACKALL, C. L. 2015. T cells expressing CD19 chimeric antigen receptors for acute lymphoblastic leukaemia in children and young adults: a phase 1 dose-escalation trial. *The Lancet,* 385**,** 517-528.

LEE, D. W., SANTOMASSO, B. D., LOCKE, F. L., GHOBADI, A., TURTLE, C. J., BRUDNO, J. N., MAUS, M. V., PARK, J. H., MEAD, E., PAVLETIC, S., GO, W. Y., ELDJEROU, L., GARDNER, R. A., FREY, N., CURRAN, K. J., PEGGS, K., PASQUINI, M., DIPERSIO, J. F., VAN DEN BRINK, M. R. M., KOMANDURI, K. V., GRUPP, S. A. & NEELAPU, S. S. 2019. ASTCT Consensus Grading for Cytokine Release Syndrome and Neurologic Toxicity Associated with Immune Effector Cells. *Biol Blood Marrow Transplant,* 25**,** 625-638.

LEE, J., FASSNACHT, M., NAIR, S., BOCZKOWSKI, D. & GILBOA, E. 2005. Tumor immunotherapy targeting fibroblast activation protein, a product expressed in tumor-associated fibroblasts. *Cancer Res,* 65**,** 11156-63.

LEE, J. M., MHAWECH-FAUCEGLIA, P., LEE, N., PARSANIAN, L. C., LIN, Y. G., GAYTHER, S. A. & LAWRENSON, K. 2013. A three-dimensional microenvironment alters protein expression and chemosensitivity of epithelial ovarian cancer cells in vitro. *Lab Invest,* 93**,** 528-42.

LEE, K. N., JACKSON, K. W., CHRISTIANSEN, V. J., LEE, C. S., CHUN, J. G. & MCKEE, P. A. 2006. Antiplasmin-cleaving enzyme is a soluble form of fibroblast activation protein. *Blood,* 107**,** 1397-404.

LEE, L., DRAPER, B., CHAPLIN, N., PHILIP, B., CHIN, M., GALAS-FILIPOWICZ, D., ONUOHA, S., THOMAS, S., BALDAN, V., BUGHDA, R., MACIOCIA, P., KOKALAKI, E., NEVES, M. P., PATEL, D., RODRIGUEZ-JUSTO, M.,

FRANCIS, J., YONG, K. & PULE, M. 2018. An APRIL-based chimeric antigen receptor for dual targeting of BCMA and TACI in multiple myeloma. *Blood,* 131**,** 746-758.

LEEN, A. M., SUKUMARAN, S., WATANABE, N., MOHAMMED, S., KEIRNAN, J., YANAGISAWA, R., ANURATHAPAN, U., RENDON, D., HESLOP, H. E., ROONEY, C. M., BRENNER, M. K. & VERA, J. F. 2014. Reversal of tumor immune inhibition using a chimeric cytokine receptor. *Mol Ther,* 22**,** 1211-1220.

LEGUT, M., DOLTON, G., MIAN, A. A., OTTMANN, O. G. & SEWELL, A. K. 2018. CRISPR-mediated TCR replacement generates superior anticancer transgenic T cells. *Blood,* 131**,** 311-322.

LI, J., O'MALLEY, M., URBAN, J., SAMPATH, P., GUO, Z. S., KALINSKI, P., THORNE, S. H. & BARTLETT, D. L. 2011. Chemokine expression from oncolytic vaccinia virus enhances vaccine therapies of cancer. *Mol Ther,* 19**,** 650-7.

LI, J., SIEGEL, D. A. & KING, J. B. 2018. Stage-specific incidence rates and trends of prostate cancer by age, race, and ethnicity, United States, 2004-2014. *Ann Epidemiol,* 28**,** 328-330.

LI, J., WANG, Z., MAO, K. & GUO, X. 2014a. Clinical significance of serum T helper 1/T helper 2 cytokine shift in patients with non-small cell lung cancer. *Oncol Lett,* 8**,** 1682-1686.

LI, Z., CHEN, L. & QIN, Z. 2009. Paradoxical roles of IL-4 in tumor immunity. *Cell Mol Immunol,* 6**,** 415-22.

LI, Z., JIANG, J., WANG, Z., ZHANG, J., XIAO, M., WANG, C., LU, Y. & QIN, Z. 2008. Endogenous interleukin-4 promotes tumor development by increasing tumor cell resistance to apoptosis. *Cancer Res,* 68**,** 8687-94.

LI, Z. Y., WANG, D. B., ZHANG, Z. P., BI, L. J., CUI, Z. Q., DENG, J. Y. & ZHANG, X. E. 2014b. The S28H mutation on mNeptune generates a brighter near-infrared monomeric fluorescent protein with improved quantum yield and pH-stability. *Acta Biochim Biophys Sin (Shanghai),* 46**,** 802-9.

LIN, H., BOLLING, S. F., LINSLEY, P. S., WEI, R. Q., GORDON, D., THOMPSON, C. B. & TURKA, L. A. 1993. Long-term acceptance of major histocompatibility complex mismatched cardiac allografts induced by CTLA4Ig plus donor-specific transfusion. *J Exp Med,* 178**,** 1801-6.

LINETTE, G. P., STADTMAUER, E. A., MAUS, M. V., RAPOPORT, A. P., LEVINE, B. L., EMERY, L., LITZKY, L., BAGG, A., CARRENO, B. M., CIMINO, P. J., BINDER-SCHOLL, G. K., SMETHURST, D. P., GERRY, A. B., PUMPHREY, N. J., BENNETT, A. D., BREWER, J. E., DUKES, J., HARPER, J., TAYTON-MARTIN, H. K., JAKOBSEN, B. K., HASSAN, N. J., KALOS, M. & JUNE, C. H. 2013. Cardiovascular toxicity and titin cross-reactivity of affinity-enhanced T cells in myeloma and melanoma. *Blood,* 122**,** 863-71.

LINSLEY, P. S., BRADY, W., URNES, M., GROSMAIRE, L. S., DAMLE, N. K. & LEDBETTER, J. A. 1991. CTLA-4 is a second receptor for the B cell activation antigen B7. *J Exp Med,* 174**,** 561-9.

LINSLEY, P. S., WALLACE, P. M., JOHNSON, J., GIBSON, M. G., GREENE, J. L., LEDBETTER, J. A., SINGH, C. & TEPPER, M. A. 1992. Immunosuppression in vivo by a soluble form of the CTLA-4 T cell activation molecule. *Science,* 257**,** 792-5.

LIPPONEN, P. K., ESKELINEN, M. J., JAUHIAINEN, K., HARJU, E. & TERHO, R. 1992. Tumour infiltrating lymphocytes as an independent prognostic factor in transitional cell bladder cancer. *Eur J Cancer,* 29a**,** 69-75.

LIU, F., QI, L., LIU, B., LIU, J., ZHANG, H., CHE, D., CAO, J., SHEN, J., GENG, J., BI, Y., YE, L., PAN, B. & YU, Y. 2015. Fibroblast activation protein

overexpression and clinical implications in solid tumors: a meta-analysis. *PLoS One,* 10**,** e0116683.

LIU, H., MOY, P., KIM, S., XIA, Y., RAJASEKARAN, A., NAVARRO, V., KNUDSEN, B. & BANDER, N. H. 1997. Monoclonal antibodies to the extracellular domain of prostate-specific membrane antigen also react with tumor vascular endothelium. *Cancer Res,* 57**,** 3629-34.

LIU, Y., ZHANG, W., CHEUNG, L. H., NIU, T., WU, Q., LI, C., VAN PELT, C. S. & ROSENBLUM, M. G. 2006. The antimelanoma immunocytokine scFvMEL/TNF shows reduced toxicity and potent antitumor activity against human tumor xenografts. *Neoplasia,* 8**,** 384-93.

LOCKE, F. L., NEELAPU, S. S., BARTLETT, N. L., LEKAKIS, L. J., MIKLOS, D., JACOBSON, C. A., BRAUNSCHWEIG, I., OLUWOLE, O., SIDDIQI, T., LIN, Y., TIMMERMAN, J., FRIEDBERG, J. W., BOT, A., ROSSI, J., NAVALE, L., JIANG, Y., AYCOCK, J., ELIAS, M., WIEZOREK, J. & GO, W. Y. 2017. Abstract CT019: Primary results from ZUMA-1: a pivotal trial of axicabtagene ciloleucel (axicel; KTE-C19) in patients with refractory aggressive non-Hodgkin lymphoma (NHL). *Cancer Research,* 77**,** CT019-CT019.

LODOLCE, J. P., BOONE, D. L., CHAI, S., SWAIN, R. E., DASSOPOULOS, T., TRETTIN, S. & MA, A. 1998. IL-15 receptor maintains lymphoid homeostasis by supporting lymphocyte homing and proliferation. *Immunity,* 9**,** 669-76.

LOEFFLER, M., KRUGER, J. A., NIETHAMMER, A. G. & REISFELD, R. A. 2006. Targeting tumor-associated fibroblasts improves cancer chemotherapy by increasing intratumoral drug uptake. *J Clin Invest,* 116**,** 1955-62.

LONG, A. H., HASO, W. M., SHERN, J. F., WANHAINEN, K. M., MURGAI, M., INGARAMO, M., SMITH, J. P., WALKER, A. J., KOHLER, M. E., VENKATESHWARA, V. R., KAPLAN, R. N., PATTERSON, G. H., FRY, T. J., ORENTAS, R. J. & MACKALL, C. L. 2015. 4-1BB costimulation ameliorates T cell exhaustion induced by tonic signaling of chimeric antigen receptors. *Nat Med,* 21**,** 581-90.

LONG, A. H., HIGHFILL, S. L., CUI, Y., SMITH, J. P., WALKER, A. J., RAMAKRISHNA, S., EL-ETRIBY, R., GALLI, S., TSOKOS, M. G., ORENTAS, R. J. & MACKALL, C. L. 2016. Reduction of MDSCs with All-trans Retinoic Acid Improves CAR Therapy Efficacy for Sarcomas. *Cancer Immunol Res,* 4**,** 869-880.

LOUIS, C. U., SAVOLDO, B., DOTTI, G., PULE, M., YVON, E., MYERS, G. D., ROSSIG, C., RUSSELL, H. V., DIOUF, O., LIU, E., LIU, H., WU, M. F., GEE, A. P., MEI, Z., ROONEY, C. M., HESLOP, H. E. & BRENNER, M. K. 2011. Antitumor activity and long-term fate of chimeric antigen receptor-positive T cells in patients with neuroblastoma. *Blood,* 118**,** 6050-6.

LU, Y. C., PARKER, L. L., LU, T., ZHENG, Z., TOOMEY, M. A., WHITE, D. E., YAO, X., LI, Y. F., ROBBINS, P. F., FELDMAN, S. A., VAN DER BRUGGEN, P., KLEBANOFF, C. A., GOFF, S. L., SHERRY, R. M., KAMMULA, U. S., YANG, J. C. & ROSENBERG, S. A. 2017. Treatment of Patients With Metastatic Cancer Using a Major Histocompatibility Complex Class II-Restricted T-Cell Receptor Targeting the Cancer Germline Antigen MAGE-A3. *J Clin Oncol,* 35**,** 3322-3329.

LU, Y. C., ZHENG, Z., ROBBINS, P. F., TRAN, E., PRICKETT, T. D., GARTNER, J. J., LI, Y. F., RAY, S., FRANCO, Z., BLISKOVSKY, V., FITZGERALD, P. C. & ROSENBERG, S. A. 2018. An Efficient Single-Cell RNA-Seq Approach to Identify Neoantigen-Specific T Cell Receptors. *Mol Ther,* 26**,** 379-389.

MA, Q., GOMES, E. M., LO, A. S. & JUNGHANS, R. P. 2014. Advanced generation anti-prostate specific membrane antigen designer T cells for prostate cancer immunotherapy. *Prostate,* 74**,** 286-96.

MACKENZIE, C. R., HIRAMA, T., DENG, S. J., BUNDLE, D. R., NARANG, S. A. & YOUNG, N. M. 1996. Analysis by surface plasmon resonance of the influence of valence on the ligand binding affinity and kinetics of an anti-carbohydrate antibody. *J Biol Chem,* 271**,** 1527-33.

MACKENZIE, K. L., FRANCO, S., MAY, C., SADELAIN, M. & MOORE, M. A. 2000. Mass cultured human fibroblasts overexpressing hTERT encounter a growth crisis following an extended period of proliferation. *Exp Cell Res,* 259**,** 336-50.

MAHER, J., BRENTJENS, R. J., GUNSET, G., RIVIERE, I. & SADELAIN, M. 2002. Human T-lymphocyte cytotoxicity and proliferation directed by a single chimeric TCRzeta /CD28 receptor. *Nat Biotechnol,* 20**,** 70-5.

MAJHAIL, N. S., HUSSEIN, M., OLENCKI, T. E., BUDD, G. T., WOOD, L., ELSON, P. & BUKOWSKI, R. M. 2004. Phase I trial of continuous infusion recombinant human interleukin-4 in patients with cancer. *Invest New Drugs,* 22**,** 421-6.

MALONEY, D. G., GRILLO-LOPEZ, A. J., BODKIN, D. J., WHITE, C. A., LILES, T. M., ROYSTON, I., VARNS, C., ROSENBERG, J. & LEVY, R. 1997. IDEC-C2B8: results of a phase I multiple-dose trial in patients with relapsed non-Hodgkin's lymphoma. *J Clin Oncol,* 15**,** 3266-74.

MARANGONI, R.G., KORMAN, B.D., WEI, J., WOOD, T.A., GRAHAM, L.V., WHITFIELD, M.L., SCHERER, P.E., TOURTELLOTTE, W.G., VARGA, J., 2015. Myofibroblasts in murine cutaneous fibrosis originate from adiponectin-positive intradermal progenitors. Arthritis Rheumatol. Hoboken NJ 67, 1062–1073. https://doi.org/10.1002/art.38990

MARGOLIN, K., ARONSON, F. R., SZNOL, M., ATKINS, M. B., GUCALP, R., FISHER, R. I., SUNDERLAND, M., DOROSHOW, J. H., ERNEST, M. L., MIER, J. W. & ET AL. 1994. Phase II studies of recombinant human interleukin-4 in advanced renal cancer and malignant melanoma. *J Immunother Emphasis Tumor Immunol,* 15**,** 147-53.

MARIATHASAN, S., TURLEY, S.J., NICKLES, D., CASTIGLIONI, A., YUEN, K., WANG, Y., KADEL, E.E.I., KOEPPEN, H., ASTARITA, J.L., CUBAS, R., JHUNJHUNWALA, S., BANCHEREAU, R., YANG, Y., GUAN, Y., CHALOUNI, C., ZIAI, J., SENBABAOGLU, Y., SANTORO, S., SHEINSON, D., HUNG, J., GILTNANE, J.M., PIERCE, A.A., MESH, K., LIANOGLOU, S., RIEGLER, J., CARANO, R.A.D., ERIKSSON, P., HOGLUND, M., SOMARRIBA, L., HALLIGAN, D.L., VAN DER HEIJDEN, M.S., LORIOT, Y., ROSENBERG, J.E., FONG, L., MELLMAN, I., CHEN, D.S., GREEN, M., DERLETH, C., FINE, G.D., HEGDE, P.S., BOURGON, R., POWLES, T., 2018. TGFbeta attenuates tumour response to PD-L1 blockade by contributing to exclusion of T cells. Nature 554, 544–548. https://doi.org/10.1038/nature25501

MAUDE, S. L., FREY, N., SHAW, P. A., APLENC, R., BARRETT, D. M., BUNIN, N. J., CHEW, A., GONZALEZ, V. E., ZHENG, Z., LACEY, S. F., MAHNKE, Y. D., MELENHORST, J. J., RHEINGOLD, S. R., SHEN, A., TEACHEY, D. T., LEVINE, B. L., JUNE, C. H., PORTER, D. L. & GRUPP, S. A. 2014. Chimeric antigen receptor T cells for sustained remissions in leukemia. *N Engl J Med,* 371**,** 1507-17.

MAUDE, S. L., LAETSCH, T. W., BUECHNER, J., RIVES, S., BOYER, M., BITTENCOURT, H., BADER, P., VERNERIS, M. R., STEFANSKI, H. E., MYERS, G. D., QAYED, M., DE MOERLOOSE, B., HIRAMATSU, H., SCHLIS, K., DAVIS, K. L., MARTIN, P. L., NEMECEK, E. R., YANIK, G. A.,

PETERS, C., BARUCHEL, A., BOISSEL, N., MECHINAUD, F., BALDUZZI, A., KRUEGER, J., JUNE, C. H., LEVINE, B. L., WOOD, P., TARAN, T., LEUNG, M., MUELLER, K. T., ZHANG, Y., SEN, K., LEBWOHL, D., PULSIPHER, M. A. & GRUPP, S. A. 2018. Tisagenlecleucel in Children and Young Adults with B-Cell Lymphoblastic Leukemia. *N Engl J Med,* 378**,** 439-448.

MAUDE, S. L., TEACHEY, D. T., RHEINGOLD, S. R., SHAW, P. A., APLENC, R., BARRETT, D. M., BARKER, C. S., CALLAHAN, C., FREY, N. V., NAZIMUDDIN, F., LACEY, S. F., ZHENG, Z., LEVINE, B., MELENHORST, J. J., MOTLEY, L., PORTER, D. L., JUNE, C. H. & GRUPP, S. A. 2016. Sustained remissions with CD19-specific chimeric antigen receptor (CAR)-modified T cells in children with relapsed/refractory ALL. *Journal of Clinical Oncology,* 34**,** 3011-3011.

MAYKEL, J., LIU, J. H., LI, H., SHULTZ, L. D., GREINER, D. L. & HOUGHTON, J. 2014. NOD-scidIl2rg (tm1Wjl) and NOD-Rag1 (null) Il2rg (tm1Wjl) : a model for stromal cell-tumor cell interaction for human colon cancer. *Dig Dis Sci,* 59**,** 1169-79.

MCCARTHY, E. F. 2006. The toxins of William B. Coley and the treatment of bone and soft-tissue sarcomas. *Iowa Orthop J,* 26**,** 154-8.

METTLIN, C. J., MURPHY, G. P., SYLVESTER, J., MCKEE, R. F., MORROW, M. & WINCHESTER, D. P. 1997. Results of hospital cancer registry surveys by the American College of Surgeons: outcomes of prostate cancer treatment by radical prostatectomy. *Cancer,* 80**,** 1875-81.

MIAO, L., LIU, Q., LIN, C.M., LUO, C., WANG, Y., LIU, L., YIN, W., HU, S., KIM, W.Y., HUANG, L., 2017. Targeting Tumor-Associated Fibroblasts for Therapeutic Delivery in Desmoplastic Tumors. Cancer Res. 77, 719–731. https://doi.org/10.1158/0008-5472.CAN-16-0866

MILLER, R. A., MALONEY, D. G., WARNKE, R. & LEVY, R. 1982. Treatment of B-cell lymphoma with monoclonal anti-idiotype antibody. *N Engl J Med,* 306**,** 517-22.

MILONE, M. C., FISH, J. D., CARPENITO, C., CARROLL, R. G., BINDER, G. K., TEACHEY, D., SAMANTA, M., LAKHAL, M., GLOSS, B., DANET-DESNOYERS, G., CAMPANA, D., RILEY, J. L., GRUPP, S. A. & JUNE, C. H. 2009. Chimeric receptors containing CD137 signal transduction domains mediate enhanced survival of T cells and increased antileukemic efficacy in vivo. *Mol Ther,* 17**,** 1453-64.

MINCIACCHI, V. R., SPINELLI, C., REIS-SOBREIRO, M., CAVALLINI, L., YOU, S., ZANDIAN, M., LI, X., MISHRA, R., CHIARUGI, P., ADAM, R. M., POSADAS, E. M., VIGLIETTO, G., FREEMAN, M. R., COCUCCI, E., BHOWMICK, N. A. & DI VIZIO, D. 2017. MYC Mediates Large Oncosome-Induced Fibroblast Reprogramming in Prostate Cancer. *Cancer Res,* 77**,** 2306-2317.

MITANI, Y., HIWATARI, M., SEKI, M., HANGAI, M. & TAKITA, J. 2019. Successful treatment of acute myeloid leukemia co-expressing NUP98/NSD1 and FLT3/ITD with preemptive donor lymphocyte infusions. *Int J Hematol*.

MITCHELL, T. C., HAMID, O., SMITH, D. C., BAUER, T. M., WASSER, J. S., OLSZANSKI, A. J., LUKE, J. J., BALMANOUKIAN, A. S., SCHMIDT, E. V., ZHAO, Y., GONG, X., MALESKI, J., LEOPOLD, L. & GAJEWSKI, T. F. 2018. Epacadostat Plus Pembrolizumab in Patients With Advanced Solid Tumors: Phase I Results From a Multicenter, Open-Label Phase I/II Trial (ECHO-202/KEYNOTE-037). *J Clin Oncol***,** Jco2018789602.

MITSUYASU, R. T., ANTON, P. A., DEEKS, S. G., SCADDEN, D. T., CONNICK, E., DOWNS, M. T., BAKKER, A., ROBERTS, M. R., JUNE, C. H., JALALI, S., LIN, A. A., PENNATHUR-DAS, R. & HEGE, K. M. 2000. Prolonged survival and tissue trafficking following adoptive transfer of CD4zeta gene-modified autologous CD4(+) and CD8(+) T cells in human immunodeficiency virus-infected subjects. *Blood,* 96**,** 785-93.

MITTAL, D., GUBIN, M. M., SCHREIBER, R. D. & SMYTH, M. J. 2014. New insights into cancer immunoediting and its three component phases--elimination, equilibrium and escape. *Curr Opin Immunol,* 27**,** 16-25.

MO, F., LIN, D., TAKHAR, M., RAMNARINE, V. R., DONG, X., BELL, R. H., VOLIK, S. V., WANG, K., XUE, H., WANG, Y., HAEGERT, A., ANDERSON, S., BRAHMBHATT, S., ERHO, N., WANG, X., GOUT, P. W., MORRIS, J., KARNES, R. J., DEN, R. B., KLEIN, E. A., SCHAEFFER, E. M., ROSS, A., REN, S., SAHINALP, S. C., LI, Y., XU, X., WANG, J., WANG, J., GLEAVE, M. E., DAVICIONI, E., SUN, Y., WANG, Y. & COLLINS, C. C. 2018. Stromal Gene Expression is Predictive for Metastatic Primary Prostate Cancer. *Eur Urol,* 73**,** 524-532.

MOCHIZUKI, D. Y., WATSON, J. & GILLIS, S. 1980. Biochemical separation of interleukin 2. *J Immunol Methods,* 39**,** 185-201.

MOHAMMED, S., SUKUMARAN, S., BAJGAIN, P., WATANABE, N., HESLOP, H. E., ROONEY, C. M., BRENNER, M. K., FISHER, W. E., LEEN, A. M. & VERA, J. F. 2017. Improving Chimeric Antigen Receptor-Modified T Cell Function by Reversing the Immunosuppressive Tumor Microenvironment of Pancreatic Cancer. *Mol Ther,* 25**,** 249-258.

MONTGOMERY, R. I., WARNER, M. S., LUM, B. J. & SPEAR, P. G. 1996. Herpes simplex virus-1 entry into cells mediated by a novel member of the TNF/NGF receptor family. *Cell,* 87**,** 427-36.

MOON, E. K., WANG, L. S., BEKDACHE, K., LYNN, R. C., LO, A., THORNE, S. H. & ALBELDA, S. M. 2018. Intra-tumoral delivery of CXCL11 via a vaccinia virus, but not by modified T cells, enhances the efficacy of adoptive T cell therapy and vaccines. *Oncoimmunology,* 7**,** e1395997.

MORALES, A. 2017. BCG: A throwback from the stone age of vaccines opened the path for bladder cancer immunotherapy. *Can J Urol,* 24**,** 8788-8793.

MORALES, A., EIDINGER, D. & BRUCE, A. W. 1976. Intracavitary Bacillus Calmette-Guerin in the treatment of superficial bladder tumors. *J Urol,* 116**,** 180-3.

MORGAN, D. A., RUSCETTI, F. W. & GALLO, R. 1976. Selective in vitro growth of T lymphocytes from normal human bone marrows. *Science,* 193**,** 1007-8.

MORGAN, R. A., CHINNASAMY, N., ABATE-DAGA, D., GROS, A., ROBBINS, P. F., ZHENG, Z., DUDLEY, M. E., FELDMAN, S. A., YANG, J. C., SHERRY, R. M., PHAN, G. Q., HUGHES, M. S., KAMMULA, U. S., MILLER, A. D., HESSMAN, C. J., STEWART, A. A., RESTIFO, N. P., QUEZADO, M. M., ALIMCHANDANI, M., ROSENBERG, A. Z., NATH, A., WANG, T., BIELEKOVA, B., WUEST, S. C., AKULA, N., MCMAHON, F. J., WILDE, S., MOSETTER, B., SCHENDEL, D. J., LAURENCOT, C. M. & ROSENBERG, S. A. 2013. Cancer regression and neurological toxicity following anti-MAGE-A3 TCR gene therapy. *J Immunother,* 36**,** 133-51.

MORGAN, R. A., DUDLEY, M. E., WUNDERLICH, J. R., HUGHES, M. S., YANG, J. C., SHERRY, R. M., ROYAL, R. E., TOPALIAN, S. L., KAMMULA, U. S., RESTIFO, N. P., ZHENG, Z., NAHVI, A., DE VRIES, C. R., ROGERS-FREEZER, L. J., MAVROUKAKIS, S. A. & ROSENBERG, S. A. 2006. Cancer regression in patients after transfer of genetically engineered lymphocytes. *Science,* 314**,** 126-9.

MORGAN, R. A., YANG, J. C., KITANO, M., DUDLEY, M. E., LAURENCOT, C. M. & ROSENBERG, S. A. 2010. Case report of a serious adverse event following the administration of T cells transduced with a chimeric antigen receptor recognizing ERBB2. *Mol Ther,* 18**,** 843-51.

MORGENROTH, A., CARTELLIERI, M., SCHMITZ, M., GUNES, S., WEIGLE, B., BACHMANN, M., ABKEN, H., RIEBER, E. P. & TEMME, A. 2007. Targeting of tumor cells expressing the prostate stem cell antigen (PSCA) using genetically engineered T-cells. *Prostate,* 67**,** 1121-31.

MORITZ, D., WELS, W., MATTERN, J. & GRONER, B. 1994. Cytotoxic T lymphocytes with a grafted recognition specificity for ERBB2-expressing tumor cells. *Proc Natl Acad Sci U S A,* 91**,** 4318-22.

MORTIER, E., ADVINCULA, R., KIM, L., CHMURA, S., BARRERA, J., REIZIS, B., MALYNN, B. A. & MA, A. 2009. Macrophage- and dendritic-cell-derived interleukin-15 receptor alpha supports homeostasis of distinct CD8+ T cell subsets. *Immunity,* 31**,** 811-22.

MOTZER, R. J., TANNIR, N. M., MCDERMOTT, D. F., ARÉN FRONTERA, O., MELICHAR, B., CHOUEIRI, T. K., PLIMACK, E. R., BARTHÉLÉMY, P., PORTA, C., GEORGE, S., POWLES, T., DONSKOV, F., NEIMAN, V., KOLLMANNSBERGER, C. K., SALMAN, P., GURNEY, H., HAWKINS, R., RAVAUD, A., GRIMM, M.-O., BRACARDA, S., BARRIOS, C. H., TOMITA, Y., CASTELLANO, D., RINI, B. I., CHEN, A. C., MEKAN, S., MCHENRY, M. B., WIND-ROTOLO, M., DOAN, J., SHARMA, P., HAMMERS, H. J. & ESCUDIER, B. 2018. Nivolumab plus Ipilimumab versus Sunitinib in Advanced Renal-Cell Carcinoma. *New England Journal of Medicine,* 378**,** 1277-1290.

MULLER, D., FREY, K. & KONTERMANN, R. E. 2008. A novel antibody-4-1BBL fusion protein for targeted costimulation in cancer immunotherapy. *J Immunother,* 31**,** 714-22.

MULLER-HERMELINK, N., BRAUMULLER, H., PICHLER, B., WIEDER, T., MAILHAMMER, R., SCHAAK, K., GHORESCHI, K., YAZDI, A., HAUBNER, R., SANDER, C. A., MOCIKAT, R., SCHWAIGER, M., FORSTER, I., HUSS, R., WEBER, W. A., KNEILLING, M. & ROCKEN, M. 2008. TNFR1 signaling and IFN-gamma signaling determine whether T cells induce tumor dormancy or promote multistage carcinogenesis. *Cancer Cell,* 13**,** 507-18.

MUSSAWY, H., VIEZENS, L., SCHROEDER, M., HETTENHAUSEN, S., SUNDERMANN, J., WELLBROCK, J., KOSSOW, K. & SCHAEFER, C. 2018. The bone microenvironment promotes tumor growth and tissue perfusion compared with striated muscle in a preclinical model of prostate cancer in vivo. *BMC Cancer,* 18**,** 979.

NADA, M. H., WANG, H., WORKALEMAHU, G., TANAKA, Y. & MORITA, C. T. 2017. Enhancing adoptive cancer immunotherapy with Vgamma2Vdelta2 T cells through pulse zoledronate stimulation. *J Immunother Cancer,* 5**,** 9.

NADLER, L. M., STASHENKO, P., HARDY, R., KAPLAN, W. D., BUTTON, L. N., KUFE, D. W., ANTMAN, K. H. & SCHLOSSMAN, S. F. 1980. Serotherapy of a patient with a monoclonal antibody directed against a human lymphoma-associated antigen. *Cancer Res,* 40**,** 3147-54.

NAMEKAWA, T., IKEDA, K., HORIE-INOUE, K. & INOUE, S. 2019. Application of Prostate Cancer Models for Preclinical Study: Advantages and Limitations of Cell Lines, Patient-Derived Xenografts, and Three-Dimensional Culture of Patient-Derived Cells. *Cells,* 8.

NARAYAN, V., GLADNEY, W., PLESA, G., VAPIWALA, N., CARPENTER, E., MAUDE, S. L., LAL, P., LACEY, S. F., MELENHORST, J. J., SEBRO, R.,

FARWELL, M., HWANG, W.-T., MONIAK, M., GILMORE, J., LLEDO, L., DENGEL, K., MARSHALL, A., COUGHLIN, C. M., JUNE, C. H. & HAAS, N. B. 2019. A phase I clinical trial of PSMA-directed/TGFβ-insensitive CAR-T cells in metastatic castration-resistant prostate cancer. *Journal of Clinical Oncology,* 37**,** TPS347-TPS347.

NATIONAL COLLABORATING CENTRE FOR CANCER (UK) Prostate Cancer: Diagnosis and Treatment. Cardiff (UK): National Collaborating Centre for Cancer (UK); 2014 Jan. (NICE Clinical Guidelines, No. 175.).

NEAL, J. T., LI, X., ZHU, J., GIANGARRA, V., GRZESKOWIAK, C. L., JU, J., LIU, I. H., CHIOU, S. H., SALAHUDEEN, A. A., SMITH, A. R., DEUTSCH, B. C., LIAO, L., ZEMEK, A. J., ZHAO, F., KARLSSON, K., SCHULTZ, L. M., METZNER, T. J., NADAULD, L. D., TSENG, Y. Y., ALKHAIRY, S., OH, C., KESKULA, P., MENDOZA-VILLANUEVA, D., DE LA VEGA, F. M., KUNZ, P. L., LIAO, J. C., LEPPERT, J. T., SUNWOO, J. B., SABATTI, C., BOEHM, J. S., HAHN, W. C., ZHENG, G. X. Y., DAVIS, M. M. & KUO, C. J. 2018. Organoid Modeling of the Tumor Immune Microenvironment. *Cell,* 175**,** 1972-1988.e16.

NEELAPU, S. S., LOCKE, F. L., BARTLETT, N. L., LEKAKIS, L. J., MIKLOS, D. B., JACOBSON, C. A., BRAUNSCHWEIG, I., OLUWOLE, O. O., SIDDIQI, T., LIN, Y., TIMMERMAN, J. M., STIFF, P. J., FRIEDBERG, J. W., FLINN, I. W., GOY, A., HILL, B. T., SMITH, M. R., DEOL, A., FAROOQ, U., MCSWEENEY, P., MUNOZ, J., AVIVI, I., CASTRO, J. E., WESTIN, J. R., CHAVEZ, J. C., GHOBADI, A., KOMANDURI, K. V., LEVY, R., JACOBSEN, E. D., WITZIG, T. E., REAGAN, P., BOT, A., ROSSI, J., NAVALE, L., JIANG, Y., AYCOCK, J., ELIAS, M., CHANG, D., WIEZOREK, J. & GO, W. Y. 2017. Axicabtagene Ciloleucel CAR T-Cell Therapy in Refractory Large B-Cell Lymphoma. *N Engl J Med,* 377**,** 2531-2544.

NEVALA, W. K., VACHON, C. M., LEONTOVICH, A. A., SCOTT, C. G., THOMPSON, M. A., MARKOVIC, S. N. & MELANOMA STUDY GROUP OF THE MAYO CLINIC CANCER, C. 2009. Evidence of systemic Th2-driven chronic inflammation in patients with metastatic melanoma. *Clin Cancer Res,* 15**,** 1931-9.

NEVEDOMSKAYA, E., BAUMGART, S. J. & HAENDLER, B. 2018. Recent Advances in Prostate Cancer Treatment and Drug Discovery. *Int J Mol Sci,* 19.

NEWICK, K., O'BRIEN, S., SUN, J., KAPOOR, V., MACEYKO, S., LO, A., PURE, E., MOON, E. & ALBELDA, S. M. 2016. Augmentation of CAR T-cell Trafficking and Antitumor Efficacy by Blocking Protein Kinase A Localization. *Cancer Immunol Res,* 4**,** 541-51.

NICHOLAOU, T., CHEN, W., DAVIS, I. D., JACKSON, H. M., DIMOPOULOS, N., BARROW, C., BROWNING, J., MACGREGOR, D., WILLIAMS, D., HOPKINS, W., MARASKOVSKY, E., VENHAUS, R., PAN, L., HOFFMAN, E. W., OLD, L. J. & CEBON, J. 2011. Immunoediting and persistence of antigen-specific immunity in patients who have previously been vaccinated with NY-ESO-1 protein formulated in ISCOMATRIX. *Cancer Immunol Immunother,* 60**,** 1625-37.

NIEDERMEYER, J., KRIZ, M., HILBERG, F., GARIN-CHESA, P., BAMBERGER, U., LENTER, M. C., PARK, J., VIERTEL, B., PUSCHNER, H., MAUZ, M., RETTIG, W. J. & SCHNAPP, A. 2000. Targeted disruption of mouse fibroblast activation protein. *Mol Cell Biol,* 20**,** 1089-94.

NIEDERMEYER, J., SCANLAN, M. J., GARIN-CHESA, P., DAIBER, C., FIEBIG, H. H., OLD, L. J., RETTIG, W. J. & SCHNAPP, A. 1997. Mouse fibroblast

activation protein: molecular cloning, alternative splicing and expression in the reactive stroma of epithelial cancers. *Int J Cancer,* 71**,** 383-9.

NISHIMURA, H., MINATO, N., NAKANO, T. & HONJO, T. 1998. Immunological studies on PD-1 deficient mice: implication of PD-1 as a negative regulator for B cell responses. *Int Immunol,* 10**,** 1563-72.

NISHIMURA, H., NOSE, M., HIAI, H., MINATO, N. & HONJO, T. 1999. Development of lupus-like autoimmune diseases by disruption of the PD-1 gene encoding an ITIM motif-carrying immunoreceptor. *Immunity,* 11**,** 141-51.

O'SULLIVAN, T., SADDAWI-KONEFKA, R., VERMI, W., KOEBEL, C. M., ARTHUR, C., WHITE, J. M., UPPALURI, R., ANDREWS, D. M., NGIOW, S. F., TENG, M. W., SMYTH, M. J., SCHREIBER, R. D. & BUI, J. D. 2012. Cancer immunoediting by the innate immune system in the absence of adaptive immunity. *J Exp Med,* 209**,** 1869-82.

OBIRI, N. I., HILLMAN, G. G., HAAS, G. P., SUD, S. & PURI, R. K. 1993. Expression of high affinity interleukin-4 receptors on human renal cell carcinoma cells and inhibition of tumor cell growth in vitro by interleukin-4. *J Clin Invest,* 91**,** 88-93.

OHSHIO, Y., TERAMOTO, K., HANAOKA, J., TEZUKA, N., ITOH, Y., ASAI, T., DAIGO, Y. & OGASAWARA, K. 2015. Cancer-associated fibroblast-targeted strategy enhances antitumor immune responses in dendritic cell-based vaccine. *Cancer Sci,* 106**,** 134-42.

OKAMURA, H., TSUTSUI, H., KOMATSU, T., YUTSUDO, M., HAKURA, A., TANIMOTO, T., TORIGOE, K., OKURA, T., NUKADA, Y., HATTORI, K., AKITA, K., NAMBA, M., TANABE, F., KONISHI, K., FUKUDA, S. & KURIMOTO, M. 1995. Cloning of a new cytokine that induces IFN-γ production by T cells. *Nature,* 378**,** 88-91.

OLSON, W. C., HESTON, W. D. & RAJASEKARAN, A. K. 2007. Clinical trials of cancer therapies targeting prostate-specific membrane antigen. *Rev Recent Clin Trials,* 2**,** 182-90.

OLVER, S., APTE, S., BAZ, A. & KIENZLE, N. 2007. The duplicitous effects of interleukin 4 on tumour immunity: how can the same cytokine improve or impair control of tumour growth? *Tissue Antigens,* 69**,** 293-8.

ONISHI, T., OHISHI, Y., GOTO, H., TOMITA, M. & ABE, K. 2001. An assessment of the immunological status of patients with renal cell carcinoma based on the relative abundance of T-helper 1- and -2 cytokine-producing CD4+ cells in peripheral blood. *BJU Int,* 87**,** 755-9.

ORIMO, A., GUPTA, P.B., SGROI, D.C., ARENZANA-SEISDEDOS, F., DELAUNAY, T., NAEEM, R., CAREY, V.J., RICHARDSON, A.L., WEINBERG, R.A., 2005. Stromal fibroblasts present in invasive human breast carcinomas promote tumor growth and angiogenesis through elevated SDF-1/CXCL12 secretion. Cell 121, 335–348. https://doi.org/10.1016/j.cell.2005.02.034

OTOMO, R., OTSUBO, C., MATSUSHIMA-HIBIYA, Y., MIYAZAKI, M., TASHIRO, F., ICHIKAWA, H., KOHNO, T., OCHIYA, T., YOKOTA, J., NAKAGAMA, H., TAYA, Y., ENARI, M., 2014. TSPAN12 is a critical factor for cancer-fibroblast cell contact-mediated cancer invasion. Proc. Natl. Acad. Sci. U. S. A. 111, 18691–18696. https://doi.org/10.1073/pnas.1412062112

OVERMAN, M. J., LONARDI, S., WONG, K. Y. M., LENZ, H. J., GELSOMINO, F., AGLIETTA, M., MORSE, M. A., VAN CUTSEM, E., MCDERMOTT, R., HILL, A., SAWYER, M. B., HENDLISZ, A., NEYNS, B., SVRCEK, M., MOSS, R. A., LEDEINE, J. M., CAO, Z. A., KAMBLE, S., KOPETZ, S. & ANDRE, T. 2018. Durable Clinical Benefit With Nivolumab Plus Ipilimumab in DNA

Mismatch Repair-Deficient/Microsatellite Instability-High Metastatic Colorectal Cancer. *J Clin Oncol,* 36**,** 773-779.

PALMER-CROCKER, R. L., HUGHES, C. C. & POBER, J. S. 1996. IL-4 and IL-13 activate the JAK2 tyrosine kinase and Stat6 in cultured human vascular endothelial cells through a common pathway that does not involve the gamma c chain. *J Clin Invest,* 98**,** 604-9.

PANSKY, A., HILDEBRAND, P., FASLER-KAN, E., BASELGIA, L., KETTERER, S., BEGLINGER, C. & HEIM, M. H. 2000. Defective Jak-STAT signal transduction pathway in melanoma cells resistant to growth inhibition by interferon-alpha. *Int J Cancer,* 85**,** 720-5.

PAPADIA, F., BASSO, V., PATUZZO, R., MAURICHI, A., DI FLORIO, A., ZARDI, L., VENTURA, E., GONZÁLEZ-IGLESIAS, R., LOVATO, V., GIOVANNONI, L., TASCIOTTI, A., NERI, D., SANTINAMI, M., MENSSEN, H. D. & DE CIAN, F. 2013. Isolated limb perfusion with the tumor-targeting human monoclonal antibody-cytokine fusion protein L19-TNF plus melphalan and mild hyperthermia in patients with locally advanced extremity melanoma. *Journal of Surgical Oncology,* 107**,** 173-179.

PARK, J. E., LENTER, M. C., ZIMMERMANN, R. N., GARIN-CHESA, P., OLD, L. J. & RETTIG, W. J. 1999. Fibroblast activation protein, a dual specificity serine protease expressed in reactive human tumor stromal fibroblasts. *J Biol Chem,* 274**,** 36505-12.

PARKHURST, M. R., YANG, J. C., LANGAN, R. C., DUDLEY, M. E., NATHAN, D. A., FELDMAN, S. A., DAVIS, J. L., MORGAN, R. A., MERINO, M. J., SHERRY, R. M., HUGHES, M. S., KAMMULA, U. S., PHAN, G. Q., LIM, R. M., WANK, S. A., RESTIFO, N. P., ROBBINS, P. F., LAURENCOT, C. M. & ROSENBERG, S. A. 2011. T cells targeting carcinoembryonic antigen can mediate regression of metastatic colorectal cancer but induce severe transient colitis. *Mol Ther,* 19**,** 620-6.

PARRY, R. V., CHEMNITZ, J. M., FRAUWIRTH, K. A., LANFRANCO, A. R., BRAUNSTEIN, I., KOBAYASHI, S. V., LINSLEY, P. S., THOMPSON, C. B. & RILEY, J. L. 2005. CTLA-4 and PD-1 receptors inhibit T-cell activation by distinct mechanisms. *Mol Cell Biol,* 25**,** 9543-53.

PASERO, C., GRAVIS, G., GUERIN, M., GRANJEAUD, S., THOMASSIN-PIANA, J., ROCCHI, P., PACIENCIA-GROS, M., POIZAT, F., BENTOBJI, M., AZARIO-CHEILLAN, F., WALZ, J., SALEM, N., BRUNELLE, S., MORETTA, A. & OLIVE, D. 2016. Inherent and Tumor-Driven Immune Tolerance in the Prostate Microenvironment Impairs Natural Killer Cell Antitumor Activity. *Cancer Res,* 76**,** 2153-65.

PATNAIK, A., KANG, S. P., RASCO, D., PAPADOPOULOS, K. P., ELASSAISS-SCHAAP, J., BEERAM, M., DRENGLER, R., CHEN, C., SMITH, L., ESPINO, G., GERGICH, K., DELGADO, L., DAUD, A., LINDIA, J. A., LI, X. N., PIERCE, R. H., YEARLEY, J. H., WU, D., LATERZA, O., LEHNERT, M., IANNONE, R. & TOLCHER, A. W. 2015. Phase I Study of Pembrolizumab (MK-3475; Anti-PD-1 Monoclonal Antibody) in Patients with Advanced Solid Tumors. *Clin Cancer Res,* 21**,** 4286-93.

PAZOLLI, E., LUO, X., BREHM, S., CARBERY, K., CHUNG, J.-J., PRIOR, J.L., DOHERTY, J., DEMEHRI, S., SALAVAGGIONE, L., PIWNICA-WORMS, D., STEWART, S.A., 2009. Senescent stromal-derived osteopontin promotes preneoplastic cell growth. Cancer Res. 69, 1230–1239. https://doi.org/10.1158/0008-5472.CAN-08-2970

PEDROZA-GONZALEZ, A., XU, K., WU, T. C., ASPORD, C., TINDLE, S., MARCHES, F., GALLEGOS, M., BURTON, E. C., SAVINO, D., HORI, T., TANAKA, Y., ZURAWSKI, S., ZURAWSKI, G., BOVER, L., LIU, Y. J., BANCHEREAU, J. & PALUCKA, A. K. 2011. Thymic stromal lymphopoietin fosters human breast tumor growth by promoting type 2 inflammation. *J Exp Med,* 208**,** 479-90.

PENN, I. 1995. Sarcomas in organ allograft recipients. *Transplantation,* 60**,** 1485-91.

PENN, I. 1999. Posttransplant malignancies. *Transplant Proc,* 31**,** 1260-2.

PETRAUSCH, U., SCHUBERTH, P. C., HAGEDORN, C., SOLTERMANN, A., TOMASZEK, S., STAHEL, R., WEDER, W. & RENNER, C. 2012. Re-directed T cells for the treatment of fibroblast activation protein (FAP)-positive malignant pleural mesothelioma (FAPME-1). *BMC Cancer,* 12**,** 615.

PETROVIC, B., LEONI, V., GATTA, V., ZAGHINI, A., VANNINI, A. & CAMPADELLI-FIUME, G. 2018. Dual Ligand Insertion in gB and gD of Oncolytic Herpes Simplex Viruses for Retargeting to a Producer Vero Cell Line and to Cancer Cells. *J Virol,* 92.

PICKLES, T., KEYES, M. & MORRIS, W. J. 2010. Brachytherapy or conformal external radiotherapy for prostate cancer: a single-institution matched-pair analysis. *Int J Radiat Oncol Biol Phys,* 76**,** 43-9.

PINTHUS, J. H., WAKS, T., KAUFMAN-FRANCIS, K., SCHINDLER, D. G., HARMELIN, A., KANETY, H., RAMON, J. & ESHHAR, Z. 2003. Immuno-gene therapy of established prostate tumors using chimeric receptor-redirected human lymphocytes. *Cancer Res,* 63**,** 2470-6.

PINTO, J. T., SUFFOLETTO, B. P., BERZIN, T. M., QIAO, C. H., LIN, S., TONG, W. P., MAY, F., MUKHERJEE, B. & HESTON, W. D. 1996. Prostate-specific membrane antigen: a novel folate hydrolase in human prostatic carcinoma cells. *Clin Cancer Res,* 2**,** 1445-51.

PLACENCIO, V. R., LI, X., SHERRILL, T. P., FRITZ, G. & BHOWMICK, N. A. 2010. Bone marrow derived mesenchymal stem cells incorporate into the prostate during regrowth. *PLoS One,* 5**,** e12920.

PORTER, D. L., HWANG, W. T., FREY, N. V., LACEY, S. F., SHAW, P. A., LOREN, A. W., BAGG, A., MARCUCCI, K. T., SHEN, A., GONZALEZ, V., AMBROSE, D., GRUPP, S. A., CHEW, A., ZHENG, Z., MILONE, M. C., LEVINE, B. L., MELENHORST, J. J. & JUNE, C. H. 2015. Chimeric antigen receptor T cells persist and induce sustained remissions in relapsed refractory chronic lymphocytic leukemia. *Sci Transl Med,* 7**,** 303ra139.

POTTER, G. A., BARRIE, S. E., JARMAN, M. & ROWLANDS, M. G. 1995. Novel Steroidal Inhibitors of Human Cytochrome P45017.alpha.-Hydroxylase-C17,20-lyase): Potential Agents for the Treatment of Prostatic Cancer. *Journal of Medicinal Chemistry,* 38**,** 2463-2471.

POWERS, D. B., AMERSDORFER, P., POUL, M., NIELSEN, U. B., SHALABY, M. R., ADAMS, G. P., WEINER, L. M. & MARKS, J. D. 2001. Expression of single-chain Fv-Fc fusions in Pichia pastoris. *J Immunol Methods,* 251**,** 123-35.

PRENDIVILLE, J., THATCHER, N., LIND, M., MCINTOSH, R., GHOSH, A., STERN, P. & CROWTHER, D. 1993. Recombinant human interleukin-4 (rhu IL-4) administered by the intravenous and subcutaneous routes in patients with advanced cancer--a phase I toxicity study and pharmacokinetic analysis. *Eur J Cancer,* 29a**,** 1700-7.

PROKOPCHUK, O., LIU, Y., HENNE-BRUNS, D. & KORNMANN, M. 2005. Interleukin-4 enhances proliferation of human pancreatic cancer cells: evidence for autocrine and paracrine actions. *Br J Cancer,* 92**,** 921-8.

PROVASI, E., GENOVESE, P., LOMBARDO, A., MAGNANI, Z., LIU, P. Q., REIK, A., CHU, V., PASCHON, D. E., ZHANG, L., KUBALL, J., CAMISA, B., BONDANZA, A., CASORATI, G., PONZONI, M., CICERI, F., BORDIGNON, C., GREENBERG, P. D., HOLMES, M. C., GREGORY, P. D., NALDINI, L. & BONINI, C. 2012. Editing T cell specificity towards leukemia by zinc finger nucleases and lentiviral gene transfer. *Nat Med,* 18**,** 807-815.

PTACKOVA, P., MUSIL, J., STACH, M., LESNY, P., NEMECKOVA, S., KRAL, V., FABRY, M. & OTAHAL, P. 2018. A new approach to CAR T-cell gene engineering and cultivation using piggyBac transposon in the presence of IL-4, IL-7 and IL-21. *Cytotherapy,* 20**,** 507-520.

PULE, M. A., STRAATHOF, K. C., DOTTI, G., HESLOP, H. E., ROONEY, C. M. & BRENNER, M. K. 2005. A chimeric T cell antigen receptor that augments cytokine release and supports clonal expansion of primary human T cells. *Mol Ther,* 12**,** 933-41.

PUZANOV, I., MILHEM, M. M., MINOR, D., HAMID, O., LI, A., CHEN, L., CHASTAIN, M., GORSKI, K. S., ANDERSON, A., CHOU, J., KAUFMAN, H. L. & ANDTBACKA, R. H. 2016. Talimogene Laherparepvec in Combination With Ipilimumab in Previously Untreated, Unresectable Stage IIIB-IV Melanoma. *J Clin Oncol,* 34**,** 2619-26.

QIU, W., HU, M., SRIDHAR, A., OPESKIN, K., FOX, S., SHIPITSIN, M., TRIVETT, M., THOMPSON, E. R., RAMAKRISHNA, M., GORRINGE, K. L., POLYAK, K., HAVIV, I. & CAMPBELL, I. G. 2008. No evidence of clonal somatic genetic alterations in cancer-associated fibroblasts from human breast and ovarian carcinomas. *Nat Genet,* 40**,** 650-5.

QUANTE, M., TU, S.P., TOMITA, H., GONDA, T., WANG, S.S.W., TAKASHI, S., BAIK, G.H., SHIBATA, W., DIPRETE, B., BETZ, K.S., FRIEDMAN, R., VARRO, A., TYCKO, B., WANG, T.C., 2011. Bone marrow-derived myofibroblasts contribute to the mesenchymal stem cell niche and promote tumor growth. Cancer Cell 19, 257–272. https://doi.org/10.1016/j.ccr.2011.01.020

QUATTRONE, F., SANCHEZ, A. M., PANNESE, M., HEMMERLE, T., VIGANO, P., CANDIANI, M., PETRAGLIA, F., NERI, D. & PANINA-BORDIGNON, P. 2015. The Targeted Delivery of Interleukin 4 Inhibits Development of Endometriotic Lesions in a Mouse Model. *Reprod Sci,* 22**,** 1143-52.

QUINTARELLI, C., ORLANDO, D., BOFFA, I., GUERCIO, M., POLITO, V. A., PETRETTO, A., LAVARELLO, C., SINIBALDI, M., WEBER, G., DEL BUFALO, F., GIORDA, E., SCARSELLA, M., PETRINI, S., PAGLIARA, D., LOCATELLI, F., DE ANGELIS, B. & CARUANA, I. 2018. Choice of costimulatory domains and of cytokines determines CAR T-cell activity in neuroblastoma. *Oncoimmunology,* 7**,** e1433518.

RAHBAR, K., AHMADZADEHFAR, H. & BOEGEMANN, M. 2018. (177)Lu-PSMA-617 radioligand therapy in mCRPC: ready for phase III trial? *Eur J Nucl Med Mol Imaging,* 45**,** 513-514.

RAHBAR, K., AHMADZADEHFAR, H., KRATOCHWIL, C., HABERKORN, U., SCHAFERS, M., ESSLER, M., BAUM, R. P., KULKARNI, H. R., SCHMIDT, M., DRZEZGA, A., BARTENSTEIN, P., PFESTROFF, A., LUSTER, M., LUTZEN, U., MARX, M., PRASAD, V., BRENNER, W., HEINZEL, A., MOTTAGHY, F. M., RUF, J., MEYER, P. T., HEUSCHKEL, M., EVESLAGE, M., BOGEMANN, M., FENDLER, W. P. & KRAUSE, B. J. 2017. German Multicenter Study Investigating 177Lu-PSMA-617 Radioligand Therapy in Advanced Prostate Cancer Patients. *J Nucl Med,* 58**,** 85-90.

RAJ, D., YANG, M. H., RODGERS, D., HAMPTON, E. N., BEGUM, J., MUSTAFA, A., LORIZIO, D., GARCES, I., PROPPER, D., KENCH, J. G., KOCHER, H. M., YOUNG, T. S., AICHER, A. & HEESCHEN, C. 2019. Switchable CAR-T cells mediate remission in metastatic pancreatic ductal adenocarcinoma. *Gut,* 68**,** 1052-1064.

RAPP, M., GRASSMANN, S., CHALOUPKA, M., LAYRITZ, P., KRUGER, S., ORMANNS, S., RATAJ, F., JANSSEN, K. P., ENDRES, S., ANZ, D. & KOBOLD, S. 2016. C-C chemokine receptor type-4 transduction of T cells enhances interaction with dendritic cells, tumor infiltration and therapeutic efficacy of adoptive T cell transfer. *Oncoimmunology,* 5**,** e1105428.

REED, J. C., MEISTER, L., TANAKA, S., CUDDY, M., YUM, S., GEYER, C. & PLEASURE, D. 1991. Differential expression of bcl2 protooncogene in neuroblastoma and other human tumor cell lines of neural origin. *Cancer Res,* 51**,** 6529-38.

RENNER, C., FISCHER, E., BAUER, S. & WUEST, T. 2012. Anti-Fibroblast Activation Protein Antibodies and Methods and Uses Thereof. 13/499,718.

RESTIFO, N. P., ESQUIVEL, F., KAWAKAMI, Y., YEWDELL, J. W., MULE, J. J., ROSENBERG, S. A. & BENNINK, J. R. 1993. Identification of human cancers deficient in antigen processing. *J Exp Med,* 177**,** 265-72.

RETTIG, W. J., CHESA, P. G., BERESFORD, H. R., FEICKERT, H. J., JENNINGS, M. T., COHEN, J., OETTGEN, H. F. & OLD, L. J. 1986. Differential expression of cell surface antigens and glial fibrillary acidic protein in human astrocytoma subsets. *Cancer Res,* 46**,** 6406-12.

RETTIG, W. J., GARIN-CHESA, P., BERESFORD, H. R., OETTGEN, H. F., MELAMED, M. R. & OLD, L. J. 1988. Cell-surface glycoproteins of human sarcomas: differential expression in normal and malignant tissues and cultured cells. *Proc Natl Acad Sci U S A,* 85**,** 3110-4.

RIBAS, A., DUMMER, R., PUZANOV, I., VANDERWALDE, A., ANDTBACKA, R. H. I., MICHIELIN, O., OLSZANSKI, A. J., MALVEHY, J., CEBON, J., FERNANDEZ, E., KIRKWOOD, J. M., GAJEWSKI, T. F., CHEN, L., GORSKI, K. S., ANDERSON, A. A., DIEDE, S. J., LASSMAN, M. E., GANSERT, J., HODI, F. S. & LONG, G. V. 2017. Oncolytic Virotherapy Promotes Intratumoral T Cell Infiltration and Improves Anti-PD-1 Immunotherapy. *Cell,* 170**,** 1109-1119.e10.

RIBAS, A., KIRKWOOD, J. M., ATKINS, M. B., WHITESIDE, T. L., GOODING, W., KOVAR, A., GILLIES, S. D., KASHALA, O. & MORSE, M. A. 2009. Phase I/II open-label study of the biologic effects of the interleukin-2 immunocytokine EMD 273063 (hu14.18-IL2) in patients with metastatic malignant melanoma. *J Transl Med,* 7**,** 68.

RIBAS, A., PUZANOV, I., GAJEWSKI, T., LONG, G. V., DUMMER, R., KIRKWOOD, J. M., VANDERWALDE, A., CEBON, J. S., MCARTHUR, G. A., GAUSE, C. K., CHEN, L., KAUFMAN, D. R., CHOU, J., ANDTBACKA, R. H. I. & HODI, F. S. 2015. A multicenter, open-label trial of talimogene laherparepvec (T-VEC) plus pembrolizumab vs pembrolizumab monotherapy in previously untreated, unresected, stage IIIB-IV melanoma. *Journal of Clinical Oncology,* 33**,** TPS9081-TPS9081.

RICE, A. E., LATCHMAN, Y. E., BALINT, J. P., LEE, J. H., GABITZSCH, E. S. & JONES, F. R. 2015. An HPV-E6/E7 immunotherapy plus PD-1 checkpoint inhibition results in tumor regression and reduction in PD-L1 expression. *Cancer Gene Ther,* 22**,** 454-62.

RICHARDS, K.E., ZELENIAK, A.E., FISHEL, M.L., WU, J., LITTLEPAGE, L.E., HILL, R., 2017. Cancer-associated fibroblast exosomes regulate survival and

proliferation of pancreatic cancer cells. Oncogene 36, 1770–1778. https://doi.org/10.1038/onc.2016.353

RIVERA, A., FU, X., TAO, L. & ZHANG, X. 2015. Expression of mouse CD47 on human cancer cells profoundly increases tumor metastasis in murine models. *BMC Cancer,* 15**,** 964.

RIVIERE, I., BROSE, K. & MULLIGAN, R. C. 1995. Effects of retroviral vector design on expression of human adenosine deaminase in murine bone marrow transplant recipients engrafted with genetically modified cells. *Proc Natl Acad Sci U S A,* 92**,** 6733-7.

ROBBINS, P. F., MORGAN, R. A., FELDMAN, S. A., YANG, J. C., SHERRY, R. M., DUDLEY, M. E., WUNDERLICH, J. R., NAHVI, A. V., HELMAN, L. J., MACKALL, C. L., KAMMULA, U. S., HUGHES, M. S., RESTIFO, N. P., RAFFELD, M., LEE, C. C., LEVY, C. L., LI, Y. F., EL-GAMIL, M., SCHWARZ, S. L., LAURENCOT, C. & ROSENBERG, S. A. 2011. Tumor regression in patients with metastatic synovial cell sarcoma and melanoma using genetically engineered lymphocytes reactive with NY-ESO-1. *J Clin Oncol,* 29**,** 917-24.

ROCHA, B. & TANCHOT, C. 2004. Towards a cellular definition of CD8+ T-cell memory: the role of CD4+ T-cell help in CD8+ T-cell responses. *Curr Opin Immunol,* 16**,** 259-63.

RODGERS, D. T., MAZAGOVA, M., HAMPTON, E. N., CAO, Y., RAMADOSS, N. S., HARDY, I. R., SCHULMAN, A., DU, J., WANG, F., SINGER, O., MA, J., NUNEZ, V., SHEN, J., WOODS, A. K., WRIGHT, T. M., SCHULTZ, P. G., KIM, C. H. & YOUNG, T. S. 2016. Switch-mediated activation and retargeting of CAR-T cells for B-cell malignancies. *Proc Natl Acad Sci U S A,* 113**,** E459-68.

ROSENBERG, S. A. 2014. IL-2: the first effective immunotherapy for human cancer. *J Immunol,* 192**,** 5451-8.

ROSENBERG, S. A., LOTZE, M. T., YANG, J. C., TOPALIAN, S. L., CHANG, A. E., SCHWARTZENTRUBER, D. J., AEBERSOLD, P., LEITMAN, S., LINEHAN, W. M., SEIPP, C. A. & ET AL. 1993. Prospective randomized trial of high-dose interleukin-2 alone or in conjunction with lymphokine-activated killer cells for the treatment of patients with advanced cancer. *J Natl Cancer Inst,* 85**,** 622-32.

ROSENBERG, S. A., PACKARD, B. S., AEBERSOLD, P. M., SOLOMON, D., TOPALIAN, S. L., TOY, S. T., SIMON, P., LOTZE, M. T., YANG, J. C., SEIPP, C. A. & ET AL. 1988. Use of tumor-infiltrating lymphocytes and interleukin-2 in the immunotherapy of patients with metastatic melanoma. A preliminary report. *N Engl J Med,* 319**,** 1676-80.

ROSENBERG, S. A., SPIESS, P. & LAFRENIERE, R. 1986. A new approach to the adoptive immunotherapy of cancer with tumor-infiltrating lymphocytes. *Science,* 233**,** 1318-21.

ROSENBERG, S. A., YANG, J. C., SHERRY, R. M., KAMMULA, U. S., HUGHES, M. S., PHAN, G. Q., CITRIN, D. E., RESTIFO, N. P., ROBBINS, P. F., WUNDERLICH, J. R., MORTON, K. E., LAURENCOT, C. M., STEINBERG, S. M., WHITE, D. E. & DUDLEY, M. E. 2011. Durable complete responses in heavily pretreated patients with metastatic melanoma using T-cell transfer immunotherapy. *Clin Cancer Res,* 17**,** 4550-7.

ROTH, M. D. & HARUI, A. 2015. Human tumor infiltrating lymphocytes cooperatively regulate prostate tumor growth in a humanized mouse model. *J Immunother Cancer,* 3**,** 12.

ROYBAL, K. T., RUPP, L. J., MORSUT, L., WALKER, W. J., MCNALLY, K. A., PARK, J. S. & LIM, W. A. 2016. Precision Tumor Recognition by T Cells With Combinatorial Antigen-Sensing Circuits. *Cell,* 164**,** 770-9.

RUBINSTEIN, N., ALVAREZ, M., ZWIRNER, N. W., TOSCANO, M. A., ILARREGUI, J. M., BRAVO, A., MORDOH, J., FAINBOIM, L., PODHAJCER, O. L. & RABINOVICH, G. A. 2004. Targeted inhibition of galectin-1 gene expression in tumor cells results in heightened T cell-mediated rejection; A potential mechanism of tumor-immune privilege. *Cancer Cell,* 5**,** 241-51.

RUDMAN, S. M., JAMESON, M. B., MCKEAGE, M. J., SAVAGE, P., JODRELL, D. I., HARRIES, M., ACTON, G., ERLANDSSON, F. & SPICER, J. F. 2011. A phase 1 study of AS1409, a novel antibody-cytokine fusion protein, in patients with malignant melanoma or renal cell carcinoma. *Clin Cancer Res,* 17**,** 1998-2005.

RUELLA, M., BARRETT, D. M., KENDERIAN, S. S., SHESTOVA, O., HOFMANN, T. J., PERAZZELLI, J., KLICHINSKY, M., AIKAWA, V., NAZIMUDDIN, F., KOZLOWSKI, M., SCHOLLER, J., LACEY, S. F., MELENHORST, J. J., MORRISSETTE, J. J., CHRISTIAN, D. A., HUNTER, C. A., KALOS, M., PORTER, D. L., JUNE, C. H., GRUPP, S. A. & GILL, S. 2016. Dual CD19 and CD123 targeting prevents antigen-loss relapses after CD19-directed immunotherapies. *J Clin Invest,* 126**,** 3814-3826.

RUSSELL, P. J., RUSSELL, P., RUDDUCK, C., TSE, B. W., WILLIAMS, E. D. & RAGHAVAN, D. 2015. Establishing prostate cancer patient derived xenografts: lessons learned from older studies. *Prostate,* 75**,** 628-36.

SADLONOVA, A., BOWE, D.B., NOVAK, Z., MUKHERJEE, S., DUNCAN, V.E., PAGE, G.P., FROST, A.R., 2009. Identification of molecular distinctions between normal breast-associated fibroblasts and breast cancer-associated fibroblasts. Cancer Microenviron. Off. J. Int. Cancer Microenviron. Soc. 2, 9–21. https://doi.org/10.1007/s12307-008-0017-0

SALMON, H., FRANCISZKIEWICZ, K., DAMOTTE, D., DIEU-NOSJEAN, M.-C., VALIDIRE, P., TRAUTMANN, A., MAMI-CHOUAIB, F., DONNADIEU, E., 2012. Matrix architecture defines the preferential localization and migration of T cells into the stroma of human lung tumors. J. Clin. Invest. 122, 899–910. https://doi.org/10.1172/JCI45817

SALTER, A. I., IVEY, R. G., KENNEDY, J. J., VOILLET, V., RAJAN, A., ALDERMAN, E. J., VOYTOVICH, U. J., LIN, C., SOMMERMEYER, D., LIU, L., WHITEAKER, J. R., GOTTARDO, R., PAULOVICH, A. G. & RIDDELL, S. R. 2018. Phosphoproteomic analysis of chimeric antigen receptor signaling reveals kinetic and quantitative differences that affect cell function. *Sci Signal,* 11.

SANCHEZ, C., CHAN, R., BAJGAIN, P., RAMBALLY, S., PALAPATTU, G., MIMS, M., ROONEY, C. M., LEEN, A. M., BRENNER, M. K. & VERA, J. F. 2013. Combining T-cell immunotherapy and anti-androgen therapy for prostate cancer. *Prostate Cancer Prostatic Dis,* 16**,** 123-31, s1.

SANDERSON, S., VALENTI, M., GOWAN, S., PATTERSON, L., AHMAD, Z., WORKMAN, P. & ECCLES, S. A. 2006. Benzoquinone ansamycin heat shock protein 90 inhibitors modulate multiple functions required for tumor angiogenesis. *Mol Cancer Ther,* 5**,** 522-32.

SANTORO, S. P., KIM, S., MOTZ, G. T., ALATZOGLOU, D., LI, C., IRVING, M., POWELL, D. J., JR. & COUKOS, G. 2015. T cells bearing a chimeric antigen receptor against prostate-specific membrane antigen mediate vascular disruption and result in tumor regression. *Cancer Immunol Res,* 3**,** 68-84.

SCHADENDORF, D., HODI, F. S., ROBERT, C., WEBER, J. S., MARGOLIN, K., HAMID, O., PATT, D., CHEN, T.-T., BERMAN, D. M. & WOLCHOK, J. D. 2015. Pooled Analysis of Long-Term Survival Data From Phase II and Phase III

Trials of Ipilimumab in Unresectable or Metastatic Melanoma. *Journal of Clinical Oncology,* 33**,** 1889-1894.

SCHER, H. I., FIZAZI, K., SAAD, F., TAPLIN, M.-E., STERNBERG, C. N., MILLER, K., WIT, R. D., MULDERS, P., HIRMAND, M., SELBY, B., BONO, J. S. D. & INVESTIGATORS, F. T. A. 2012. Effect of MDV3100, an androgen receptor signaling inhibitor (ARSI), on overall survival in patients with prostate cancer postdocetaxel: Results from the phase III AFFIRM study. *Journal of Clinical Oncology,* 30**,** LBA1-LBA1.

SCHRECENGOST, R. & KNUDSEN, K. E. 2013. Molecular pathogenesis and progression of prostate cancer. *Semin Oncol,* 40**,** 244-58.

SCHULER, T., KORNIG, S. & BLANKENSTEIN, T. 2003. Tumor rejection by modulation of tumor stromal fibroblasts. *J Exp Med,* 198**,** 1487-93.

SCHUSTER, S. J., BISHOP, M. R., TAM, C., WALLER, E. K., BORCHMANN, P., MCGUIRK, J., JÄGER, U., JAGLOWSKI, S., ANDREADIS, C., WESTIN, J., FLEURY, I., BACHANOVA, V., FOLEY, S. R., HO, P. J., MIELKE, S., HOLTE, H., ANAK, O., PACAUD, L., AWASTHI, R., TAI, F., SALLES, G. & MAZIARZ, R. 2017. GLOBAL PIVOTAL PHASE 2 TRIAL OF THE CD19-TARGETED THERAPY CTL019 IN ADULT PATIENTS WITH RELAPSED OR REFRACTORY (R/R) DIFFUSE LARGE B-CELL LYMPHOMA (DLBCL)—AN INTERIM ANALYSIS. *Hematological Oncology,* 35**,** 27-27.

SCOTT, A. M., WISEMAN, G., WELT, S., ADJEI, A., LEE, F. T., HOPKINS, W., DIVGI, C. R., HANSON, L. H., MITCHELL, P., GANSEN, D. N., LARSON, S. M., INGLE, J. N., HOFFMAN, E. W., TANSWELL, P., RITTER, G., COHEN, L. S., BETTE, P., ARVAY, L., AMELSBERG, A., VLOCK, D., RETTIG, W. J. & OLD, L. J. 2003. A Phase I dose-escalation study of sibrotuzumab in patients with advanced or metastatic fibroblast activation protein-positive cancer. *Clin Cancer Res,* 9**,** 1639-47.

SENGER, D. R., PERRUZZI, C. A., FEDER, J. & DVORAK, H. F. 1986. A highly conserved vascular permeability factor secreted by a variety of human and rodent tumor cell lines. *Cancer Res,* 46**,** 5629-32.

SERGANOVA, I., MOROZ, E., COHEN, I., MOROZ, M., MANE, M., ZURITA, J., SHENKER, L., PONOMAREV, V. & BLASBERG, R. 2017. Enhancement of PSMA-Directed CAR Adoptive Immunotherapy by PD-1/PD-L1 Blockade. *Mol Ther Oncolytics,* 4**,** 41-54.

SFANOS, K. S., BRUNO, T. C., MARIS, C. H., XU, L., THOBURN, C. J., DEMARZO, A. M., MEEKER, A. K., ISAACS, W. B. & DRAKE, C. G. 2008. Phenotypic analysis of prostate-infiltrating lymphocytes reveals TH17 and Treg skewing. *Clin Cancer Res,* 14**,** 3254-61.

SHAFREN, D. R., AU, G. G., NGUYEN, T., NEWCOMBE, N. G., HALEY, E. S., BEAGLEY, L., JOHANSSON, E. S., HERSEY, P. & BARRY, R. D. 2004. Systemic therapy of malignant human melanoma tumors by a common cold-producing enterovirus, coxsackievirus a21. *Clin Cancer Res,* 10**,** 53-60.

SHAFREN, D. R., SYLVESTER, D., JOHANSSON, E. S., CAMPBELL, I. G. & BARRY, R. D. 2005. Oncolysis of human ovarian cancers by echovirus type 1. *Int J Cancer,* 115**,** 320-8.

SHAN, F., CLOSE, D. A., CAMARCO, D. P. & JOHNSTON, P. A. 2018. High-Content Screening Comparison of Cancer Drug Accumulation and Distribution in Two-Dimensional and Three-Dimensional Culture Models of Head and Neck Cancer. *Assay Drug Dev Technol,* 16**,** 27-50.

SHANER, N. C., CAMPBELL, R. E., STEINBACH, P. A., GIEPMANS, B. N., PALMER, A. E. & TSIEN, R. Y. 2004. Improved monomeric red, orange and

yellow fluorescent proteins derived from Discosoma sp. red fluorescent protein. *Nat Biotechnol,* 22**,** 1567-72.

SHANKARAN, V., IKEDA, H., BRUCE, A. T., WHITE, J. M., SWANSON, P. E., OLD, L. J. & SCHREIBER, R. D. 2001. IFNgamma and lymphocytes prevent primary tumour development and shape tumour immunogenicity. *Nature,* 410**,** 1107-11.

SHERMAN, M.H., YU, R.T., ENGLE, D.D., DING, N., ATKINS, A.R., TIRIAC, H., COLLISSON, E.A., CONNOR, F., VAN DYKE, T., KOZLOV, S., MARTIN, P., TSENG, T.W., DAWSON, D.W., DONAHUE, T.R., MASAMUNE, A., SHIMOSEGAWA, T., APTE, M.V., WILSON, J.S., NG, B., LAU, S.L., GUNTON, J.E., WAHL, G.M., HUNTER, T., DREBIN, J.A., O'DWYER, P.J., LIDDLE, C., TUVESON, D.A., DOWNES, M., EVANS, R.M., 2014. Vitamin D receptor-mediated stromal reprogramming suppresses pancreatitis and enhances pancreatic cancer therapy. Cell 159, 80–93. https://doi.org/10.1016/j.cell.2014.08.007

SHIROTA, H., KLINMAN, D. M., ITO, S. E., ITO, H., KUBO, M. & ISHIOKA, C. 2017. IL4 from T Follicular Helper Cells Downregulates Antitumor Immunity. *Cancer Immunol Res,* 5**,** 61-71.

SHULTZ, L. D., GOODWIN, N., ISHIKAWA, F., HOSUR, V., LYONS, B. L. & GREINER, D. L. 2014. Human cancer growth and therapy in immunodeficient mouse models. *Cold Spring Harb Protoc,* 2014**,** 694-708.

SHUSTERMAN, S., LONDON, W. B., GILLIES, S. D., HANK, J. A., VOSS, S. D., SEEGER, R. C., REYNOLDS, C. P., KIMBALL, J., ALBERTINI, M. R., WAGNER, B., GAN, J., EICKHOFF, J., DESANTES, K. B., COHN, S. L., HECHT, T., GADBAW, B., REISFELD, R. A., MARIS, J. M. & SONDEL, P. M. 2010. Antitumor activity of hu14.18-IL2 in patients with relapsed/refractory neuroblastoma: a Children's Oncology Group (COG) phase II study. *J Clin Oncol,* 28**,** 4969-75.

SILVER, D. A., PELLICER, I., FAIR, W. R., HESTON, W. D. & CORDON-CARDO, C. 1997. Prostate-specific membrane antigen expression in normal and malignant human tissues. *Clin Cancer Res,* 3**,** 81-5.

SIMPKINS, S.A., HANBY, A.M., HOLLIDAY, D.L., SPEIRS, V., 2012. Clinical and functional significance of loss of caveolin-1 expression in breast cancer-associated fibroblasts. J. Pathol. 227, 490–498. https://doi.org/10.1002/path.403

SINGH, H., SERRANO, L. M., PFEIFFER, T., OLIVARES, S., MCNAMARA, G., SMITH, D. D., AL-KADHIMI, Z., FORMAN, S. J., GILLIES, S. D., JENSEN, M. C., COLCHER, D., RAUBITSCHEK, A. & COOPER, L. J. N. 2007. Combining Adoptive Cellular and Immunocytokine Therapies to Improve Treatment of B-Lineage Malignancy. *Cancer Research,* 67**,** 2872-2880.

SIU, L. L., STEEGHS, N., MENIAWY, T., JOERGER, M., SPRATLIN, J. L., ROTTEY, S., NAGRIAL, A., COOPER, A., MEIER, R., GUAN, X., PHILLIPS, P., BAJAJ, G., GOKEMEIJER, J., KORMAN, A. J., AUNG, K. L. & CARLINO, M. S. 2017. Preliminary results of a phase I/IIa study of BMS-986156 (glucocorticoid-induced tumor necrosis factor receptor–related gene [GITR] agonist), alone and in combination with nivolumab in pts with advanced solid tumors. *Journal of Clinical Oncology,* 35**,** 104-104.

SLOVIN, S. F., WANG, X., HULLINGS, M., ARAUZ, G., BARTIDO, S., LEWIS, J. S., SCHÖDER, H., ZANZONICO, P., SCHER, H. I. & RIVIERE, I. 2013. Chimeric antigen receptor (CAR+) modified T cells targeting prostate specific membrane antigen (PSMA) in patients (pts) with castrate metastatic prostate cancer (CMPC). *Journal of Clinical Oncology,* 31**,** TPS3115-TPS3115.

SMITH, K. D., MEZHIR, J. J., BICKENBACH, K., VEERAPONG, J., CHARRON, J., POSNER, M. C., ROIZMAN, B. & WEICHSELBAUM, R. R. 2006. Activated MEK suppresses activation of PKR and enables efficient replication and in vivo oncolysis by Deltagamma(1)34.5 mutants of herpes simplex virus 1. *J Virol,* 80**,** 1110-20.

SMYTH, M. J., TANIGUCHI, M. & STREET, S. E. 2000a. The anti-tumor activity of IL-12: mechanisms of innate immunity that are model and dose dependent. *J Immunol,* 165**,** 2665-70.

SMYTH, M. J., THIA, K. Y., STREET, S. E., MACGREGOR, D., GODFREY, D. I. & TRAPANI, J. A. 2000b. Perforin-mediated cytotoxicity is critical for surveillance of spontaneous lymphoma. *J Exp Med,* 192**,** 755-60.

SOMMERMEYER, D., HUDECEK, M., KOSASIH, P. L., GOGISHVILI, T., MALONEY, D. G., TURTLE, C. J. & RIDDELL, S. R. 2016. Chimeric antigen receptor-modified T cells derived from defined CD8+ and CD4+ subsets confer superior antitumor reactivity in vivo. *Leukemia,* 30**,** 492-500.

SONG, D. G., YE, Q., POUSSIN, M., HARMS, G. M., FIGINI, M. & POWELL, D. J., JR. 2012. CD27 costimulation augments the survival and antitumor activity of redirected human T cells in vivo. *Blood,* 119**,** 696-706.

SPITALERI, G., BERARDI, R., PIERANTONI, C., DE PAS, T., NOBERASCO, C., LIBBRA, C., GONZALEZ-IGLESIAS, R., GIOVANNONI, L., TASCIOTTI, A., NERI, D., MENSSEN, H. D. & DE BRAUD, F. 2013. Phase I/II study of the tumour-targeting human monoclonal antibody-cytokine fusion protein L19-TNF in patients with advanced solid tumours. *J Cancer Res Clin Oncol,* 139**,** 447-55.

STADLER, W. M., RYBAK, M. E. & VOGELZANG, N. J. 1995. A phase II study of subcutaneous recombinant human interleukin-4 in metastatic renal cell carcinoma. *Cancer,* 76**,** 1629-33.

STANCOVSKI, I., SCHINDLER, D. G., WAKS, T., YARDEN, Y., SELA, M. & ESHHAR, Z. 1993. Targeting of T lymphocytes to Neu/HER2-expressing cells using chimeric single chain Fv receptors. *J Immunol,* 151**,** 6577-82.

STASHENKO, P., NADLER, L. M., HARDY, R. & SCHLOSSMAN, S. F. 1980. Characterization of a human B lymphocyte-specific antigen. *J Immunol,* 125**,** 1678-85.

STRAATHOF, K. C., PULE, M. A., YOTNDA, P., DOTTI, G., VANIN, E. F., BRENNER, M. K., HESLOP, H. E., SPENCER, D. M. & ROONEY, C. M. 2005. An inducible caspase 9 safety switch for T-cell therapy. *Blood,* 105**,** 4247-54.

STREET, S. E., TRAPANI, J. A., MACGREGOR, D. & SMYTH, M. J. 2002. Suppression of lymphoma and epithelial malignancies effected by interferon gamma. *J Exp Med,* 196**,** 129-34.

STREET, S. E. A., CRETNEY, E. & SMYTH, M. J. 2001. Perforin and interferon-γ activities independently control tumor initiation, growth, and metastasis. *Blood,* 97**,** 192-197.

STRONG, J. E., COFFEY, M. C., TANG, D., SABININ, P. & LEE, P. W. 1998. The molecular basis of viral oncolysis: usurpation of the Ras signaling pathway by reovirus. *Embo j,* 17**,** 3351-62.

SU, S., CHEN, J., YAO, H., LIU, J., YU, S., LAO, L., WANG, M., LUO, M., XING, Y., CHEN, F., HUANG, D., ZHAO, J., YANG, L., LIAO, D., SU, F., LI, M., LIU, Q., SONG, E., 2018. CD10(+)GPR77(+) Cancer-Associated Fibroblasts Promote Cancer Formation and Chemoresistance by Sustaining Cancer Stemness. Cell 172, 841-856.e16. https://doi.org/10.1016/j.cell.2018.01.00

SUN, Y.B.Y., QU, X., CARUANA, G., LI, J., 2016. The origin of renal fibroblasts/myofibroblasts and the signals that trigger fibrosis. Differ. Res. Biol. Divers. 92, 102–107. https://doi.org/10.1016/j.diff.2016.05.008

SUKUMARAN, S., WATANABE, N., BAJGAIN, P., RAJA, K., MOHAMMED, S., FISHER, W. E., BRENNER, M. K., LEEN, A. M. & VERA, J. F. 2018. Enhancing the Potency and Specificity of Engineered T Cells for Cancer Treatment. *Cancer Discov,* 8**,** 972-987.

TAKAHASHI, H., SAKAKURA, K., KAWABATA-IWAKAWA, R., ROKUDAI, S., TOYODA, M., NISHIYAMA, M., CHIKAMATSU, K., 2015. Immunosuppressive activity of cancer-associated fibroblasts in head and neck squamous cell carcinoma. Cancer Immunol. Immunother. CII 64, 1407–1417. https://doi.org/10.1007/s00262-015-1742-0

TAKESHI, U., SADAR, M. D., SUZUKI, H., AKAKURA, K., SAKAMOTO, S., SHIMBO, M., SUYAMA, T., IMAMOTO, T., KOMIYA, A., YUKIO, N. & ICHIKAWA, T. 2005. Interleukin-4 in patients with prostate cancer. *Anticancer Res,* 25**,** 4595-8.

TAMADA, K., GENG, D., SAKODA, Y., BANSAL, N., SRIVASTAVA, R., LI, Z. & DAVILA, E. 2012. Redirecting gene-modified T cells toward various cancer types using tagged antibodies. *Clin Cancer Res,* 18**,** 6436-45.

TAMMANA, S., HUANG, X., WONG, M., MILONE, M. C., MA, L., LEVINE, B. L., JUNE, C. H., WAGNER, J. E., BLAZAR, B. R. & ZHOU, X. 2010. 4-1BB and CD28 signaling plays a synergistic role in redirecting umbilical cord blood T cells against B-cell malignancies. *Hum Gene Ther,* 21**,** 75-86.

TANG, D. G., LI, L., CHOPRA, D. P. & PORTER, A. T. 1998. Extended survivability of prostate cancer cells in the absence of trophic factors: increased proliferation, evasion of apoptosis, and the role of apoptosis proteins. *Cancer Res,* 58**,** 3466-79.

TANG, X., TU, G., YANG, G., WANG, X., KANG, L., YANG, L., ZENG, H., WAN, X., QIAO, Y., CUI, X., LIU, M., HOU, Y., 2019. Autocrine TGF-beta1/miR-200s/miR-221/DNMT3B regulatory loop maintains CAF status to fuel breast cancer cell proliferation. Cancer Lett. 452, 79–89. https://doi.org/10.1016/j.canlet.2019.02.044

TANOUE, K., ROSEWELL SHAW, A., WATANABE, N., PORTER, C., RANA, B., GOTTSCHALK, S., BRENNER, M. & SUZUKI, M. 2017. Armed Oncolytic Adenovirus-Expressing PD-L1 Mini-Body Enhances Antitumor Effects of Chimeric Antigen Receptor T Cells in Solid Tumors. *Cancer Res,* 77**,** 2040-2051.

TAWARA, I., KAGEYAMA, S., MIYAHARA, Y., FUJIWARA, H., NISHIDA, T., AKATSUKA, Y., IKEDA, H., TANIMOTO, K., TERAKURA, S., MURATA, M., INAGUMA, Y., MASUYA, M., INOUE, N., KIDOKORO, T., OKAMOTO, S., TOMURA, D., CHONO, H., NUKAYA, I., MINENO, J., NAOE, T., EMI, N., YASUKAWA, M., KATAYAMA, N. & SHIKU, H. 2017. Safety and persistence of WT1-specific T-cell receptor gene-transduced lymphocytes in patients with AML and MDS. *Blood,* 130**,** 1985-1994.

TAYLOR, C. W., LEBLANC, M., FISHER, R. I., MOORE, D. F., SR., ROACH, R. W., ELIAS, L. & MILLER, T. P. 2000. Phase II evaluation of interleukin-4 in patients with non-Hodgkin's lymphoma: a Southwest Oncology Group trial. *Anticancer Drugs,* 11**,** 695-700.

TCHOU, J., ZHAO, Y., LEVINE, B. L., ZHANG, P. J., DAVIS, M. M., MELENHORST, J. J., KULIKOVSKAYA, I., BRENNAN, A. L., LIU, X., LACEY, S. F., POSEY, A. D., JR., WILLIAMS, A. D., SO, A., CONEJO-GARCIA, J. R., PLESA, G., YOUNG, R. M., MCGETTIGAN, S., CAMPBELL, J., PIERCE, R. H., MATRO, J. M., DEMICHELE, A. M., CLARK, A. S.,

COOPER, L. J., SCHUCHTER, L. M., VONDERHEIDE, R. H. & JUNE, C. H. 2017. Safety and Efficacy of Intratumoral Injections of Chimeric Antigen Receptor (CAR) T Cells in Metastatic Breast Cancer. *Cancer Immunol Res,* 5**,** 1152-1161.

TEACHEY, D. T., LACEY, S. F., SHAW, P. A., MELENHORST, J. J., MAUDE, S. L., FREY, N., PEQUIGNOT, E., GONZALEZ, V. E., CHEN, F., FINKLESTEIN, J., BARRETT, D. M., WEISS, S. L., FITZGERALD, J. C., BERG, R. A., APLENC, R., CALLAHAN, C., RHEINGOLD, S. R., ZHENG, Z., ROSE-JOHN, S., WHITE, J. C., NAZIMUDDIN, F., WERTHEIM, G., LEVINE, B. L., JUNE, C. H., PORTER, D. L. & GRUPP, S. A. 2016. Identification of Predictive Biomarkers for Cytokine Release Syndrome after Chimeric Antigen Receptor T-cell Therapy for Acute Lymphoblastic Leukemia. *Cancer Discov,* 6**,** 664-79.

TEICHGRABER, V., MONASTERIO, C., CHAITANYA, K., BOGER, R., GORDON, K., DIETERLE, T., JAGER, D. & BAUER, S. 2015. Specific inhibition of fibroblast activation protein (FAP)-alpha prevents tumor progression in vitro. *Adv Med Sci,* 60**,** 264-72.

TENG, M. W., VESELY, M. D., DURET, H., MCLAUGHLIN, N., TOWNE, J. E., SCHREIBER, R. D. & SMYTH, M. J. 2012. Opposing roles for IL-23 and IL-12 in maintaining occult cancer in an equilibrium state. *Cancer Res,* 72**,** 3987-96.

TEPPER, R. I., COFFMAN, R. L. & LEDER, P. 1992. An eosinophil-dependent mechanism for the antitumor effect of interleukin-4. *Science,* 257**,** 548-51.

THOMAS, D.A., MASSAGUE, J., 2005. TGF-beta directly targets cytotoxic T cell functions during tumor evasion of immune surveillance. Cancer Cell 8, 369–380. https://doi.org/10.1016/j.ccr.2005.10.012

TODARO, M., ALEA, M. P., DI STEFANO, A. B., CAMMARERI, P., VERMEULEN, L., IOVINO, F., TRIPODO, C., RUSSO, A., GULOTTA, G., MEDEMA, J. P. & STASSI, G. 2007. Colon cancer stem cells dictate tumor growth and resist cell death by production of interleukin-4. *Cell Stem Cell,* 1**,** 389-402.

TODARO, M., LOMBARDO, Y., FRANCIPANE, M. G., ALEA, M. P., CAMMARERI, P., IOVINO, F., DI STEFANO, A. B., DI BERNARDO, C., AGRUSA, A., CONDORELLI, G., WALCZAK, H. & STASSI, G. 2008. Apoptosis resistance in epithelial tumors is mediated by tumor-cell-derived interleukin-4. *Cell Death Differ,* 15**,** 762-72.

TODARO, M., ZERILLI, M., RICCI-VITIANI, L., BINI, M., PEREZ ALEA, M., MARIA FLORENA, A., MICELI, L., CONDORELLI, G., BONVENTRE, S., DI GESU, G., DE MARIA, R. & STASSI, G. 2006. Autocrine production of interleukin-4 and interleukin-10 is required for survival and growth of thyroid cancer cells. *Cancer Res,* 66**,** 1491-9.

TOI, M., BICKNELL, R. & HARRIS, A. L. 1992. Inhibition of colon and breast carcinoma cell growth by interleukin-4. *Cancer Res,* 52**,** 275-9.

TOPALIAN, S. L., SOLOMON, D., AVIS, F. P., CHANG, A. E., FREERKSEN, D. L., LINEHAN, W. M., LOTZE, M. T., ROBERTSON, C. N., SEIPP, C. A., SIMON, P. & ET AL. 1988. Immunotherapy of patients with advanced cancer using tumor-infiltrating lymphocytes and recombinant interleukin-2: a pilot study. *J Clin Oncol,* 6**,** 839-53.

TOPP, M. S., PAPADIMITRIOU, C. A., EITELBACH, F., KOENIGSMANN, M., OELMANN, E., KOEHLER, B., OBERBERG, D., REUFI, B., STEIN, H., THIEL, E. & ET AL. 1995. Recombinant human interleukin 4 has antiproliferative activity on human tumor cell lines derived from epithelial and nonepithelial histologies. *Cancer Res,* 55**,** 2173-6.

TOYODA, H., WIMMER, E. & CELLO, J. 2011. Oncolytic poliovirus therapy and immunization with poliovirus-infected cell lysate induces potent antitumor immunity against neuroblastoma in vivo. *Int J Oncol,* 38**,** 81-7.

TRAN, C., OUK, S., CLEGG, N. J., CHEN, Y., WATSON, P. A., ARORA, V., WONGVIPAT, J., SMITH-JONES, P. M., YOO, D., KWON, A., WASIELEWSKA, T., WELSBIE, D., CHEN, C. D., HIGANO, C. S., BEER, T. M., HUNG, D. T., SCHER, H. I., JUNG, M. E. & SAWYERS, C. L. 2009. Development of a second-generation antiandrogen for treatment of advanced prostate cancer. *Science,* 324**,** 787-90.

TRAN, E., AHMADZADEH, M., LU, Y. C., GROS, A., TURCOTTE, S., ROBBINS, P. F., GARTNER, J. J., ZHENG, Z., LI, Y. F., RAY, S., WUNDERLICH, J. R., SOMERVILLE, R. P. & ROSENBERG, S. A. 2015. Immunogenicity of somatic mutations in human gastrointestinal cancers. *Science,* 350**,** 1387-90.

TRAN, E., CHINNASAMY, D., YU, Z., MORGAN, R. A., LEE, C. C., RESTIFO, N. P. & ROSENBERG, S. A. 2013. Immune targeting of fibroblast activation protein triggers recognition of multipotent bone marrow stromal cells and cachexia. *J Exp Med,* 210**,** 1125-35.

TRAN, E., TURCOTTE, S., GROS, A., ROBBINS, P. F., LU, Y. C., DUDLEY, M. E., WUNDERLICH, J. R., SOMERVILLE, R. P., HOGAN, K., HINRICHS, C. S., PARKHURST, M. R., YANG, J. C. & ROSENBERG, S. A. 2014. Cancer immunotherapy based on mutation-specific CD4+ T cells in a patient with epithelial cancer. *Science,* 344**,** 641-5.

TRAVERS, M. T., BARRETT-LEE, P. J., BERGER, U., LUQMANI, Y. A., GAZET, J. C., POWLES, T. J. & COOMBES, R. C. 1988. Growth factor expression in normal, benign, and malignant breast tissue. *Br Med J (Clin Res Ed),* 296**,** 1621-4.

TRUONG, L. D., KADMON, D., MCCUNE, B. K., FLANDERS, K. C., SCARDINO, P. T. & THOMPSON, T. C. 1993. Association of transforming growth factor-beta 1 with prostate cancer: an immunohistochemical study. *Hum Pathol,* 24**,** 4-9.

TSANG, J. Y. S., CHAN, K. W., NI, Y. B., HLAING, T., HU, J., CHAN, S. K., CHEUNG, S. Y. & TSE, G. M. 2017. Expression and Clinical Significance of Herpes Virus Entry Mediator (HVEM) in Breast Cancer. *Ann Surg Oncol,* 24**,** 4042-4050.

TUBB, V. M., SCHRIKKEMA, D. S., CROFT, N. P., PURCELL, A. W., LINNEMANN, C., FRERIKS, M. R., CHEN, F., LONG, H. M., LEE, S. P. & BENDLE, G. M. 2018. Isolation of T cell receptors targeting recurrent neoantigens in hematological malignancies. *J Immunother Cancer,* 6**,** 70.

TURTLE, C. J., HANAFI, L. A., BERGER, C., GOOLEY, T. A., CHERIAN, S., HUDECEK, M., SOMMERMEYER, D., MELVILLE, K., PENDER, B., BUDIARTO, T. M., ROBINSON, E., STEEVENS, N. N., CHANEY, C., SOMA, L., CHEN, X., YEUNG, C., WOOD, B., LI, D., CAO, J., HEIMFELD, S., JENSEN, M. C., RIDDELL, S. R. & MALONEY, D. G. 2016. CD19 CAR-T cells of defined CD4+:CD8+ composition in adult B cell ALL patients. *J Clin Invest,* 126**,** 2123-38.

TUXHORN, J. A., AYALA, G. E., SMITH, M. J., SMITH, V. C., DANG, T. D. & ROWLEY, D. R. 2002a. Reactive stroma in human prostate cancer: induction of myofibroblast phenotype and extracellular matrix remodeling. *Clin Cancer Res,* 8**,** 2912-23.

TUXHORN, J. A., MCALHANY, S. J., DANG, T. D., AYALA, G. E. & ROWLEY, D. R. 2002b. Stromal cells promote angiogenesis and growth of human prostate tumors in a differential reactive stroma (DRS) xenograft model. *Cancer Res,* 62**,** 3298-307.

URBANSKA, K., LANITIS, E., POUSSIN, M., LYNN, R. C., GAVIN, B. P., KELDERMAN, S., YU, J., SCHOLLER, N. & POWELL, D. J., JR. 2012. A universal strategy for adoptive immunotherapy of cancer through use of a novel T-cell antigen receptor. *Cancer Res,* 72**,** 1844-52.

UUSI-KERTTULA, H., LEGUT, M., DAVIES, J., JONES, R., HUDSON, E., HANNA, L., STANTON, R. J., CHESTER, J. D. & PARKER, A. L. 2015. Incorporation of Peptides Targeting EGFR and FGFR1 into the Adenoviral Fiber Knob Domain and Their Evaluation as Targeted Cancer Therapies. *Hum Gene Ther,* 26**,** 320-9.

VAN DEN BROEK, M. E., KAGI, D., OSSENDORP, F., TOES, R., VAMVAKAS, S., LUTZ, W. K., MELIEF, C. J., ZINKERNAGEL, R. M. & HENGARTNER, H. 1996. Decreased tumor surveillance in perforin-deficient mice. *J Exp Med,* 184**,** 1781-90.

VAN DEN HEUVEL, M. M., VERHEIJ, M., BOSHUIZEN, R., BELDERBOS, J., DINGEMANS, A. M., DE RUYSSCHER, D., LAURENT, J., TIGHE, R., HAANEN, J. & QUARATINO, S. 2015. NHS-IL2 combined with radiotherapy: preclinical rationale and phase Ib trial results in metastatic non-small cell lung cancer following first-line chemotherapy. *J Transl Med,* 13**,** 32.

VAN DER STEGEN, S. J., HAMIEH, M. & SADELAIN, M. 2015. The pharmacology of second-generation chimeric antigen receptors. *Nat Rev Drug Discov,* 14**,** 499-509.

VAN SCHALKWYK, M. C., PAPA, S. E., JEANNON, J. P., GUERRERO URBANO, T., SPICER, J. F. & MAHER, J. 2013. Design of a phase I clinical trial to evaluate intratumoral delivery of ErbB-targeted chimeric antigen receptor T-cells in locally advanced or recurrent head and neck cancer. *Hum Gene Ther Clin Dev,* 24**,** 134-42.

VÁZQUEZ-REY, M. & LANG, D. A. 2011. Aggregates in monoclonal antibody manufacturing processes. *Biotechnology and Bioengineering,* 108**,** 1494-1508.

VELDSCHOLTE, J., RIS-STALPERS, C., KUIPER, G. G., JENSTER, G., BERREVOETS, C., CLAASSEN, E., VAN ROOIJ, H. C., TRAPMAN, J., BRINKMANN, A. O. & MULDER, E. 1990. A mutation in the ligand binding domain of the androgen receptor of human LNCaP cells affects steroid binding characteristics and response to anti-androgens. *Biochem Biophys Res Commun,* 173**,** 534-40.

VENMAR, K. T., CARTER, K. J., HWANG, D. G., DOZIER, E. A. & FINGLETON, B. 2014. IL4 receptor ILR4alpha regulates metastatic colonization by mammary tumors through multiple signaling pathways. *Cancer Res,* 74**,** 4329-40.

VIAUD, S., MA, J. S. Y., HARDY, I. R., HAMPTON, E. N., BENISH, B., SHERWOOD, L., NUNEZ, V., ACKERMAN, C. J., KHIALEEVA, E., WEGLARZ, M., LEE, S. C., WOODS, A. K. & YOUNG, T. S. 2018. Switchable control over in vivo CAR T expansion, B cell depletion, and induction of memory. *Proc Natl Acad Sci U S A,* 115**,** E10898-e10906.

VIBHAKAR, R., JUAN, G., TRAGANOS, F., DARZYNKIEWICZ, Z. & FINGER, L. R. 1997. Activation-induced expression of human programmed death-1 gene in T-lymphocytes. *Exp Cell Res,* 232**,** 25-8.

VILLALOBOS-HERNANDEZ, A., BOBBALA, D., KANDHI, R., KHAN, M. G., MAYHUE, M., DUBOIS, C. M., FERBEYRE, G., SAUCIER, C., RAMANATHAN, S. & ILANGUMARAN, S. 2017. SOCS1 inhibits migration and invasion of prostate cancer cells, attenuates tumor growth and modulates the tumor stroma. *Prostate Cancer Prostatic Dis,* 20**,** 36-47.

VOELKEL-JOHNSON, C., KING, D. L. & NORRIS, J. S. 2002. Resistance of prostate cancer cells to soluble TNF-related apoptosis-inducing ligand (TRAIL/Apo2L)

can be overcome by doxorubicin or adenoviral delivery of full-length TRAIL. *Cancer Gene Ther,* 9**,** 164-72.

VOLPERT, O. V., FONG, T., KOCH, A. E., PETERSON, J. D., WALTENBAUGH, C., TEPPER, R. I. & BOUCK, N. P. 1998. Inhibition of angiogenesis by interleukin 4. *J Exp Med,* 188**,** 1039-46.

VON BOEHMER, L., MATTLE, M., BODE, P., LANDSHAMMER, A., SCHAFER, C., NUBER, N., RITTER, G., OLD, L., MOCH, H., SCHAFER, N., JAGER, E., KNUTH, A. & VAN DEN BROEK, M. 2013. NY-ESO-1-specific immunological pressure and escape in a patient with metastatic melanoma. *Cancer Immun,* 13**,** 12.

VORMOOR, B., KNIZIA, H. K., BATEY, M. A., ALMEIDA, G. S., WILSON, I., DILDEY, P., SHARMA, A., BLAIR, H., HIDE, I. G., HEIDENREICH, O., VORMOOR, J., MAXWELL, R. J. & BACON, C. M. 2014. Development of a preclinical orthotopic xenograft model of ewing sarcoma and other human malignant bone disease using advanced in vivo imaging. *PLoS One,* 9**,** e85128.

WALLIN, J. J., BENDELL, J. C., FUNKE, R., SZNOL, M., KORSKI, K., JONES, S., HERNANDEZ, G., MIER, J., HE, X., HODI, F. S., DENKER, M., LEVEQUE, V., CANAMERO, M., BABITSKI, G., KOEPPEN, H., ZIAI, J., SHARMA, N., GAIRE, F., CHEN, D. S., WATERKAMP, D., HEGDE, P. S. & MCDERMOTT, D. F. 2016. Atezolizumab in combination with bevacizumab enhances antigen-specific T-cell migration in metastatic renal cell carcinoma. *Nat Commun,* 7**,** 12624.

WALSENG, E., KOKSAL, H., SEKTIOGLU, I. M., FANE, A., SKORSTAD, G., KVALHEIM, G., GAUDERNACK, G., INDERBERG, E. M. & WALCHLI, S. 2017. A TCR-based Chimeric Antigen Receptor. *Sci Rep,* 7**,** 10713.

WALTER, K., OMURA, N., HONG, S. M., GRIFFITH, M. & GOGGINS, M. 2008. Pancreatic cancer associated fibroblasts display normal allelotypes. *Cancer Biol Ther,* 7**,** 882-8.

WANG, L. C., LO, A., SCHOLLER, J., SUN, J., MAJUMDAR, R. S., KAPOOR, V., ANTZIS, M., COTNER, C. E., JOHNSON, L. A., DURHAM, A. C., SOLOMIDES, C. C., JUNE, C. H., PURE, E. & ALBELDA, S. M. 2014. Targeting fibroblast activation protein in tumor stroma with chimeric antigen receptor T cells can inhibit tumor growth and augment host immunity without severe toxicity. *Cancer Immunol Res,* 2**,** 154-66.

WANG, W., LI, Q., TAKEUCHI, S., YAMADA, T., KOIZUMI, H., NAKAMURA, T., MATSUMOTO, K., MUKAIDA, N., NISHIOKA, Y., SONE, S., NAKAGAWA, T., UENAKA, T. & YANO, S. 2012. Met kinase inhibitor E7050 reverses three different mechanisms of hepatocyte growth factor-induced tyrosine kinase inhibitor resistance in EGFR mutant lung cancer. *Clin Cancer Res,* 18**,** 1663-71.

WEIDE, B., EIGENTLER, T. K., PFLUGFELDER, A., ZELBA, H., MARTENS, A., PAWELEC, G., GIOVANNONI, L., RUFFINI, P. A., ELIA, G., NERI, D., GUTZMER, R., BECKER, J. C. & GARBE, C. 2014. Intralesional treatment of stage III metastatic melanoma patients with L19-IL2 results in sustained clinical and systemic immunologic responses. *Cancer Immunol Res,* 2**,** 668-78.

WELT, S., DIVGI, C. R., SCOTT, A. M., GARIN-CHESA, P., FINN, R. D., GRAHAM, M., CARSWELL, E. A., COHEN, A., LARSON, S. M., OLD, L. J. & ET AL. 1994. Antibody targeting in metastatic colon cancer: a phase I study of monoclonal antibody F19 against a cell-surface protein of reactive tumor stromal fibroblasts. *J Clin Oncol,* 12**,** 1193-203.

WEN, Y., WANG, C. T., MA, T. T., LI, Z. Y., ZHOU, L. N., MU, B., LENG, F., SHI, H. S., LI, Y. O. & WEI, Y. Q. 2010. Immunotherapy targeting fibroblast

activation protein inhibits tumor growth and increases survival in a murine colon cancer model. *Cancer Sci,* 101**,** 2325-32.

WENDT, M. K., MOLTER, J., FLASK, C. A. & SCHIEMANN, W. P. 2011. In vivo dual substrate bioluminescent imaging. *J Vis Exp*.

WILKIE, S., BURBRIDGE, S. E., CHIAPERO-STANKE, L., PEREIRA, A. C., CLEARY, S., VAN DER STEGEN, S. J., SPICER, J. F., DAVIES, D. M. & MAHER, J. 2010. Selective expansion of chimeric antigen receptor-targeted T-cells with potent effector function using interleukin-4. *J Biol Chem,* 285**,** 25538-44.

WILKIE, S., VAN SCHALKWYK, M. C., HOBBS, S., DAVIES, D. M., VAN DER STEGEN, S. J., PEREIRA, A. C., BURBRIDGE, S. E., BOX, C., ECCLES, S. A. & MAHER, J. 2012. Dual targeting of ErbB2 and MUC1 in breast cancer using chimeric antigen receptors engineered to provide complementary signaling. *J Clin Immunol,* 32**,** 1059-70.

WILKINSON, S. E., FURIC, L., BUCHANAN, G., LARSSON, O., PEDERSEN, J., FRYDENBERG, M., RISBRIDGER, G. P. & TAYLOR, R. A. 2013. Hedgehog signaling is active in human prostate cancer stroma and regulates proliferation and differentiation of adjacent epithelium. *Prostate,* 73**,** 1810-23.

WOLCHOK, J. D., CHIARION-SILENI, V., GONZALEZ, R., RUTKOWSKI, P., GROB, J. J., COWEY, C. L., LAO, C. D., WAGSTAFF, J., SCHADENDORF, D., FERRUCCI, P. F., SMYLIE, M., DUMMER, R., HILL, A., HOGG, D., HAANEN, J., CARLINO, M. S., BECHTER, O., MAIO, M., MARQUEZ-RODAS, I., GUIDOBONI, M., MCARTHUR, G., LEBBE, C., ASCIERTO, P. A., LONG, G. V., CEBON, J., SOSMAN, J., POSTOW, M. A., CALLAHAN, M. K., WALKER, D., ROLLIN, L., BHORE, R., HODI, F. S. & LARKIN, J. 2017. Overall Survival with Combined Nivolumab and Ipilimumab in Advanced Melanoma. *N Engl J Med,* 377**,** 1345-1356.

WRIGHT, G. L., JR., GROB, B. M., HALEY, C., GROSSMAN, K., NEWHALL, K., PETRYLAK, D., TROYER, J., KONCHUBA, A., SCHELLHAMMER, P. F. & MORIARTY, R. 1996. Upregulation of prostate-specific membrane antigen after androgen-deprivation therapy. *Urology,* 48**,** 326-34.

WRIGHT, G. L., JR., HALEY, C., BECKETT, M. L. & SCHELLHAMMER, P. F. 1995. Expression of prostate-specific membrane antigen in normal, benign, and malignant prostate tissues. *Urol Oncol,* 1**,** 18-28.

WU, C. Y., ROYBAL, K. T., PUCHNER, E. M., ONUFFER, J. & LIM, W. A. 2015. Remote control of therapeutic T cells through a small molecule-gated chimeric receptor. *Science,* 350**,** aab4077.

WU, X., PENG, M., HUANG, B., ZHANG, H., WANG, H., HUANG, B., XUE, Z., ZHANG, L., DA, Y., YANG, D., YAO, Z. & ZHANG, R. 2013. Immune microenvironment profiles of tumor immune equilibrium and immune escape states of mouse sarcoma. *Cancer Lett,* 340**,** 124-33.

YANG, X., LIN, Y., SHI, Y., LI, B., LIU, W., YIN, W., DANG, Y., CHU, Y., FAN, J., HE, R., 2016. FAP Promotes Immunosuppression by Cancer-Associated Fibroblasts in the Tumor Microenvironment via STAT3-CCL2 Signaling. Cancer Res. 76, 4124–4135. https://doi.org/10.1158/0008-5472.CAN-15-2973

YANG, Y., KOHLER, M. E., CHIEN, C. D., SAUTER, C. T., JACOBY, E., YAN, C., HU, Y., WANHAINEN, K., QIN, H. & FRY, T. J. 2017. TCR engagement negatively affects CD8 but not CD4 CAR T cell expansion and leukemic clearance. *Sci Transl Med,* 9.

YEKU, O., LI, X. & BRENTJENS, R. J. 2017a. Adoptive T-Cell Therapy for Solid Tumors. *Am Soc Clin Oncol Educ Book,* 37**,** 193-204.

YEKU, O. O., PURDON, T. J., KONERU, M., SPRIGGS, D. & BRENTJENS, R. J. 2017b. Armored CAR T cells enhance antitumor efficacy and overcome the tumor microenvironment. *Sci Rep,* 7**,** 10541.

ZACHARAKIS, N., CHINNASAMY, H., BLACK, M., XU, H., LU, Y.-C., ZHENG, Z., PASETTO, A., LANGHAN, M., SHELTON, T., PRICKETT, T., GARTNER, J., JIA, L., TREBSKA-MCGOWAN, K., SOMERVILLE, R. P., ROBBINS, P. F., ROSENBERG, S. A., GOFF, S. L. & FELDMAN, S. A. 2018. Immune recognition of somatic mutations leading to complete durable regression in metastatic breast cancer. *Nature Medicine,* 24**,** 724-730.

ZHAND, S., HOSSEINI, S. M., TABARRAEI, A., SAEIDI, M., JAZI, M. S., KALANI, M. R. & MORADI, A. 2018. Oral poliovirus vaccine-induced programmed cell death involves both intrinsic and extrinsic pathways in human colorectal cancer cells. *Oncolytic Virother,* 7**,** 95-105.

ZHANG, G., WANG, L., CUI, H., WANG, X., ZHANG, G., MA, J., HAN, H., HE, W., WANG, W., ZHAO, Y., LIU, C., SUN, M. & GAO, B. 2014. Anti-melanoma activity of T cells redirected with a TCR-like chimeric antigen receptor. *Sci Rep,* 4**,** 3571.

ZHANG, K. X., MATSUI, Y., HADASCHIK, B. A., LEE, C., JIA, W., BELL, J. C., FAZLI, L., SO, A. I. & RENNIE, P. S. 2010. Down-regulation of type I interferon receptor sensitizes bladder cancer cells to vesicular stomatitis virus-induced cell death. *Int J Cancer,* 127**,** 830-8.

ZHANG, L., KERKAR, S. P., YU, Z., ZHENG, Z., YANG, S., RESTIFO, N. P., ROSENBERG, S. A. & MORGAN, R. A. 2011a. Improving adoptive T cell therapy by targeting and controlling IL-12 expression to the tumor environment. *Mol Ther,* 19**,** 751-9.

ZHANG, L., MORGAN, R. A., BEANE, J. D., ZHENG, Z., DUDLEY, M. E., KASSIM, S. H., NAHVI, A. V., NGO, L. T., SHERRY, R. M., PHAN, G. Q., HUGHES, M. S., KAMMULA, U. S., FELDMAN, S. A., TOOMEY, M. A., KERKAR, S. P., RESTIFO, N. P., YANG, J. C. & ROSENBERG, S. A. 2015. Tumor-infiltrating lymphocytes genetically engineered with an inducible gene encoding interleukin-12 for the immunotherapy of metastatic melanoma. *Clin Cancer Res,* 21**,** 2278-88.

ZHANG, Q., CHEN, L., HELFAND, B. T., JANG, T. L., SHARMA, V., KOZLOWSKI, J., KUZEL, T. M., ZHU, L. J., YANG, X. J., JAVONOVIC, B., GUO, Y., LONNING, S., HARPER, J., TEICHER, B. A., BRENDLER, C., YU, N., CATALONA, W. J. & LEE, C. 2011b. TGF-beta regulates DNA methyltransferase expression in prostate cancer, correlates with aggressive capabilities, and predicts disease recurrence. *PLoS One,* 6**,** e25168.

ZHAO, J., ZHAO, J. & PERLMAN, S. 2012. Differential effects of IL-12 on Tregs and non-Treg T cells: roles of IFN-gamma, IL-2 and IL-2R. *PLoS One,* 7**,** e46241.

ZHAO, S., SHEN, W., YU, J. & WANG, L. 2018. TBX21 predicts prognosis of patients and drives cancer stem cell maintenance via the TBX21-IL-4 pathway in lung adenocarcinoma. *Stem Cell Res Ther,* 9**,** 89.

ZHAO, Z., CONDOMINES, M., VAN DER STEGEN, S. J. C., PERNA, F., KLOSS, C. C., GUNSET, G., PLOTKIN, J. & SADELAIN, M. 2015. Structural Design of Engineered Costimulation Determines Tumor Rejection Kinetics and Persistence of CAR T Cells. *Cancer Cell,* 28**,** 415-428.

ZHONG, X. S., MATSUSHITA, M., PLOTKIN, J., RIVIERE, I. & SADELAIN, M. 2010. Chimeric antigen receptors combining 4-1BB and CD28 signaling domains augment PI3kinase/AKT/Bcl-XL activation and CD8+ T cell-mediated tumor eradication. *Mol Ther,* 18**,** 413-20.

ZHOU, S., KHANAL, S. & ZHANG, H. 2019. Risk of immune-related adverse events associated with ipilimumab-plus-nivolumab and nivolumab therapy in cancer patients. *Ther Clin Risk Manag,* 15**,** 211-221.

ZHUANG, X., KAUL, B., BENTLEY, M., NAGY, Z., GIRAUDO, E., BENDLE, G., GILHAM, D., BICKNELL, R. & LEE, S. P. 2014. Abstract LB-256: Immunotherapy using genetically modified T lymphocytes to target CLEC14A on the tumor vasculature. *Cancer Research,* 74**,** LB-256-LB-256.

ZIANI, L., SAFTA-SAADOUN, T.B., GOURBEIX, J., CAVALCANTI, A., ROBERT, C., FAVRE, G., CHOUAIB, S., THIERY, J., 2017. Melanoma-associated fibroblasts decrease tumor cell susceptibility to NK cell-mediated killing through matrix-metalloproteinases secretion. Oncotarget 8, 19780–19794. https://doi.org/10.18632/oncotarget.15540